NASA/TM-2007-214867

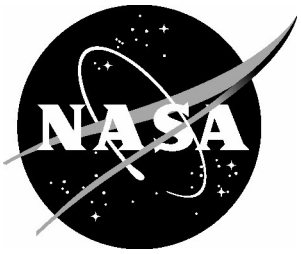

Wall Boundary Layer Measurements for the NASA Langley Transonic Dynamics Tunnel

Carol D. Wieseman, and Robert M. Bennett
Langley Research Center, Hampton, Virginia

April 2007

The NASA STI Program Office . . . in Profile

Since its founding, NASA has been dedicated to the advancement of aeronautics and space science. The NASA Scientific and Technical Information (STI) Program Office plays a key part in helping NASA maintain this important role.

The NASA STI Program Office is operated by Langley Research Center, the lead center for NASA's scientific and technical information. The NASA STI Program Office provides access to the NASA STI Database, the largest collection of aeronautical and space science STI in the world. The Program Office is also NASA's institutional mechanism for disseminating the results of its research and development activities. These results are published by NASA in the NASA STI Report Series, which includes the following report types:

- TECHNICAL PUBLICATION. Reports of completed research or a major significant phase of research that present the results of NASA programs and include extensive data or theoretical analysis. Includes compilations of significant scientific and technical data and information deemed to be of continuing reference value. NASA counterpart of peer-reviewed formal professional papers, but having less stringent limitations on manuscript length and extent of graphic presentations.

- TECHNICAL MEMORANDUM. Scientific and technical findings that are preliminary or of specialized interest, e.g., quick release reports, working papers, and bibliographies that contain minimal annotation. Does not contain extensive analysis.

- CONTRACTOR REPORT. Scientific and technical findings by NASA-sponsored contractors and grantees.

- CONFERENCE PUBLICATION. Collected papers from scientific and technical conferences, symposia, seminars, or other meetings sponsored or co-sponsored by NASA.

- SPECIAL PUBLICATION. Scientific, technical, or historical information from NASA programs, projects, and missions, often concerned with subjects having substantial public interest.

- TECHNICAL TRANSLATION. English-language translations of foreign scientific and technical material pertinent to NASA's mission.

Specialized services that complement the STI Program Office's diverse offerings include creating custom thesauri, building customized databases, organizing and publishing research results ... even providing videos.

For more information about the NASA STI Program Office, see the following:

- Access the NASA STI Program Home Page at ***http://www.sti.nasa.gov***

- E-mail your question via the Internet to help@sti.nasa.gov

- Fax your question to the NASA STI Help Desk at (301) 621-0134

- Phone the NASA STI Help Desk at (301) 621-0390

- Write to:
  NASA STI Help Desk
  NASA Center for AeroSpace Information
  7115 Standard Drive
  Hanover, MD 21076-1320

NASA/TM-2007-214867

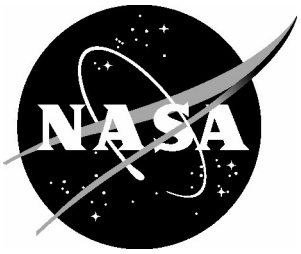

Wall Boundary Layer Measurements for the NASA Langley Transonic Dynamics Tunnel

Carol D. Wieseman and Robert M. Bennett
Langley Research Center, Hampton, Virginia

National Aeronautics and
Space Administration

Langley Research Center
Hampton, Virginia 23681-2199

April 2007

Available from:

NASA Center for AeroSpace Information (CASI)
7115 Standard Drive
Hanover, MD 21076-1320
(301) 621-0390

National Technical Information Service (NTIS)
5285 Port Royal Road
Springfield, VA 22161-2171
(703) 605-6000

Abstract

Measurements of the boundary layer parameters in the NASA Langley Transonic Dynamics Tunnel were conducted during extensive calibration activities following the facility conversion from a Freon-12 heavy-gas test medium to R-134a. Boundary-layer rakes were mounted on the wind-tunnel walls, ceiling, and floor. Measurements were made throughout the tunnel operational envelope in both heavy gas and air and without a model in the test section at three tunnel stations. Configuration variables included open and closed east sidewall wall slots, air and R-134a test media, reentry flap settings, and stagnation pressures over the full range of tunnel operation.

The boundary layer thickness varied considerably for the six rakes. The thickness for the east wall was considerably larger than the thicknesses measured by the other rakes and was also larger than previously reported. There generally was some reduction in thickness at supersonic Mach numbers, but the effects of stagnation pressure, and test medium were not extensive.

Nomenclature

a	speed of sound (ft/sec)
δ	boundary layer thickness, inches
δ^*	boundary layer displacement thickness, inches
γ	ratio of specific heats
θ	boundary layer momentum thickness, inches
ρ	density, slugs/ft^3
C	Velocity profile coefficient (used in equation 11)
Fs	reentry flap setting, figure 5
H	boundary layer shape factor
M	Mach number
P	tunnel static pressure, psf
P_r	Prandtl number
P_t	stagnation pressure
q	dynamic pressure, psf
r	recovery factor, $=\sqrt[3]{P_r}$
R_n	Reynold's number
T	temperature, deg F
Titer	in figures – results with temperature iterated
T0	in figures – results using stagnation temperature
TS	tunnel station, ft
WOZP	wind off zero Tab Point
Tab Pt	data point
V	velocity, ft/sec

V_{ref}	velocity used for determining boundary layer thickness, ft/sec ($.995V_e$)
x_R	gas purity

EW	East Wall
WWTHERMO	temperature measured at West wall rake, TS 72, deg F
EWTHERMO	temperature measured at East wall rake, TS 72, deg F
ECTHERMO	temperature measured at East ceiling location, TS 72, deg F
WCTHERMO	temperature measured at West ceiling location, TS 72, deg F
EFTHERMO	temperature measured at East Floor location, TS 72, deg F
WFTHERMO	temperature measured at West Floor location, TS 72, deg F
TS	tunnel station

Subscripts

ad	adiabatic wall
bl	boundary layer
e	edge
t	stagnation condition
w	wall
∞	free stream conditions
ref	free stream conditions

Introduction

The NASA Langley Transonic Dynamics Tunnel (TDT) is a continuous-flow, closed circuit, slotted-throat wind tunnel that has a test section that is 16-feet square with filleted corners. This wind tunnel was originally constructed as a 19-foot diameter subsonic pressure tunnel in 1938 (ref.1). During the 1950s, the tunnel was converted to a transonic tunnel using air or a heavy gas, dichlorodifluoromethane (R-12, Freon-12), for aeroelastic testing (ref. 2). Environmental concerns in the late 1980s regarding the use of R-12 (a chloroflourocarbon or CFC) as a test gas led to the conversion of the tunnel to a more environmentally acceptable refrigerant 1,1,1,2-tetraflouroethane (R-134a, a hydrofluorocarbon or HFC). The use of the heavy gas improves the simulation accuracy of flexible vehicles for aeroelastic model design. This facility was described in an internal Report (Aeroelasticity Branch Staff: *The Langley Transonic Dynamics Tunnel*. LWP-799, Sep. 1969). The TDT conversion was completed in 1997 and is described in references 3-4. Wind tunnel characterization and calibration tests were performed in 1998 after the conversion was complete.

The calibration tests for the TDT included measurements to evaluate performance, flow quality, and overall tunnel characteristics. Calibration results for the TDT are presented in references 5-9. Similar calibration tests for some other wind tunnels are given in references 10-14. One portion of the calibration effort was to measure the boundary layer on the walls of the TDT test section. Knowledge of the wall boundary layer thickness and other parameters is particularly desirable for use as boundary conditions for wall-mounted models. Here, the models may require special treatment such as standoffs from the wall or splitter plate to prevent the wall flow field from distorting the aerodynamic characteristics. For the TDT, models are sometimes mounted to a wall, and at other times on the floor as well as mounting on the centerline with a sting or cables. Furthermore in a slotted-wall wind tunnel such as the TDT, the boundary layer can be quite complex due to the flow through the slots. Measurements of the wall boundary layers were made with six rakes, one on each wall and two each on the floor and ceiling at points centered between the slots. Measurements were made for a wide range of test conditions, at three locations along the

tunnel, and included the effects of wall temperature. A semi-automated procedure for online evaluation of the results was developed and used during the test.

This report documents the results for the boundary layer measurements for the tunnel without a model in the test section. Configuration variables included open and closed east sidewall wall slots, air and R-134a test media, reentry flap settings, and stagnation pressures over the full range of tunnel operation.

Wind Tunnel

The TDT is a continuous-flow transonic wind tunnel that has many features that make it suitable for aeroelastic testing. The facility is capable of attaining Mach numbers between near zero to 1.2 using either air or R-134a as a test medium. Stagnation pressures from 50 psf to atmospheric pressure are possible and dynamic pressures up to 550 psf are possible using R-134a as a test medium.

An aerial photograph of the TDT is shown in figure 1. Figures 2 and 3 provide drawings of the layout of the TDT. The major components of the TDT include a steel pressure shell, settling chamber, contraction section, slotted test section with plenum chamber, diffuser section, electric drive system with 47-blade fan, and a high-volume gas handling system for heavy gas operations. The whole tunnel encloses a volume of about a million cubic feet. The test section is 16 ft-by-16 ft with corner fillets, making the cross-sectional area approximately 248 ft^2. It is surrounded by a 60 ft diameter plenum chamber and has three slots in both the ceiling and the floor and two slots on each of the walls to provide adequate area for flow expansion and therefore enable transonic testing. The shape of the slots is designed to provide a nearly gradient free region of flow at transonic speeds in the vicinity of a model.

The test chamber, which can be isolated from the rest of the tunnel using the butterfly and gate valves, shown in figure 2, is composed of the 16-foot square test section and the 60-foot diameter plenum chamber that surrounds it. The flow is powered by a 30,000 hp fan drive motor and enhanced by the reentry flap settings and remotely controlled pre-rotation vanes. The pre-rotation vanes are located directly upstream of the fan blades as shown in figure 2 and are remotely adjustable. The vanes only pivot about their spanwise axes to change the angle of flow impinging on the fan blades. Smaller pre-rotation vane angles are needed to attain higher speeds but greater angles provide better operating efficiency. In standard operations, the pre-rotation vanes are only rotated at the upper limits of the drive motor rotational speed when additional velocity is required. Tunnel cooling is provided at the turning vanes downstream of the motor to limit temperature to a maximum of approximately 130 ^oF. The tunnel is equipped with two screens, one a model debris catch screen upstream of the pre-rotation vanes and the other a flow-smoothing screen near the downstream tip of the fan motor nacelle.

During operations above M=0.85, double-hinged re-entry flaps in the floor and ceiling are progressively opened to allow flow that exits the test section through the transonic slots to re-enter the main flow in the diffuser section. A down-stream view, showing the tunnel flow re-entry flaps outlined, is presented in figure 4. This figure also shows the slots located on the walls and ceiling of the test section (the floor slots are covered in this photograph and are not visible). A schematic of the reentry flap operation and the schedule of the flaps are shown in figure 5. A view of the sidewall slots is shown in figure 6.

An early description of the TDT test section geometry is given in an internal report (Aeroelasticity Branch Staff: *The Langley Transonic Dynamics Tunnel*. LWP-799, Sept. 1969).

Description and Location of Rakes

The six boundary layer rakes were mounted as shown in figure 7. One was mounted on the center of each sidewall and the other four were centered between the slots on the floor and ceiling. These were located nominally at Tunnel Stations 62, 72, or 75 as sketched in figure 8. Detailed locations at the various tunnel stations are given in table 1.

The rakes were of conventional design for wind tunnel measurements. A photograph of a typical rake is shown in figure 9 with the detailed dimensions given by the drawing in figure 10. The length of the rakes was 12.5 inches. The "root" of the rakes was flush with the wall or ceiling or floor. The tubes were clustered more closely near the root and were of smaller diameter near the root. The design location and tube diameters are given in table 2. The corresponding design and measured tube locations for each rake are presented in table 3. The design and measured locations correspond quite closely.

Instrumentation and Data Collection

The instrumentation for the test consisted of the normal flow measurement instrumentation for total pressure, static pressure, total temperature, and static temperature for defining the wind tunnel test conditions. In addition wind tunnel temperature measurements were made with thermocouples near each rake location at tunnel station 72. The thermocouples were not moved to other tunnel stations with the rakes, but used in place near tunnel station 72.

The tubes for the rakes were connected with flexible tubing to commercial quick disconnects which facilitated movement of the rakes without reconnecting the flexible tubes. These tubes from the rakes were then connected to electronically-scanned pressure (ESP) modules. The digital data for the rake pressures from the ESP modules were transmitted to a data station, and recorded electronically. These data were processed with the tunnel data system (ref. 15-16) and displayed in the test section and printed.

Calculation of Boundary Layer Parameters

Boundary layer parameters (ref. 17) were calculated for each rake from the total pressures measured with the rake tubes using standard definitions of the displacement thickness, δ^*, and the momentum thickness, θ, which are

$$\delta^* = \int_0^\infty \left(1 - \frac{\rho V}{\rho_e V_e}\right) dy \qquad (1)$$

and,

$$\theta = \int_0^\infty \frac{\rho V}{\rho_e V_e}\left(1 - \frac{V}{V_e}\right) dy \qquad (2)$$

where distance, y, is measured from the root of the rake, density $\rho = \rho(y)$ and velocity $V = V(y)$, and the subscript "e" indicates the edge of the boundary layer. The upper limit of the integral is also at the edge of the boundary layer in practice since the integrand goes to zero in the freestream. The shape factor is calculated from

$$H = \frac{\delta^*}{\theta} \tag{3}$$

The boundary layer thickness, δ, is determined as the position where V is 0.995 V_e, since V asymptotically approaches V_e. The integrals in equations 1 and 2 are straightforward to perform when given ρ and V. In this case they have been evaluated with a trapezoidal rule of integration for unequal spacing and with V = 0, the no slip boundary condition, applied at the wall.

Two methods for evaluating ρ and V have been used. The first one considered constant stagnation temperature throughout the boundary layer, and the other varied the stagnation temperature such that the wall temperature matches the measured value.

Calculation with Constant Boundary Layer Stagnation Temperature

From the basic wind tunnel instrumentation, the stagnation pressure, P_{t_∞}, static pressure, P_∞, stagnation temperature, T_o, and gas purity, x_R are determined. With these parameters, the wind tunnel flow parameters are calculated using the program developed for the mixture of R-134a and air treated as a real gas (ref. 18). Thus, freestream values of Mach number, M_∞, velocity, V_∞, dynamic pressure, q_∞, static temperature, T_∞, density, ρ_∞, the ratio of specific heats for the mixture, γ_∞, Reynolds number, R_n, and Prandtl number P_r are calculated by the wind tunnel parameter program. The conventional constant static pressure assumption for an attached boundary layer is applied throughout the boundary layer, thus $p_i = p_\infty$ for each tube in the rakes, where "i" refers to the number of the tube. If, in addition, the boundary layer is considered isoenergetic, T_o is constant and applicable to each tube. With the measured value of stagnation pressure for each tube, P_{t_i}, the values of P_{t_i}, p_∞, T_o, and x_R are available to calculate the local density and velocity for equations 1 and 2 from the wind tunnel parameters program.

Calculation Including Wall Temperature

The actual wall temperature in the wind tunnel may be affected by several factors in addition to the flow. The test section walls are connected to the tunnel shell that can act as a heat sink and is affected by atmospheric temperature and possibly other factors. For adiabatic wall boundary layers Schlichting (ref. 17, pp 332-339) gives the boundary layer temperature profile as

$$\frac{T_{bl}}{T_\infty} = 1 + r_\infty \left(\frac{\gamma_\infty - 1}{2}\right) M_\infty^2 \left[1 - \left(\frac{V}{V_\infty}\right)^2\right] + \left(\frac{T_w - T_{ad}}{T_\infty}\right)\left[1 - \frac{V}{V_\infty}\right] \tag{4}$$

Here,

$$\frac{T_{ad}}{T_\infty} = 1 + r_\infty \left(\frac{\gamma_\infty - 1}{2}\right) M_\infty^2 \tag{5}$$

is the adiabatic wall temperature ratio and the recovery factor is given by (ref. 17, pp 712-724)

$$r_\infty = \sqrt[3]{P_{r,\infty}} \tag{6}$$

Again, with measured values of H_∞, p_∞, T_o, x_R from the wind tunnel instrumentation, the wind tunnel parameter program for the mixture of air and R-134a gives freestream values M_∞, V_∞, q_∞, T_∞, ρ_∞, γ_∞, R_n, P_r, and also static temperature T_∞. In this case, T_w = T at the wall which is measured at each rake location. Given the measured value of P_{t_i} for each tube, Equation 4 is iteratively solved to determine the local temperature and velocity in the boundary layer. Equation 4 can be rewritten as

$$T = 1 + A(1 - u^2) + B(1 - u) \tag{7}$$

where

$$T = T_{bl} \Big/ T_\infty, \quad u = V \Big/ V_\infty, \quad A = r_\infty \left(\frac{\gamma_\infty - 1}{2} \right) M_\infty^2, \quad and \quad B = \frac{T_w - T_{ad}}{T_\infty} \tag{8}$$

Note that for a given test condition A is a constant for all rakes. However, B contains the variable wall temperature T_w. T_w is assumed constant for each rake and test condition by neglecting the small variations in r and γ through the boundary layer, which is consistent with the assumptions used in deriving equation 4.

An interval half-stepping method is used to determine T and is described as follows. Let T_{bl} represent the result of equation 4, and T_{tp} the corresponding value from the tunnel parameter program (ref. 18). Then, T_o must be iteratively solved through the boundary layer, consistent with u, to satisfy

$$\Delta T = T_{tp} - T_{bl} = 0 \tag{9}$$

The iteration is performed by

$$T_o^{m+1} = T_o^m - h_I \, \Delta T \frac{dT_o^m}{dT_{tp}} \tag{10}$$

where h_I is the incremental factor for the iteration (0.5 for half interval iteration). In equation 10, $\frac{dT_o^m}{dT_{tp}}$ is evaluated by differences, where T_o is incremented by δ_T and is evaluated using the tunnel parameter program (ref. 18). The value of ΔT is set to 5^o and T is converged to 0.5^o in the program.

Power Law Fit of Boundary Layer Velocity Profile

Turbulent boundary layers at large Reynolds numbers can in many cases be approximated with a fractional power law fit (refs. 17, 19 and LWP-799 of Sept. 1969) of the type

$$V = C y^{1/N} \tag{11}$$

where N is not necessarily an integer and can be on the order of 7 for air. For a boundary layer rake, V is determined for each tube i, with i = 1, m. The fit is calculated as shown in Equations 12-15.

$$\left(\frac{V}{V_e}\right)=\left(\frac{y}{\delta}\right)^{\frac{1}{N}} \tag{12}$$

$$\ln\left(\frac{V}{V_e}\right)=\frac{1}{N}\ln\left(\frac{y}{\delta}\right)=\frac{1}{N}\left[\ln(y)-\ln(\delta)\right] \tag{13}$$

$$\ln(y)=\ln(\delta)+N\ln\left(\frac{V}{V_{ref}}\right) \tag{14}$$

or

$$Y=A+Bx \tag{15}$$

Using a least squares fit of the data one obtains A and B from which the boundary layer thickness and N can be calculated directly.

Since $V_e = C\delta^{1/N}$, the constant C is defined by equation 16

$$C=\frac{V_e}{\delta^{1/N}} \tag{16}$$

For the boundary layer profile, the edge velocity was calculated as 0.995 times the average of the points outside the boundary layer. The range of points used was specified interactively. If the boundary layer was thick enough that there weren't points on the rake to be averaged, then the tunnel velocity was used.

Trapezoidal Rule for Boundary Layer Integrals

Integration of integrals of equations 1 and 2 is performed by an unequispaced trapezoidal rule which is straightforward. For these cases, the boundary condition of V = 0.0 at the wall is applied. The form implemented in the program is given here.

$$S=\tfrac{1}{2}\left[(y_1-y_0)f_0+(y_n-y_{n-1})f_n+\sum_{i=1}^{n-1}(y_{i+1}-y_{i-1})f_i\right] \tag{17}$$

where f_i represents the integrand of equation 1 or 2 evaluated for the rake tube at $y = y_i$, the subscript 0 for conditions at the wall, and n is the number of tubes in the boundary layer. For δ^*, $f_0 = 1$ as $V = 0$ at $y = y_0 = 0$, giving

$$\delta^*=\tfrac{1}{2}\left[y_0+(y_n-y_{n-1})f_n+\sum_{i=1}^{n-1}(y_{i+1}-y_{i-1})f_i\right] \tag{18}$$

Formally $f_n = 0$ at the edge of the boundary layer. Similarly, for θ, $f_0 = 0$ at the wall and formally $f_n = 0$ at the edge of the boundary layer also. The summation is then,

$$\theta = \tfrac{1}{2}\left[(y_n - y_{n-1}) f_n + \sum_{i=1}^{n-1} (y_{i+1} - y_{i-1}) f_i \right] \tag{19}$$

These sums are generated in a subroutine with V_i , ρ_i, and y_i as input arrays.

Implementation of Boundary Layer Calculations

The above procedures have been implemented in a series of interactive programs using Matlab® that permitted display and evaluation of the elements of the analysis and displaying of the results while online as shown in figure 11. First, the measured pressures, H_i, are displayed versus rake tube location for each rake. The mean pressures, maximum values, and minimum values are displayed for the measured results based on 5 seconds of data acquired at 500 samples/second. These same values are also tabulated along with root-mean-square (rms) values in a spread-sheet and printed. The calculated mean velocities, V_i, and densities, ρ_i, are plotted in similar fashion.

In addition, the velocities, V_i, are plotted against the tube location, y, in both linear and log-log form as shown in figure 12. From these figures, the indices of any bad tubes were selected. There is a change in slope between the boundary layer and the freestream. The index of the rake closest to the boundary layer edge was manually chosen based on visual inspection of these plots, shown in figure 12. The index of the starting point of the freestream was also manually selected. The freestream value of the velocity was calculated as an average of the outer measurements. If there were no outer measurements due to the thickness of the boundary layer exceeding the length of the rake, the tunnel free-stream value was chosen. The boundary layer thickness was then calculated from equations 14-15.

Evaluating the integrals given by equations 1 and 2 by the summations indicated by equations 18 and 19 yielded δ^* and θ. The plots of V_i are then displayed normalized by V_e, and plotted against the tube location y_i as normalized by the boundary layer thickness δ with the fitted curve of equation 11 plotted along with the data. Numerical values of δ, δ^*, and θ are also printed on the plot and indicated as vertical lines (fig. 12).

Measurement Program

Configuration variables included open and closed east sidewall wall slots, air and R-134a test media, reentry flap settings, and stagnation pressures over the full range of tunnel operation. Figures 13a and 13b show the TDT operating boundaries as a function of Mach number and dynamic pressure for air and R-134a. Superimposed on these figures are the open-slot test conditions of the points which are presented in this paper. A detailed presentation of the test conditions and configurations for each test point is given in table 4.

Except for the very low pressure conditions, the measurement program encompassed most of the operating conditions of the TDT with the rakes located at station 72 and for the slots open. A somewhat reduced set of conditions were explored for the other configurations.

Results and Discussion

Presentation of Data

The results are generally given in the form of plots of values of boundary layer parameters δ, δ^*, and θ, and the velocity profile coefficients C and N versus Mach number. The results determined without considering wall temperature are presented for the various configurations in the figures as shown in the following chart.

Chart of Figures of Boundary Layer Results And Comparisons

Figures	Test Media	Slots	Flap Settings	$P_{t\infty}$ (psf)	Tunnel Station
15	Air	All slots open	standard	varies	72
16	Air	East wall slots closed	standard	varies	72
17	R-134a	All slots open	standard	varies	72
18	R-134a	East wall slots closed	standard	varies	72
19	Air	All slots open	varies	400 psf	72
20	Air	East wall slots closed	varies	400 psf	72
21	R-134a	varies	standard	400 psf	72
22	R-134a	varies	standard	700 psf	72
23	R-134a	varies	standard	1000 psf	72
24	R-134a	varies	standard	1800 psf	72
25	R-134a	East wall slots closed	standard	700 psf	varies
26	R-134a	East wall slots closed	standard	1000 psf	varies
27	R-134a	East wall slots closed	standard	1800 psf	varies
28	air	All slots open	standard	400 psf	72
29	air	East wall slots closed	standard	varies	72
30	R-134a	All slots open	standard	varies	72
31	R-134a	East wall slots closed	standard	varies	72

The measured wall, static, and stagnation temperatures are presented as a function of adiabatic wall temperature in figure 32. Boundary layer results using the wall temperature measurements are compared with those using adiabatic wall conditions in figure 33.

Overall Trends

There are a large number of results for the several configurations presented in this report. The results will not be discussed in detail, but a few overall trends will be presented.

In figure 15, the boundary layer results at tunnel station 72 are given versus Mach number with air as the test medium, standard flap settings, and with the east wall slots open. The east wall boundary layer is significantly thicker than those for the west wall, ceiling, and floor. It is also significantly thicker than values given in reference TDT paper LWP-799, Sept. 1969. There is also significant rake-to-rake variation in the boundary layer thickness. The following sketch shows the distribution of boundary layer thickness, δ, around the tunnel for Mach 0.8, q=141 psf, Tab Pt=1020.

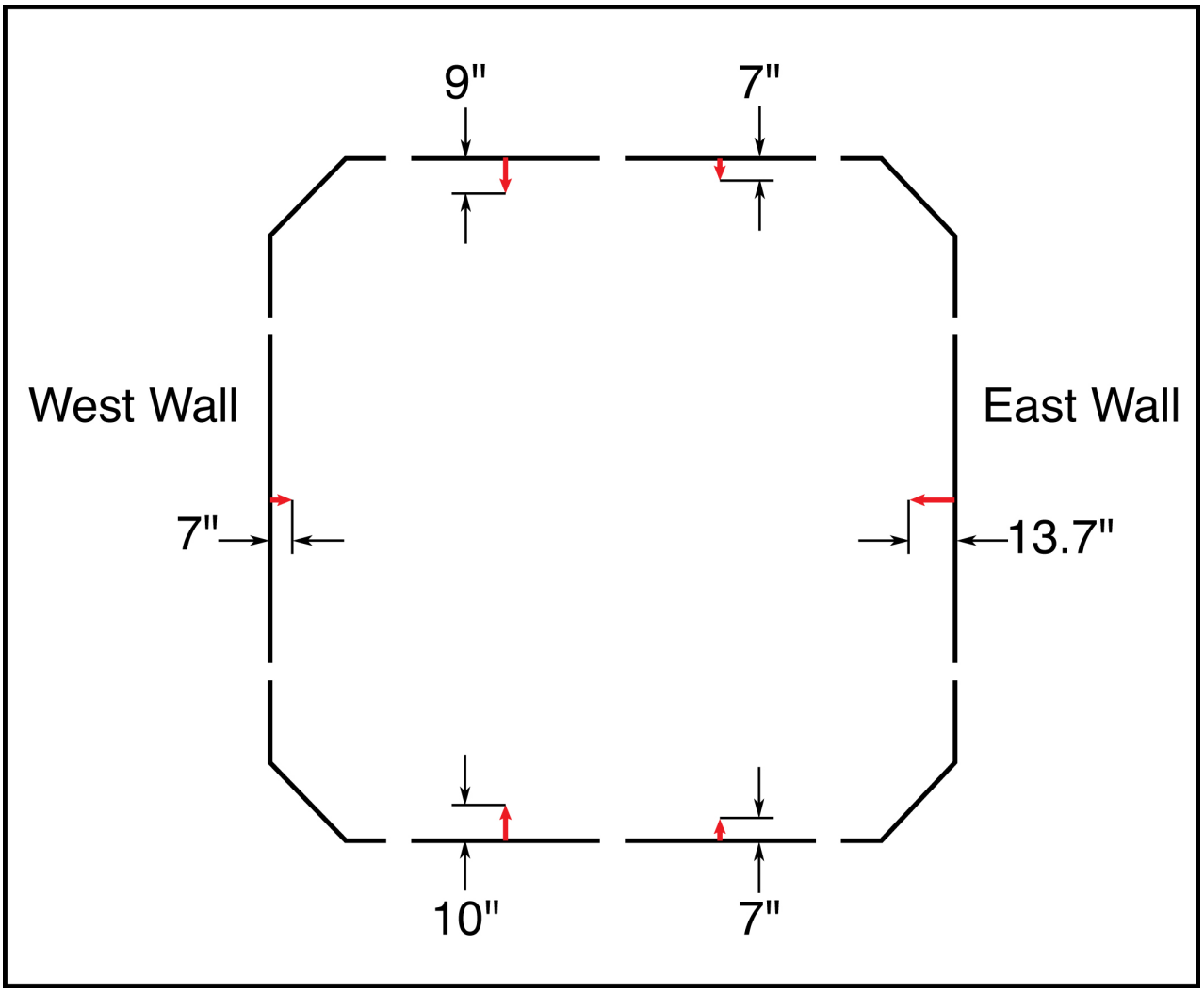

Generally the east wall boundary layer is thickest, east floor and ceiling thin, west wall thin, and west floor and ceiling thicker. However these are only one or two points on each wall and caution should be exercised in drawing general conclusions about the boundary layer properties between the measurements. The flow about the slots can be very complex with associated changes in the boundary layer near the slots. There is a small decrease in thickness with Mach number that is more apparent at supersonic Mach numbers. The boundary layer thickness is also somewhat reduced for the higher stagnation pressures. The corresponding data with the east wall slots closed show little influence on the boundary layer properties of slots-open or slots-closed configurations (figure 16). The value of N in the exponential fit is near 9 as expected from reference 17 for air.

The results obtained using R-134a as a test medium are presented in figures 17-18. The magnitudes and trends are quite similar to those in air. The values of N for R-134a are somewhat higher than those for air.

The effects of varying the reentry flap position on the boundary layer parameters in air is given in figure 19 with all slots open and in figure 20 with the east wall slots closed. Although there are some detailed differences, overall there is not a large effect on boundary layer properties of flap setting.

The direct comparison of the boundary layer parameters with the east wall slots open and closed is given

in figures 21-24. The effect on the boundary layer parameters of closing the wall slots is not large even for the east wall rake location.

Comparisons of the boundary layer parameters measured at the three streamwise locations along the tunnel with the east wall slots closed are shown in figures 25-27. Generally the results indicate growth of the boundary layer from tunnel station 62 to tunnel stations 72. However the results for station 75 vary in relation to station 72. In the case of the east wall rake, there is a reduction in the boundary layer thickness from station 72 to station 75. Apparently this aft location may be influenced by the proximity of the flap and diffuser.

Boundary layer parameters for all six rakes are compared directly or summarized for various tunnel configurations in figures 28-31.

The measured wall temperatures at the rake locations and tunnel static and stagnation temperature are shown compared with adiabatic wall temperatures in figure 32. The east floor temperature gage failed and thus the east floor temperatures are not available. The wall temperatures depend somewhat on tunnel operations since the soak time from ambient conditions may affect the wall temperatures. Differences of up to about 20 degrees F are evident in figure 32. Corresponding boundary layer parameters including wall temperature and using adiabatic wall temperatures are given in figure 33. The effect of the wall temperature differing from adiabatic appears to be quite small.

Concluding Remarks

Tunnel wall boundary layer measurements were made in the NASA Langley Transonic Dynamics Tunnel during extensive calibration activities following the facility conversion from a Freon-12 heavy-gas test medium to R-134a. Six boundary-layer rakes were mounted on the wind-tunnel walls, ceiling, and floor. Measurements were made over the range of the tunnel operation envelope in both heavy gas and air and without a model in the test section at three tunnel stations. Configuration variables included open and closed east sidewall wall slots, air and R-134a test media, reentry flap settings, and stagnation pressures over the full range of tunnel operation. Resulting data were reduced to traditional boundary layer thickness parameters using a power law representation of the velocity profile.

The boundary layer thickness varied considerably for the six rakes. The boundary layer thickness for the east wall was considerably larger than those for the others. This result for the east wall rake was also larger than previously reported. There generally was some reduction in boundary layer thickness at supersonic Mach numbers, but the effects of stagnation pressure, and test medium on the boundary layer properties were not extensive.

References

1. *Notes on the Proceedings of the 1939 Meeting of the Aircraft Industry with the National Advisory Committee for Aeronautics*. Journal of the Aeronautical Sciences, Vol. 6, No. 7, May 1939, pp 299-301.

2. Moxey, R. L.: *Transonic Dynamics Wind Tunnel*. Compressed Air Magazine, Vol. 68, No. 10, Oct. 1963, pp 8-13.

3. Cole, Stanley C., and Rivera, Jose, A., Jr.: *The New Heavy Gas Testing Capability in the NASA Langley Transonic Dynamics Tunnel.* Paper No. 4, Presented at the Royal Aeronautical Society Wind Tunnels and Wind Tunnel Test Techniques Forum, Churchill College, Cambridge, Cambridge, UK, April 14-16, 1997.

4. Corliss, James M.; and Cole, Stanley R.: *Heavy Gas Conversion of the NASA Langley Transonic Dynamics Tunnel.* AIAA Paper 98-2710, June 1998.

5. Florance, James R.; and Rivera, Jose' A., Jr.: *Sidewall Mach Number Distributions Obtained During the NASA Langley Transonic Dynamics Tunnel Calibration*. NASA/TM-2001-211019, June, 2001.

6. Wieseman, Carol D.; and Sleeper, Robert K.: *Measurements of Flow Turbulence in the NASA Langley Transonic Dynamics Tunnel*. NASA/TM-2005-213529, Feb. 2005.

7. Schuster, David M.: *Aerodynamic Measurements on a Large Splitter Plate for the NASA Transonic Dynamics Tunnel*. NASA/TM-2001-210828, March 2001.

8. Yeager, William T., Wilbur, Matthew L., Rivera, Jose A., Mirick, Paul. *Flow Angularity Measurements in the NASA-Langley Transonic Dynamics Tunnel*, NASA TM-2005-213946, .Dec. 2005.

9. Piatak, David J., *Survey of Primary Flow Measurement Parameters at the NASA Langley Transonic Dynamics Tunnel,* NASA/TM-2003-212413, June 2003.

10. Jackson, Charlie E.; Corlett, William A.; and Monta, William J.: *Description and Calibration of the Langley Unitary Plan Wind Tunnel.* NASA TP-1905, Nov. 1981.

11. Capone, Francis J.; Bangert, Linda S.; Asbury, Scott C.; Mills, Charles T. L.; and Bare, Ann T.: *The NASA Langley 16-Foot Transonic Tunnel - Historical Overview, Facility Description, Calibration, Flow Characteristics, and Test Capabilities*. NASA TP-3521, Sept. 1995.

12. Brooks, Cuyler W., Jr.; Harris, Charles D.; and Reagon, Particia G.: *The NASA Langley 8-Foot Transonic Pressure Tunnel Calibration.* NASA TP- 3437, August 1994.

13. Gentry, Garl L.; Quinto P. Frank; Gatlin Gregory M.; and Applin, Zachary T.: *The Langley 14- by 22-Foot Subsonic Tunnel: Description, Flow Characteristics, and Guide for Users.* NASA TP-3008, Sept. 1990.

14. Harvey, William D.; Stainback, P. Calvin; and Owen, F. Kevin: *Evaluation of Flow Quality in Two Large NASA Wind Tunnels at Transonic Speeds.* NASA TP-1737, Dec. 1980.

15. Wieseman, Carol D.; and Hoadley, Sherwood, T.: *Versatile Software Package for Near Real-Time Analysis of Experimental Data.* AIAA Paper 98-2722, June 1998.

16. Bryant, C.; and Hoadley , S. T.: *Open Architecture Dynamic Data System at Langley's Transonic Dynamics Tunnel.* AAIA Paper 98-0343, Jan. 1998.

17. Schlichting, Hermann: *Boundary Layer Theory*. Translated by J. Kestin. McGraw Hill Book Co., New York, NY, 7th edition, c.1979.

18. Kvaternik, Raymond G.: *Computer Programs for Calculating the Isentropic Flow Properties for Mixtures of R-134a and Air.* NASA/TM-2000-210622, Nov. 2000.

19. Allen, Jerry M.: *A Simple Method of Calculating Power-Law Velocity Profile Exponents from Experimental Data*. NASA TM X-72000, Oct. 1974.

Table 1. Boundary Layer Rake Locations in the Wind Tunnel

	Rake	Tunnel Station	Height from Tunnel Centerline	Horizontal Distance from tunnel centerline
Forward Location	East Wall	62’ 0”	3” Above Centerline	Wall
	East Ceiling	62’ 0”	Ceiling	Centered Between Slots
	West Ceiling	62’ 0”	Ceiling	Centered Between Slots
	West Wall	62’ 0”	14” Below Centerline	Wall
	West Floor	62’ 0”	Floor	Centered Between Slots
	East Floor	62’ 0”	Floor	Centered Between Slots
Center Location	East Wall	71’ 7”	Centered	Wall
	East Ceiling	72’ 0”	Ceiling	Centered Between Slots
	West Ceiling	72’ 0”	Ceiling	Centered Between Slots
	West Wall	72’ 0”	Centered	Wall
	West Floor	72’ 0”	Floor	Centered Between Slots
	East Floor	72’ 0”	Floor	Centered Between Slots
Aft Location	East Wall	75’ 0”	3” Above Centerline	Wall
	East Ceiling	75’ 0”	Ceiling	Centered Between Slots
	West Ceiling	75’ 0”	Ceiling	Centered Between Slots
	West Wall	75’ 0”	3” Below Centerline	Wall
	West Floor	75’ 0”	Floor	Centered Between Slots
	East Floor	75’ 0”	Floor	Centered Between Slots

Table 2. Rake Tube Design Locations and Diameters

Tube number	Design y-Location, in	Outside Tube Diameter, in	Inside Tube Diameter, in
1	0.125	0.060	0.040
2	0.250	0.060	0.040
3	0.500	0.060	0.040
4	0.750	0.060	0.040
5	1.000	0.060	0.040
6	1.250	0.090	0.060
7	1.500	0.090	0.060
8	1.750	0.090	0.060
9	2.000	0.090	0.060
10	2.375	0.090	0.060
11	2.750	0.090	0.060
12	3.125	0.090	0.060
13	3.500	0.090	0.060
14	3.875	0.090	0.060
15	4.250	0.090	0.060
16	4.625	0.090	0.060
17	5.000	0.090	0.060
18	5.500	0.090	0.060
19	6.000	0.090	0.060
20	6.500	0.090	0.060
21	7.000	0.090	0.060
22	7.500	0.090	0.060
23	8.000	0.090	0.060
24	8.750	0.090	0.060
25	9.500	0.090	0.060
26	10.250	0.090	0.060
27	11.000	0.090	0.060
28	12.000	0.090	0.060

Table 3. Design and Measured Tube Locations for Each Rake, inches

Tube number	Design	EW (East Wall)	EC (East Ceiling)	WC (West Ceiling)	WW (West Wall)	WF (West Floor)	EF (East Floor)
1	0.125	0.125	0.124	0.126	0.126	0.127	0.129
2	0.250	0.255	0.255	0.255	0.252	0.255	0.252
3	0.500	0.501	0.503	0.498	0.504	0.502	0.503
4	0.750	0.750	0.751	0.750	0.755	0.752	0.754
5	1.000	0.999	1.004	1.004	1.000	1.005	1.003
6	1.250	1.253	1.254	1.252	1.252	1.252	1.251
7	1.500	1.496	1.505	1.502	1.499	1.501	1.504
8	1.750	1.750	1.754	1.748	1.749	1.745	1.748
9	2.000	2.001	2.001	1.997	2.000	1.999	2.000
10	2.375	2.371	2.371	2.376	2.374	2.370	2.375
11	2.750	2.751	2.751	2.753	2.759	2.754	2.751
12	3.125	3.123	3.123	3.127	3.129	3.122	3.128
13	3.500	3.496	3.505	3.497	3.500	3.499	3.496
14	3.875	3.877	3.879	3.874	3.873	3.872	3.878
15	4.250	4.255	4.250	4.245	4.250	4.250	4.254
16	4.625	4.620	4.628	4.630	4.626	4.630	4.624
17	5.000	4.999	4.997	5.001	5.002	4.996	5.003
18	5.500	5.497	5.505	5.499	5.502	5.501	5.504
19	6.000	5.999	6.004	6.002	6.004	5.995	5.995
20	6.500	6.500	6.503	6.498	6.498	6.505	6.502
21	7.000	6.998	6.999	7.000	6.999	7.003	7.003
22	7.500	7.503	7.505	7.504	7.533	7.503	7.502
23	8.000	8.002	8.005	7.998	7.999	8.002	8.000
24	8.750	8.750	8.754	8.752	8.746	8.748	8.751
25	9.500	9.501	9.499	9.502	9.495	9.499	9.501
26	10.250	10.246	10.253	10.245	10.248	10.247	10.249
27	11.000	11.001	11.005	11.004	11.005	10.996	10.998
28	12.000	11.995	12.005	11.999	12.005	11.996	11.998

Table 4. Test Conditions

Run	Tab Pt	WOZP	M	q psf	$P_{t\infty}$ psf	P_{∞} psf	T_o °F	γ_{∞}	a ft/sec	Rn*10^{-6}	FLAP Setting	EW Slots	Rakes location
44	898	887	1.17	106.38	258.6	110.7	122.3	1.4	1047.3	0.513	F4	Closed	TS 72
44	900	887	1.10	100.00	252.3	118.5	118.3	1.4	1057.7	0.501	F4	Closed	TS 72
44	902	887	1.05	96.34	250.5	124.6	117.2	1.4	1065.4	0.495	F4	Closed	TS 72
44	904	887	1.00	91.66	247.8	130.9	116.0	1.4	1073.4	0.486	F3	Closed	TS 72
44	906	887	0.95	86.89	245.7	137.4	112.1	1.4	1078.6	0.478	F3	Closed	TS 72
44	908	887	0.90	82.00	244.5	144.6	111.2	1.4	1086.3	0.468	F3	Closed	TS 72
44	910	887	0.80	70.36	238.9	156.6	107.1	1.4	1098.4	0.439	F1	Closed	TS 72
44	912	887	0.50	33.02	222.6	187.5	98.0	1.4	1129.4	0.306	F1	Closed	TS 72
45	925	919	0.25	16.46	394.9	378.2	91.3	1.4	1143.3	0.298	F1	Closed	TS 72
45	926	919	0.50	61.16	414.2	349.1	99.7	1.4	1131.1	0.567	F1	Closed	TS 72
45	927	919	0.60	83.96	425.1	333.3	103.8	1.4	1123.7	0.660	F1	Closed	TS 72
45	930	919	0.70	107.89	439.4	317.9	110.8	1.4	1117.7	0.740	F1	Closed	TS 72
45	931	919	0.75	121.24	447.7	308.5	114.1	1.4	1113.1	0.781	F1	Closed	TS 72
45	932	919	0.80	133.74	455.5	299.0	116.9	1.4	1108.2	0.817	F1	Closed	TS 72
45	933	919	0.80	134.58	457.4	299.9	117.9	1.4	1109.0	0.819	F2	Closed	TS 72
45	935	919	0.85	146.75	465.4	290.2	120.9	1.4	1103.9	0.851	F2	Closed	TS 72
45	936	919	0.90	158.36	473.5	280.6	125.2	1.4	1099.9	0.878	F2	Closed	TS 72
45	937	919	0.50	62.82	425.9	359.0	108.8	1.4	1140.4	0.570	F2	Closed	TS 72
45	938	919	0.50	62.36	425.5	359.2	107.1	1.4	1138.8	0.570	F3	Closed	TS 72
45	939	919	0.80	135.37	462.1	303.9	119.0	1.4	1110.5	0.824	F3	Closed	TS 72
45	940	919	0.90	159.64	477.2	282.8	123.5	1.4	1098.3	0.888	F3	Closed	TS 72
45	941	919	0.95	171.60	486.6	273.0	127.3	1.4	1093.3	0.915	F3	Closed	TS 72
45	942	919	0.97	177.81	491.7	267.6	129.5	1.4	1090.6	0.928	F3	Closed	TS 72
45	943	919	1.00	183.29	496.5	263.0	132.1	1.4	1088.7	0.938	F3	Closed	TS 72
45	944	919	1.02	188.99	501.9	258.3	134.3	1.4	1086.3	0.950	F3	Closed	TS 72
45	945	919	0.50	63.86	433.7	365.8	109.7	1.4	1141.3	0.579	F4	Closed	TS 72
45	946	919	0.80	138.43	471.2	309.2	122.6	1.4	1113.5	0.835	F4	Closed	TS 72
45	947	919	0.90	163.14	487.0	288.2	128.4	1.4	1102.7	0.897	F4	Closed	TS 72
45	948	919	1.00	186.63	504.9	267.0	135.5	1.4	1091.6	0.948	F4	Closed	TS 72
46	955	951	0.25	29.00	686.5	657.1	95.7	1.4	1147.8	0.516	F1	Closed	TS 72
46	956	951	0.50	106.45	721.4	608.1	106.6	1.4	1138.2	0.971	F1	Closed	TS 72
46	957	951	0.60	146.24	742.9	583.1	112.9	1.4	1132.8	1.128	F1	Closed	TS 72
46	958	951	0.70	189.31	766.9	553.4	120.2	1.4	1126.4	1.268	F1	Closed	TS 72
46	959	951	0.75	211.76	782.2	539.1	125.6	1.4	1124.3	1.330	F1	Closed	TS 72
46	961	951	0.25	49.08	1187.0	1137.2	99.6	1.4	1152.0	0.874	F1	Closed	TS 72
46	962	951	0.25	49.39	1185.9	1135.7	100.4	1.4	1152.7	0.875	F2	Closed	TS 72
46	963	951	0.25	49.29	1184.2	1134.2	99.4	1.4	1151.7	0.876	F3	Closed	TS 72
46	964	951	0.25	49.64	1182.5	1132.1	98.3	1.4	1150.5	0.880	F4	Closed	TS 72
46	965	951	0.48	172.01	1243.0	1060.8	109.7	1.4	1143.2	1.612	F4	Closed	TS 72
46	966	951	0.48	174.39	1244.7	1059.9	110.3	1.4	1143.5	1.621	F3	Closed	TS 72
46	967	951	0.49	177.06	1246.2	1058.3	110.6	1.4	1143.3	1.633	F2	Closed	TS 72
46	968	951	0.49	177.74	1247.8	1059.1	111.4	1.4	1144.1	1.634	F1	Closed	TS 72
47	973	970	0.25	88.76	2110.4	2020.2	92.7	1.4	1144.7	1.593	F1	Closed	TS 72
47	974	970	0.25	88.45	2105.0	2015.1	92.2	1.4	1144.2	1.590	F2	Closed	TS 72

Table 4. Test Conditions, cont.

Run	Tab Pt	WOZP	Mach	q psf	$P_{t\infty}$ psf	P_{∞} psf	T_o (deg F)	γ_{∞}	a ft/sec	R_n $*10^{-6}$	FLAP Setting	EW Slots	Rakes location
47	975	970	0.25	88.18	2104.5	2014.9	92.5	1.4	1144.5	1.586	F3	Closed	TS 72
47	976	970	0.25	87.99	2104.7	2015.3	92.3	1.4	1144.3	1.585	F4	Closed	TS 72
47	977	970	0.49	312.20	2178.1	1846.6	106.0	1.4	1138.5	2.895	F4	Closed	TS 72
47	978	970	0.49	311.95	2160.9	1829.5	109.1	1.4	1141.4	2.862	F3	Closed	TS 72
47	979	970	0.50	313.66	2146.2	1812.6	110.2	1.4	1142.1	2.853	F2	Closed	TS 72
47	980	970	0.50	313.03	2135.2	1802.3	111.1	1.4	1142.8	2.837	F1	Closed	TS 72
49	1001	994	1.17	104.44	254.1	109.0	122.6	1.4	1048.0	0.503	F4	Open	TS 72
49	1003	994	1.00	88.82	240.3	127.1	112.5	1.4	1070.3	0.475	F3	Open	TS 72
49	1005	994	0.80	67.34	228.7	149.9	106.2	1.4	1097.6	0.421	F1	Open	TS 72
50	1014	1011	1.00	185.68	502.5	265.8	125.9	1.4	1082.9	0.963	F4	Open	TS 72
50	1016	1011	0.95	176.26	499.0	279.4	127.7	1.4	1093.3	0.938	F4	Open	TS 72
50	1018	1011	0.90	165.51	493.6	291.8	126.8	1.4	1101.0	0.913	F4	Open	TS 72
50	1020	1011	0.80	141.45	480.3	314.7	122.3	1.4	1113.0	0.852	F4	Open	TS 72
50	1023	1011	0.50	65.71	441.4	371.4	105.4	1.4	1136.7	0.598	F4	Open	TS 72
50	1025	1011	1.00	188.44	510.6	270.6	130.1	1.4	1087.0	0.969	F3	Open	TS 72
50	1027	1011	0.95	178.74	506.3	283.7	130.4	1.4	1095.9	0.946	F3	Open	TS 72
50	1029	1011	0.90	167.71	500.8	296.4	129.4	1.4	1103.6	0.920	F3	Open	TS 72
50	1031	1011	0.80	143.10	487.5	320.1	125.1	1.4	1116.0	0.859	F3	Open	TS 72
50	1033	1011	0.50	66.38	448.6	378.0	109.2	1.4	1140.7	0.601	F3	Open	TS 72
50	1036	1011	0.90	167.94	501.2	296.5	126.7	1.4	1101.1	0.927	F2	Open	TS 72
50	1038	1011	0.80	143.42	488.7	321.0	124.5	1.4	1115.5	0.862	F2	Open	TS 72
50	1040	1011	0.50	66.76	450.7	379.7	109.1	1.4	1140.5	0.604	F2	Open	TS 72
50	1043	1011	0.80	143.45	489.2	321.4	122.2	1.4	1113.3	0.867	F1	Open	TS 72
50	1045	1011	0.70	117.72	477.0	344.2	118.3	1.4	1124.6	0.792	F1	Open	TS 72
50	1047	1011	0.50	67.22	453.0	381.4	107.7	1.4	1139.1	0.610	F1	Open	TS 72
51	1062	1059	0.50	107.61	726.3	611.7	101.0	1.4	1132.3	0.992	F1	Open	TS 72
51	1063	1059	0.70	190.22	771.8	557.3	115.6	1.4	1122.0	1.288	F1	Open	TS 72
52	1069	1065	0.49	178.96	1252.6	1062.7	106.4	1.4	1139.0	1.661	F1	Open	TS 72
52	1070	1065	0.49	178.31	1254.3	1065.1	107.1	1.4	1139.8	1.657	F2	Open	TS 72
52	1071	1065	0.48	175.07	1255.4	1069.9	107.4	1.4	1140.7	1.642	F3	Open	TS 72
52	1072	1065	0.48	172.53	1256.8	1074.1	108.7	1.4	1142.5	1.627	F4	Open	TS 72
52	1073	1065	0.48	301.85	2159.0	1839.1	114.8	1.4	1148.0	2.782	F4	Open	TS 72
52	1074	1065	0.49	300.37	2130.6	1812.1	117.1	1.4	1150.1	2.742	F3	Open	TS 72
52	1075	1065	0.49	303.61	2116.6	1794.2	117.9	1.4	1150.4	2.741	F2	Open	TS 72
52	1076	1065	0.49	304.70	2114.2	1790.5	118.7	1.4	1151.0	2.739	F1	Open	TS 72
54	1106	1103	0.30	9.36	195.5	185.9	87.1	1.11	552.2	0.442	F4	Open	TS 72
54	1107	1103	0.50	24.49	202.2	176.1	89.6	1.11	551.2	0.694	F4	Open	TS 72
54	1108	1103	0.60	34.07	207.9	170.6	92.4	1.11	551.0	0.805	F4	Open	TS 72
54	1109	1103	1.05	78.22	231.3	127.5	100.4	1.11	544.5	1.097	F4	Open	TS 72
54	1110	1103	1.10	82.72	236.1	123.4	101.3	1.11	543.7	1.115	F4	Open	TS 72
54	1111	1103	1.19	90.45	245.4	115.4	106.7	1.11	543.4	1.130	F4	Open	TS 72
54	1112	1103	1.00	75.53	233.3	135.8	103.5	1.11	547.4	1.094	F3	Open	TS 72
54	1113	1103	0.95	71.18	231.8	142.3	101.9	1.11	548.0	1.083	F3	Open	TS 72

Table 4. Test Conditions, cont.

Run	Tab Pt	WOZP	Mach	q psf	$P_{t\infty}$ psf	P_{∞} psf	T_o ^oF	γ_{∞}	a ft/sec	R_n $*10^{-6}$	FLAP Setting	EW Slots	Rakes location
54	1114	1103	0.90	66.53	230.2	148.5	100.7	1.11	548.7	1.065	F3	Open	TS 72
54	1115	1103	0.80	56.42	226.1	159.8	98.5	1.11	550.0	1.010	F1	Open	TS 72
54	1116	1103	0.50	25.91	214.5	186.9	94.0	1.11	553.3	0.727	F1	Open	TS 72
55	1125	1122	0.50	87.59	728.6	635.4	90.8	1.11	550.3	2.487	F1	Open	TS 72
55	1126	1122	0.60	121.01	744.2	611.8	93.9	1.11	550.3	2.870	F1	Open	TS 72
55	1127	1122	0.70	157.88	761.7	583.1	97.4	1.11	550.2	3.204	F1	Open	TS 72
55	1128	1122	0.80	194.82	780.6	551.6	101.0	1.11	549.9	3.470	F1	Open	TS 72
55	1129	1122	0.90	232.10	802.6	517.4	104.2	1.11	549.1	3.685	F3	Open	TS 72
55	1130	1122	0.95	249.76	813.8	499.4	106.5	1.11	549.0	3.760	F3	Open	TS 72
59	1174	1171	0.98	262.51	832.5	497.5	115.4	1.11	546.0	3.839	F3	Open	TS 72
59	1175	1171	1.00	270.51	840.6	491.6	120.0	1.11	547.6	3.839	F3	Open	TS 72
59	1176	1171	1.02	280.12	849.0	482.3	121.9	1.11	547.7	3.867	F3	Open	TS 72
59	1178	1171	1.05	290.84	863.9	478.1	126.3	1.11	549.1	3.893	F4	Open	TS 72
59	1179	1171	1.10	307.67	880.5	460.6	130.1	1.11	549.5	3.923	F4	Open	TS 72
62	1219	1212	0.08	3.50	997.6	994.1	100.4	1.11	548.2	0.614	F1	Open	TS 72
62	1220	1212	0.10	5.32	998.5	993.2	100.4	1.11	548.2	0.770	F1	Open	TS 72
62	1221	1212	0.20	21.62	1004.8	983.0	101.7	1.11	548.4	1.512	F1	Open	TS 72
62	1222	1212	0.30	47.90	1015.7	966.7	104.6	1.11	549.2	2.214	F1	Open	TS 72
62	1223	1212	0.50	125.56	1047.2	913.5	107.3	1.11	548.3	3.506	F1	Open	TS 72
62	1224	1212	0.60	173.94	1069.4	878.9	110.6	1.11	548.5	4.049	F1	Open	TS 72
62	1225	1212	0.70	226.09	1094.9	839.0	114.6	1.11	548.7	4.509	F1	Open	TS 72
62	1226	1212	0.80	278.95	1123.5	795.6	119.7	1.11	549.2	4.865	F1	Open	TS 72
62	1227	1212	0.90	334.43	1158.9	747.8	123.6	1.11	553.1	5.118	F3	Open	TS 72
63	1233	1230	0.95	358.01	1172.1	721.7	121.9	1.11	551.2	5.261	F3	Open	TS 72
63	1234	1230	0.98	373.48	1186.9	710.5	125.9	1.11	552.4	5.298	F3	Open	TS 72
63	1235	1230	1.00	385.81	1200.9	703.3	128.3	1.11	552.9	5.340	F3	Open	TS 72
63	1236	1230	1.02	400.15	1214.4	690.7	132.9	1.11	554.3	5.349	F3	Open	TS 72
63	1239	1230	1.05	414.87	1233.6	683.4	137.2	1.11	555.6	5.379	F3	Open	TS 72
63	1241	1230	1.12	445.52	1261.7	647.7	138.3	1.11	554.3	5.470	F3	Open	TS 72
64	1249	1244	0.09	5.50	1371.4	1365.9	107.6	1.11	558.5	0.859	F1	Open	TS 72
64	1251	1244	0.10	7.55	1371.3	1363.7	101.2	1.11	555.4	1.021	F1	Open	TS 72
64	1252	1244	0.20	29.93	1378.2	1348.0	102.0	1.11	555.4	2.029	F1	Open	TS 72
64	1253	1244	0.30	65.80	1390.7	1323.4	102.6	1.11	555.1	2.996	F1	Open	TS 72
65	1259	1256	0.04	1.85	1787.0	1785.2	97.5	1.11	553.7	0.568	F1	Open	TS 72
65	1260	1256	0.09	7.20	1788.0	1780.8	97.6	1.11	553.6	1.206	F1	Open	TS 72
65	1261	1256	0.10	9.79	1788.9	1779.1	97.8	1.11	553.7	1.334	F1	Open	TS 72
65	1262	1256	0.20	38.15	1799.6	1761.1	99.9	1.11	554.4	2.646	F1	Open	TS 72
65	1263	1256	0.30	85.23	1817.7	1730.6	100.4	1.11	553.9	3.915	F1	Open	TS 72
65	1265	1256	0.50	225.74	1877.5	1637.1	105.2	1.11	554.2	6.197	F1	Open	TS 72
65	1266	1256	0.6	311.81	1918.4	1577	108.2	1.11	554.2	7.152	F1	Open	TS 72
65	1267	1256	0.7	409.06	1969.2	1505.8	113.5	1.11	555	7.969	F1	Open	TS 72
65	1268	1256	0.8	504.78	2024.8	1430.9	121.7	1.11	557	8.549	F1	Open	TS 72
65	1269	1256	0.85	556.64	2054.4	1384.1	124.4	1.11	557.1	8.827	F1	Open	TS 72

Table 4. Test Conditions, cont.

Run	Tab Pt	WOZP	Mach	q psf	$P_{t\infty}$ psf	P_{∞} psf	T_o °F	γ_{∞}	a ft/sec	Rn *E-6	FLAP Setting	EW Slots	Rakes location
65	1270	1256	0.5	230.46	1908.8	1663.3	115.3	1.11	559	6.139	F1	Open	TS 72
66	1279	1273	1.2	90	243.2	113	112.5	1.11	543.7	1.105	F4	closed	TS 72
67	1285	1282	0.5	88.08	726.4	632.5	100.9	1.11	550.6	2.455	F1	closed	TS 72
67	1286	1282	0.7	156.93	756.9	579.3	106.5	1.11	550.1	3.147	F1	closed	TS 72
67	1287	1282	0.8	193.97	776.4	548.2	110.7	1.11	550	3.405	F1	closed	TS 72
67	1288	1282	0.9	229.98	797	514.4	112.3	1.11	548.6	3.623	F2	closed	TS 72
67	1289	1282	0.95	249.1	811.2	497.4	115.4	1.11	548.8	3.704	F3	closed	TS 72
67	1290	1282	1	265.17	823.2	481	118.1	1.11	548.8	3.758	F3	closed	TS 72
67	1291	1282	1.05	283.12	840.3	464.7	121.6	1.11	549.1	3.812	F4	closed	TS 72
67	1292	1282	1.1	299.61	856.6	447.7	125.1	1.11	549.3	3.845	F4	closed	TS 72
67	1294	1282	1.2	334.53	903.4	416.5	137.4	1.11	551.9	3.864	F4	closed	TS 72
67	1295	1282	1	271.71	841.1	489.8	124.9	1.11	551.9	3.773	F4	closed	TS 72
67	1296	1282	0.95	254.89	830.1	508.9	122.9	1.11	552.2	3.717	F4	closed	TS 72
67	1297	1282	0.5	90.31	751.1	655	112.3	1.11	555.9	2.455	F4	closed	TS 72
68	1303	1300	0.5	124.61	1038.8	906.1	105.7	1.11	554.3	3.431	F1	Closed	TS 72
68	1304	1300	0.7	223.35	1082	829.3	110.7	1.11	553.5	4.418	F1	Closed	TS 72
68	1305	1300	0.8	276.63	1109.2	783.9	115.1	1.11	553.6	4.783	F1	Closed	TS 72
68	1306	1300	0.9	328.54	1139.9	736.2	119.6	1.11	553.5	5.055	F2	Closed	TS 72
68	1307	1300	0.95	355.39	1160.4	712.9	122.7	1.11	553.7	5.169	F3	Closed	TS 72
68	1308	1300	1	379.61	1178	687.8	125.2	1.11	553.6	5.253	F3	Closed	TS 72
68	1309	1300	1.05	404.46	1202	665.8	129.8	1.11	554.5	5.312	F4	Closed	TS 72
68	1311	1300	1.12	440.4	1240.3	630.6	134.8	1.11	554.6	5.391	F4	Closed	TS 72
68	1312	1300	0.5	129.75	1066.7	928.4	114	1.11	558.1	3.468	F4	Closed	TS 72
70	1336	1331	0.5	229.46	1912.2	1667.8	110	1.11	547.2	6.383	F1	Closed	TS 72
70	1337	1331	0.7	411.24	1998.2	1532.8	116.5	1.11	547.4	8.192	F1	Closed	TS 72
70	1338	1331	0.8	510.05	2054.3	1454.4	121.8	1.11	548.1	8.87	F1	Closed	TS 72
70	1339	1331	0.86	570.78	2092.9	1403.6	126.7	1.11	549.1	9.167	F1	Closed	TS 72
70	1340	1331	0.5	232.06	1935	1687.8	112.7	1.11	548.5	6.408	F2	Closed	TS 72
70	1341	1331	0.5	231.22	1931.2	1685	111.6	1.11	547.9	6.411	F3	Closed	TS 72
70	1342	1331	0.5	231.24	1929.6	1683.3	109.9	1.11	547.1	6.442	F4	Closed	TS 72
70	1345	1331	0.85	557.06	2086.5	1418.2	121.6	1.11	547	9.209	F2	Closed	TS 72
86	1610	1607	0.5	87.3	723.6	630.7	103.9	1.11	556.5	2.389	F1	Closed	TS 62
86	1611	1607	0.7	156.33	753.3	576.3	109	1.11	555.7	3.075	F1	Closed	TS 62
86	1612	1607	0.8	192.89	771.5	544.6	112.1	1.11	555.1	3.331	F1	Closed	TS 62
86	1613	1607	0.9	229.4	792.7	510.7	116	1.11	554.7	3.528	F2	Closed	TS 62
86	1614	1607	0.95	247.99	806	493.4	118.4	1.11	554.5	3.611	F3	Closed	TS 62
86	1615	1607	1	263.45	817.1	477.3	120.3	1.11	556.5	3.645	F3	Closed	TS 62
86	1616	1607	1.05	281.6	834.3	460.7	124.3	1.11	556.9	3.695	F4	Closed	TS 62
86	1617	1607	1.1	297.41	850.3	444.9	128	1.11	557.2	3725	F4	Closed	TS 62
86	1618	1607	1.2	329.99	893.2	415.5	139.7	1.11	559.6	3.743	F4	Closed	TS 62
87	1624	1621	1.05	396.19	1175.1	649.5	123.4	1.11	553.6	5.25	F4	Closed	TS 62

Table 4. Test Conditions, concluded.

Run	Tab Pt	WOZP	Mach	q psf	$P_{t\infty}$ psf	P_{∞} psf	T_o °F	γ_{∞}	a ft/sec	Rn $*10^{-6}$	FLAP Setting	EW Slots	Rakes location
87	1625	1621	1.13	431.53	1213.3	622	131.8	1.11	555.7	5.288	F4	Closed	TS 62
87	1626	1621	1	376.65	1167.7	681.2	126.3	1.11	556.3	5.162	F3	Closed	TS 62
87	1627	1621	0.95	353.98	1155.4	709.7	125.1	1.11	557	5.087	F3	Closed	TS 62
87	1628	1621	0.9	329.82	1141.4	735.8	124.7	1.11	558.1	4.97	F2	Closed	TS 62
87	1629	1621	0.8	279.1	1115.1	786.5	122.2	1.11	559.1	4.696	F1	Closed	TS 62
87	1630	1621	0.7	225.9	1090	834.3	118.7	1.11	559.5	4.34	F1	Closed	TS 62
87	1631	1621	0.5	126.88	1047	911.8	112.6	1.11	559.8	3.392	F1	Closed	TS 62
88	1637	1635	0.5	226.24	1898.8	1658	118.4	1.11	557	6.091	F1	Closed	TS 62
88	1638	1635	0.5	227.33	1907.6	1665.6	120.9	1.11	558.2	6.073	F2	Closed	TS 62
88	1640	1635	0.5	226.69	1881.3	1639.8	108.9	1.11	552.5	6.214	F3	Closed	TS 62
88	1641	1635	0.5	224.86	1881.4	1642	108.4	1.11	552.2	6.196	F4	Closed	TS 62
88	1642	1635	0.7	403.31	1958.5	1502.2	113.8	1.11	551.8	7.973	F1	Closed	TS 62
88	1643	1635	0.8	501.19	2010.5	1420.7	117.8	1.11	551.7	8.651	F1	Closed	TS 62
88	1644	1635	0.86	557.08	2043.3	1371	121.2	1.11	552.2	8.944	F1	Closed	TS 62
88	1645	1635	0.86	555.71	2049.1	1379.5	123.1	1.11	553.1	8.915	F2	Closed	TS 62
90	1667	1664	0.5	89.15	741.5	646.5	107.8	1.11	553.8	2.453	F1	Closed	TS 75
90	1668	1664	0.7	159.94	771.7	590.7	112.9	1.11	553	3.154	F1	Closed	TS 75
90	1669	1664	0.8	197.57	790.4	557.9	115.7	1.11	552.3	3.422	F1	Closed	TS 75
90	1670	1664	0.9	233.03	810.2	524.2	118	1.11	551.3	3.625	F2	Closed	TS 75
90	1671	1664	0.95	252.06	823.5	506.3	120	1.11	550.9	3.714	F3	Closed	TS 75
90	1672	1664	1	268.77	835	488.3	121.9	1.11	550.6	3.774	F3	Closed	TS 75
90	1673	1664	1.05	287.06	851.9	471	124.6	1.11	550.5	3.835	F4	Closed	TS 75
90	1674	1664	1.1	303.07	867.6	454.3	127.8	1.11	550.6	3.867	F4	Closed	TS 75
90	1675	1664	1.21	338.19	912.6	420.2	139.1	1.11	554.7	3.865	F4	Closed	TS 75
91	1681	1678	0.5	124.88	1034.2	901.2	109	1.11	555.8	3.399	F1	Closed	TS 75
91	1682	1678	0.7	223.65	1076.2	822.9	113.5	1.11	554.8	4.372	F1	Closed	TS 75
91	1683	1678	0.8	274.93	1101.4	778	116.6	1.11	554.3	4.732	F1	Closed	TS 75
91	1685	1678	0.9	327.08	1131.6	729.4	120.2	1.11	553.7	5.016	F2	Closed	TS 75
91	1686	1678	0.95	352.22	1149.4	705.8	122.7	1.11	553.7	5.121	F3	Closed	TS 75
91	1687	1678	1	375.57	1166.3	681.6	125.5	1.11	553.8	5.196	F3	Closed	TS 75
91	1688	1678	1.05	401.9	1191.1	657.4	129.8	1.11	554.4	5.264	F4	Closed	TS 75
91	1689	1678	1.12	434.15	1224.4	624.1	136.3	1.11	555.4	5.302	F4	Closed	TS 75
92	1695	1691	0.5	224.92	1872.7	1633.1	107	1.11	549.3	6.24	F1	Closed	TS 75
92	1696	1691	0.5	224.81	1873	1640.1	107.3	1.11	549.5	6.166	F2	Closed	TS 75
92	1697	1691	0.5	224	1874.4	1635.9	106.1	1.11	548.9	6.255	F3	Closed	TS 75
92	1698	1691	0.5	224.72	1877.3	1638	107	1.11	549.3	6.253	F4	Closed	TS 75
92	1699	1691	0.84	532.28	2019.9	1383.9	118.5	1.11	549.2	8.874	F2	Closed	TS 75
92	1700	1691	0.84	541.4	2029.7	1380.5	121.6	1.11	550.5	8.876	F1	Closed	TS 75
92	1701	1691	0.8	501.72	2015.2	1424.8	121.2	1.11	551.2	8.641	F1	Closed	TS 75
92	1702	1691	0.7	408.31	1975.3	1512.9	120	1.11	552.4	7.973	F1	Closed	TS 75

Figure 1. Aerial view of the NASA Langley Transonic Dynamics Tunnel.

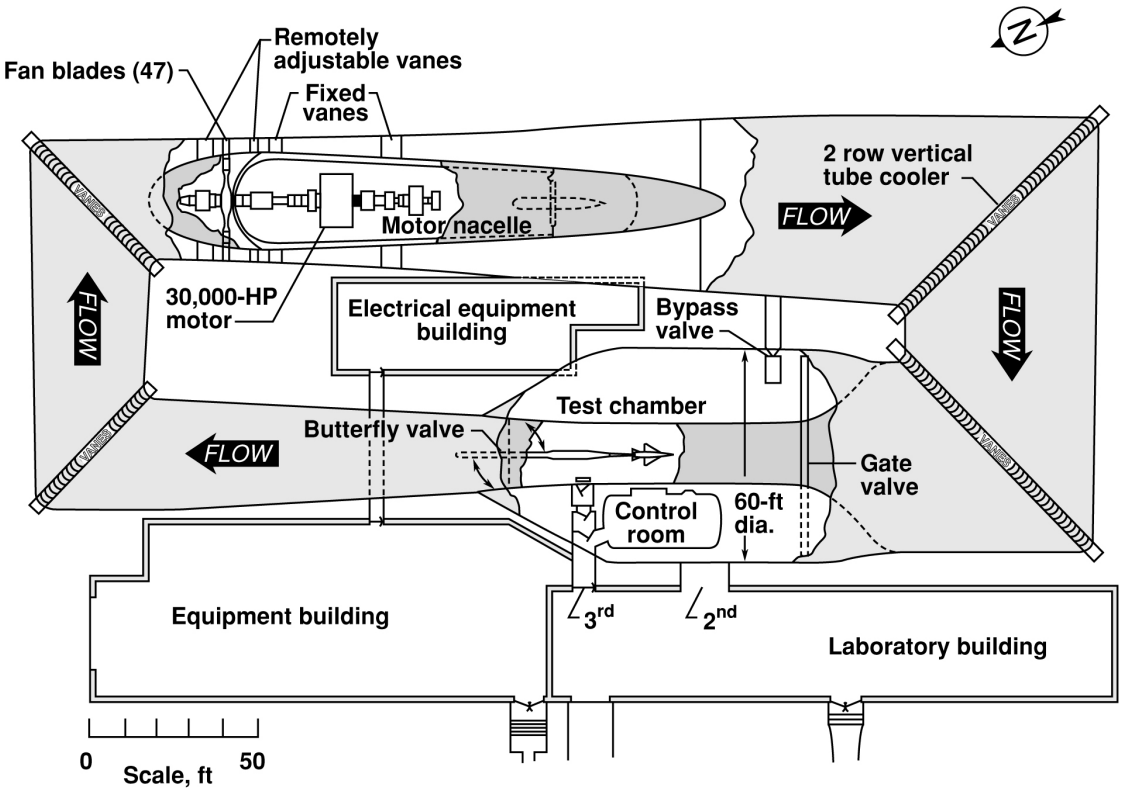

Figure 2. Planview drawing of the Transonic Dynamics Tunnel.

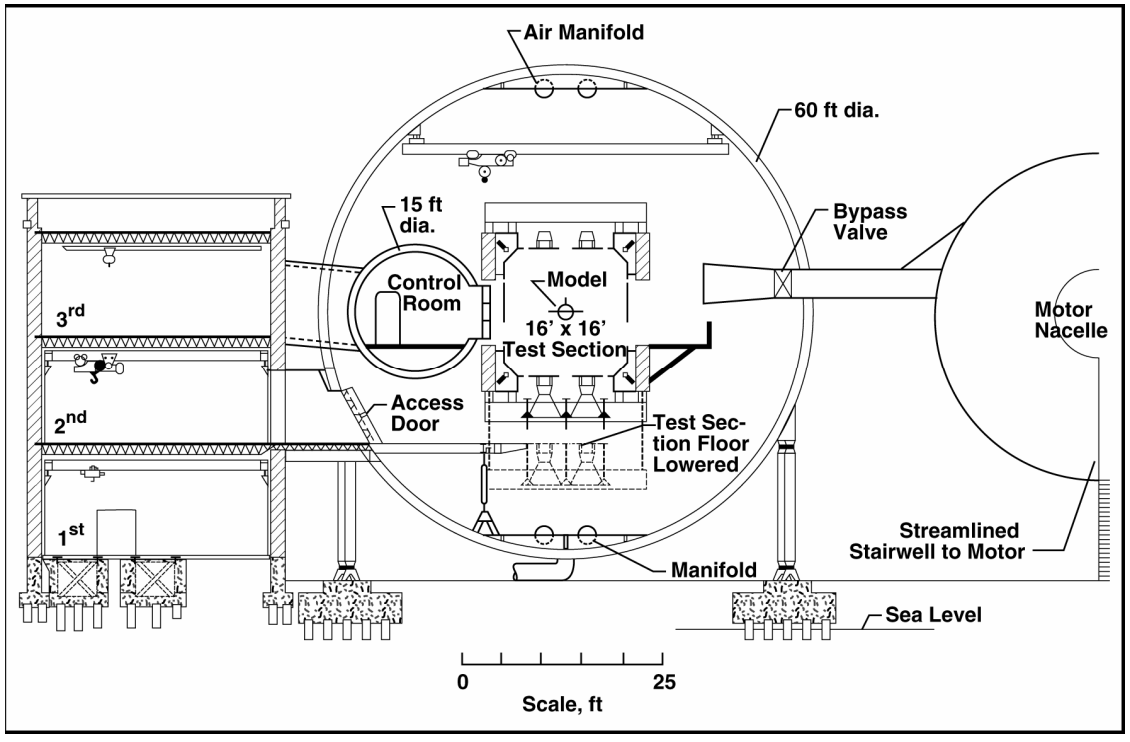

Figure 3. Cross section of the Transonic Dynamics Tunnel near the model testing location.

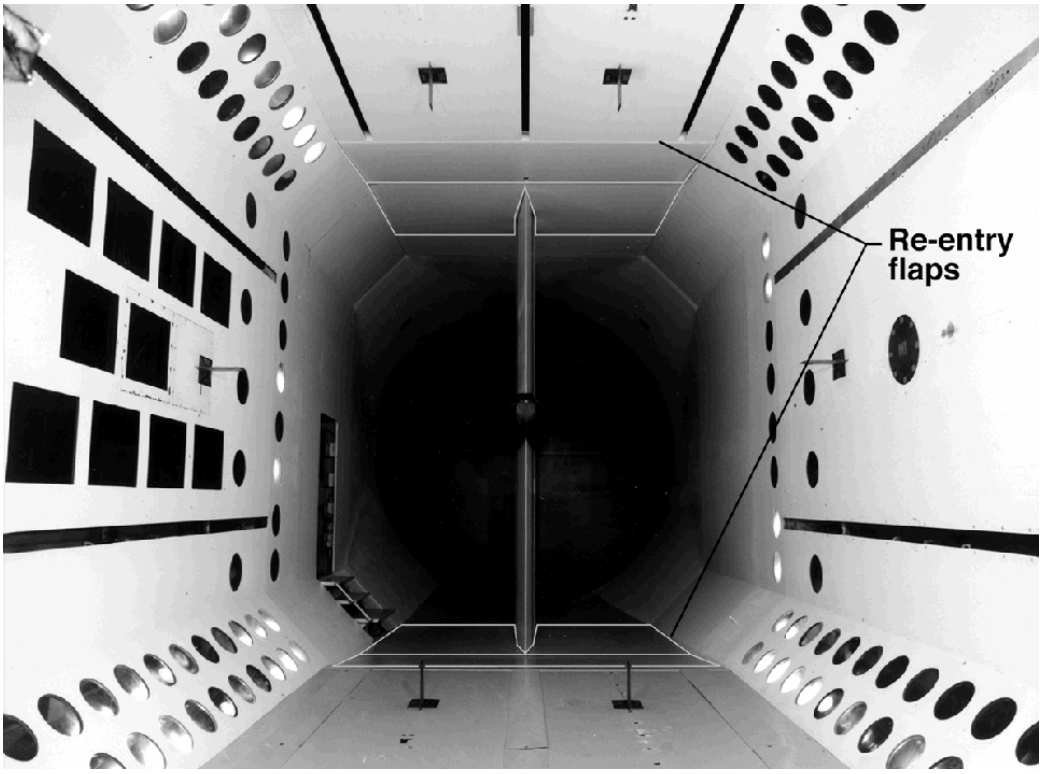

Figure 4. Photograph of the TDT test section with the reentry flaps shown outlined.

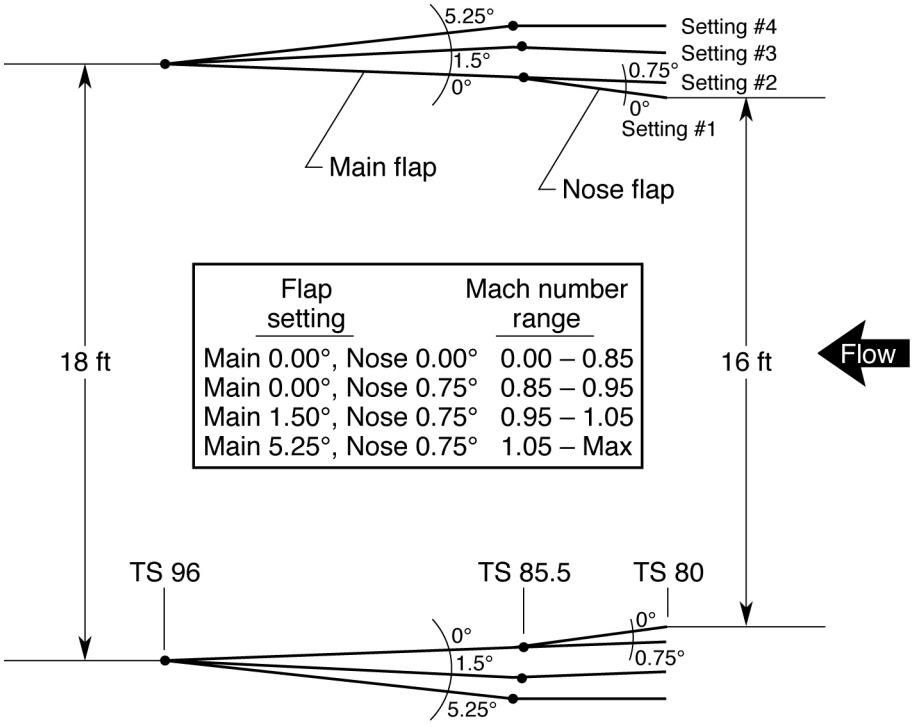

Figure 5. Schematic of reentry flap operation.

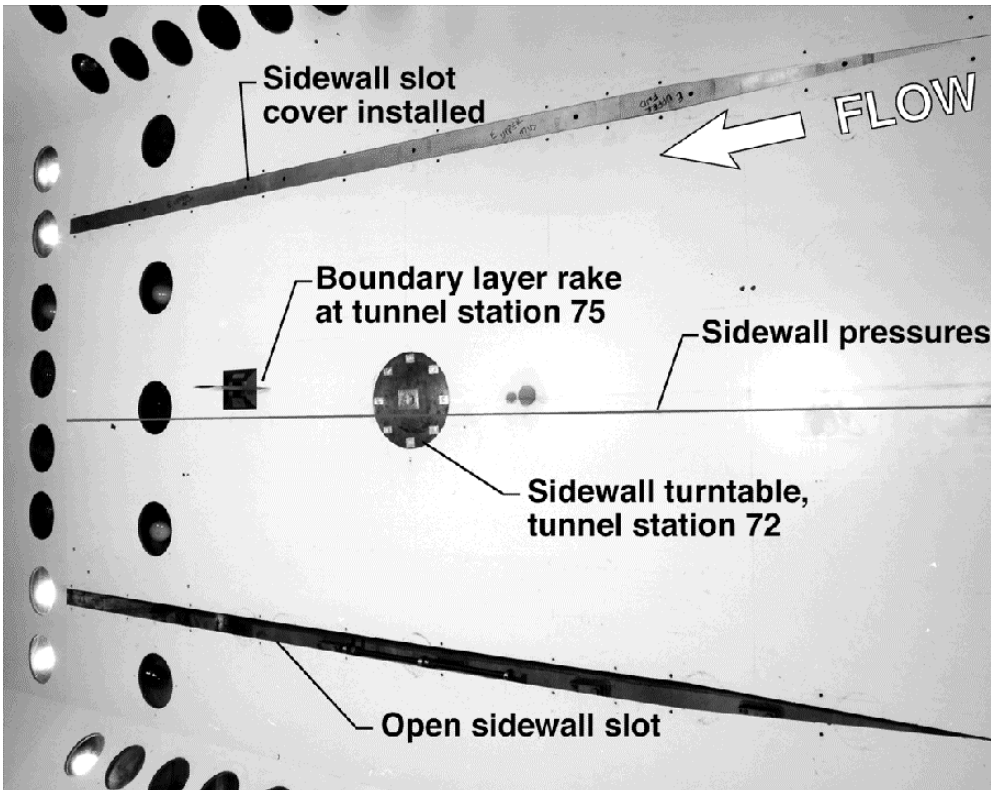

Figure 6. Photograph of test section sidewall showing sidewall slots.

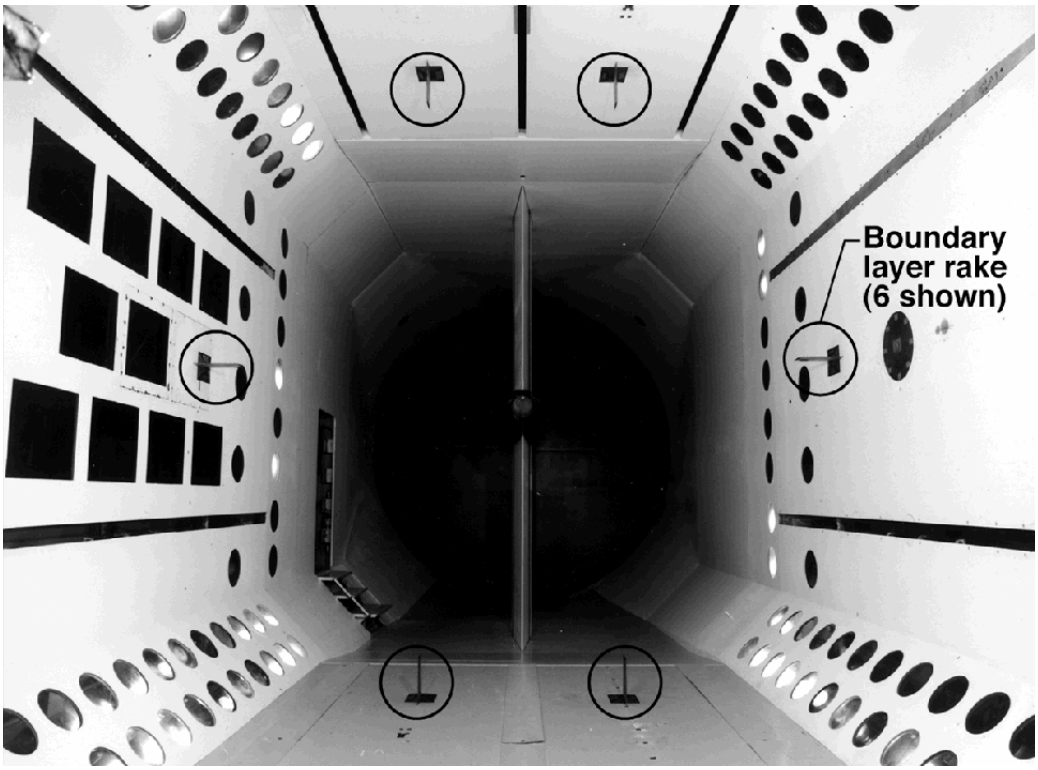

Figure 7. Photograph of the boundary layer rakes mounted in the TDT test section at the aft location.

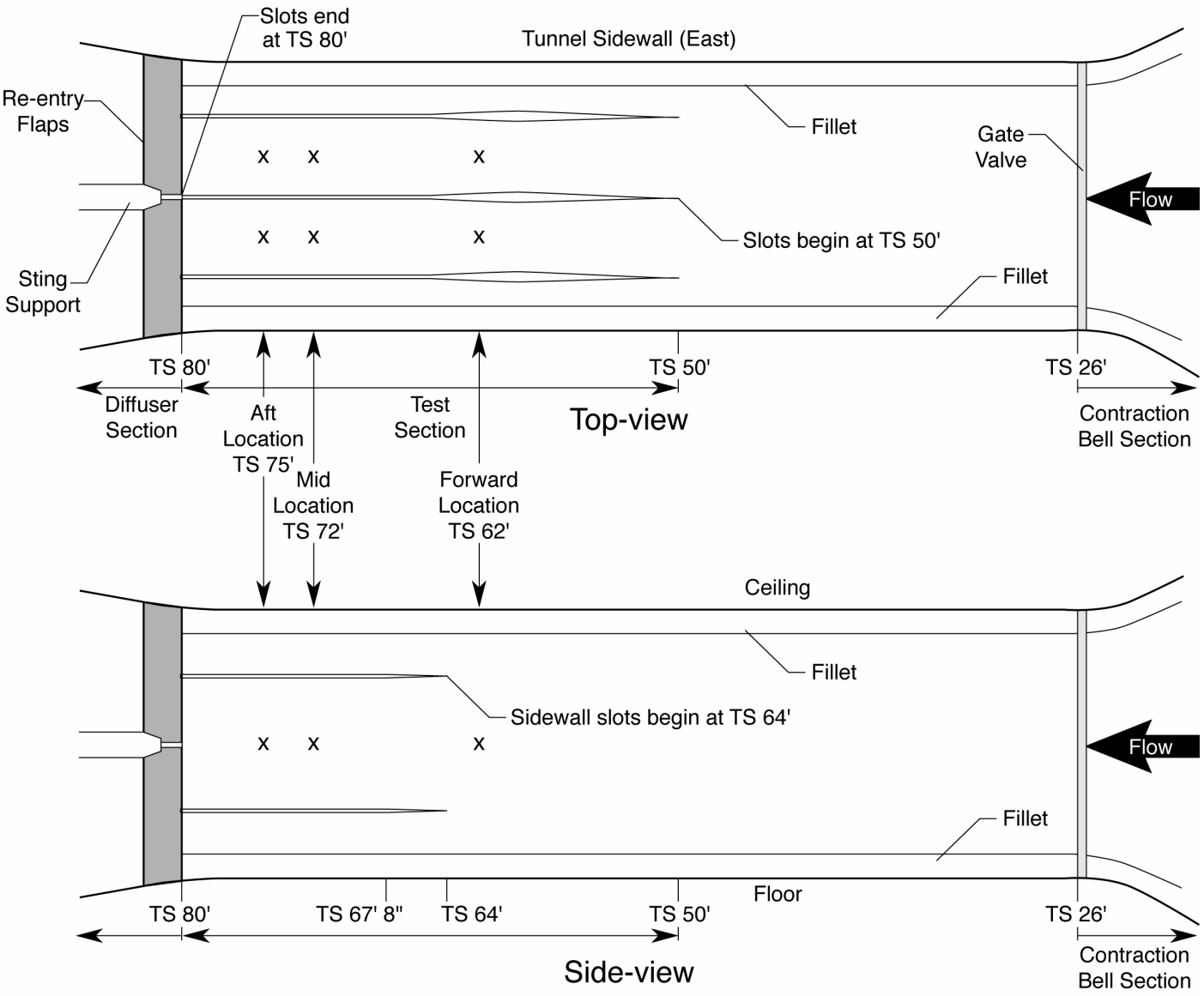

Figure 8. Sketch of the rake locations in the test section of the Transonic Dynamics Tunnel.

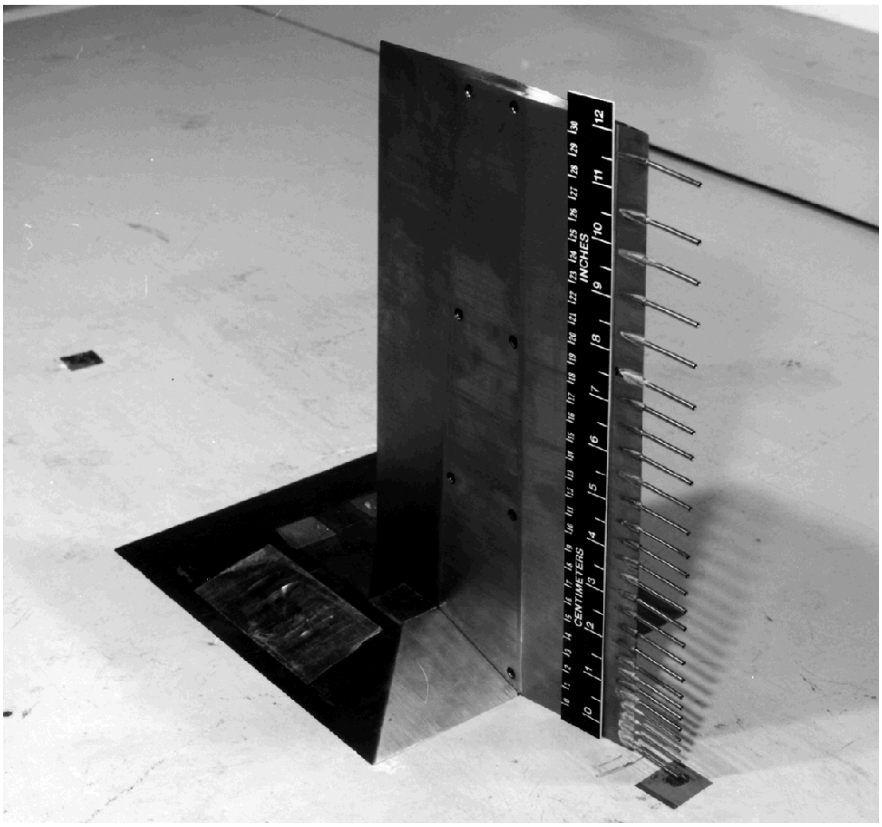

Figure 9. Boundary layer rake mounted in the test section.

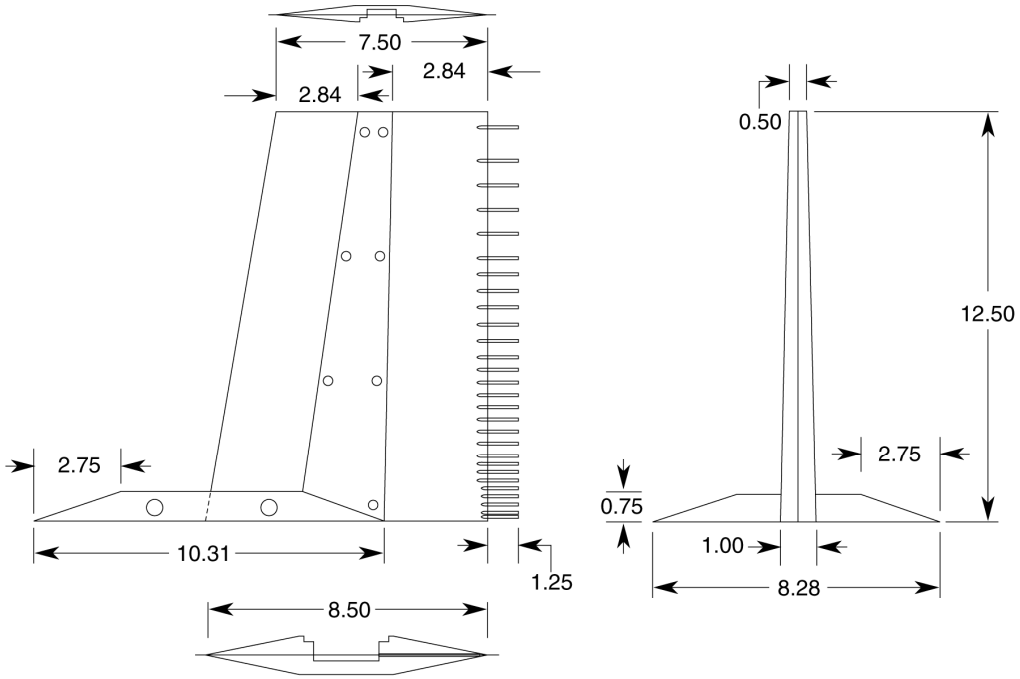

Figure 10. Sketch of a boundary layer rake. Dimensions in inches.

Figure 11. Boundary layer data reduction station in TDT control room.

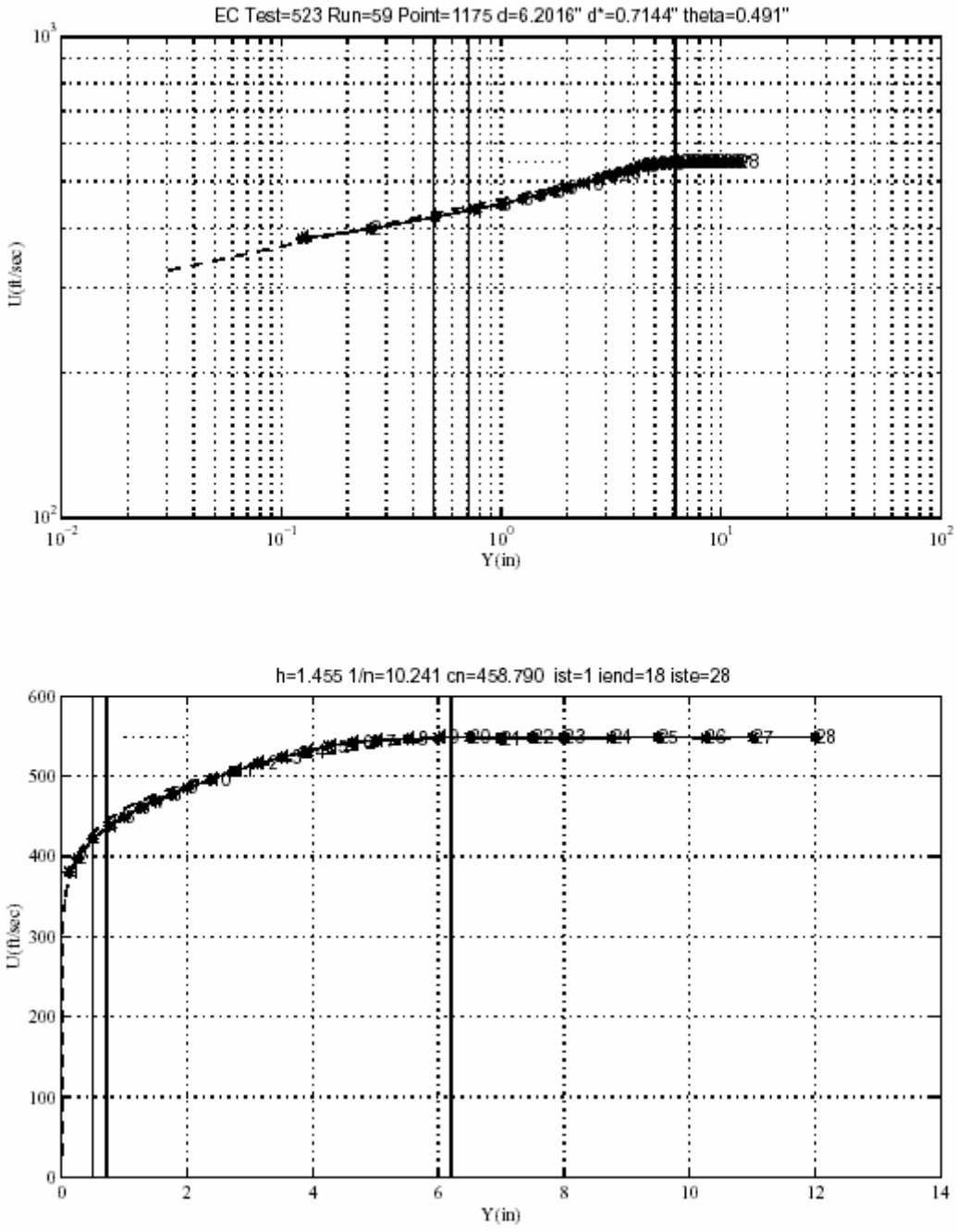

Figure 12. Example plots from boundary layer data reduction station. Top plot is log-log. Bottom plot is linear format.

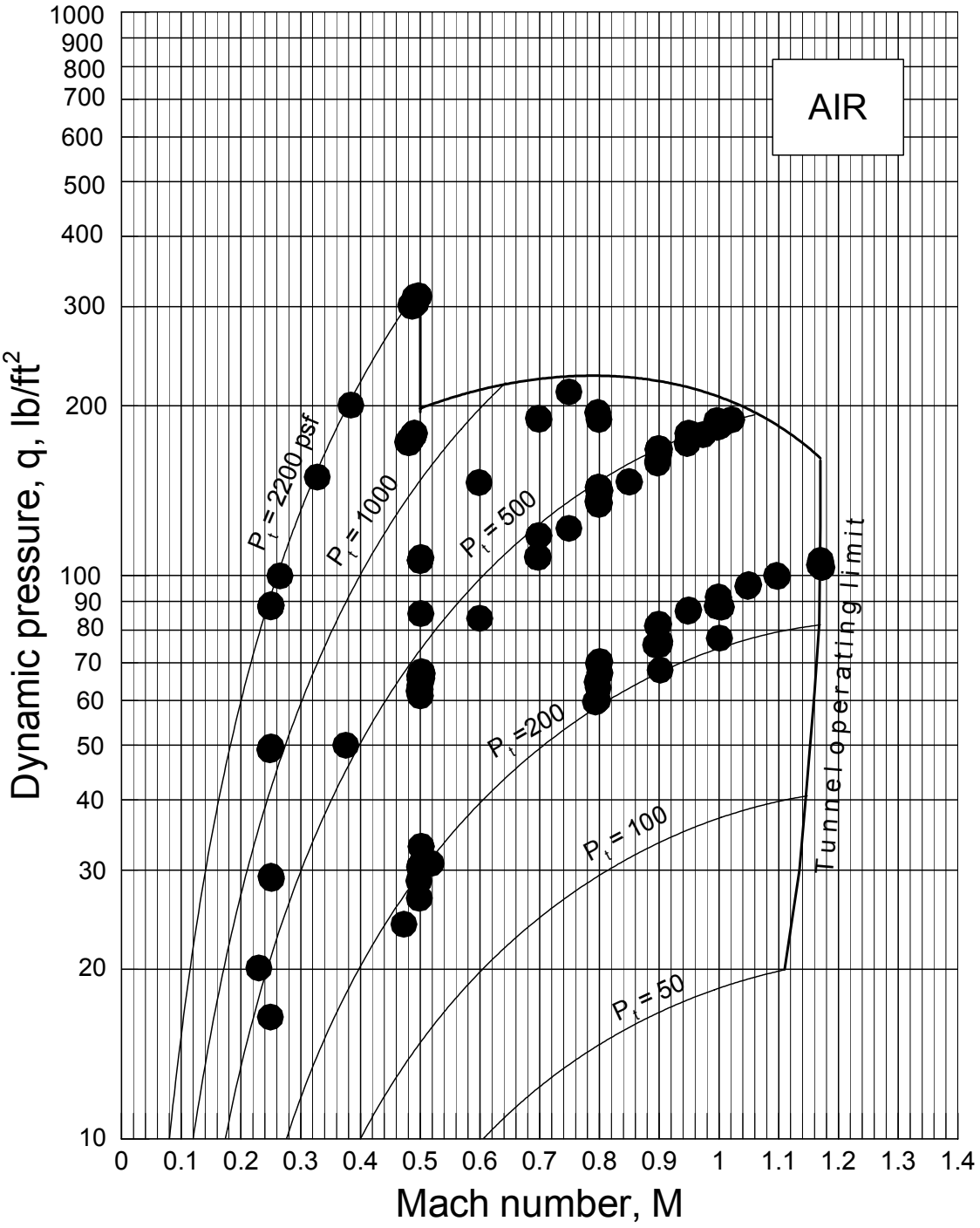

Figure 13. Operational boundary for the Transonic Dynamics Tunnel and test conditions in air.

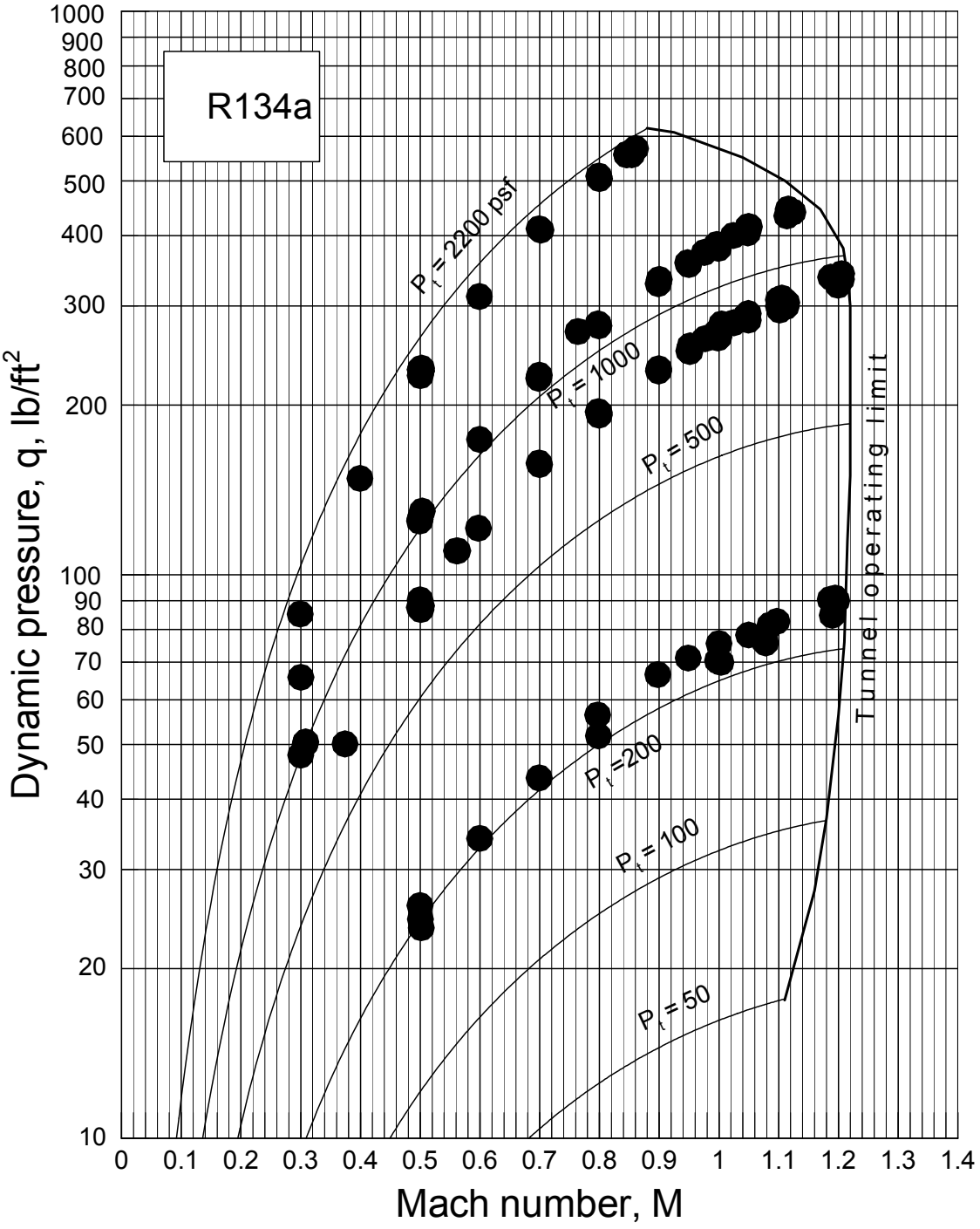

Figure 14. Operational boundary for the Transonic Dynamics Tunnel and test conditions in R-134a.

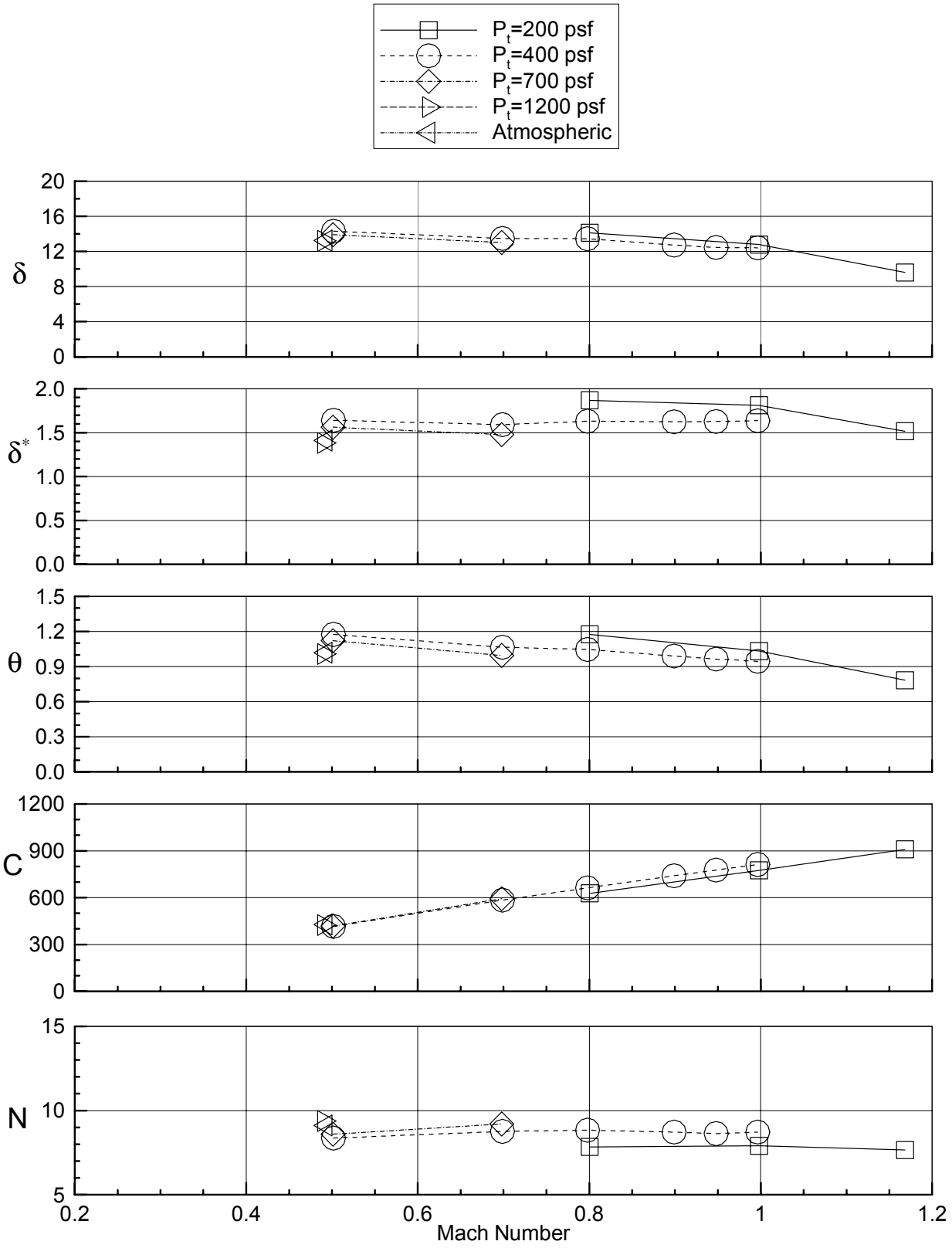

a) East wall rake

Figure 15. Boundary layer parameters for air, all slots open, TS 72, standard flap settings.

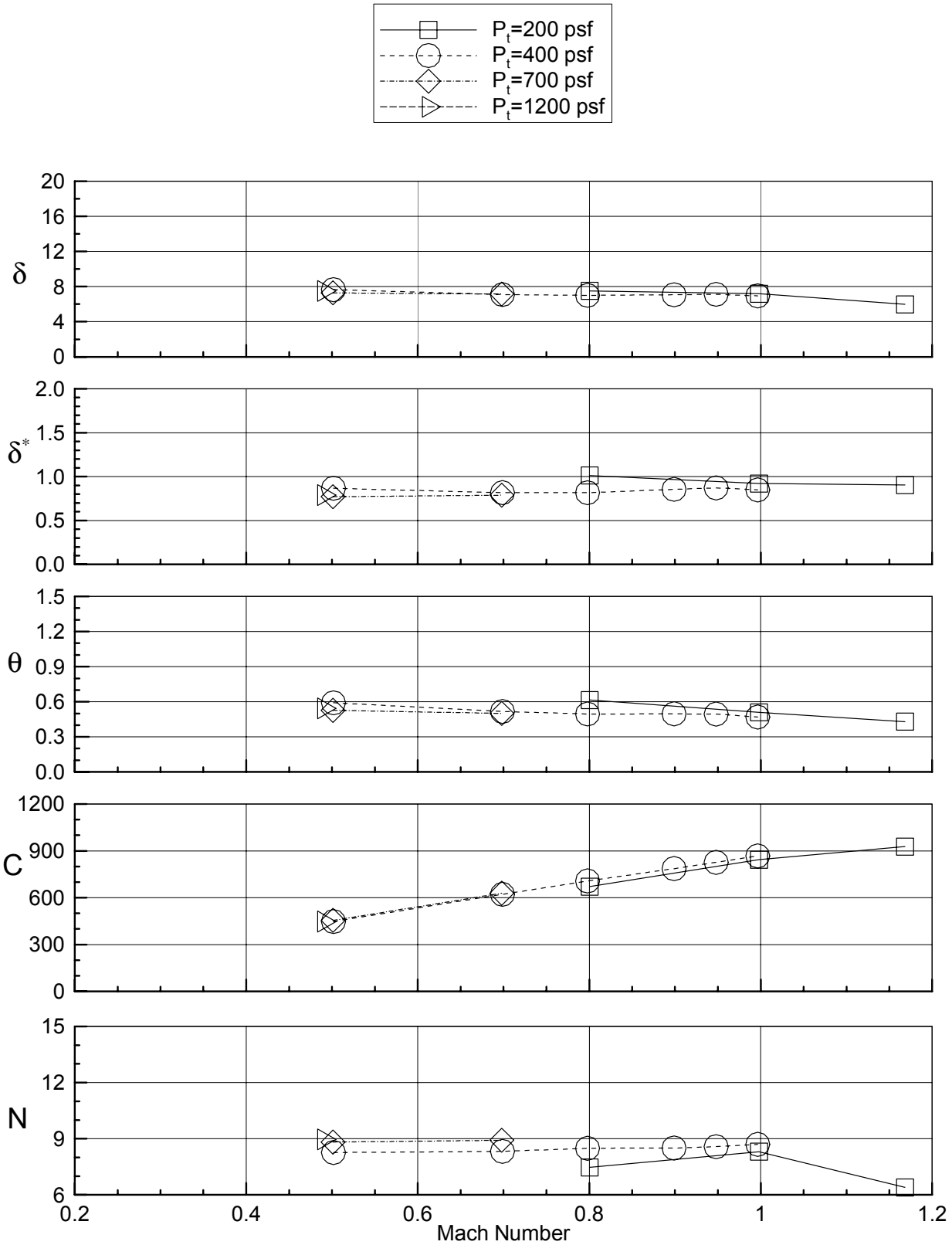

b) East ceiling rake

Figure 15. - continued.

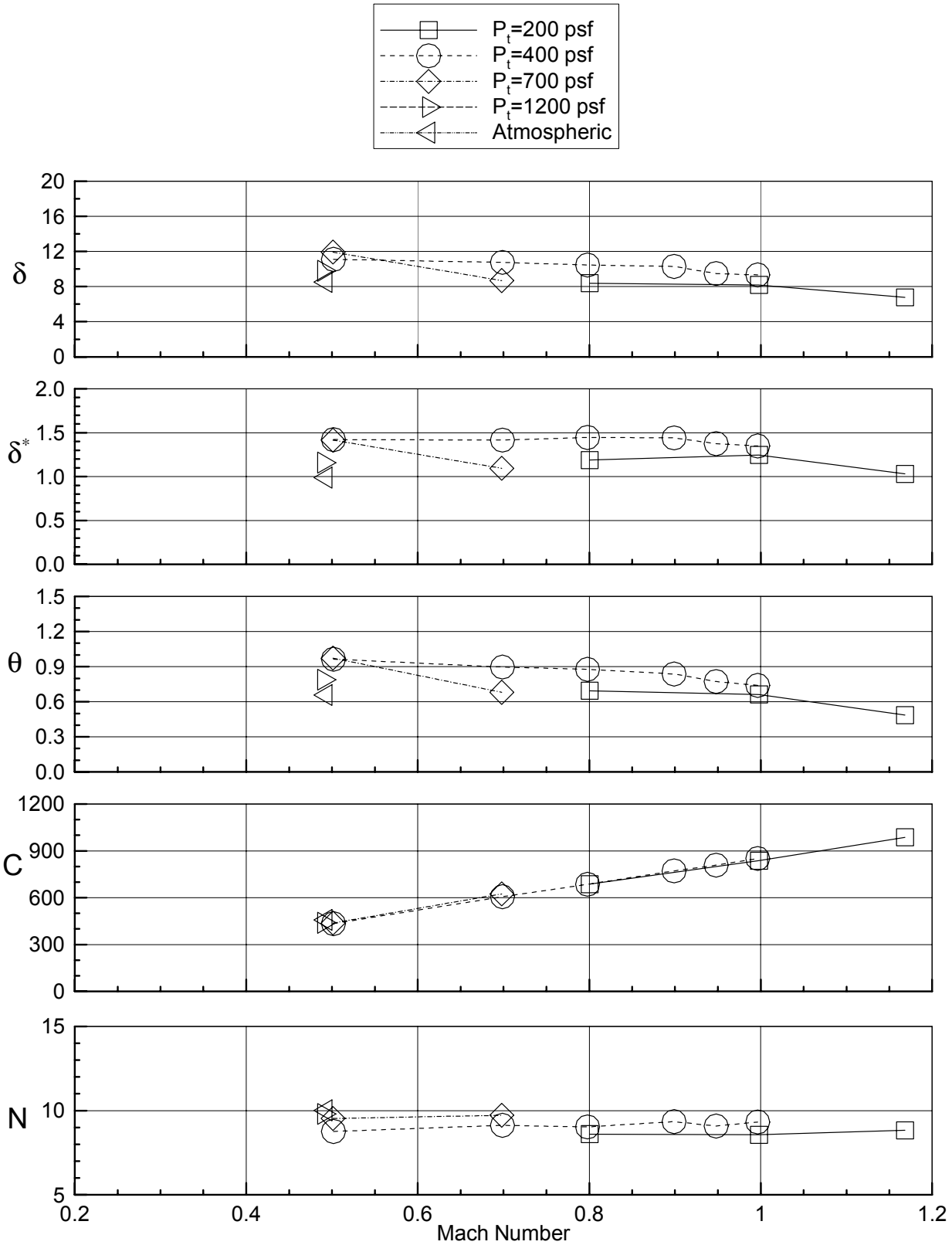

c) West ceiling rake

Figure 15. - continued.

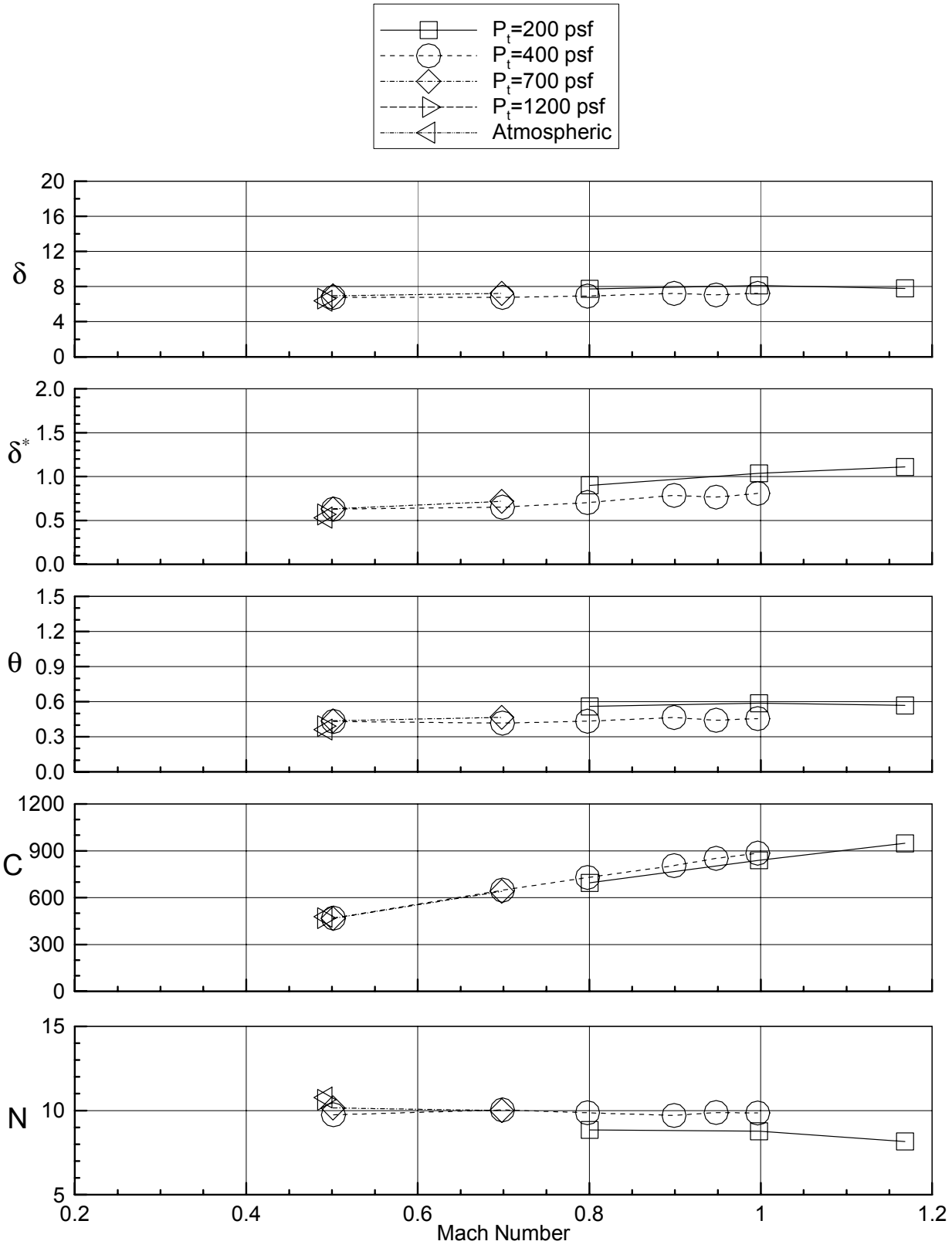

d) West wall rake

Figure 15. - continued.

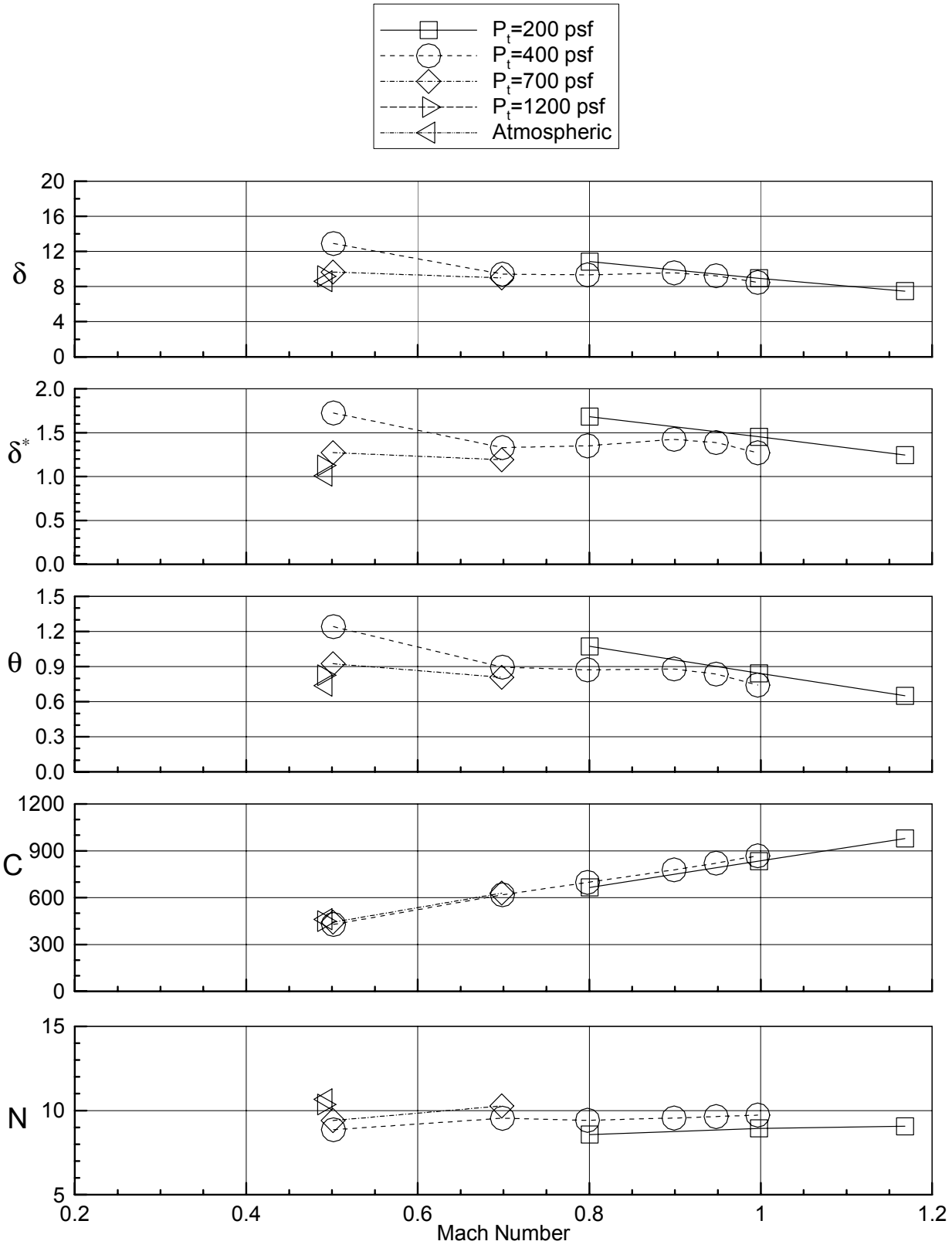

e) West floor rake

Figure 15. - continued.

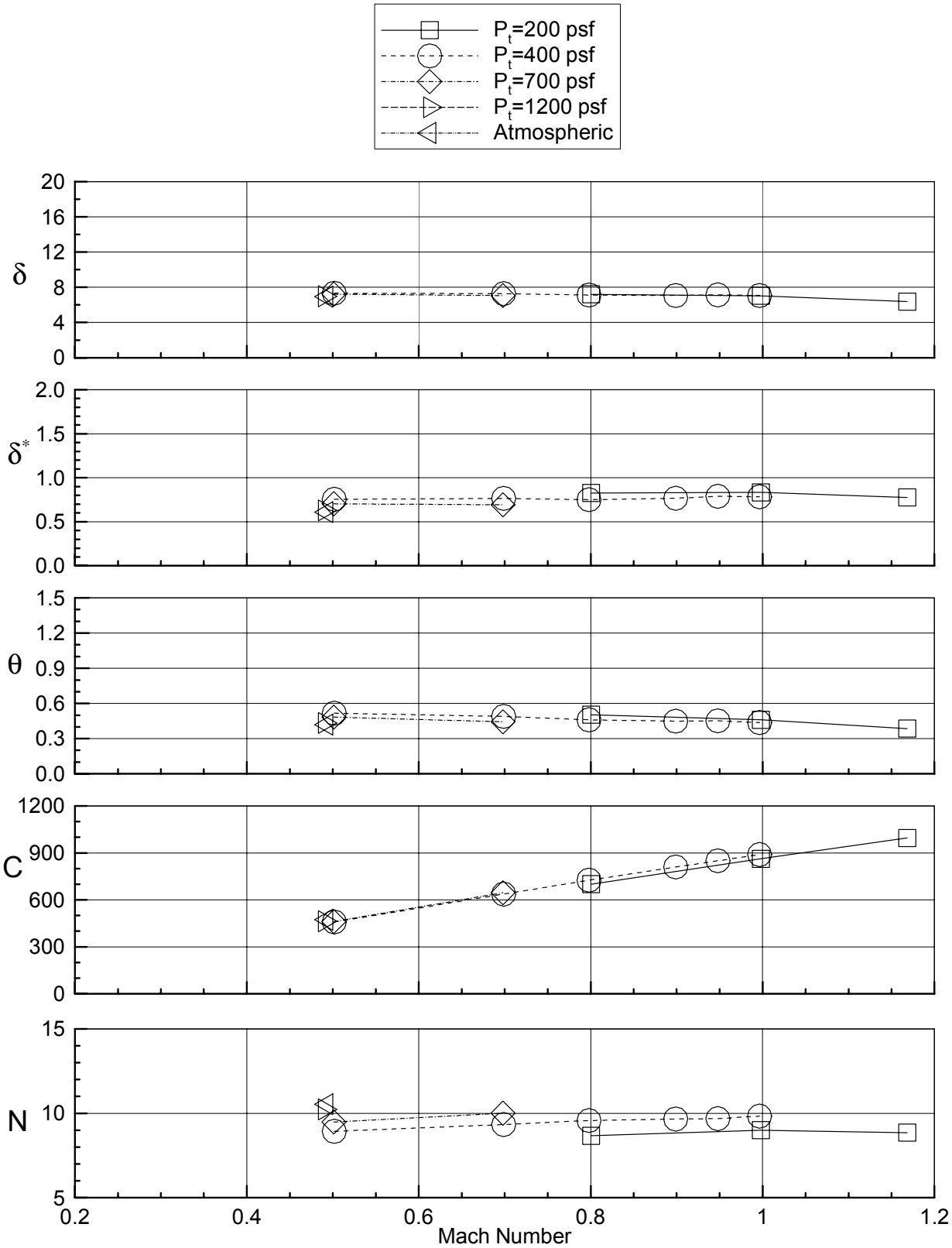

f) East floor rake

Figure 15. - continued.

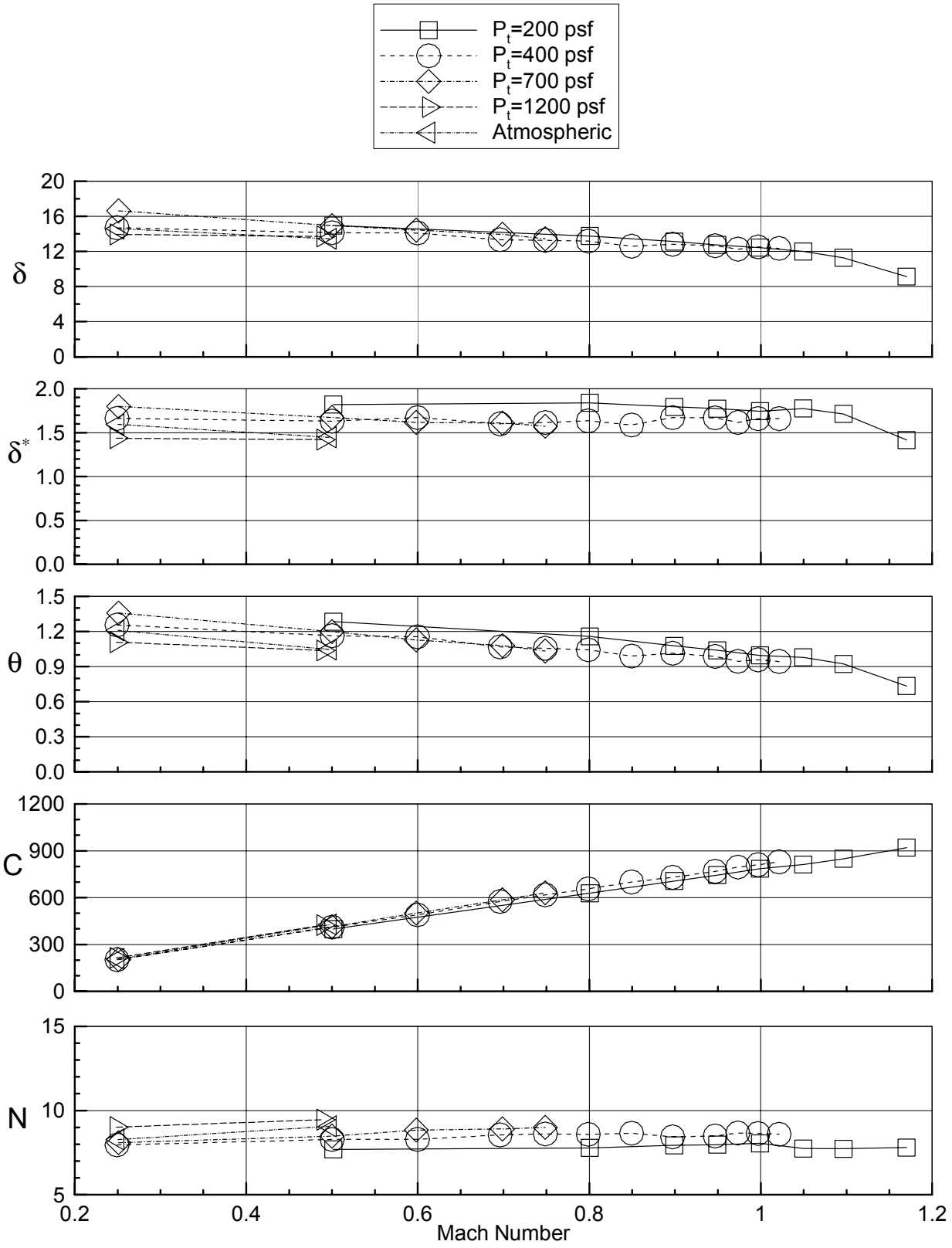

a) East wall rake

Figure 16. Boundary layer parameters for air, East Wall slots closed, TS 72, standard flap settings.

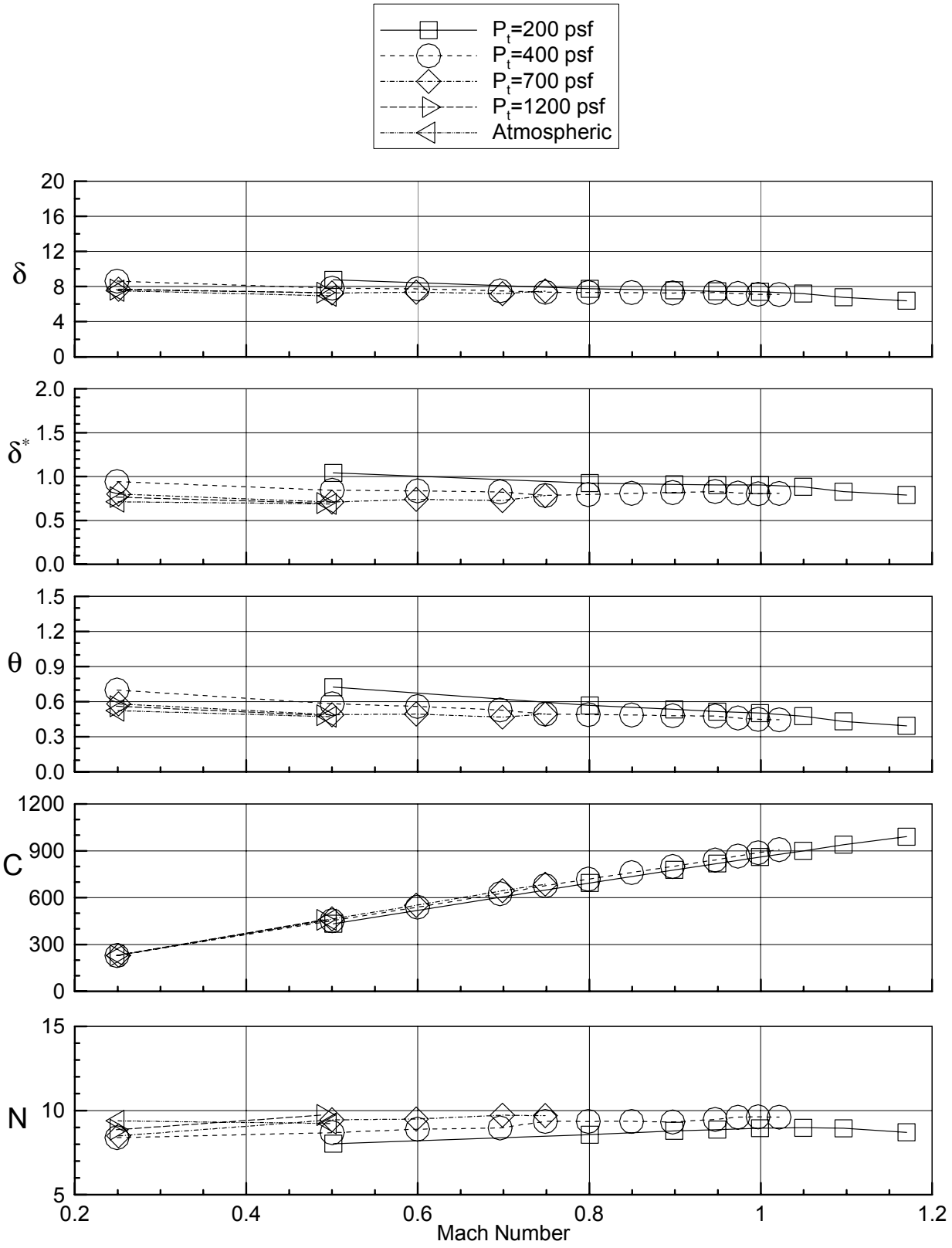

b) East ceiling rake

Figure 16. - continued.

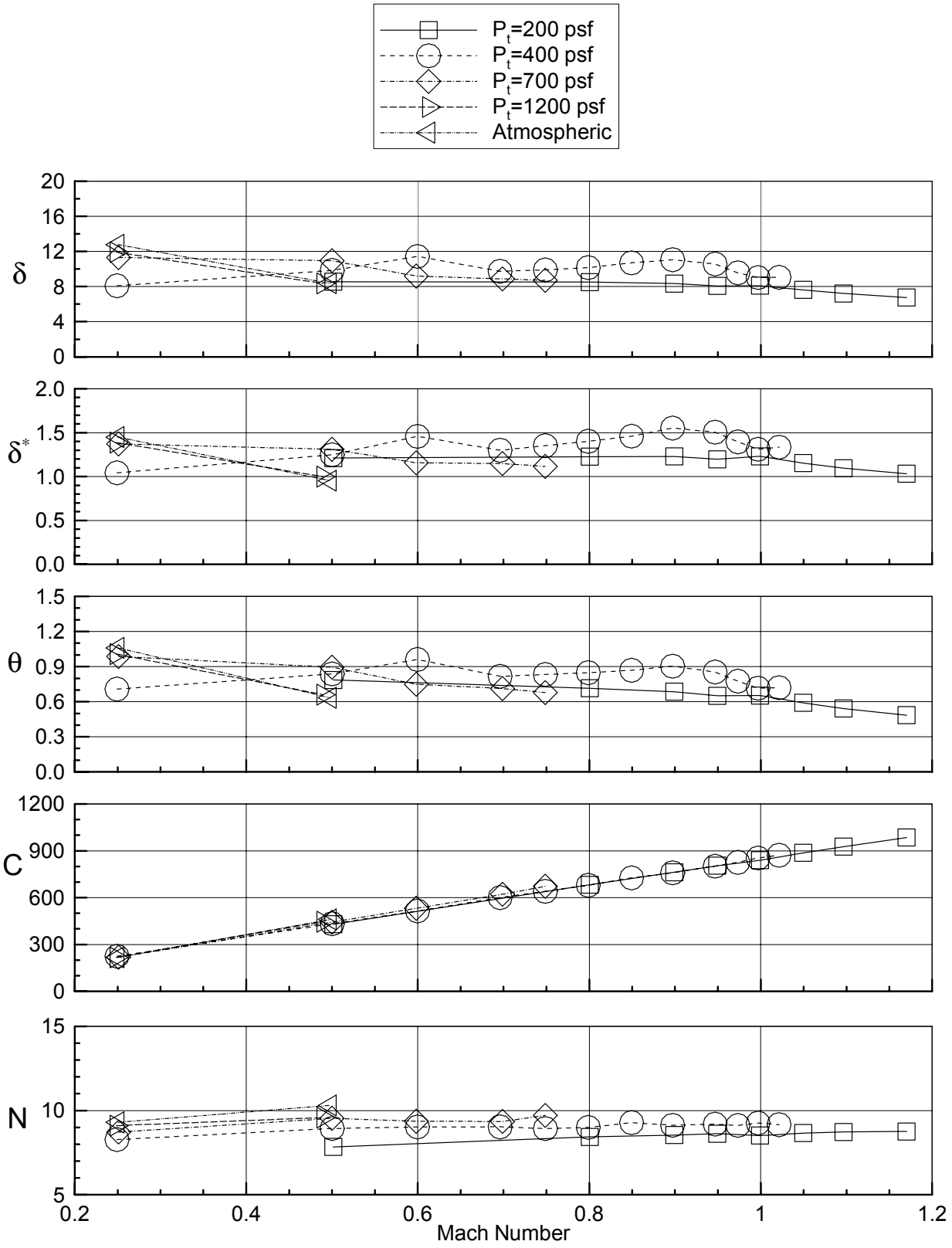

c) West ceiling rake

Figure 16. - continued.

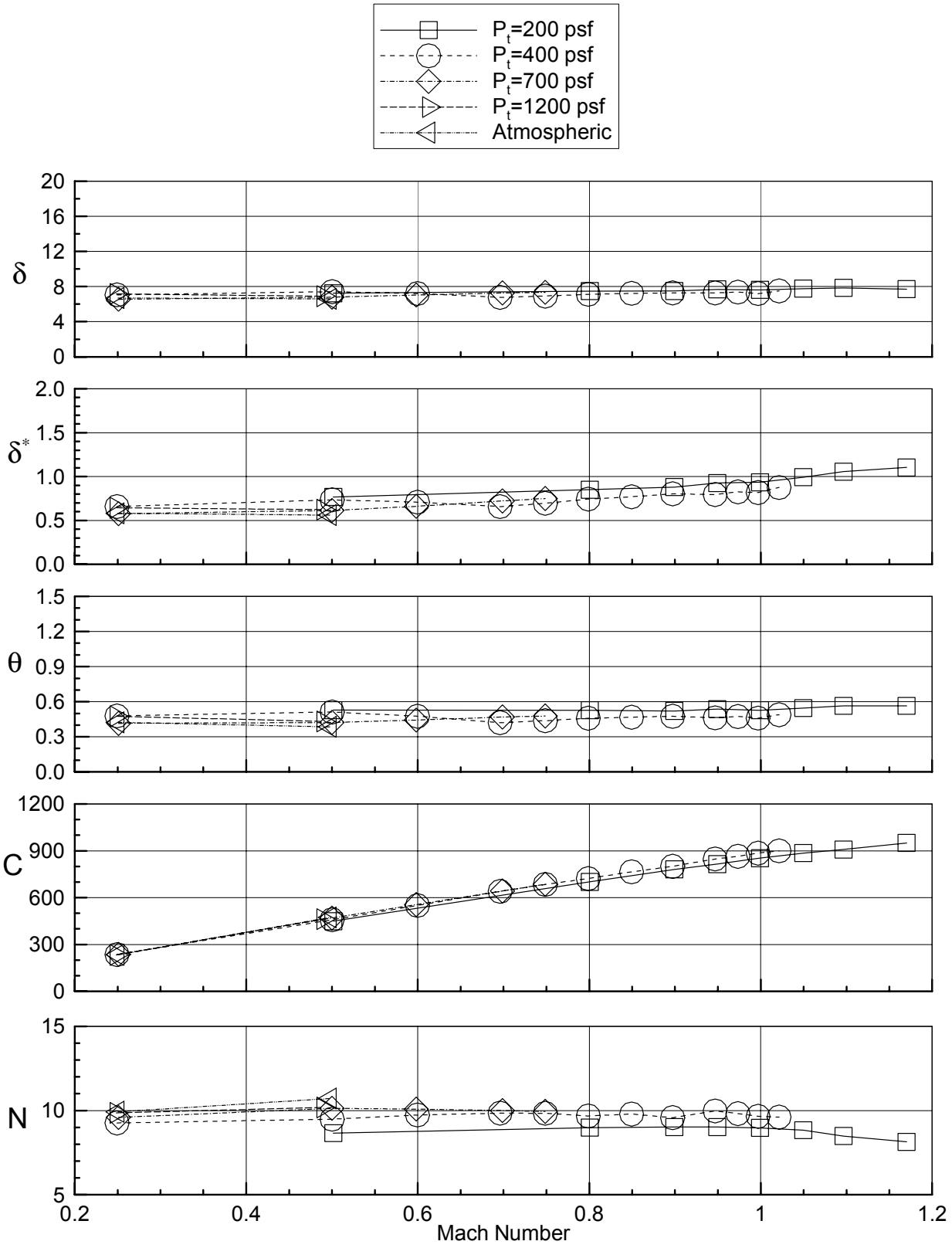

d) West wall rake

Figure 16. - continued.

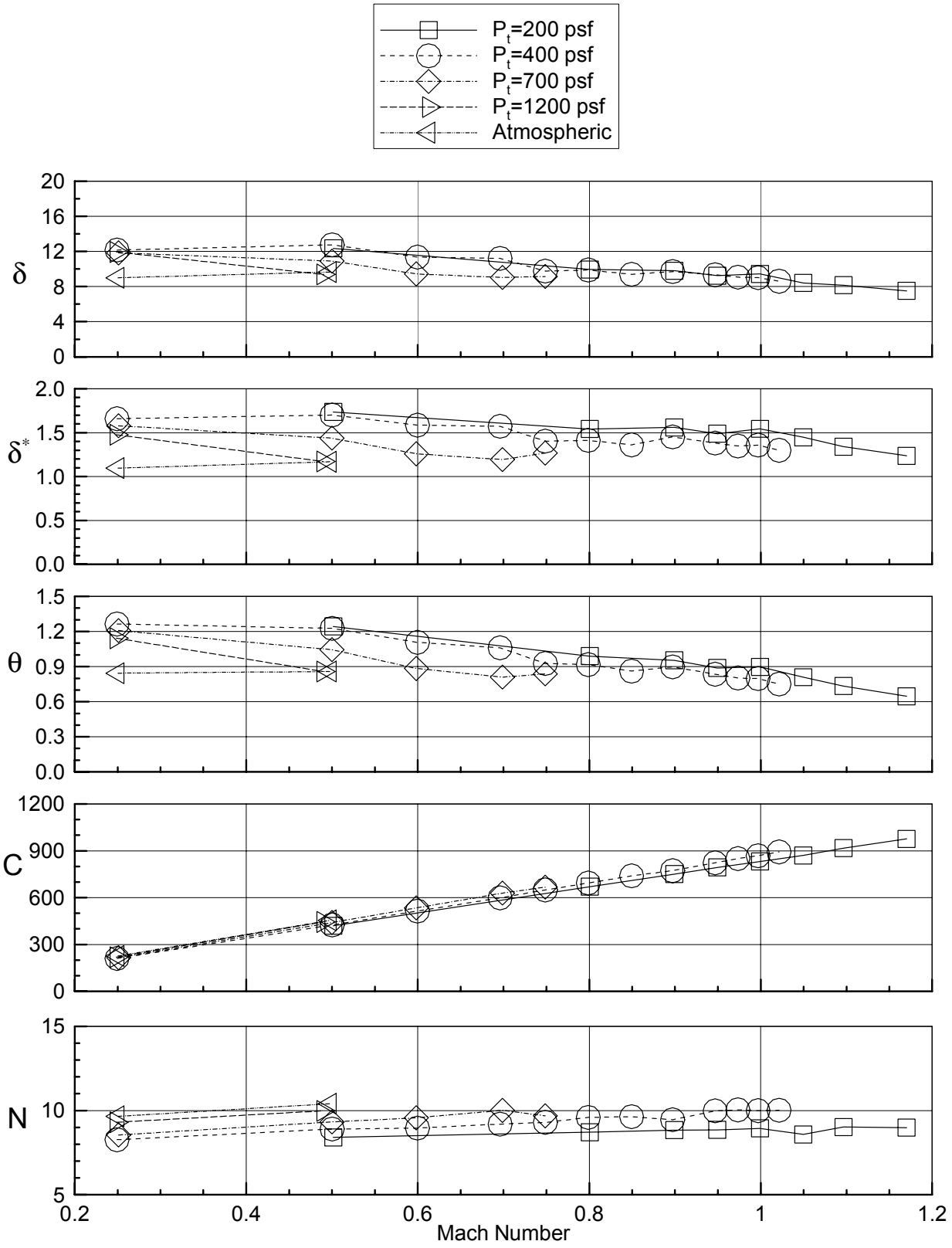

e) West floor rake

Figure 16. - continued.

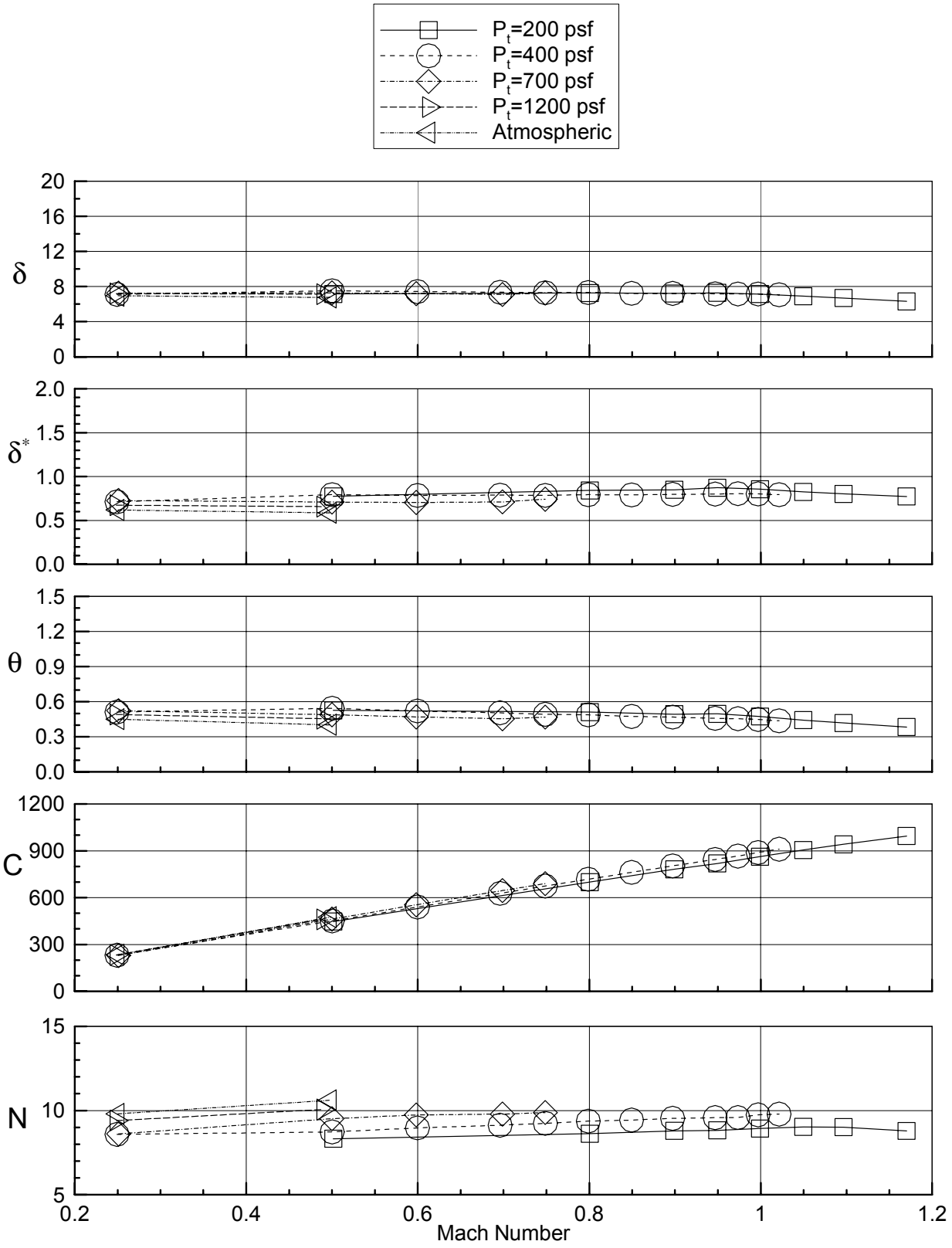

f) East floor rake

Figure 16. - continued.

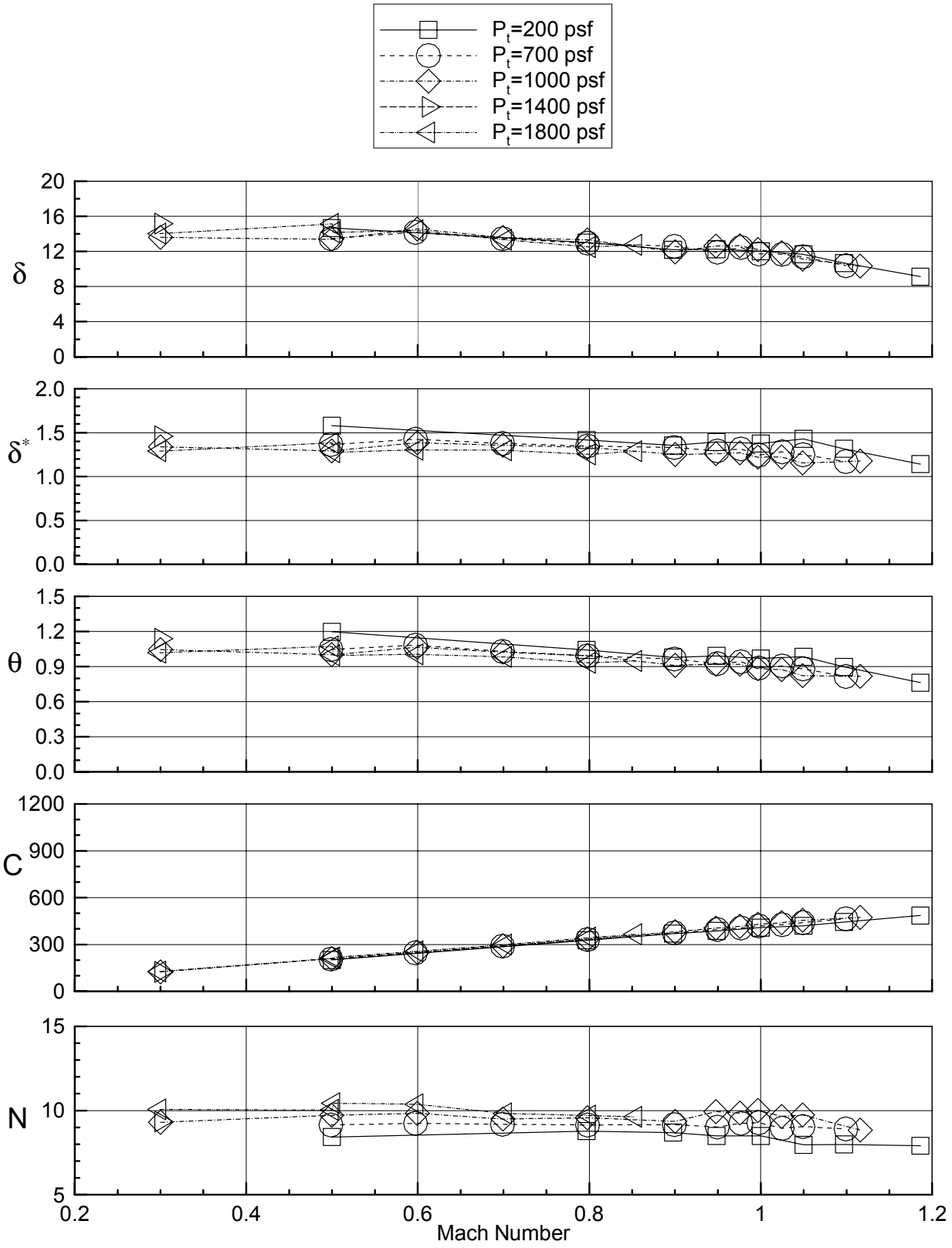

a) East wall rake

Figure 17. Boundary layer parameters for R-134a, all slots open, TS 72, standard flap settings.

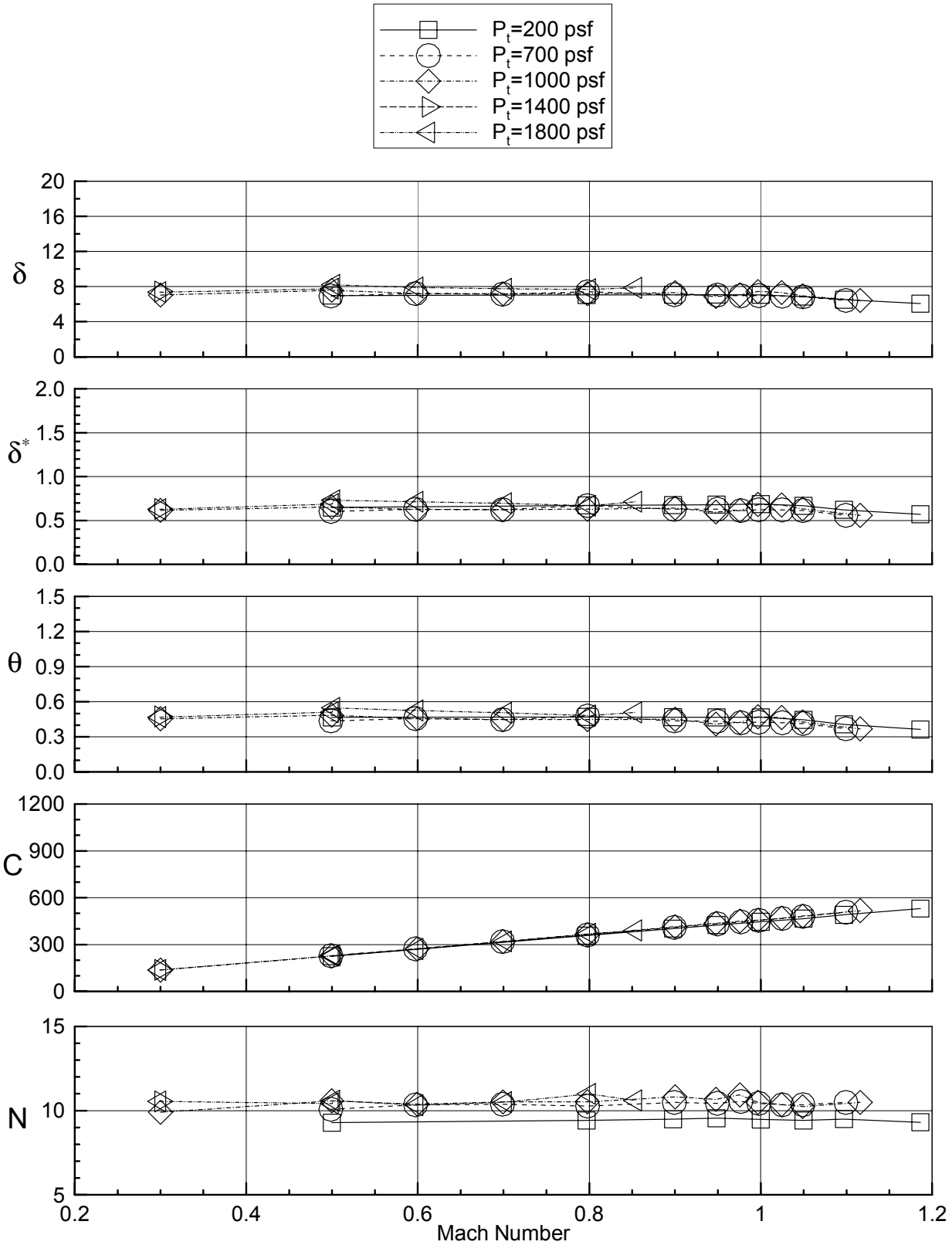

b) East ceiling rake

Figure 17. - continued.

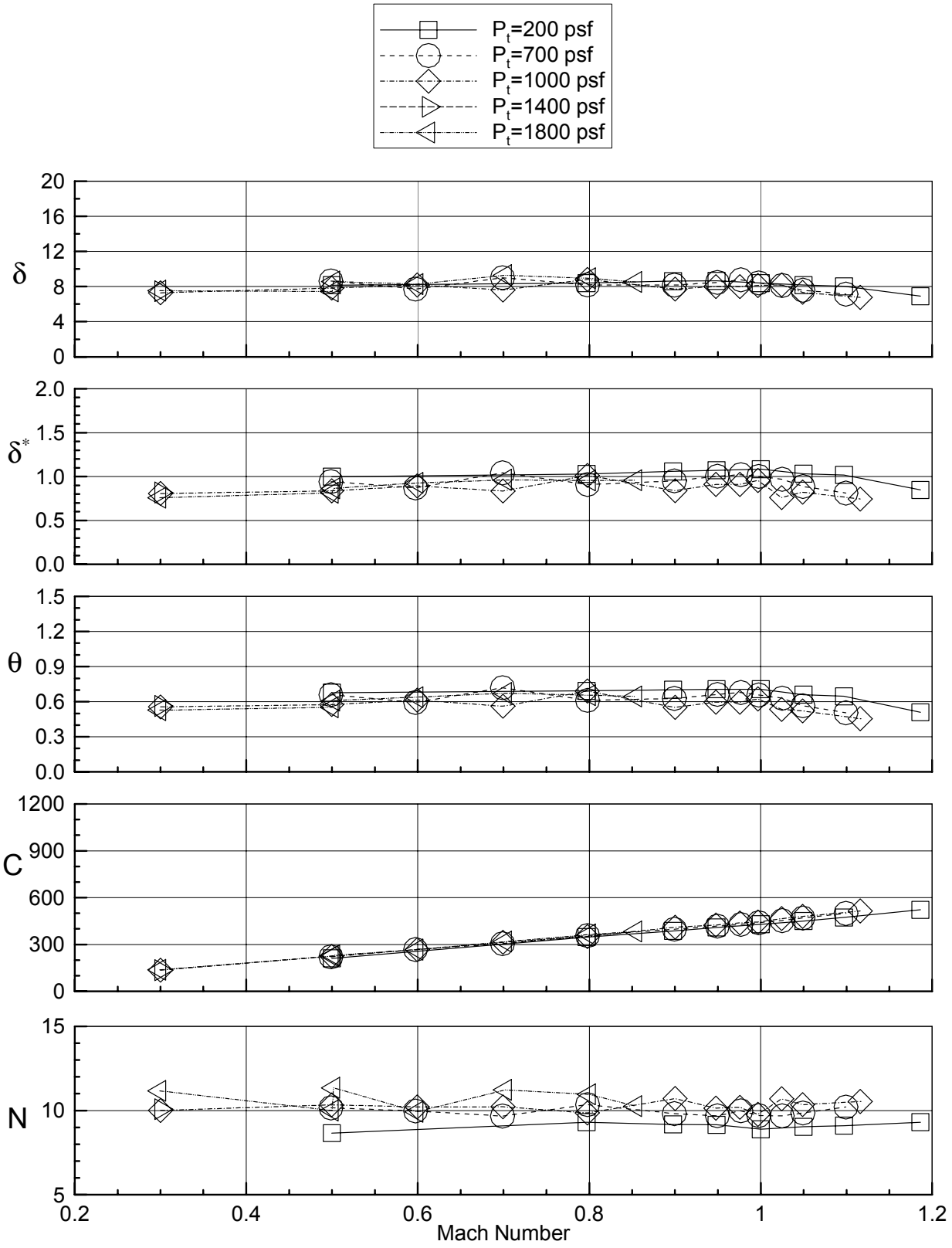

c) West ceiling rake

Figure 17. - continued.

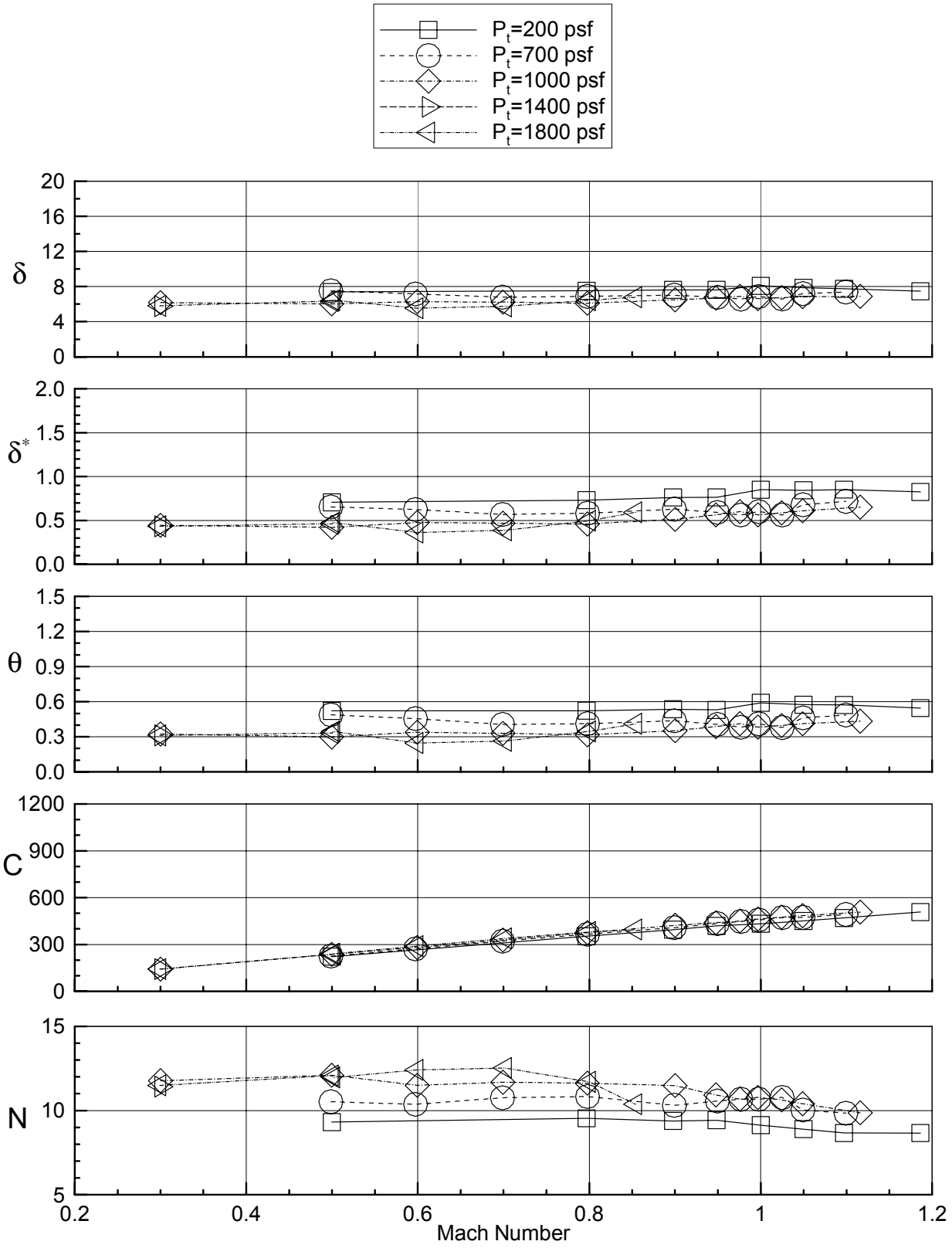

d) West wall rake

Figure 17. - continued.

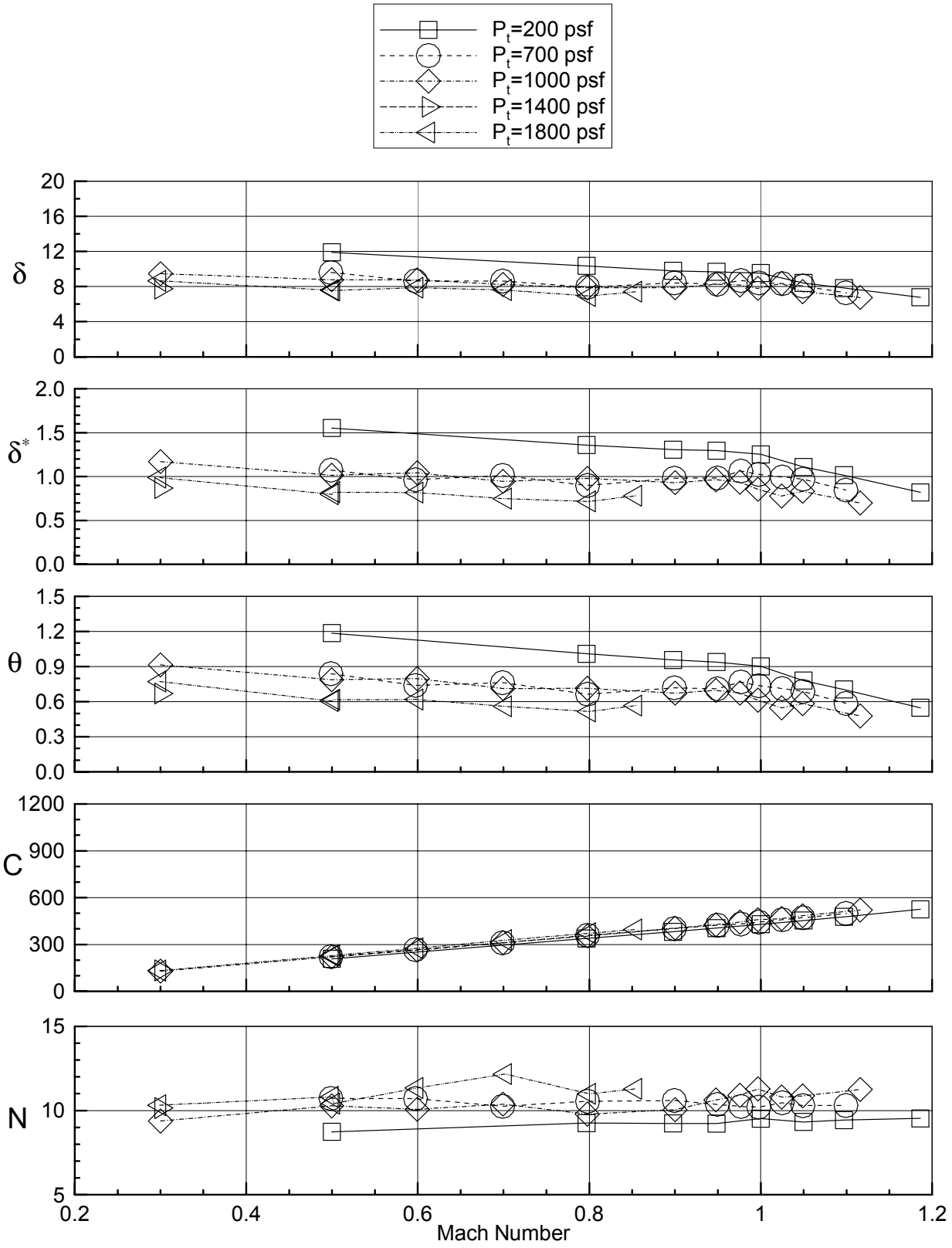

e) West floor rake

Figure 17. - continued.

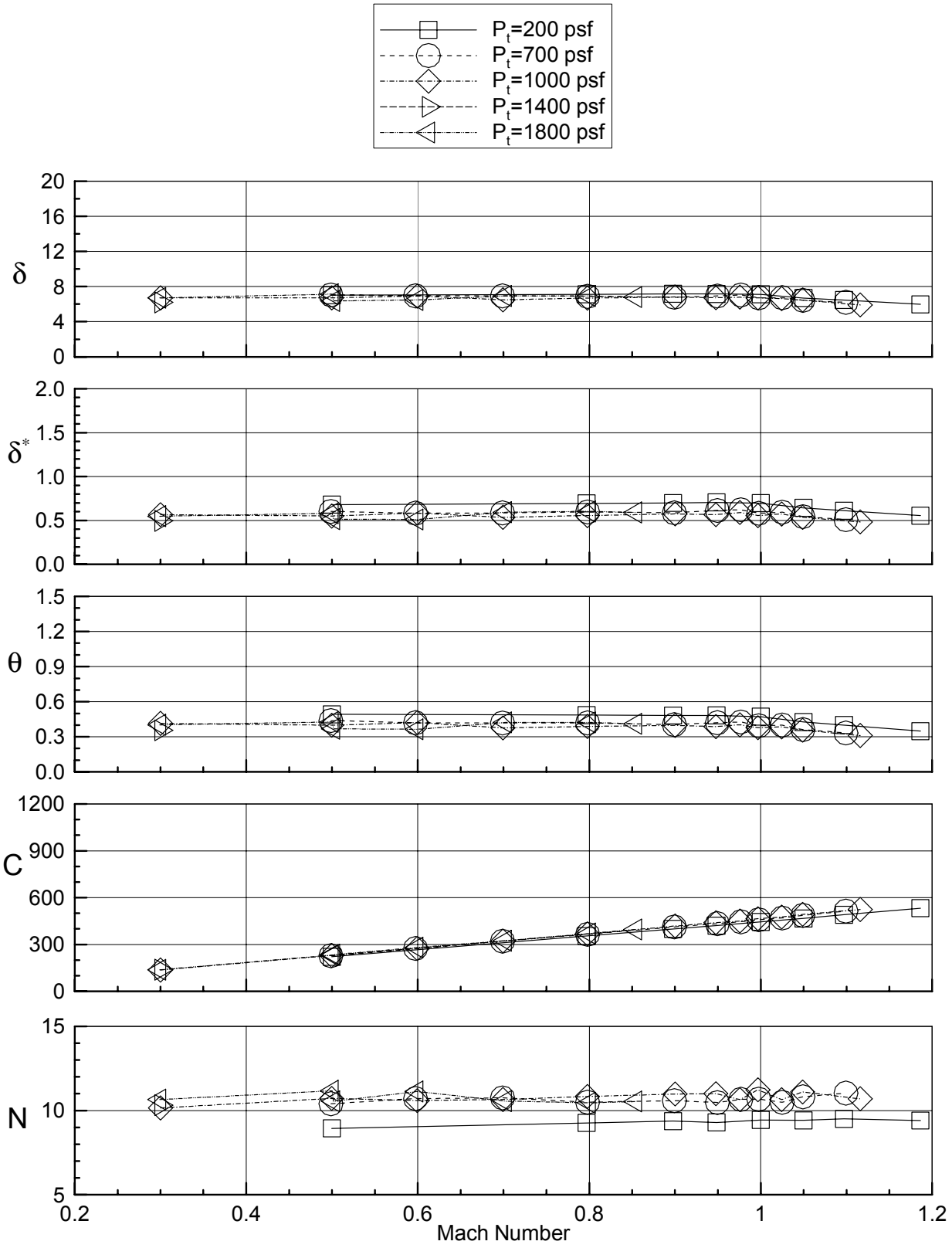

f) East floor rake

Figure 17. - continued.

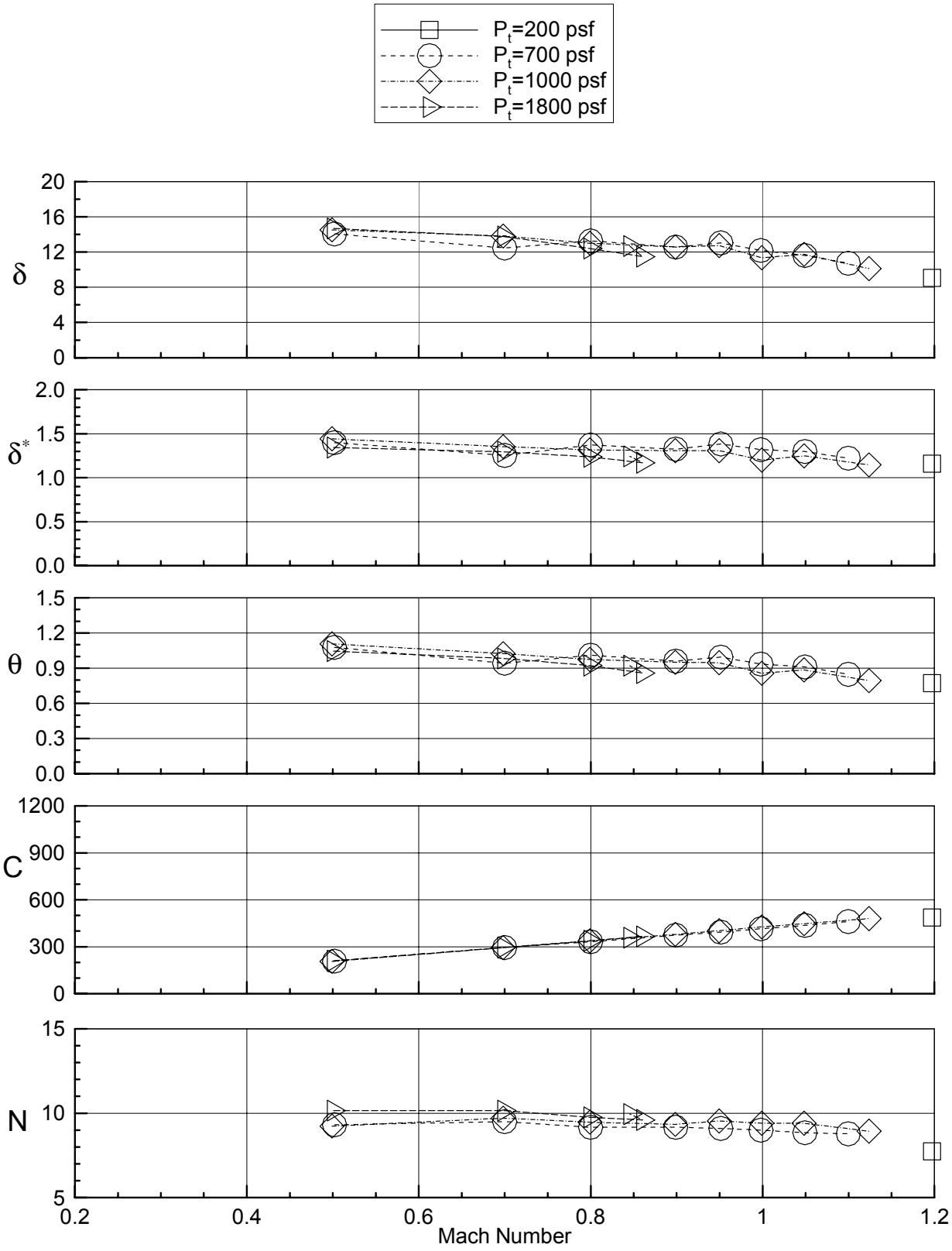

a) East wall rake

Figure 18. Boundary layer parameters for R-134a, East Wall slots closed, TS 72, standard flap settings

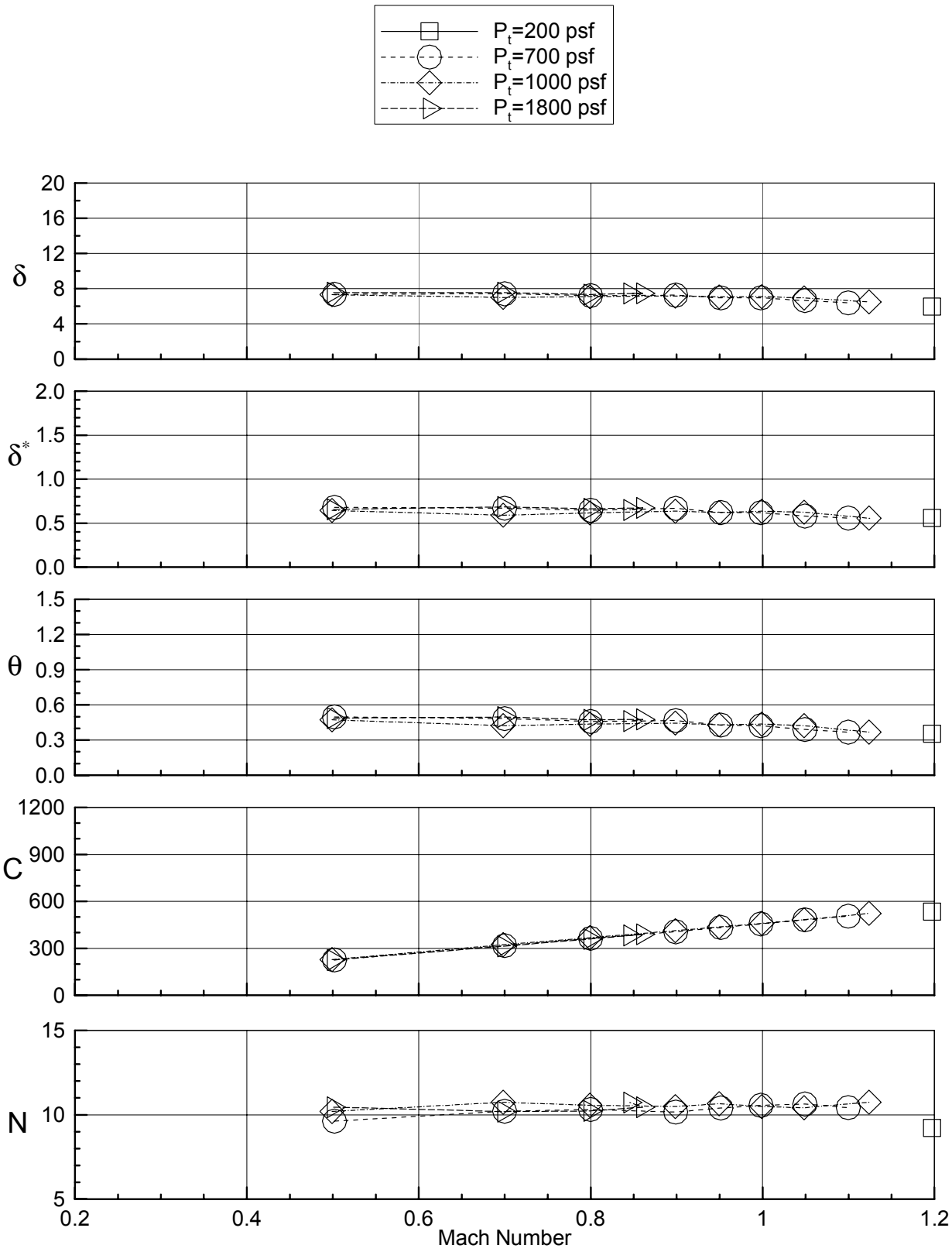

b) East ceiling rake

Figure 18. - continued.

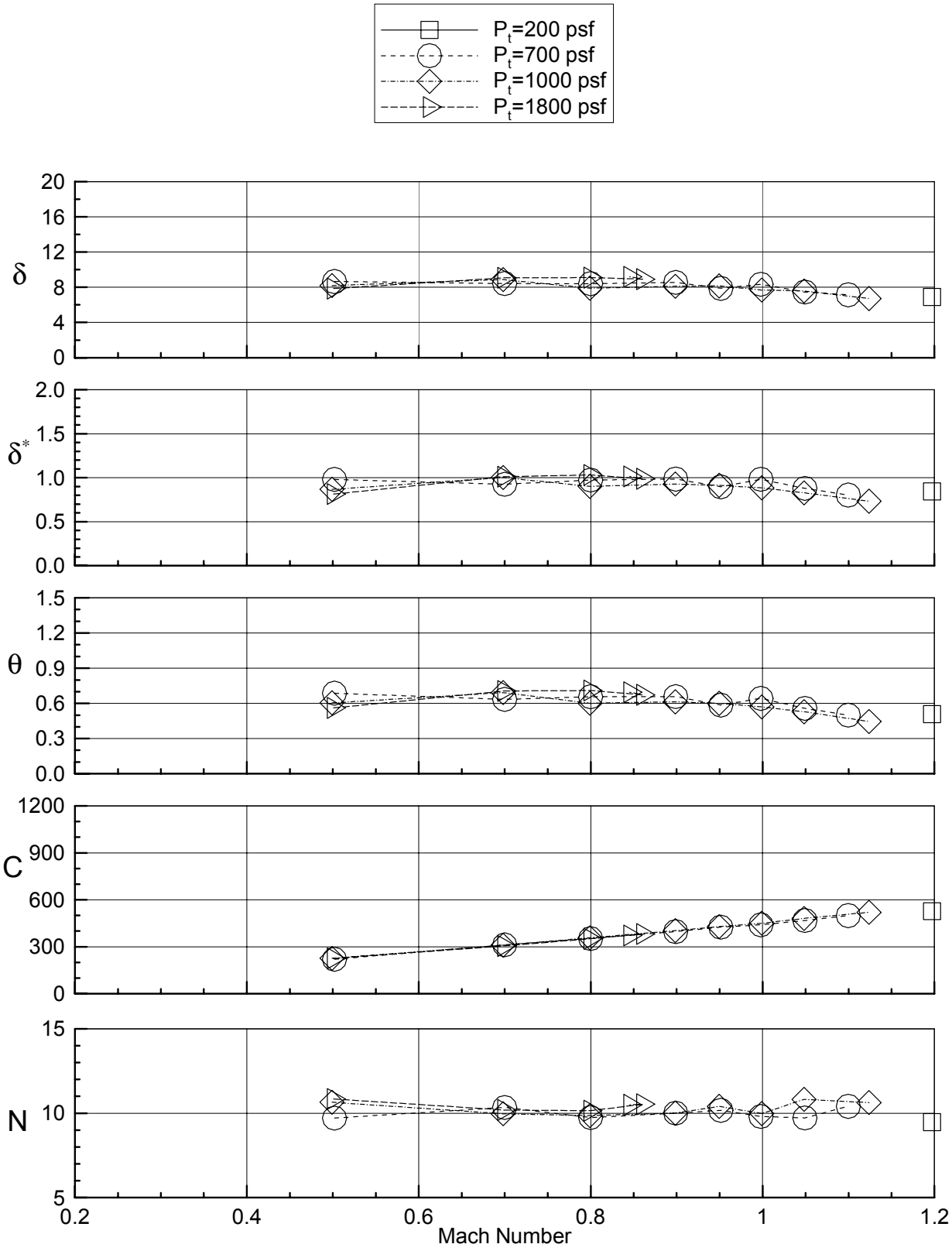

c) West ceiling rake

Figure 18. - continued.

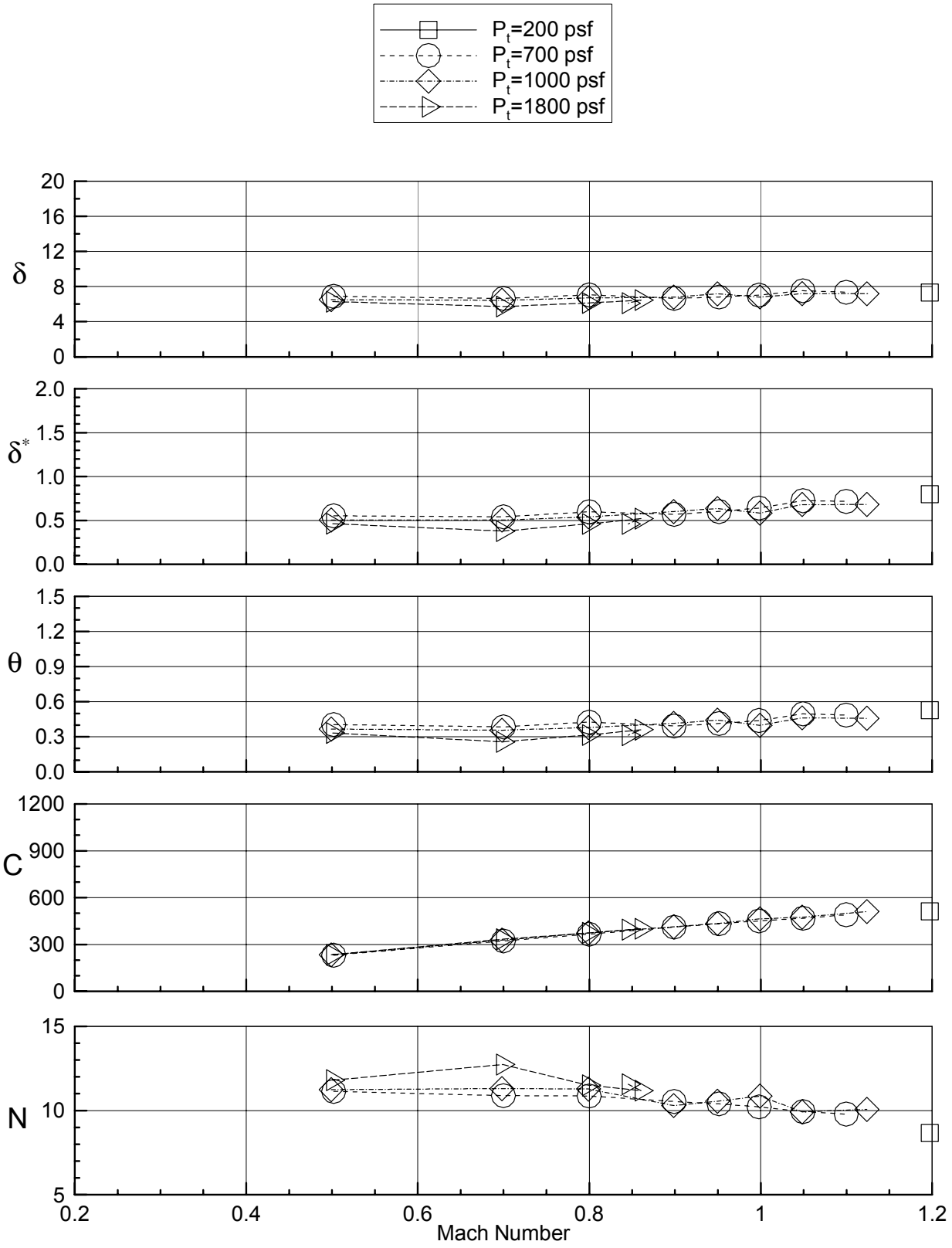

d) West wall rake

Figure 18. - continued.

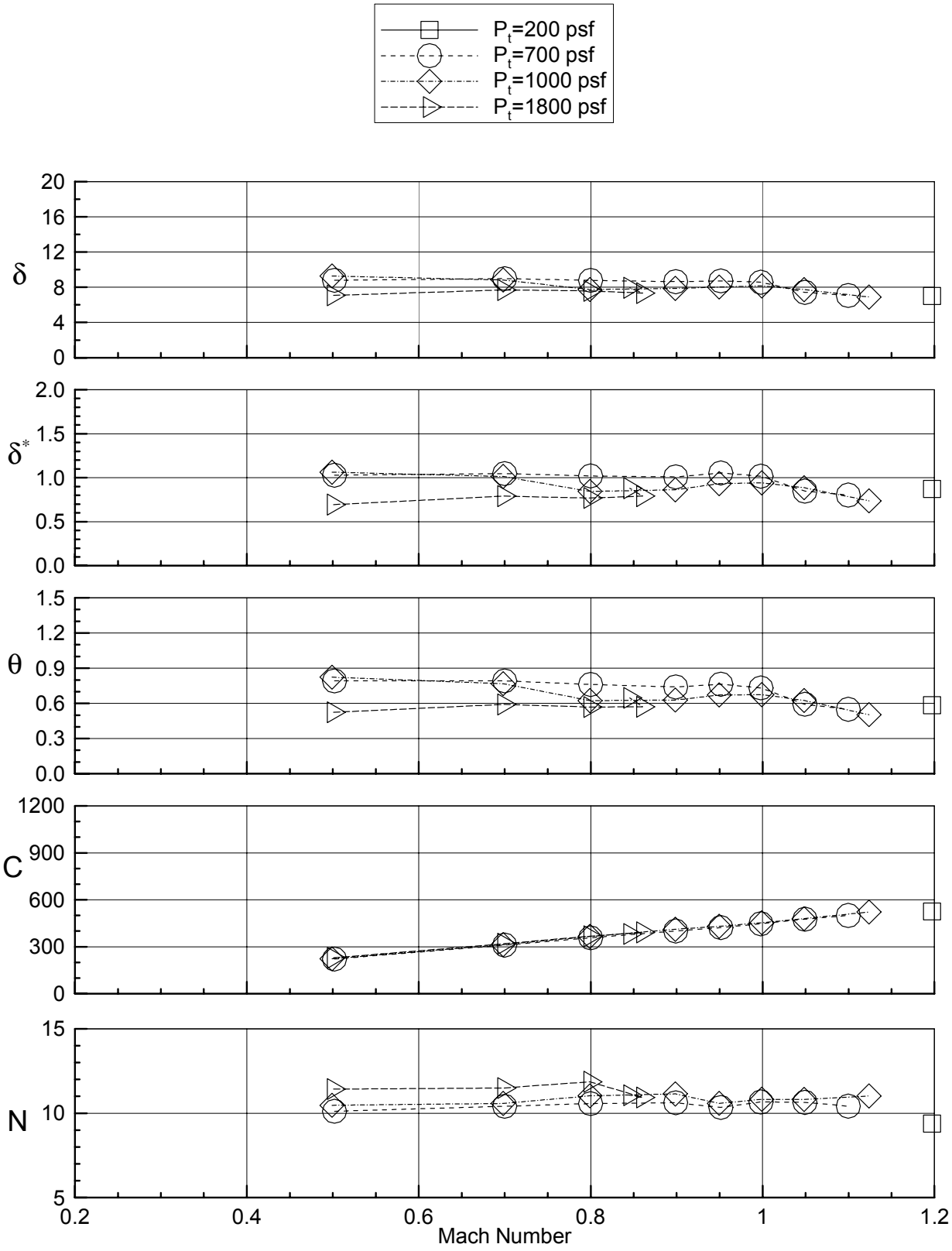

e) West floor rake

Figure 18. - continued.

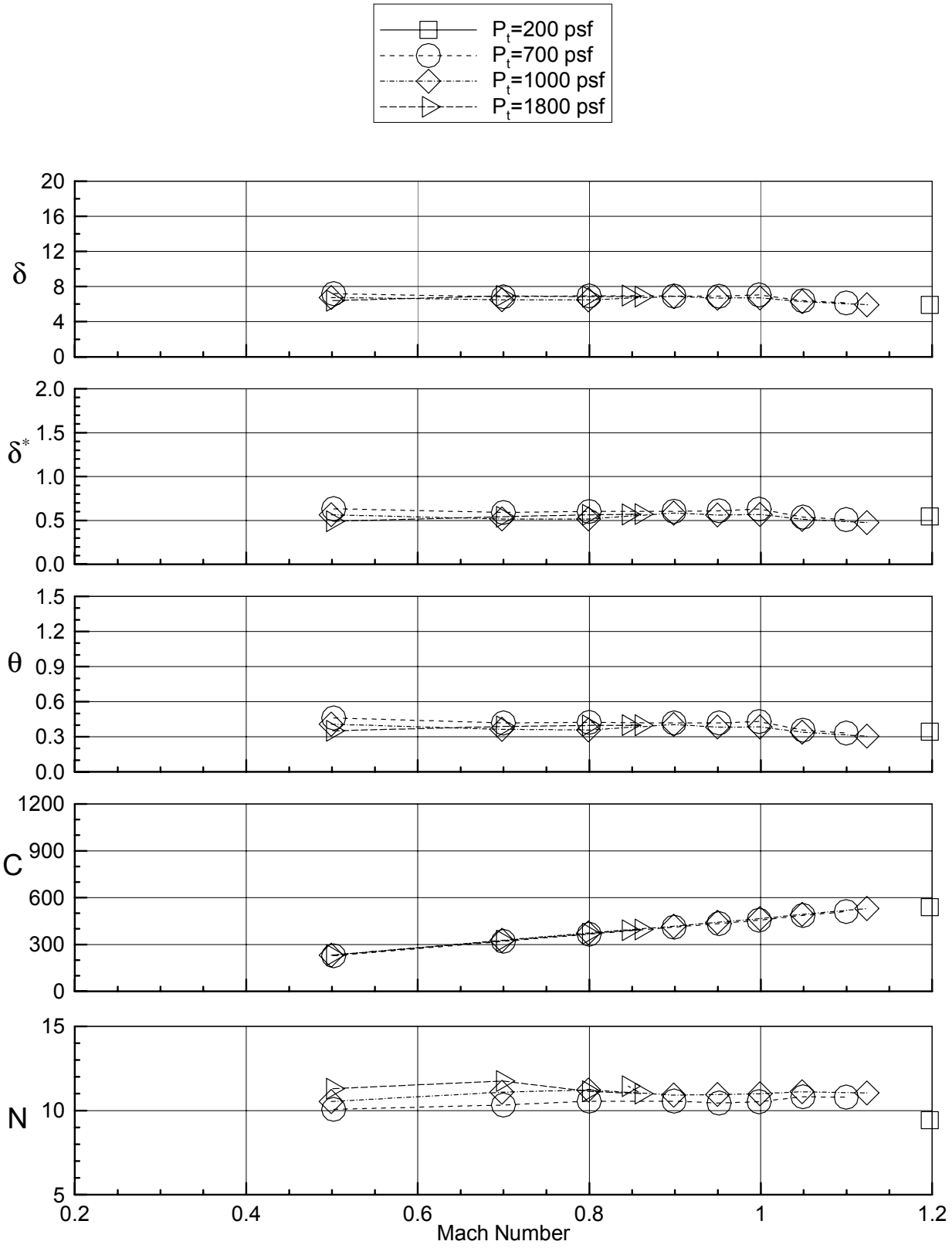

f) East floor rake

Figure 18. - continued.

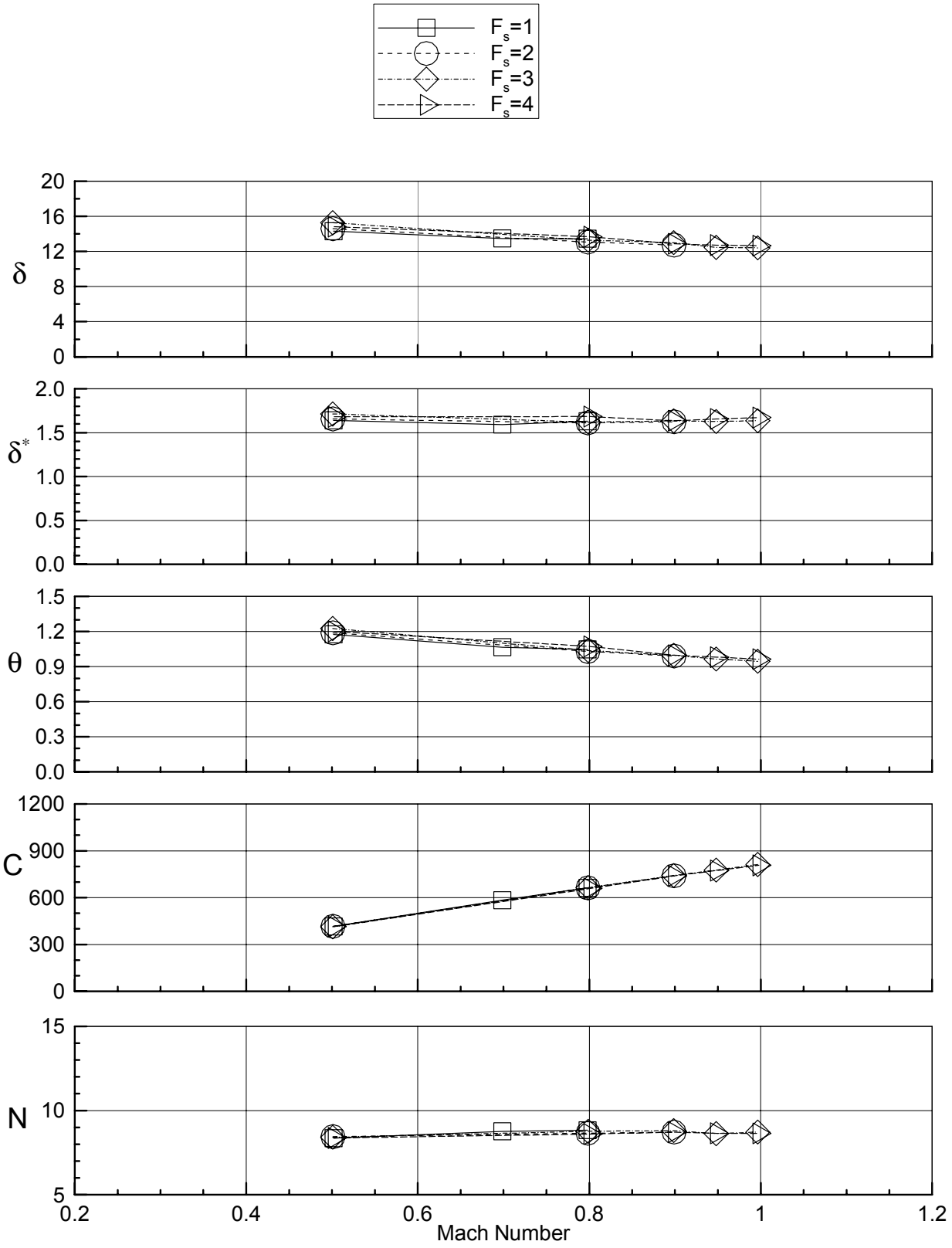

a) East wall rake

Figure 19. Boundary layer parameters for air, P_t=400 psf, all slots open, TS 72, effect of flap settings

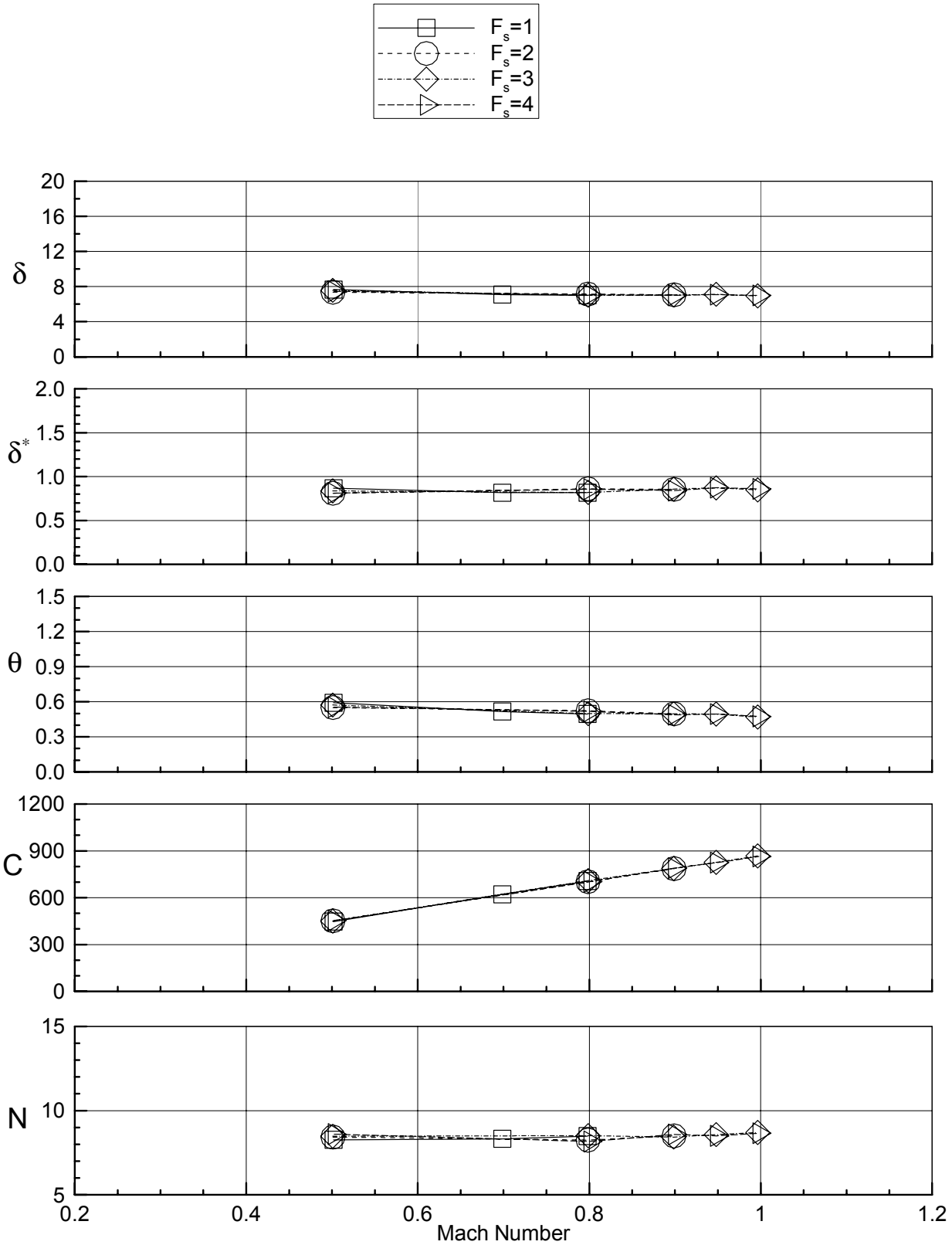

b) East ceiling rake

Figure 19. - continued.

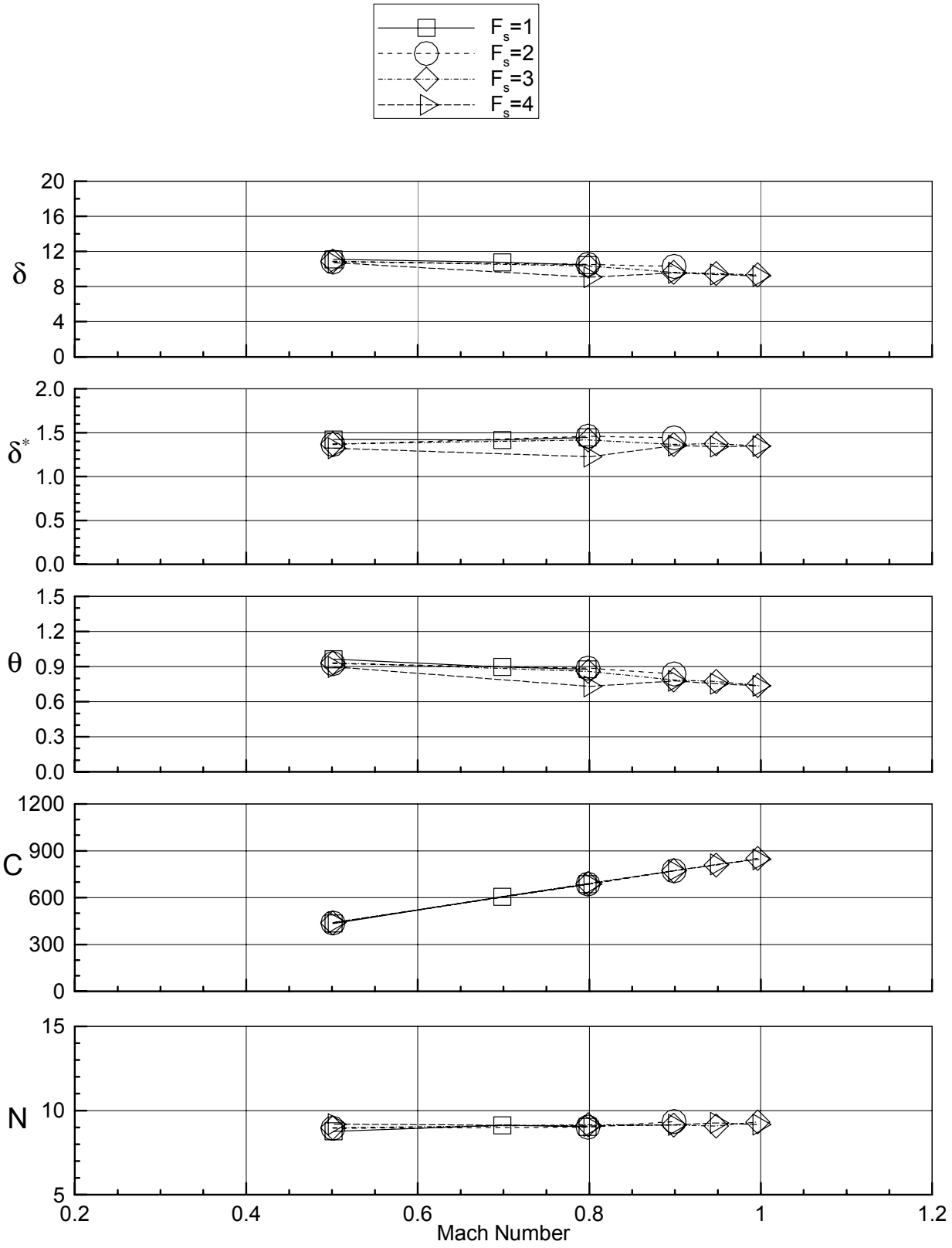

c) West ceiling rake

Figure 19. - continued.

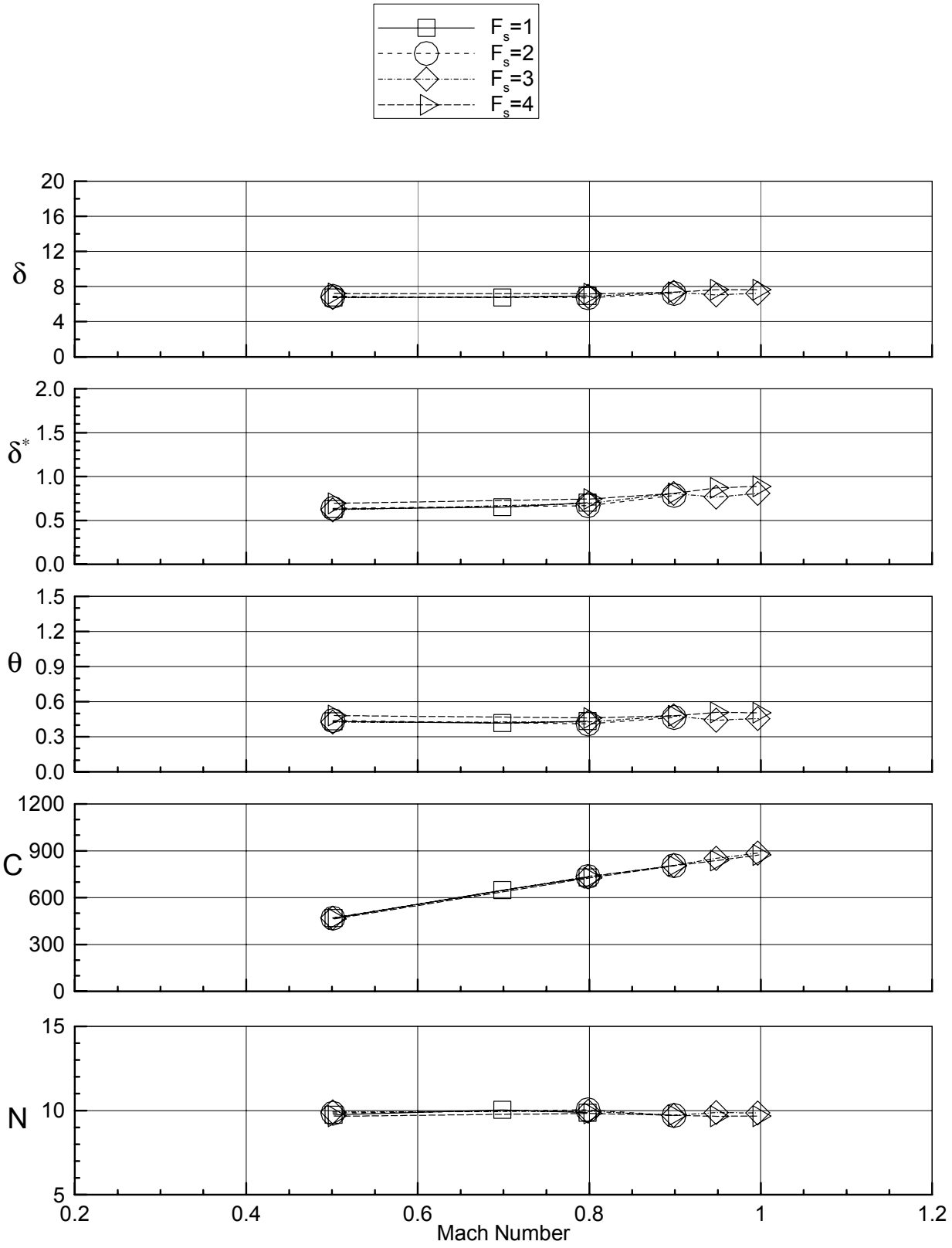

d) West wall rake

Figure 19. - continued.

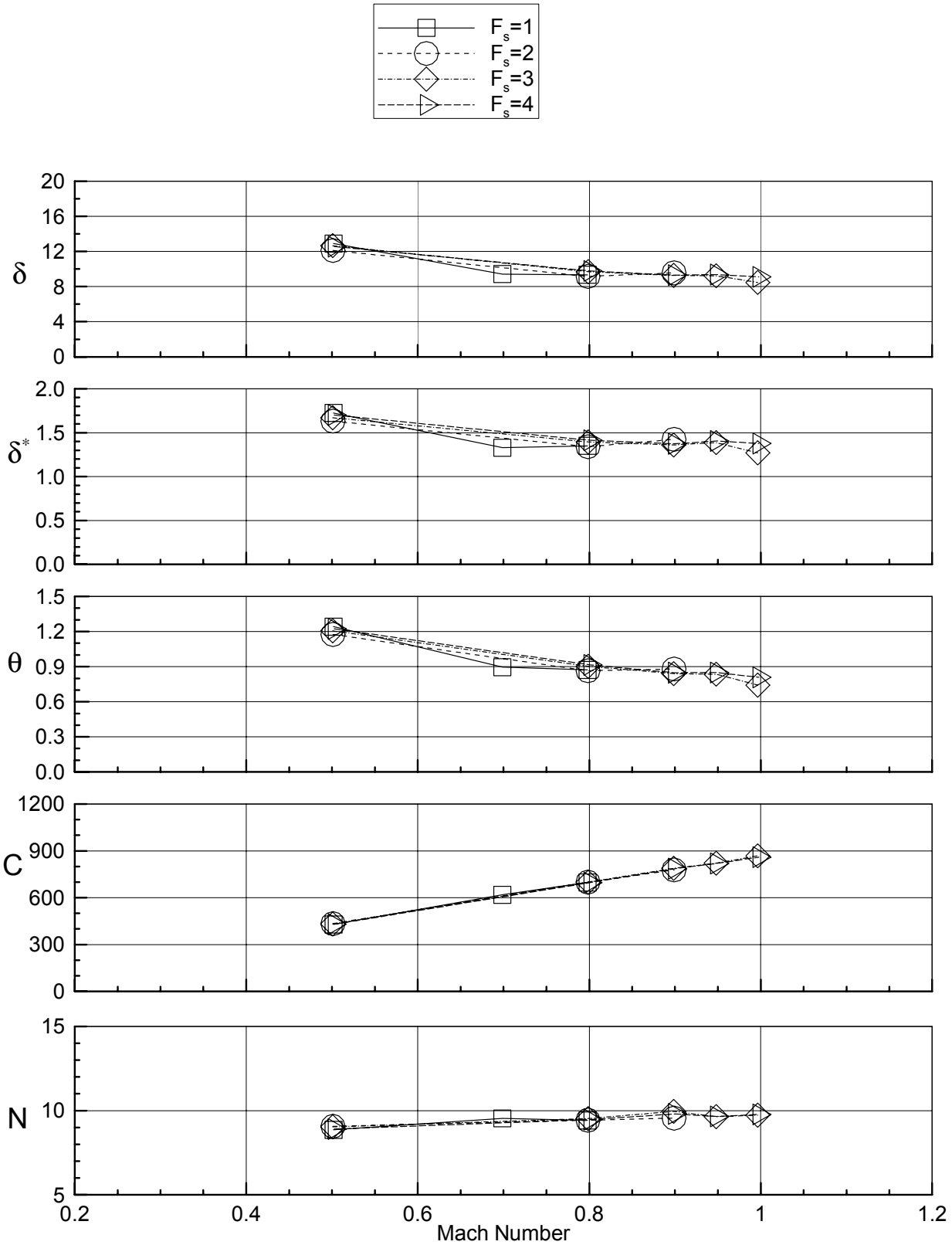

e) West floor rake

Figure 19. - continued.

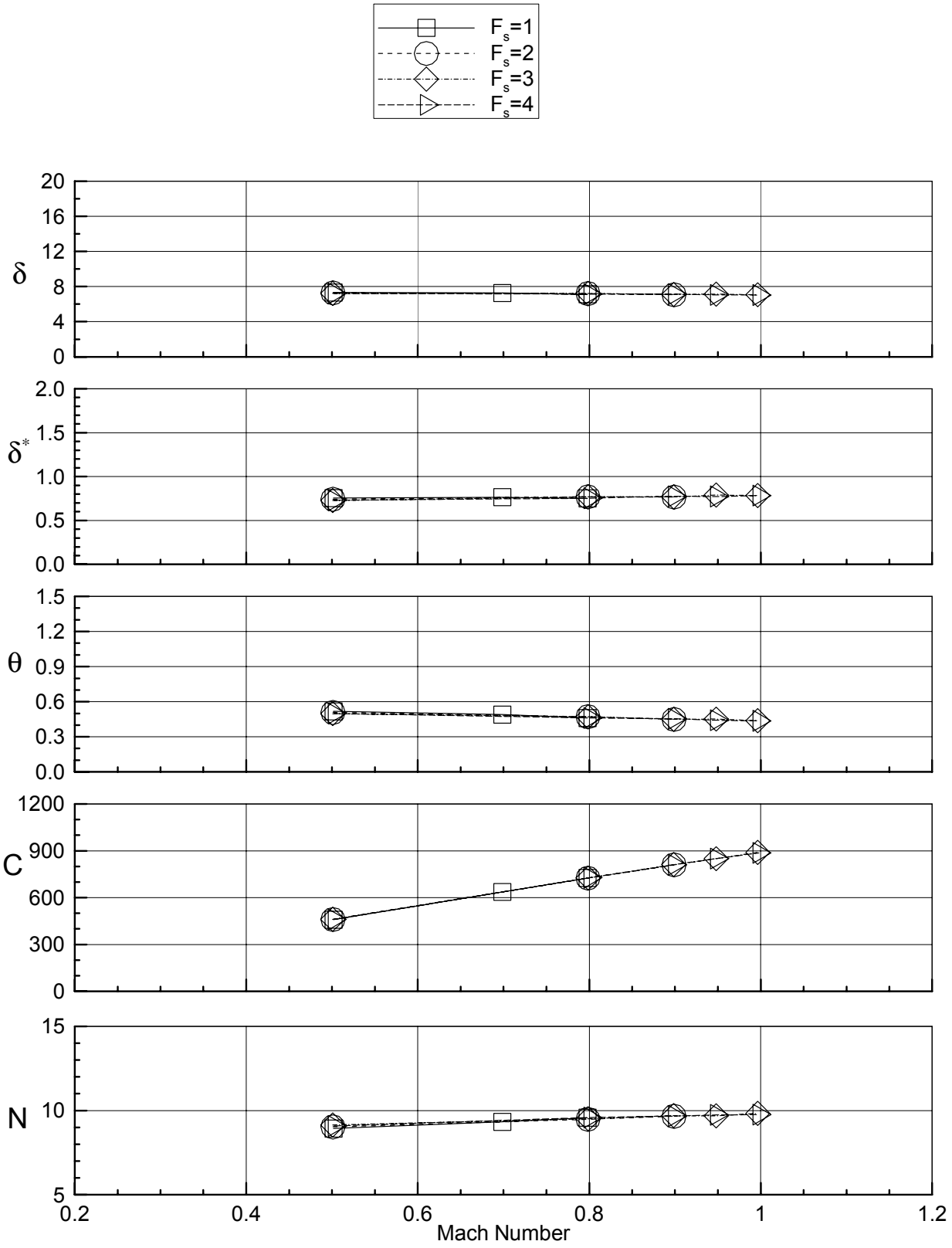

f) East floor rake

Figure 19. - continued.

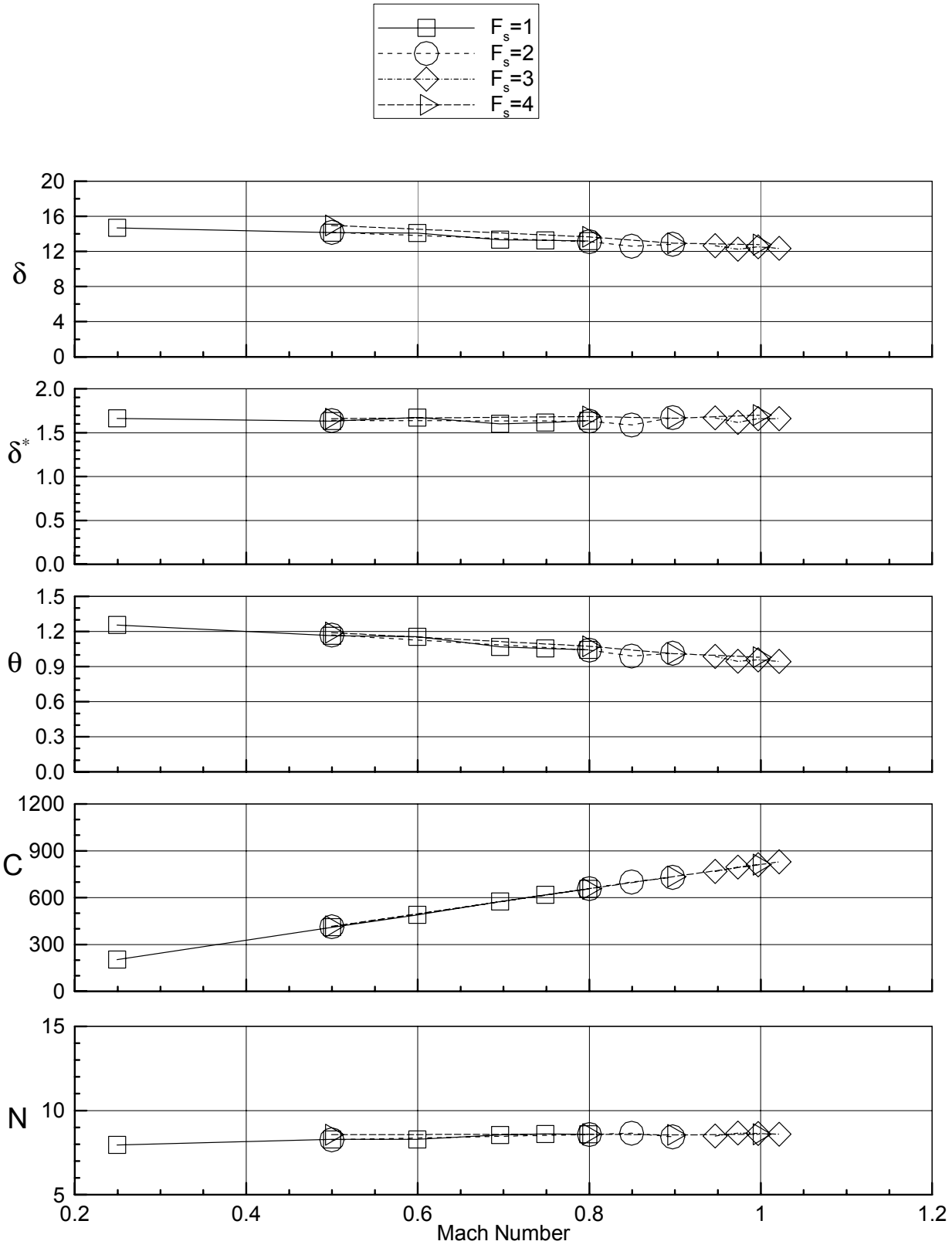

a) East wall rake

Figure 20. Boundary layer parameters for air, P_t=400 psf, East Wall slots closed, TS 72, effect of flap settings

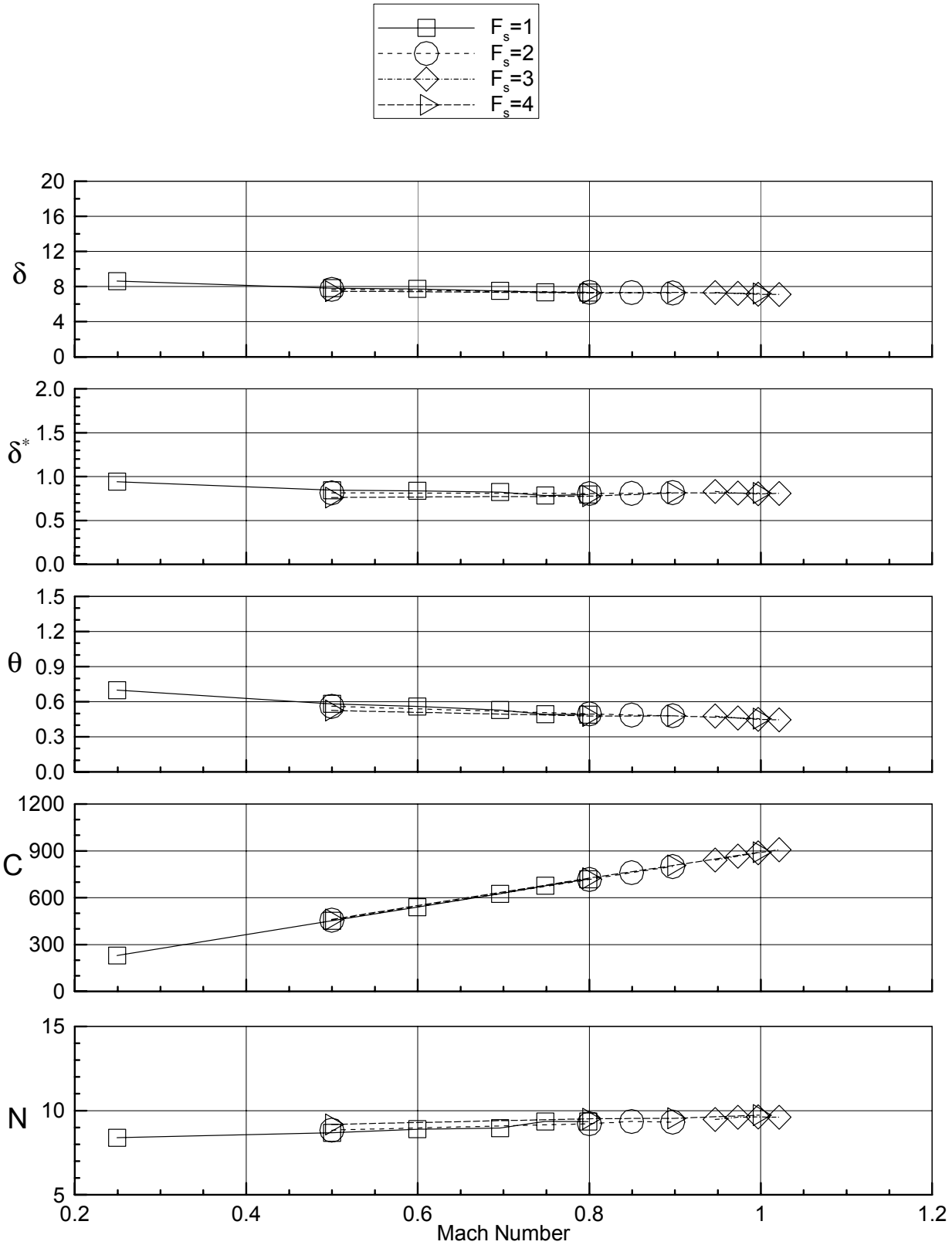

b) East ceiling rake

Figure 20. - continued.

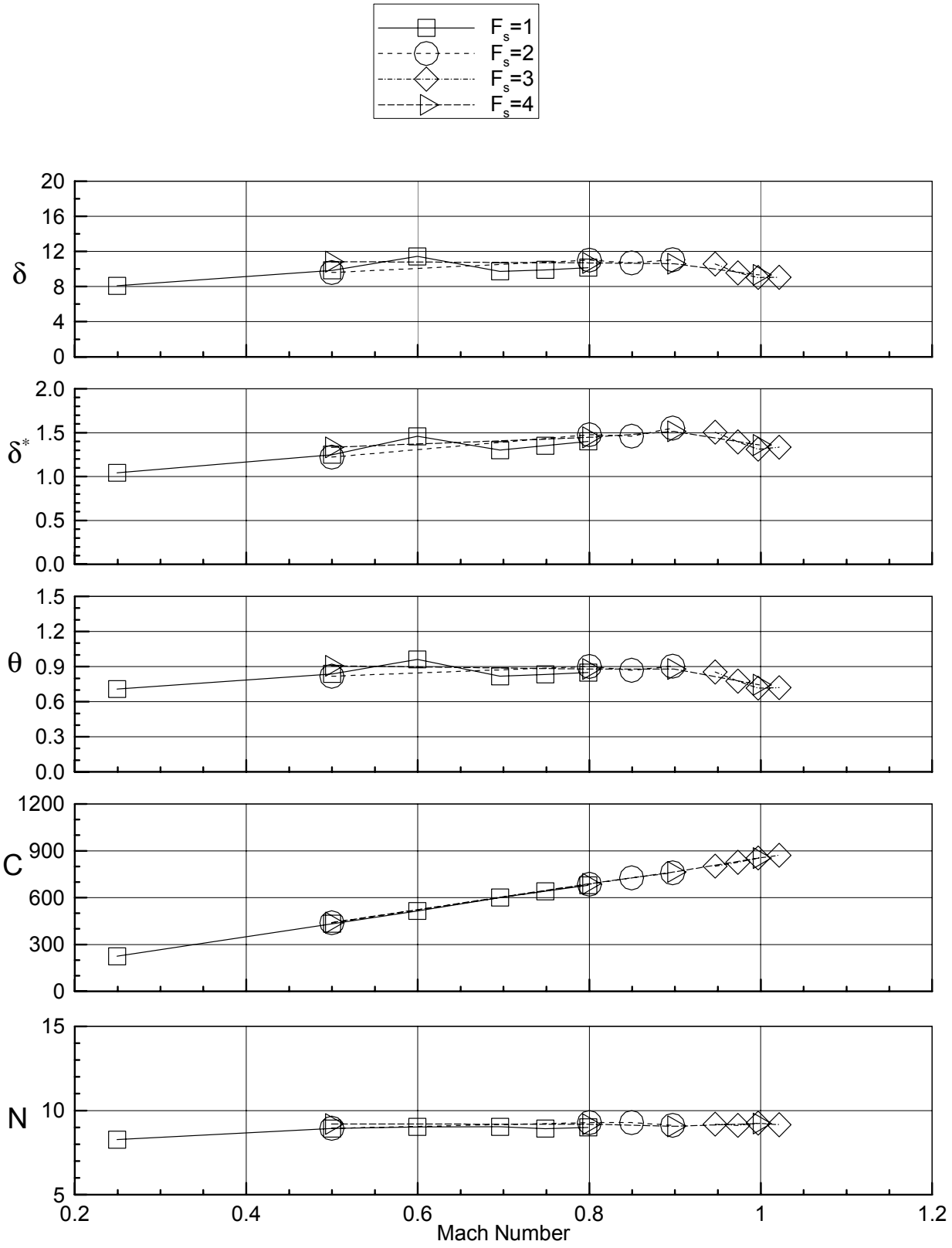

c) West ceiling rake

Figure 20. - continued.

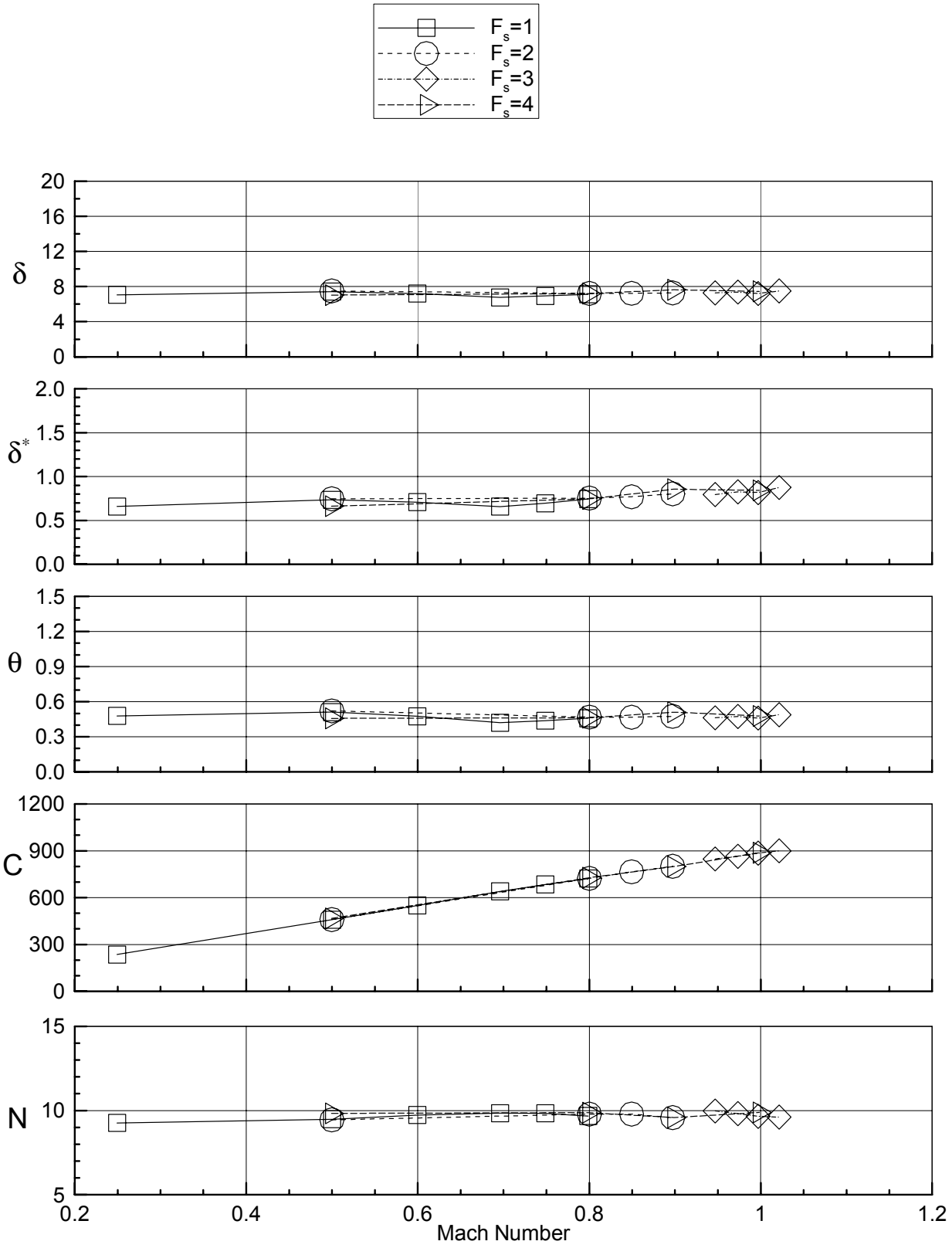

d) West wall rake

Figure 20. - continued.

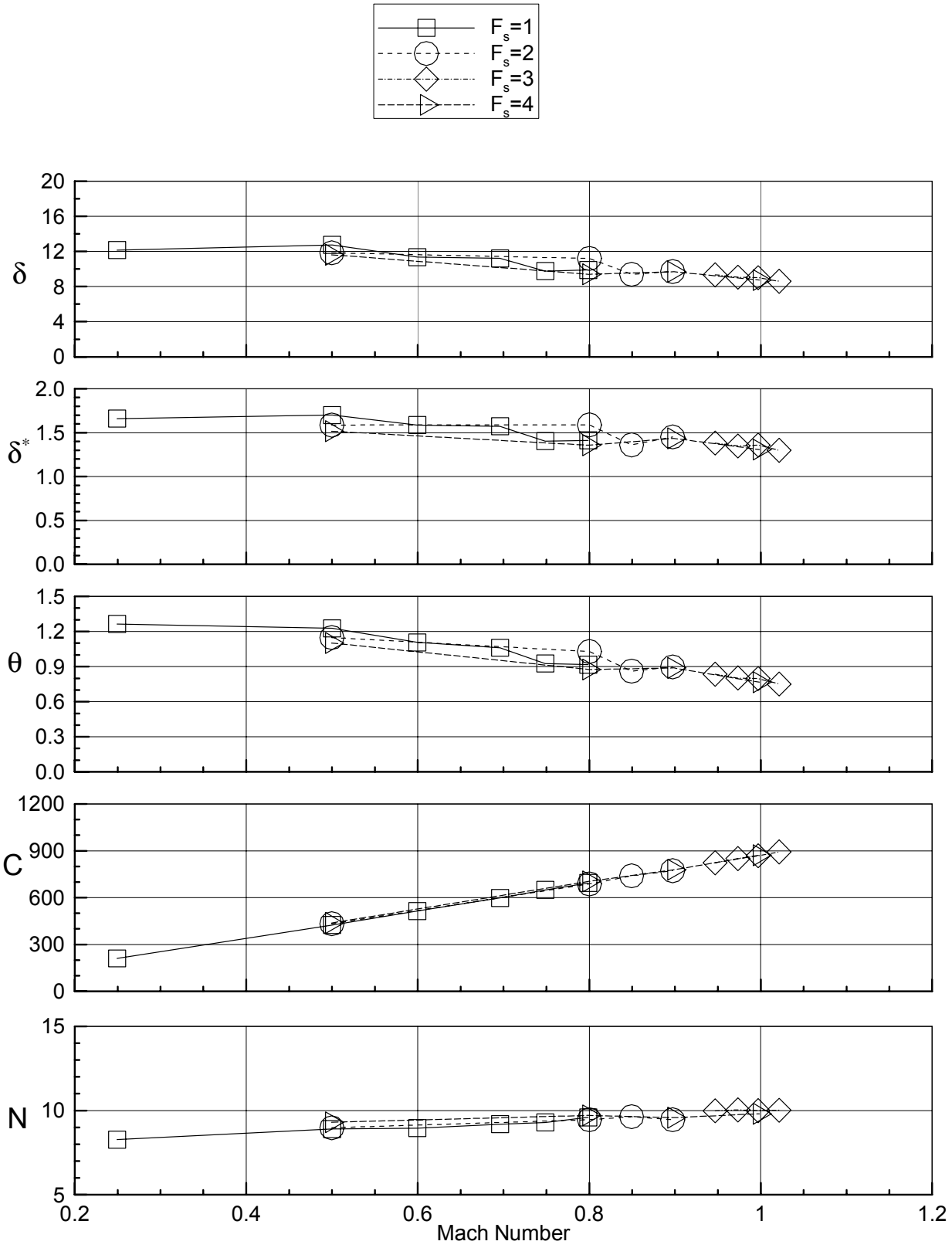

e) West floor rake

Figure 20. - continued.

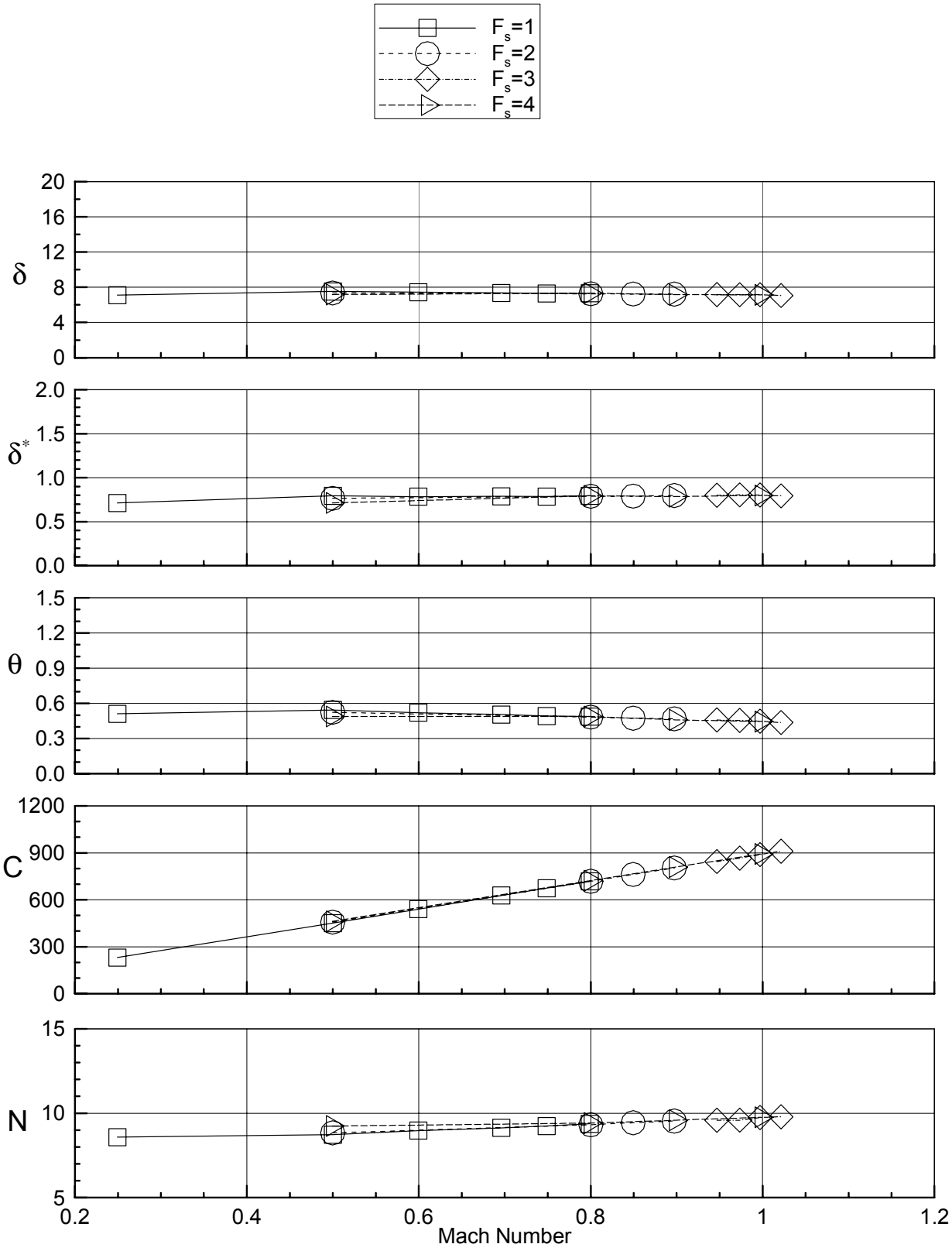

f) East floor rake

Figure 20. - continued.

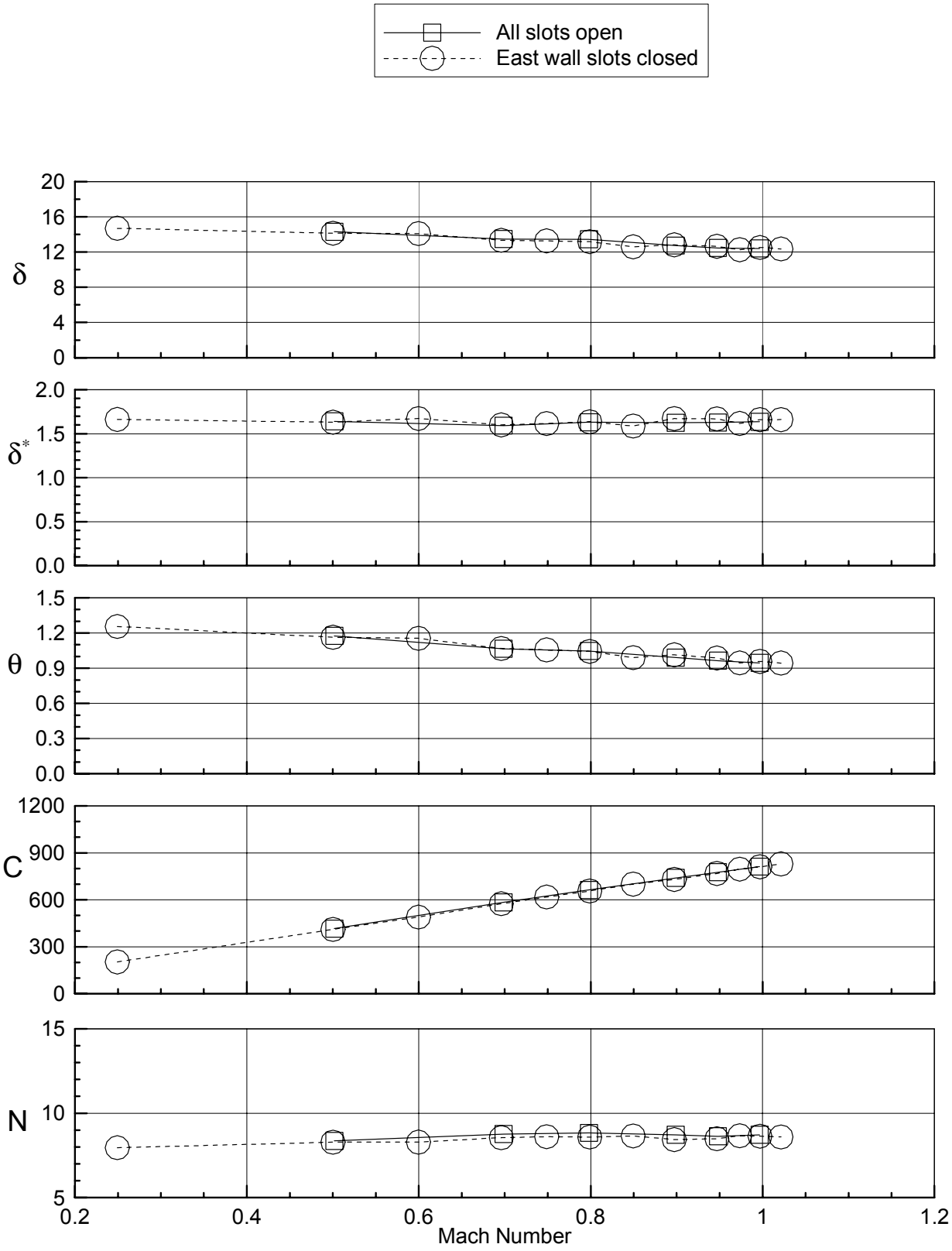

a) East wall rake

Figure 21. Boundary layer parameters for air, P_t=400 psf, standard flap settings, TS 72, slot effect.

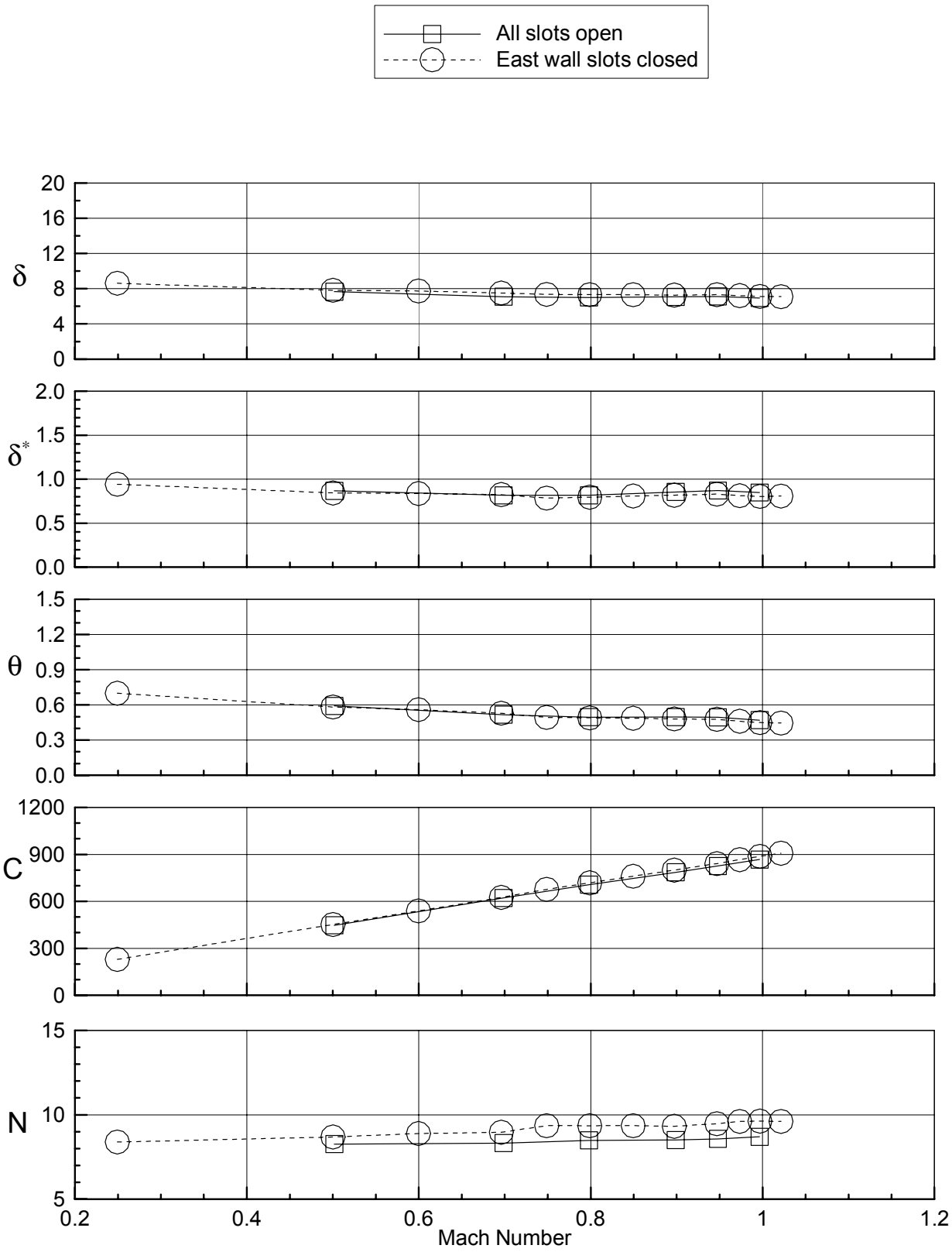

b) East ceiling rake

Figure 21. - continued.

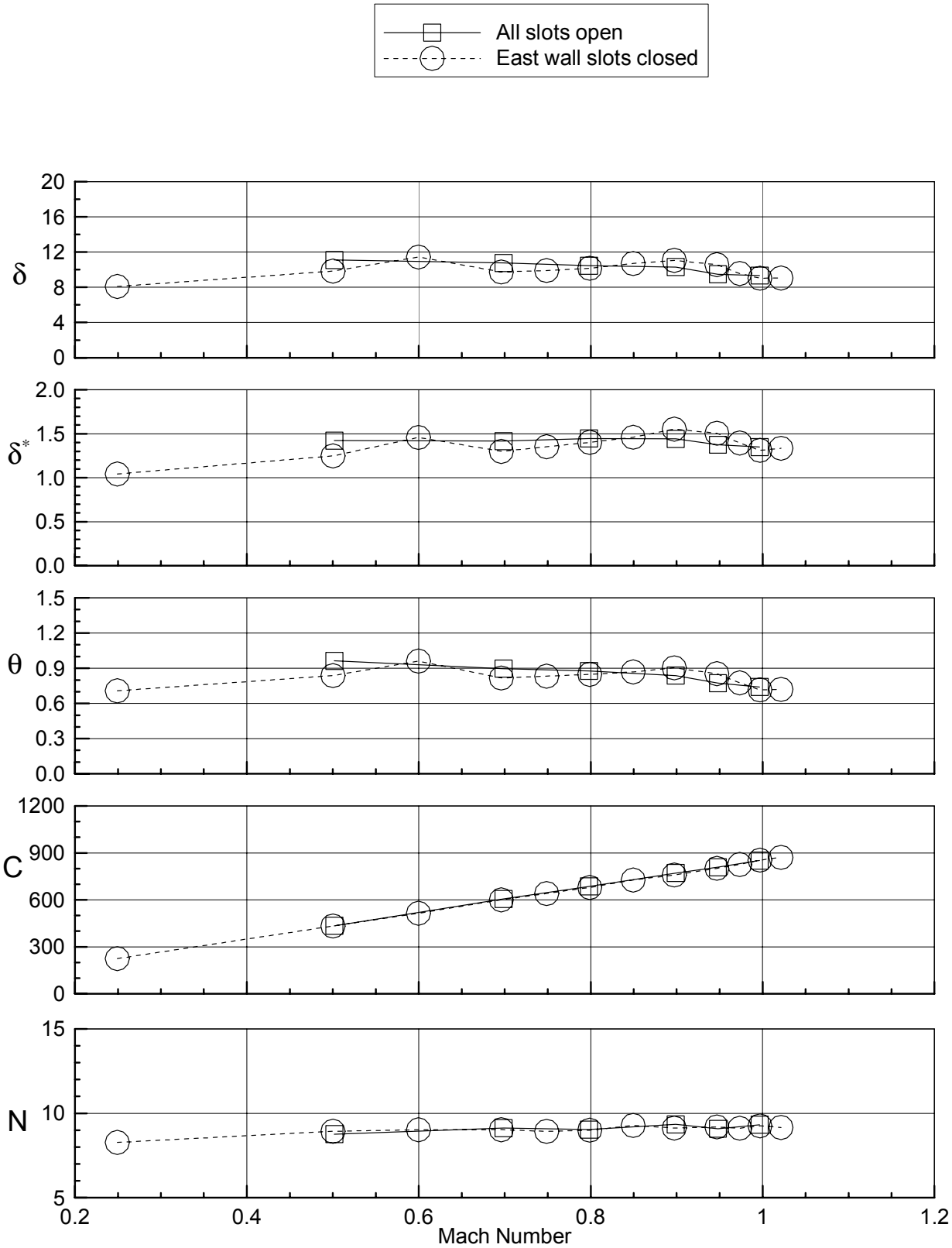

c) West ceiling rake

Figure 21. - continued.

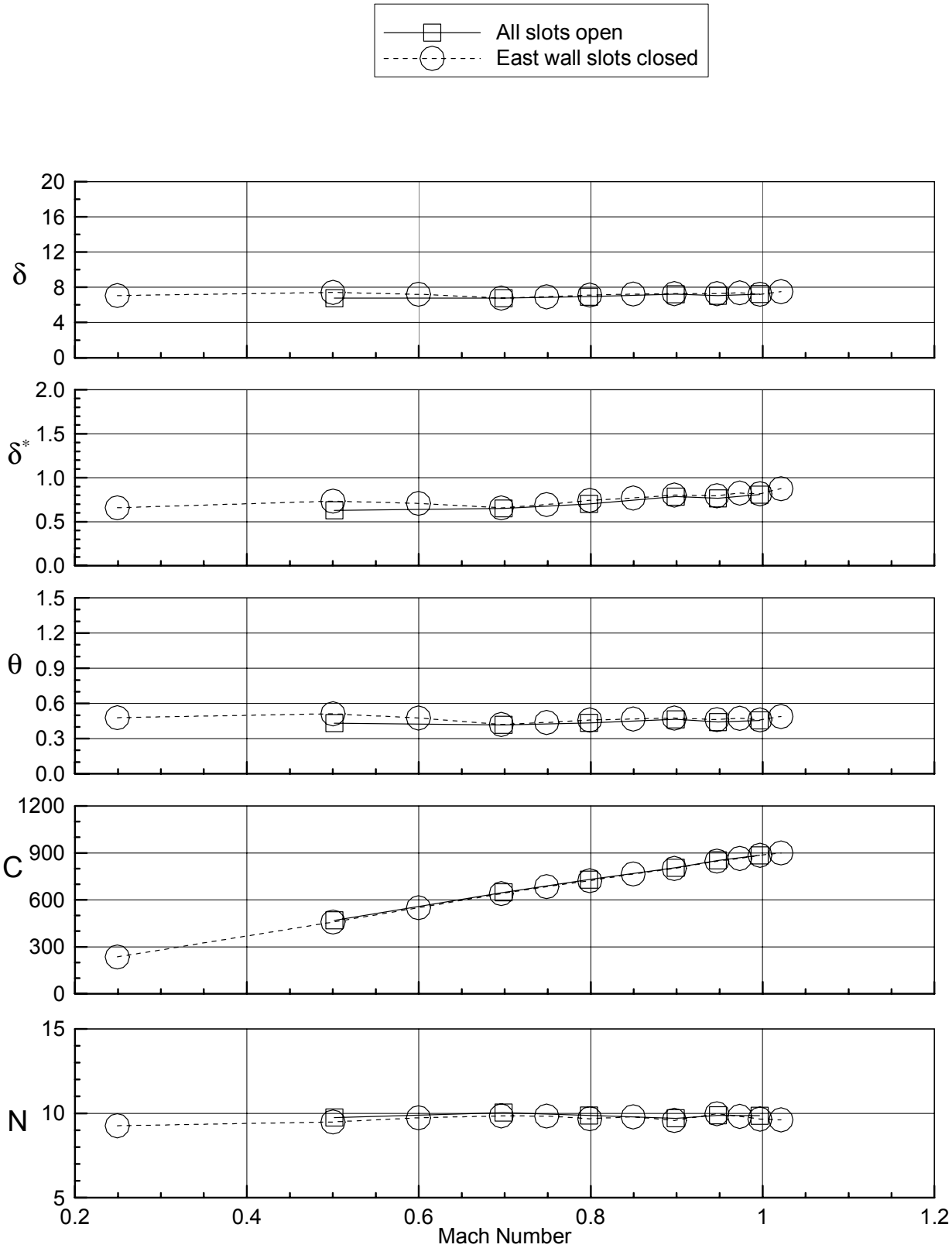

d) West wall rake

Figure 21. - continued.

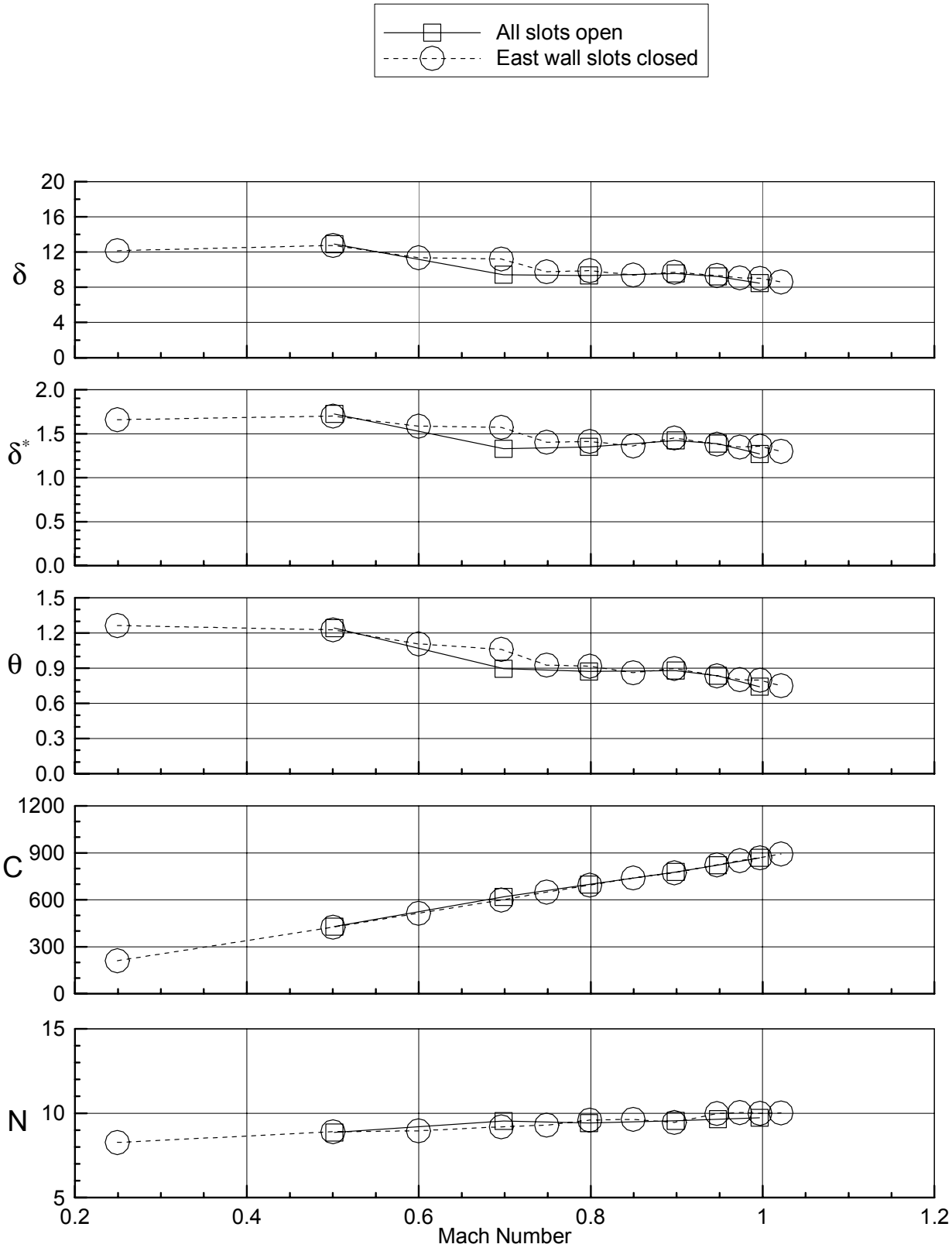

e) West floor rake

Figure 21. - continued.

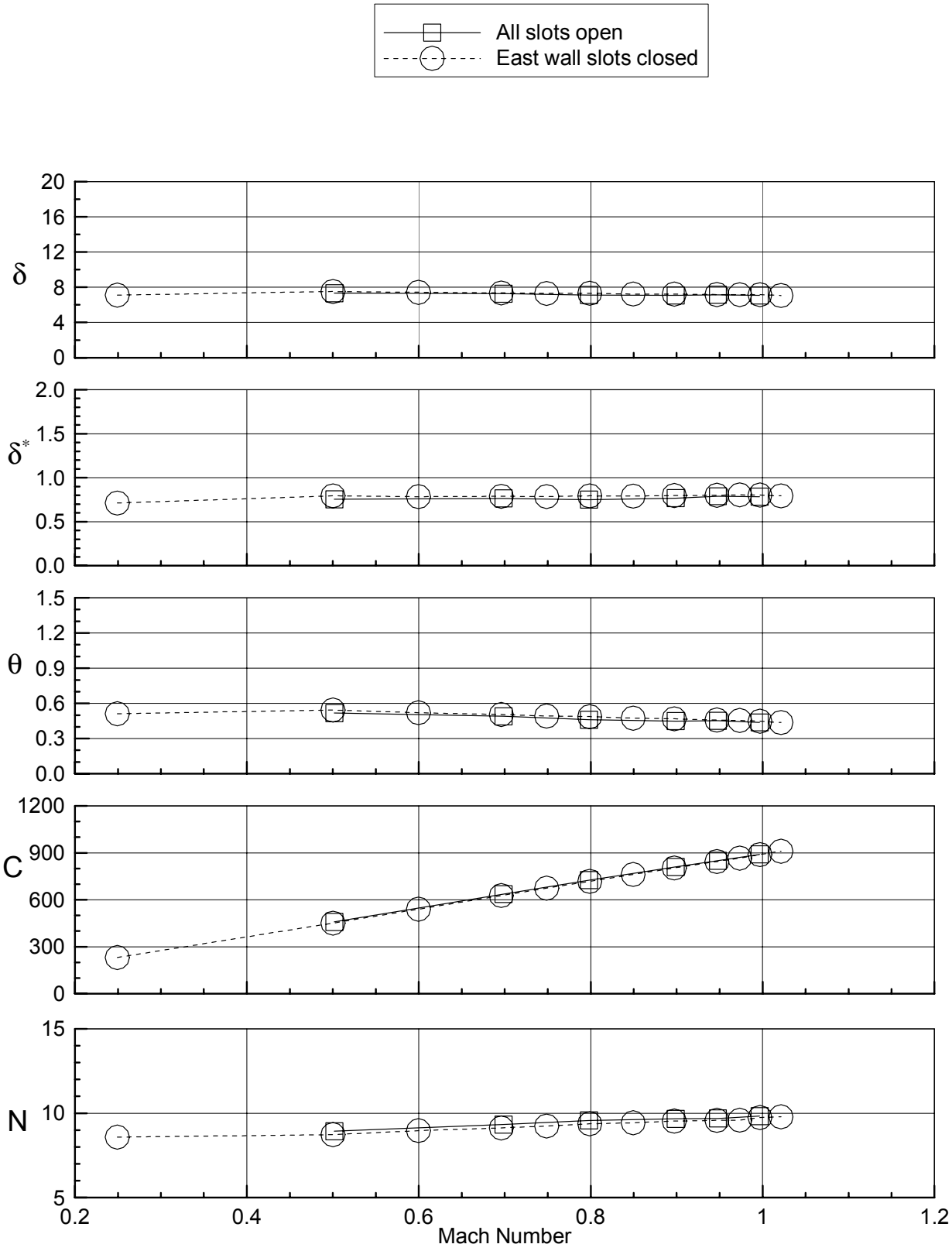

f) East floor rake

Figure 21. - continued.

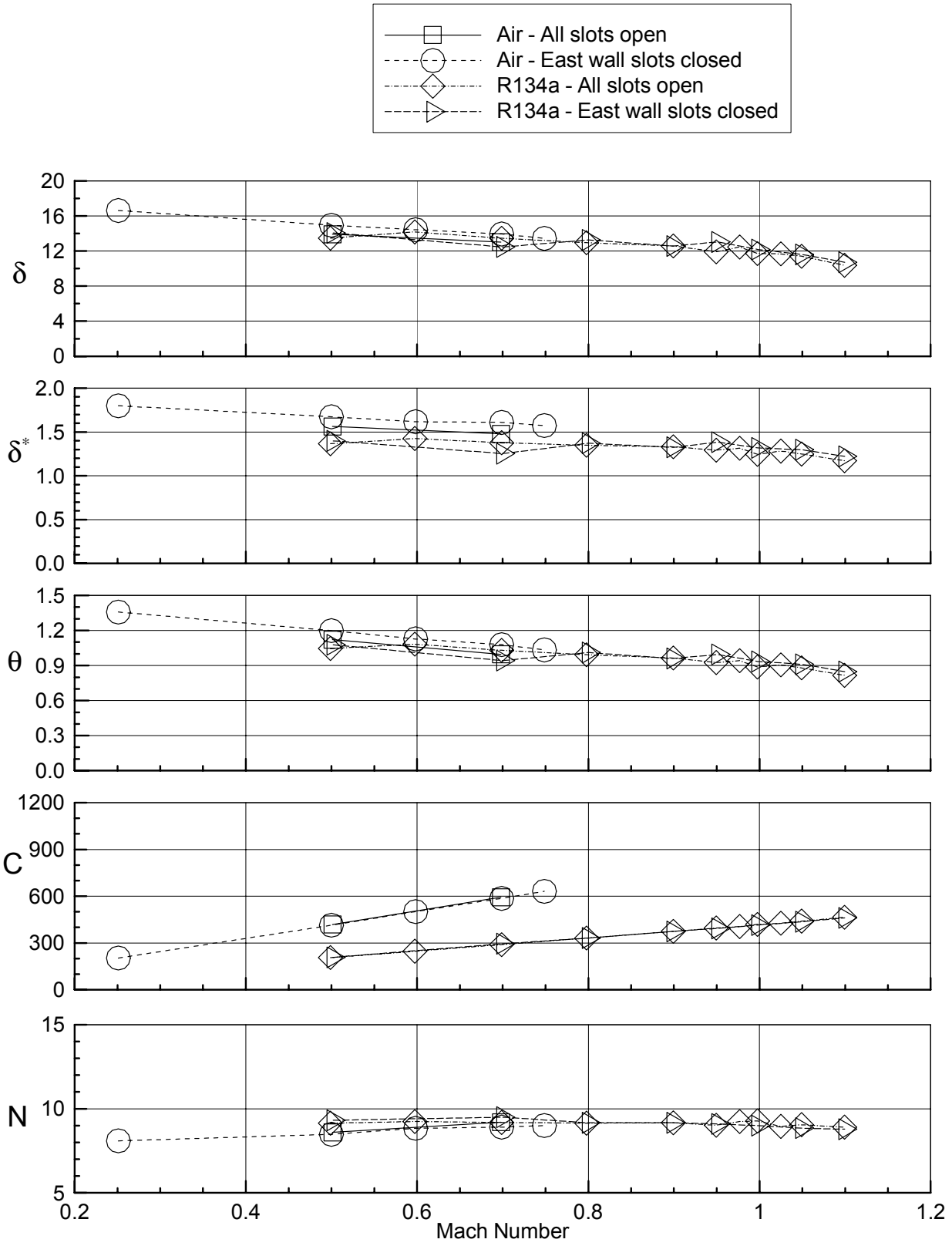

a) East wall rake

Figure 22. Boundary layer parameters for air and R-134a, standard flap settings, P_t=700 psf, TS 72, slot effect.

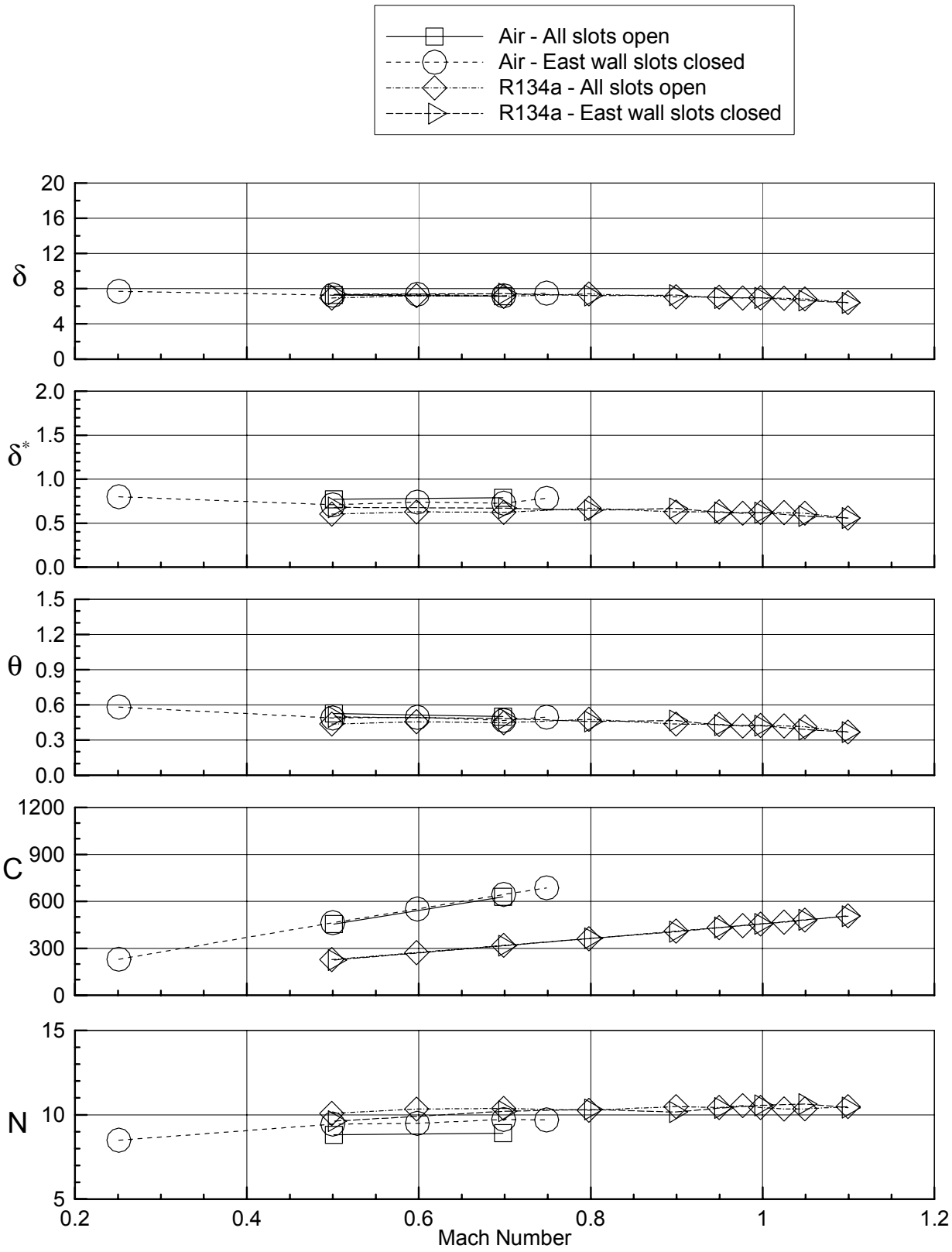

b) East ceiling rake

Figure 22. - continued.

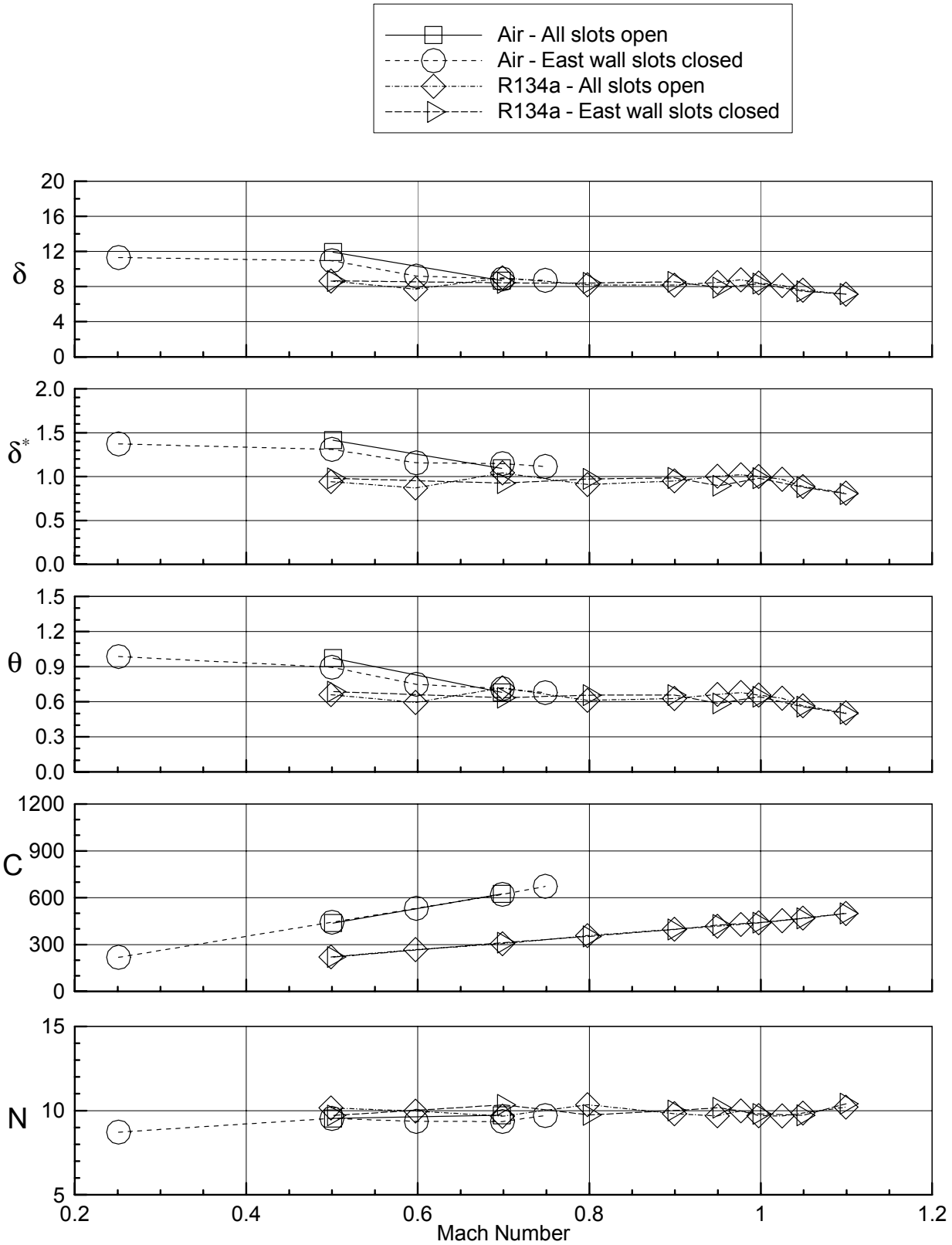

c) West ceiling rake

Figure 22. - continued.

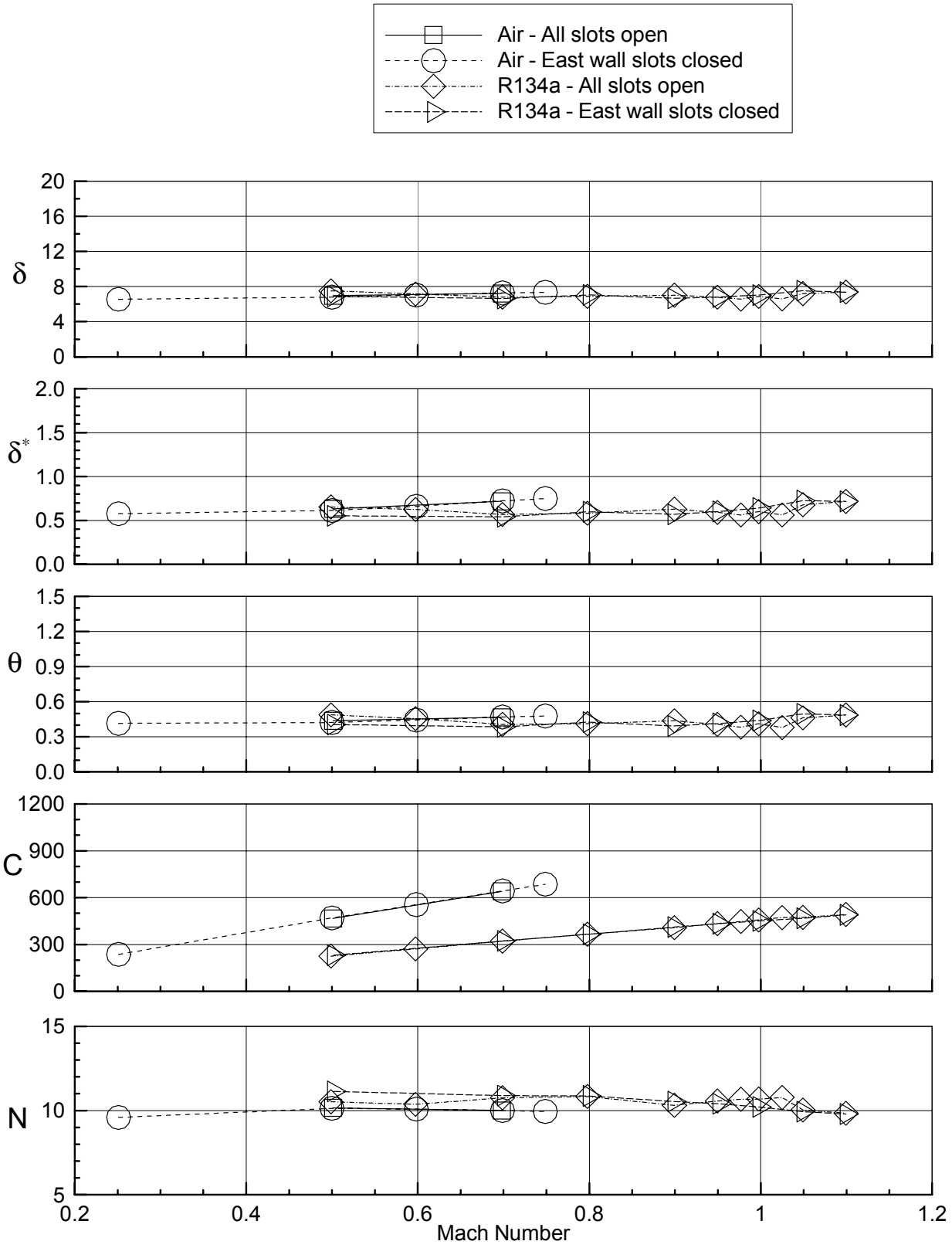

d) West wall rake

Figure 22. - continued.

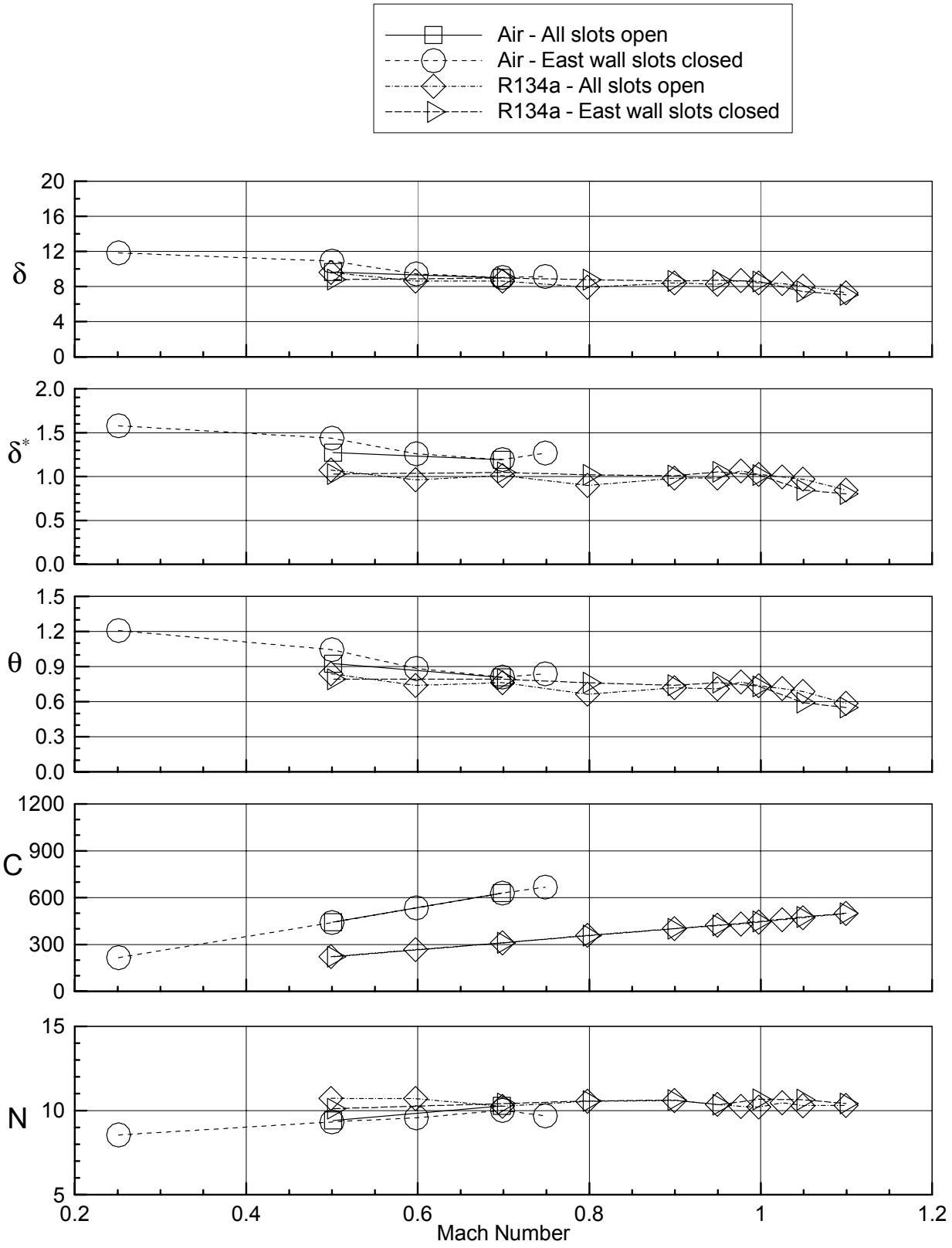

e) West floor rake

Figure 22. - continued.

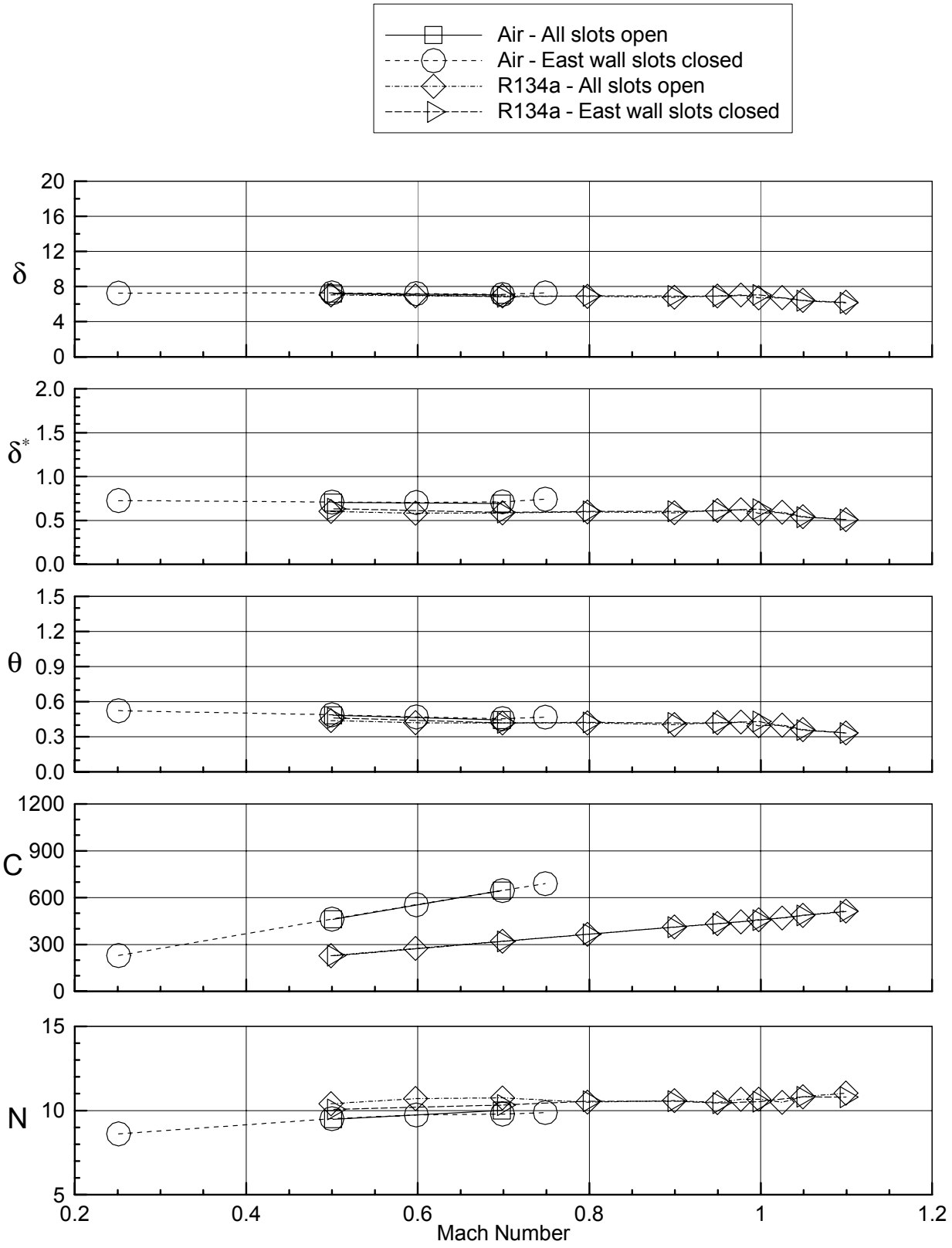

f) East floor rake

Figure 22. - continued.

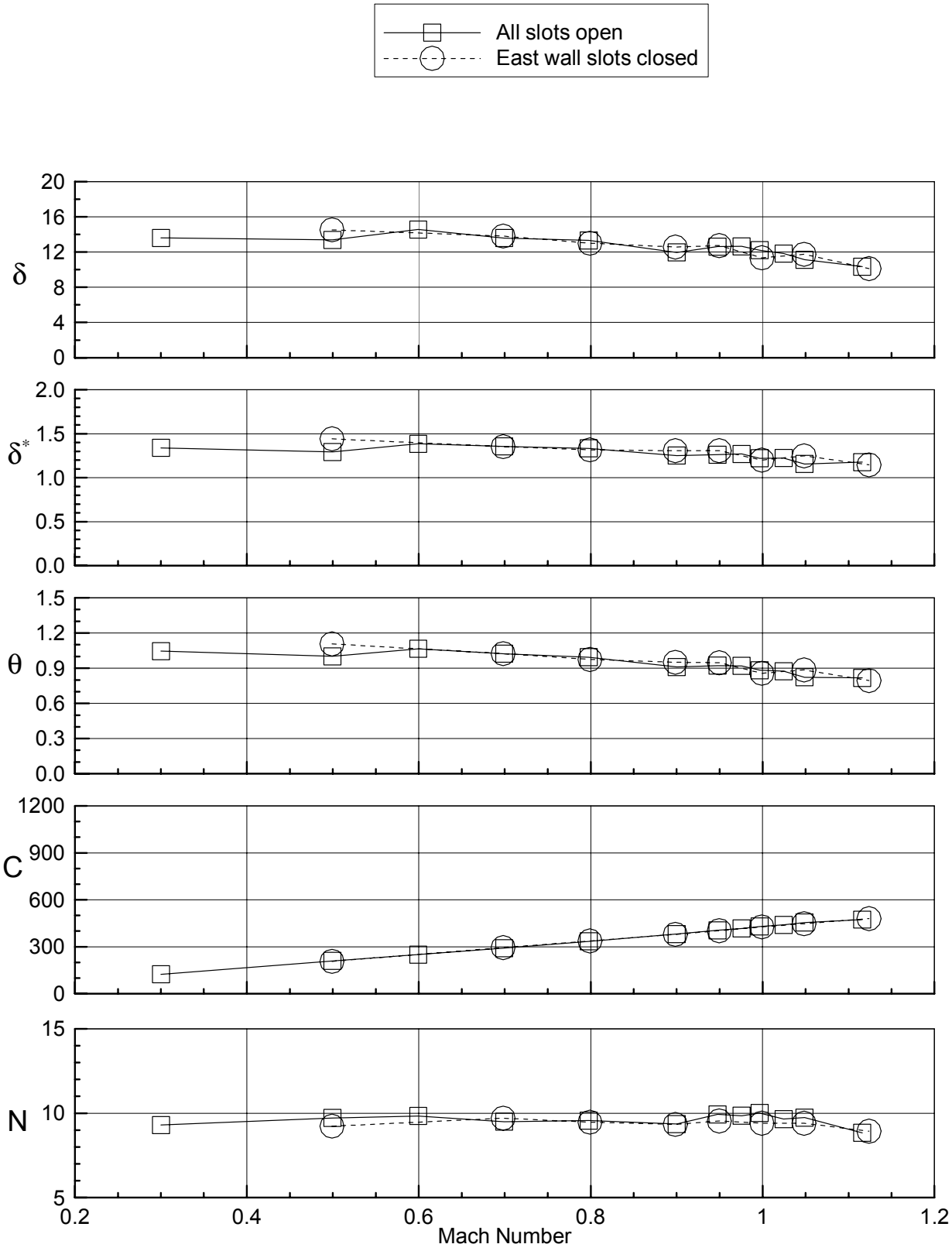

a) East wall rake

Figure 23. Boundary layer parameters for R-134a, P_t=1000 psf, standard flap settings, TS 72, slot effect

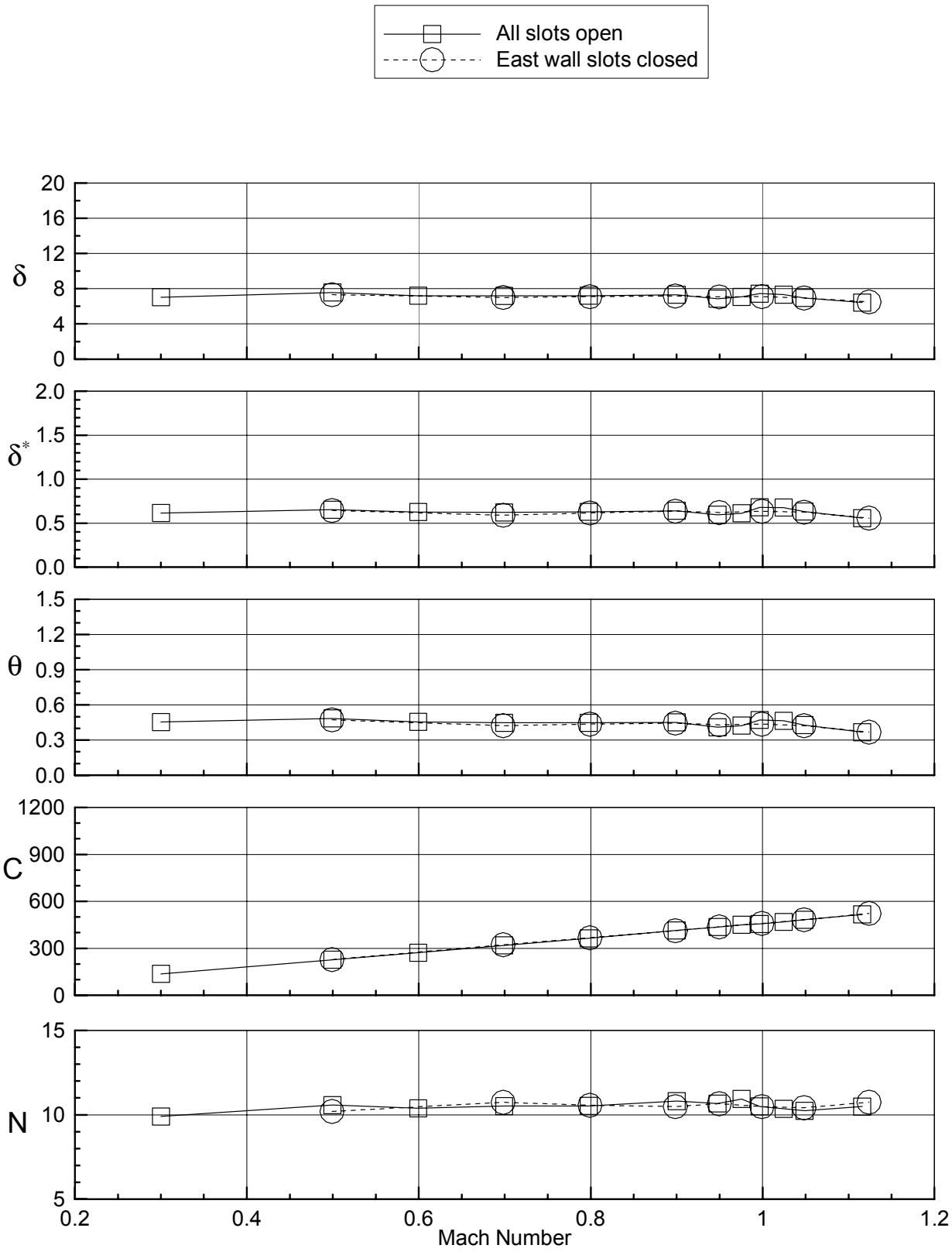

b) East ceiling rake

Figure 23. - continued.

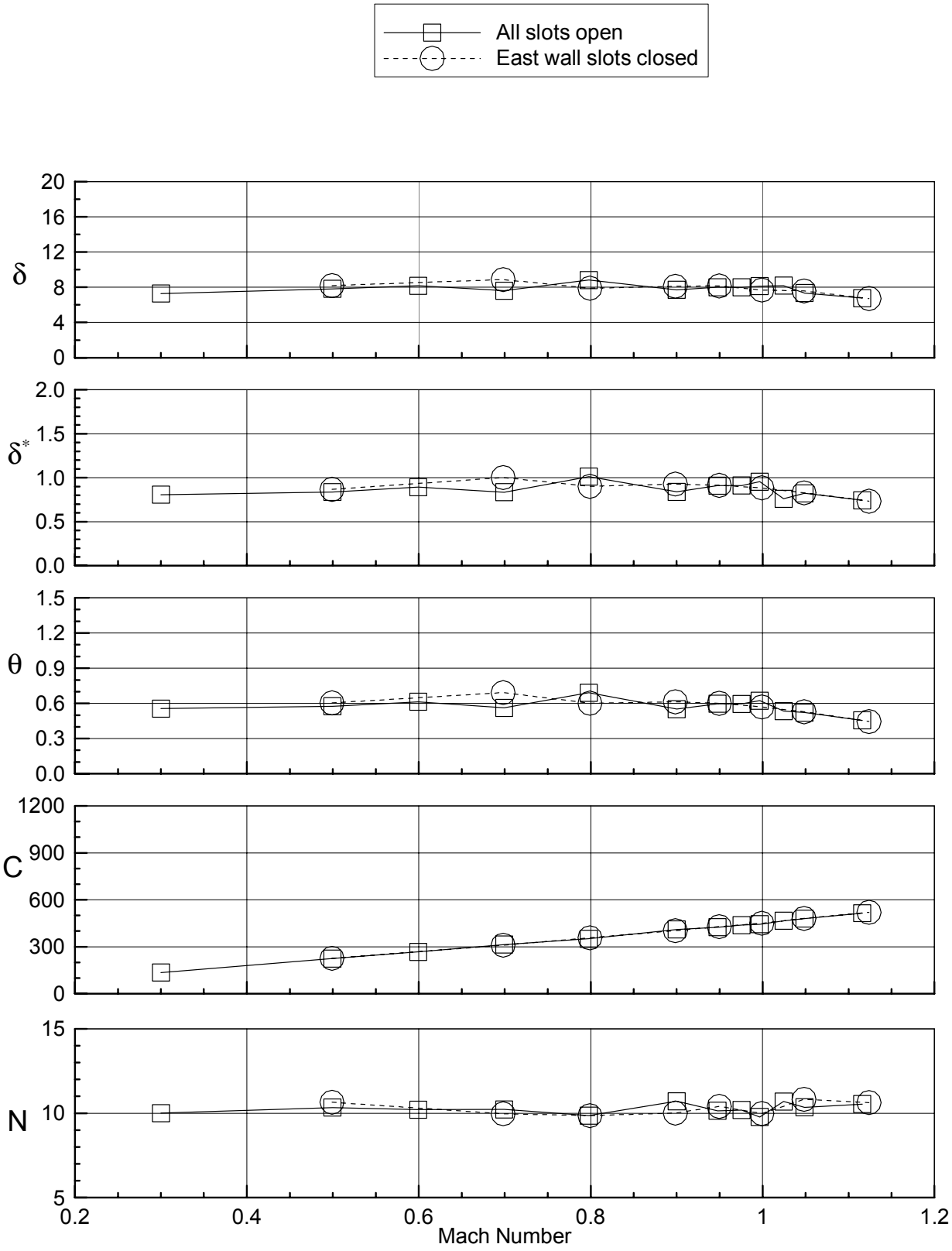

c) West ceiling rake

Figure 23. - continued.

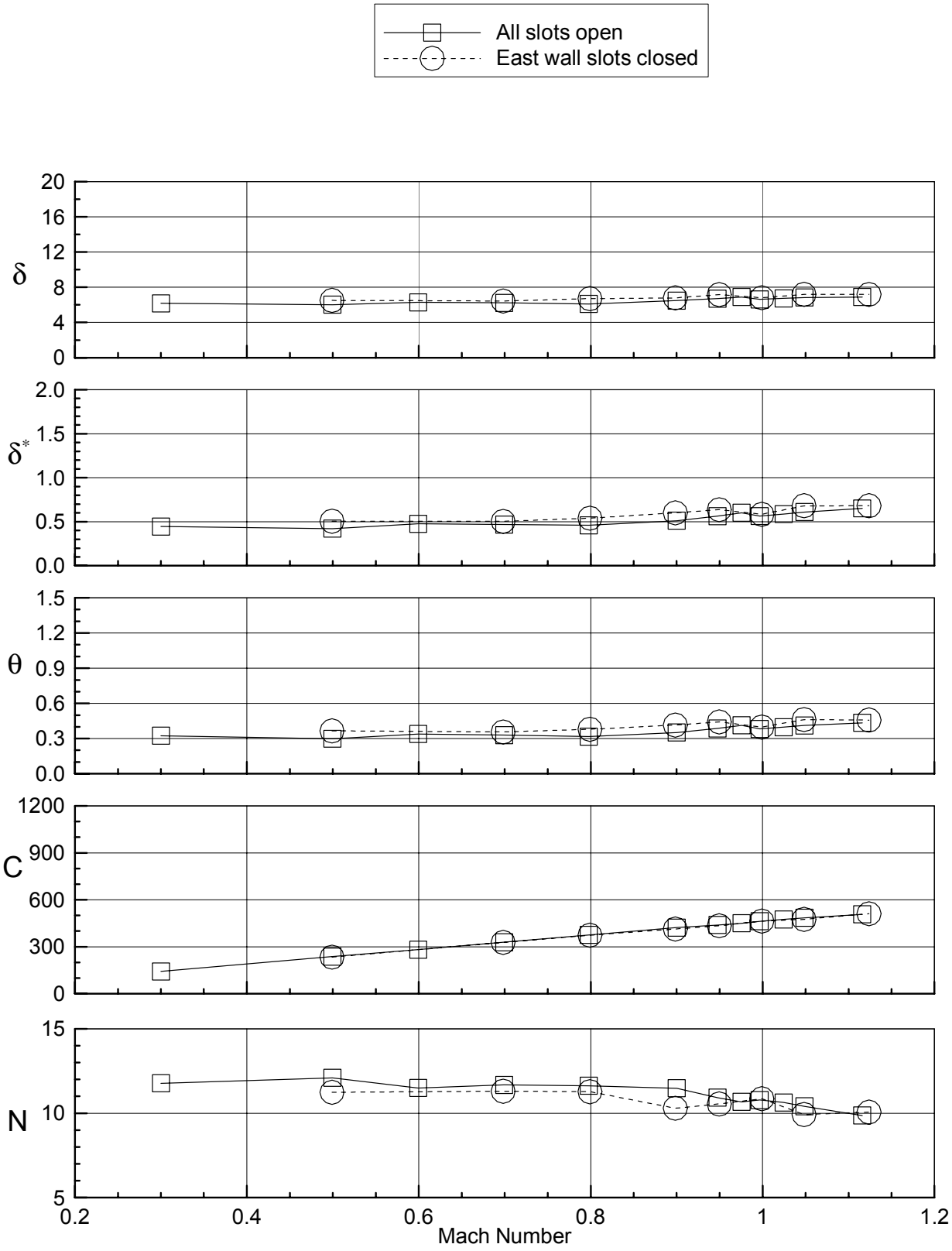

d) West wall rake

Figure 23. - continued.

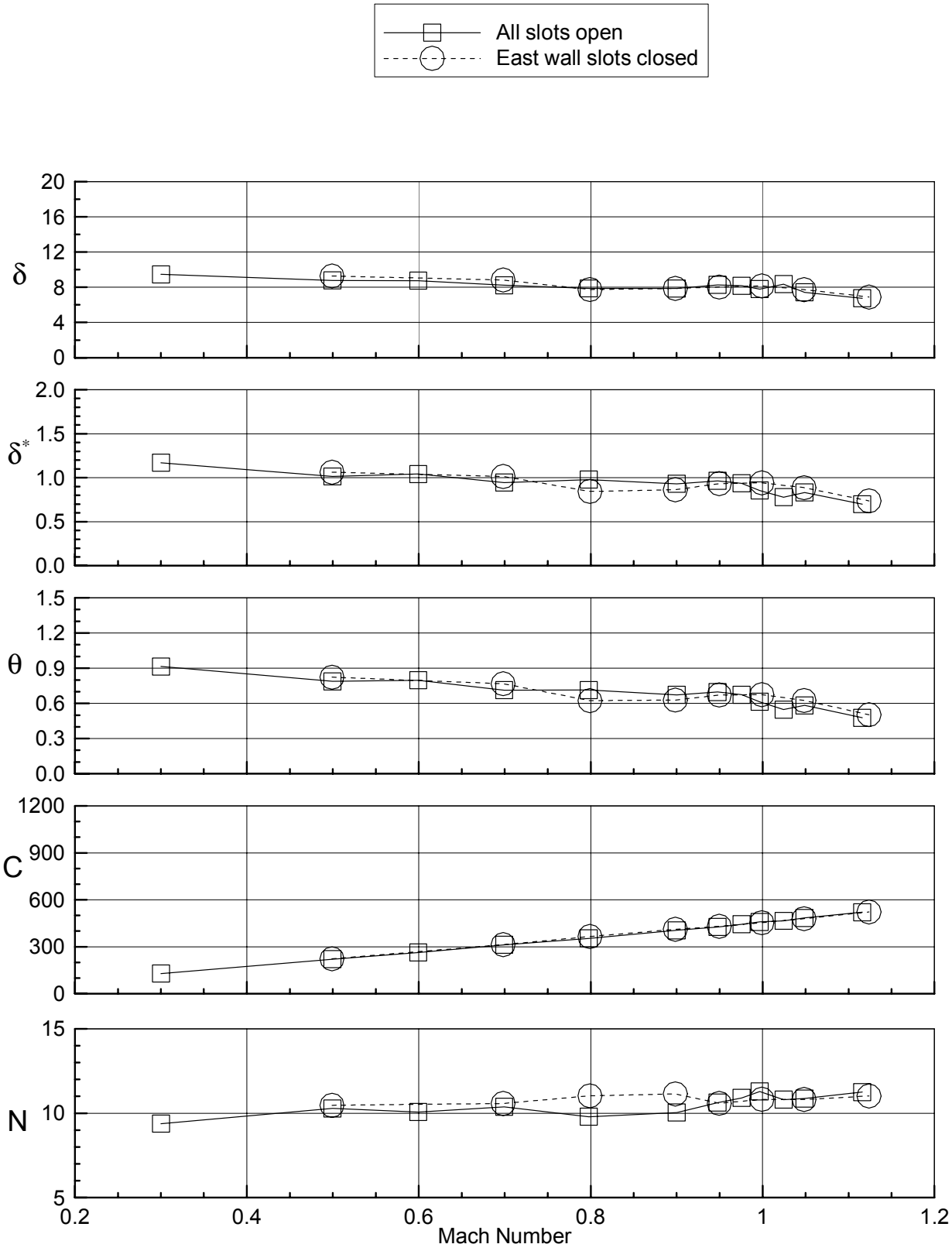

e) West floor rake

Figure 23. - continued.

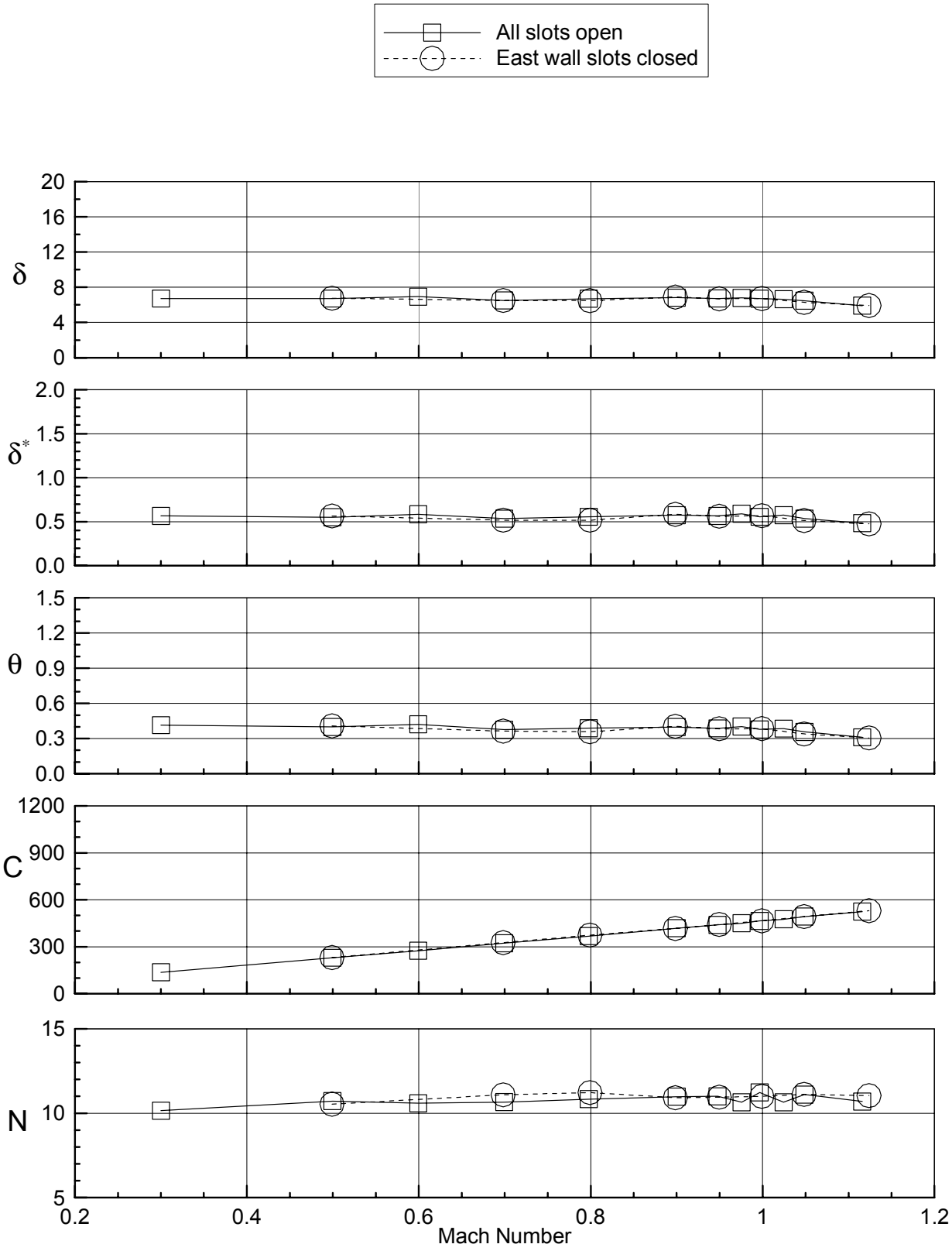

f) East floor rake

Figure 23. - continued.

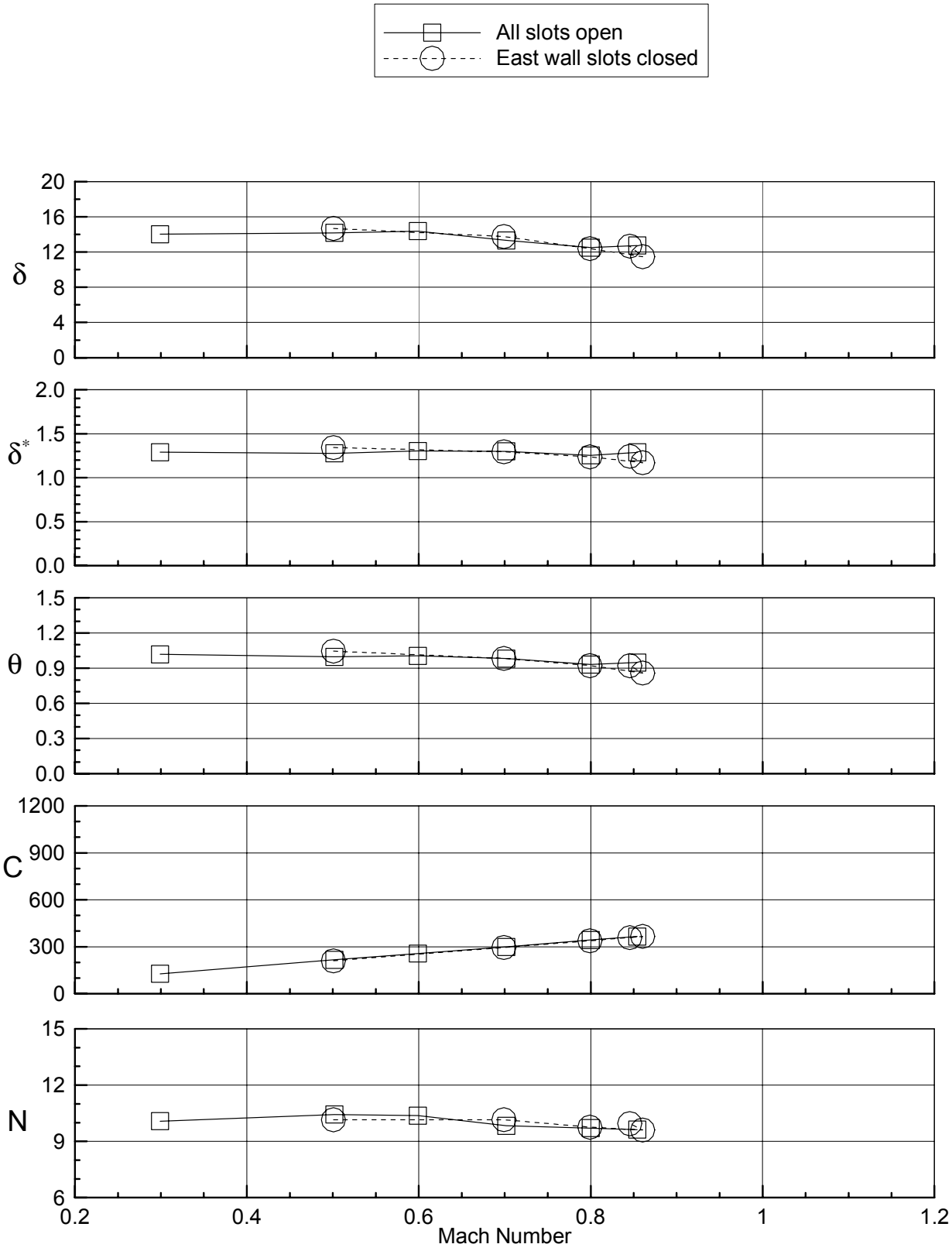

a) East wall rake

Figure 24. Boundary layer parameters for R-134a, P_t=1800 psf, standard flap settings, TS 72, slot effect.

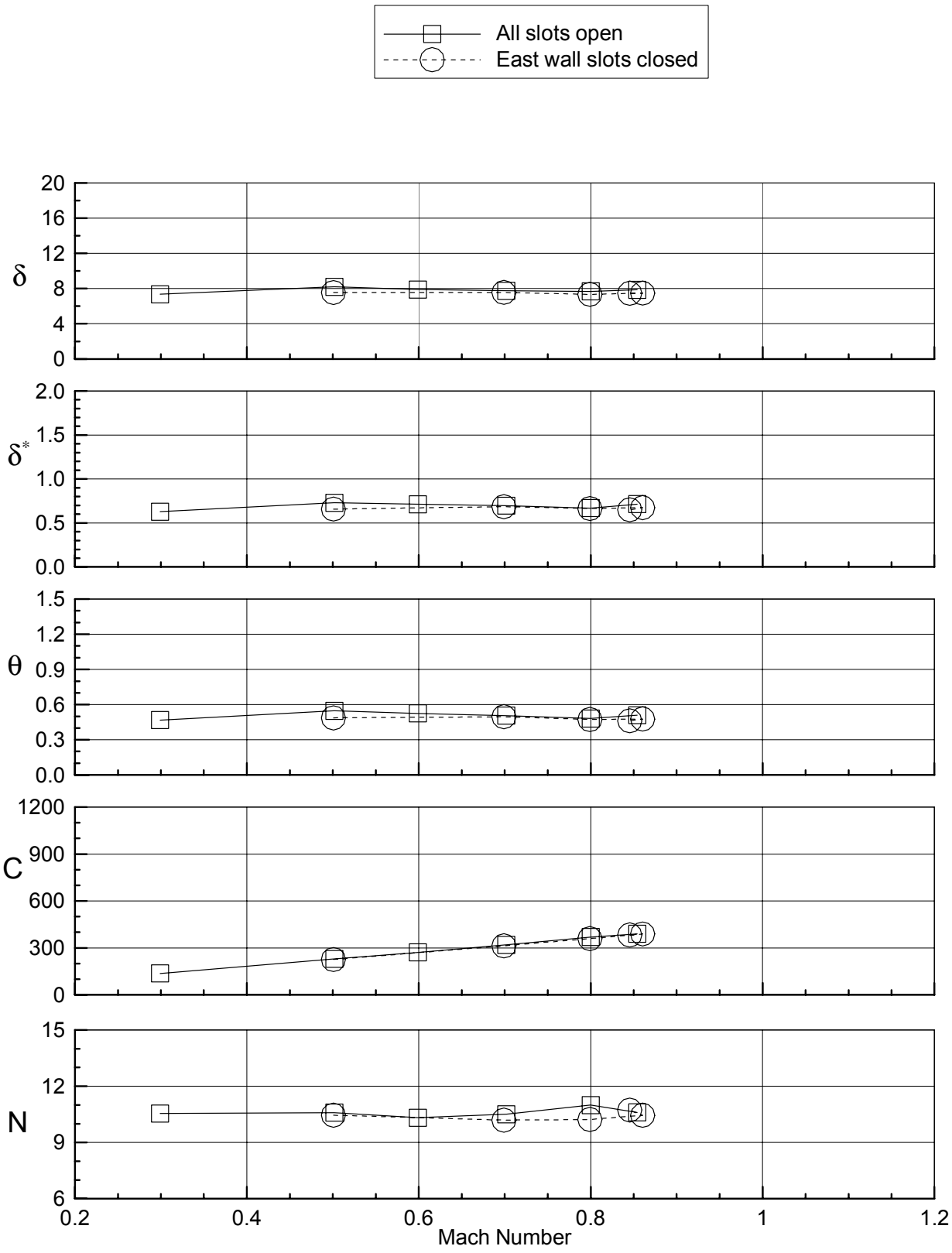

b) East ceiling rake

Figure 24. - continued.

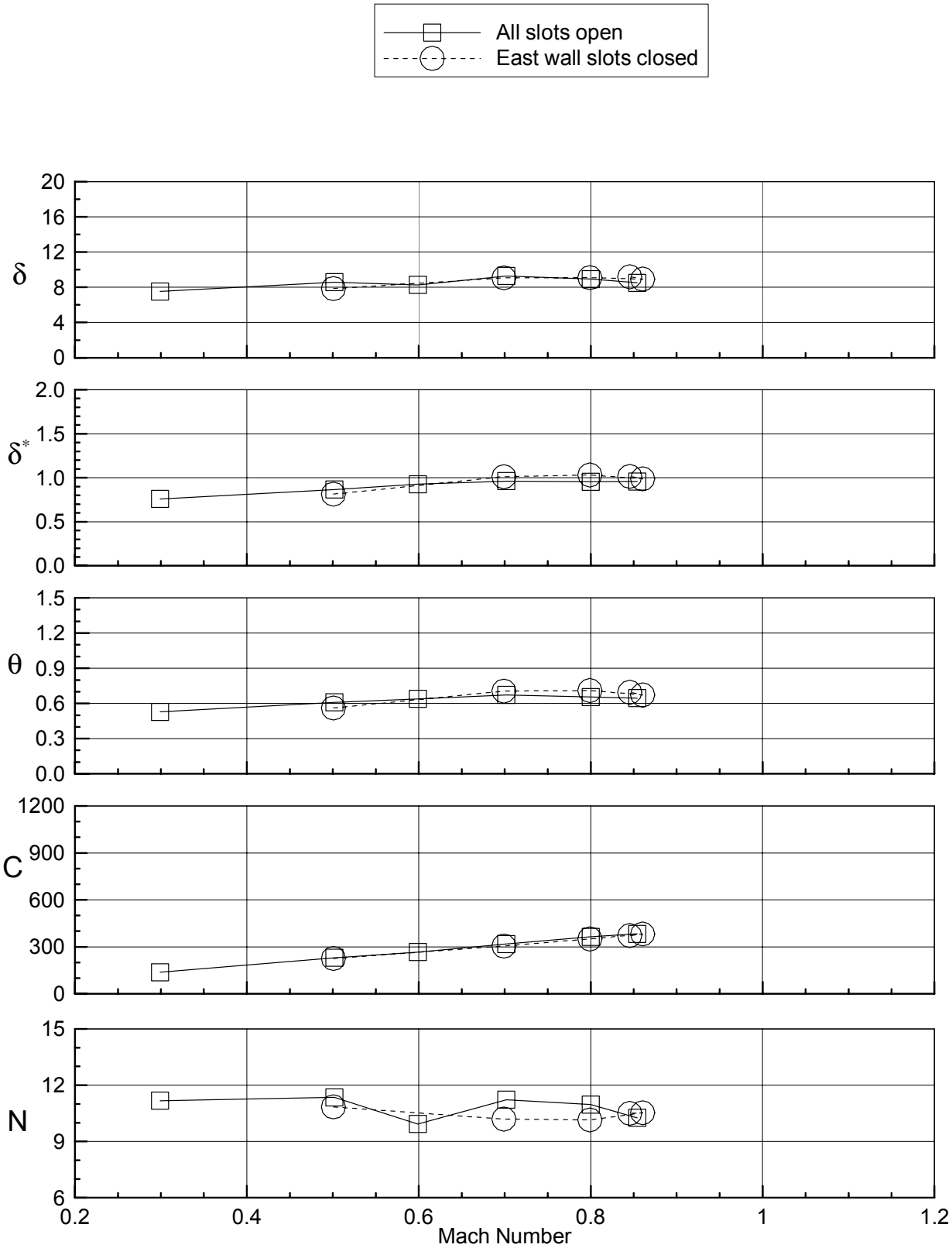

c) West ceiling rake

Figure 24. - continued.

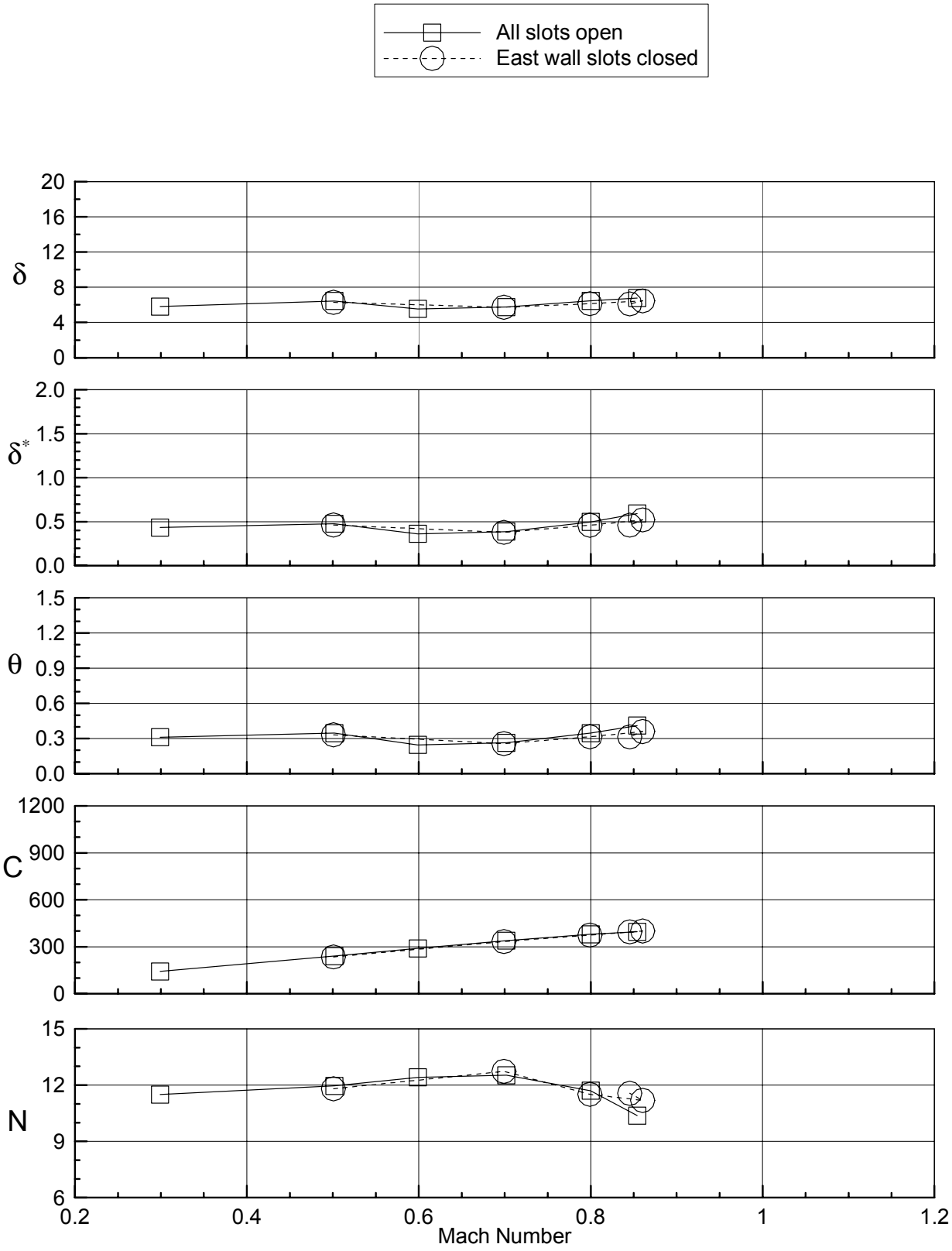

d) West wall rake

Figure 24. - continued.

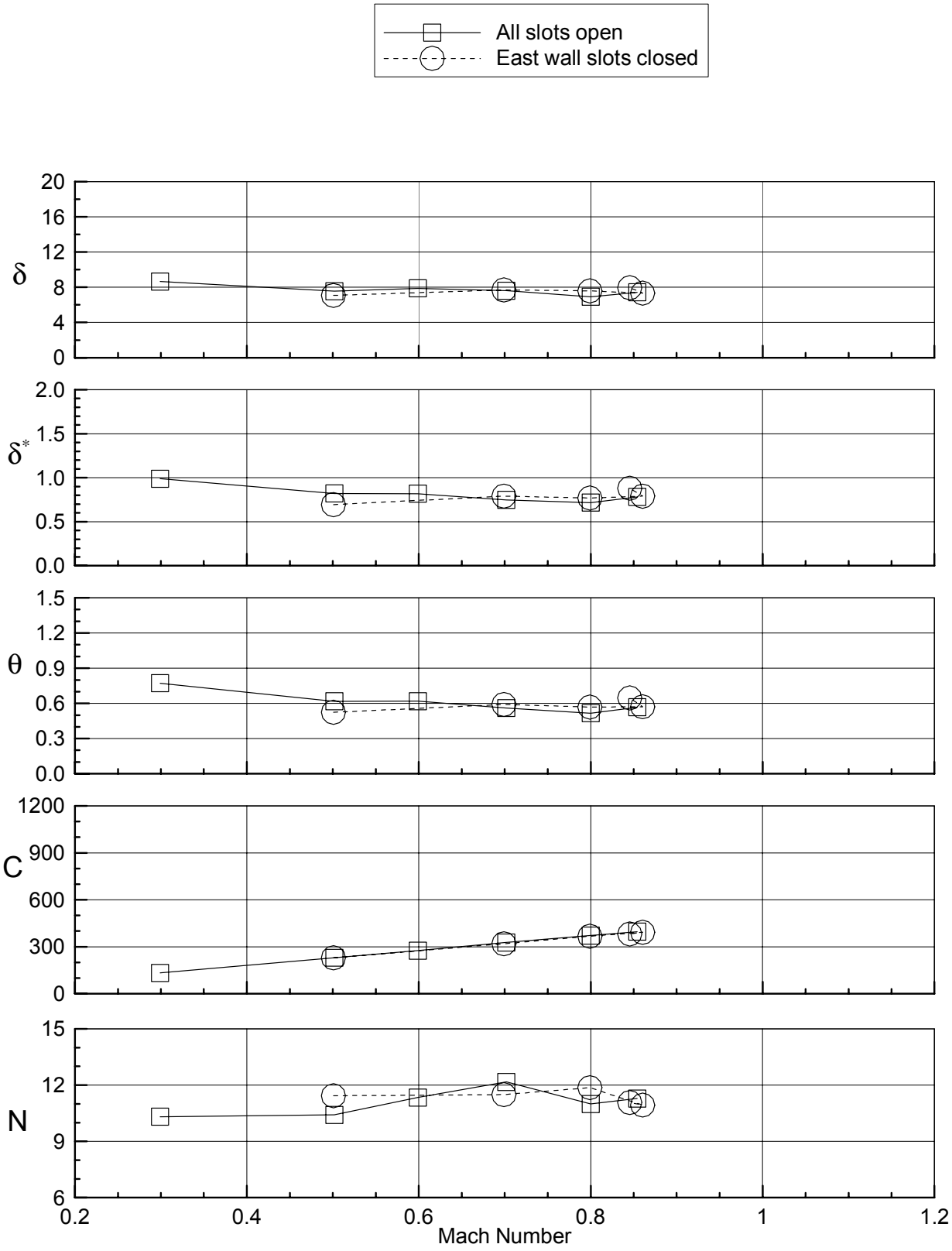

e) West floor rake

Figure 24. - continued.

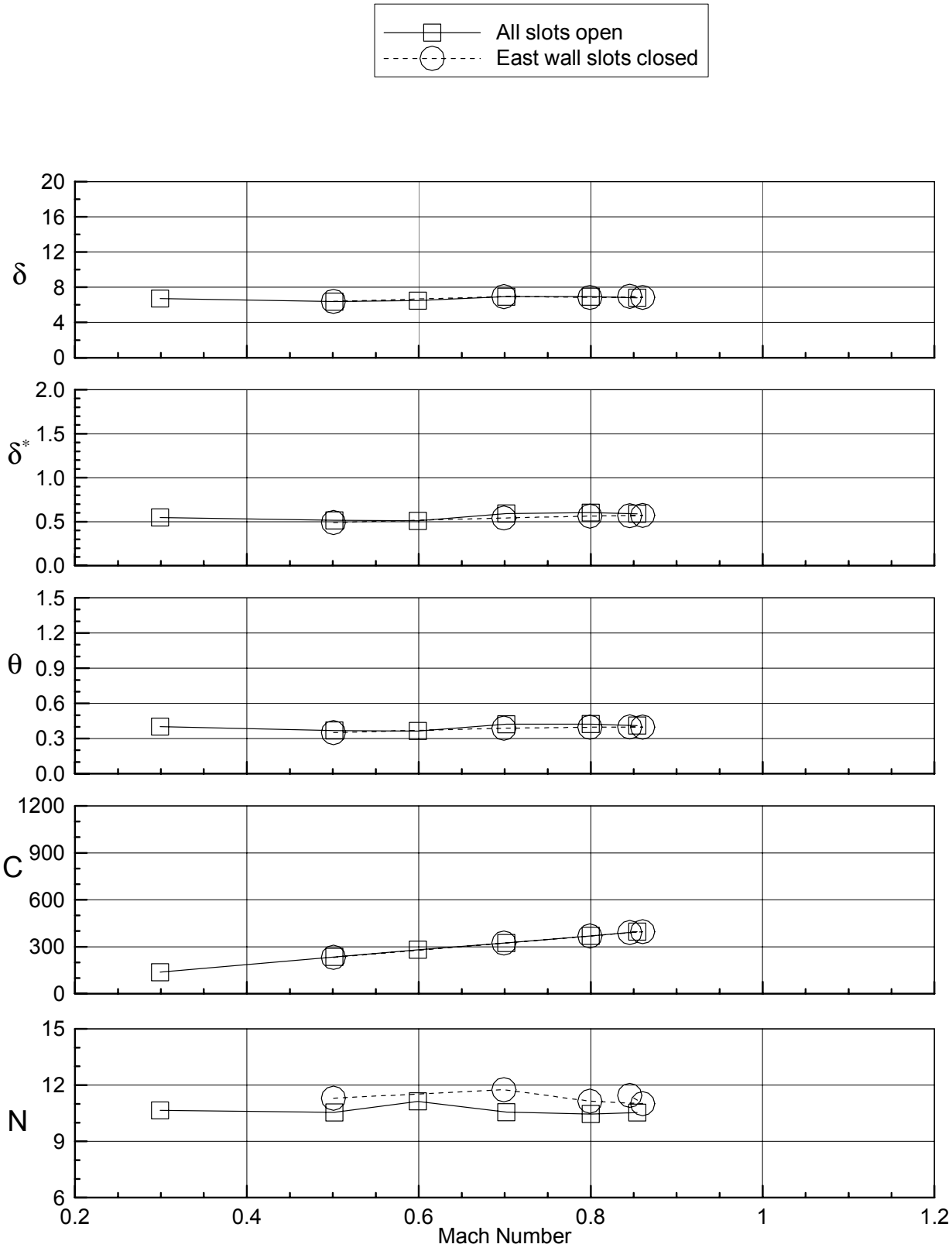

f) East floor rake

Figure 24. - continued.

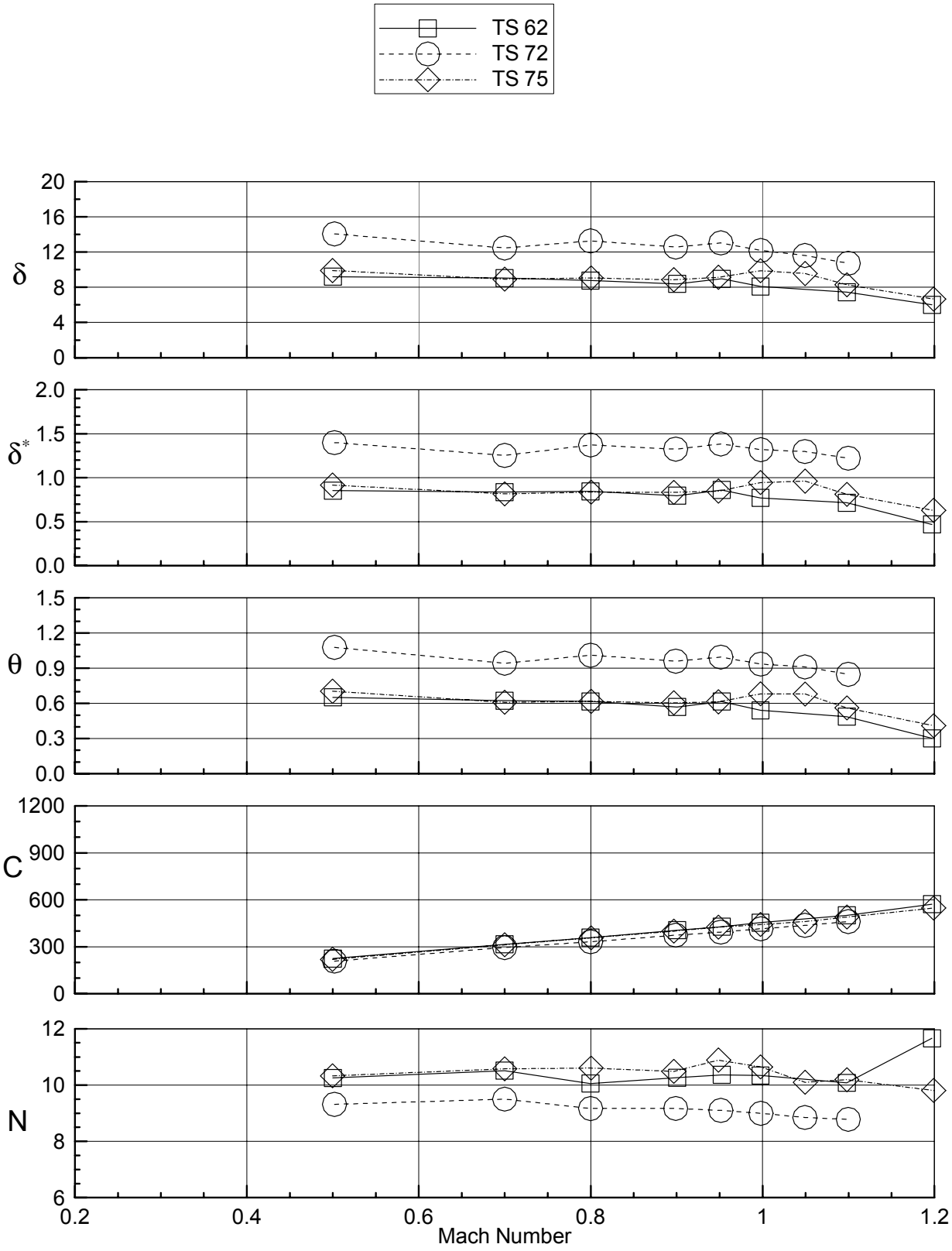

a) East wall rake

Figure 25. Boundary layer parameters for R-134a, East Wall slots closed, standard flap settings, P_t=700 psf.

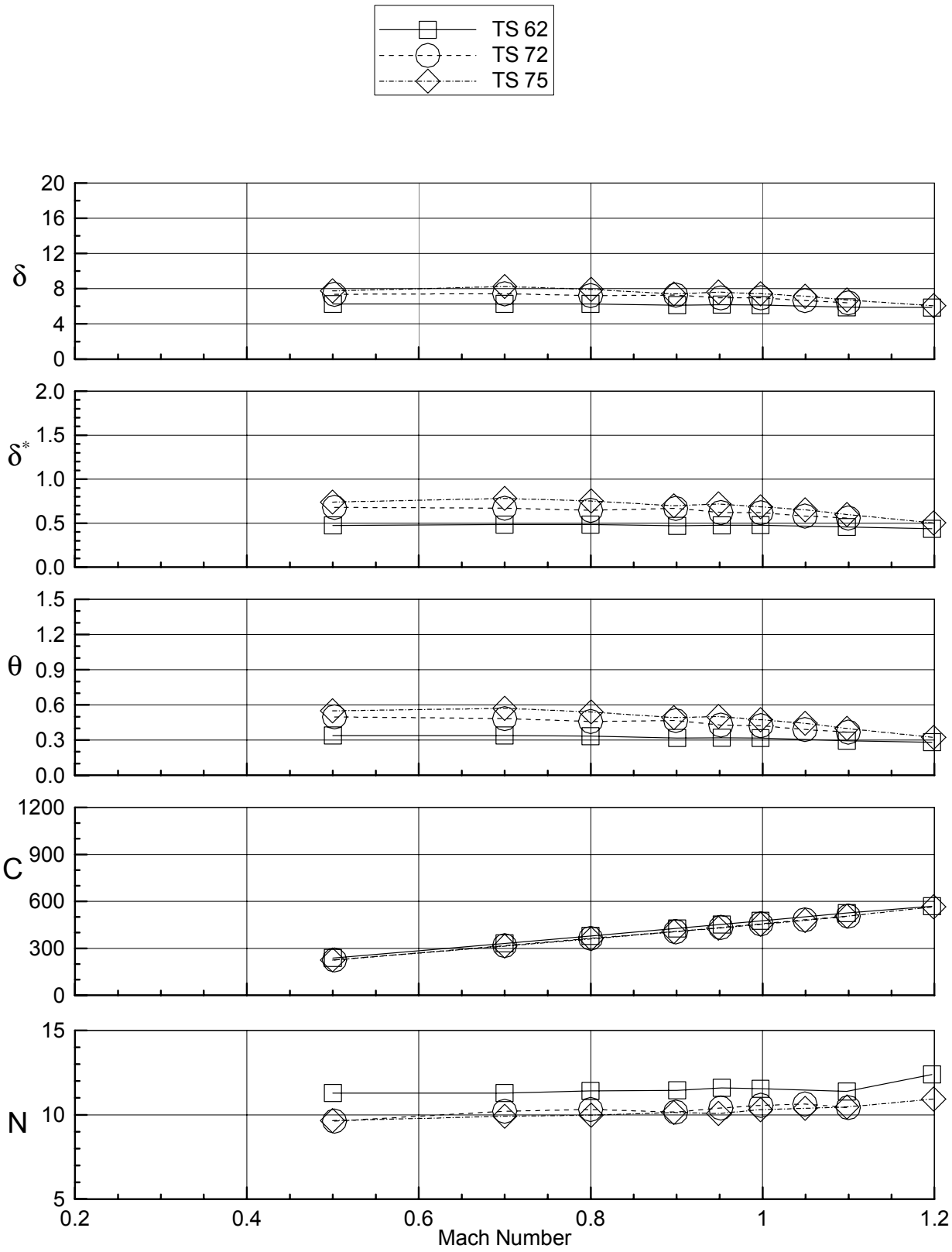

b) East ceiling rake

Figure 25. - continued.

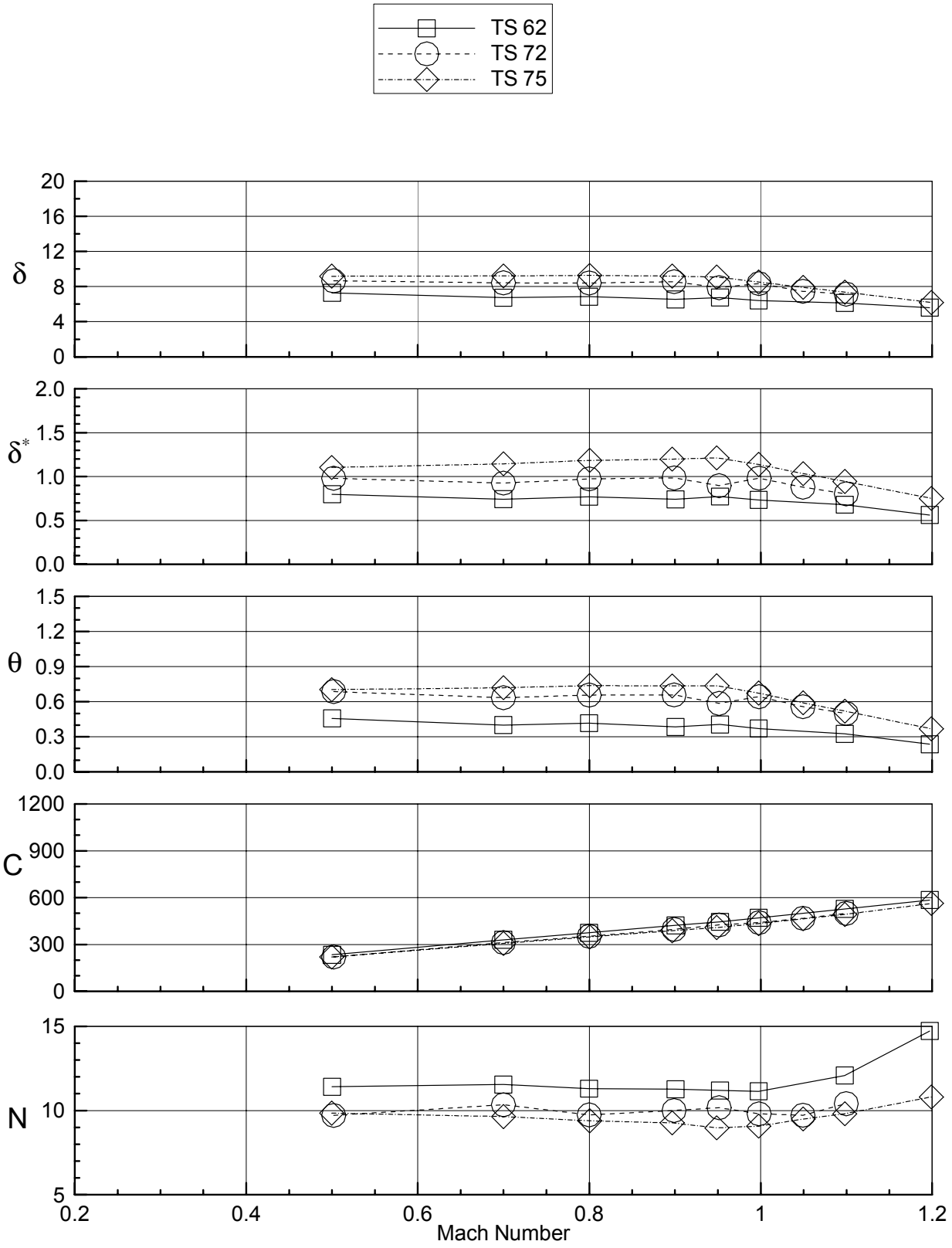

c) West ceiling rake

Figure 25. - continued.

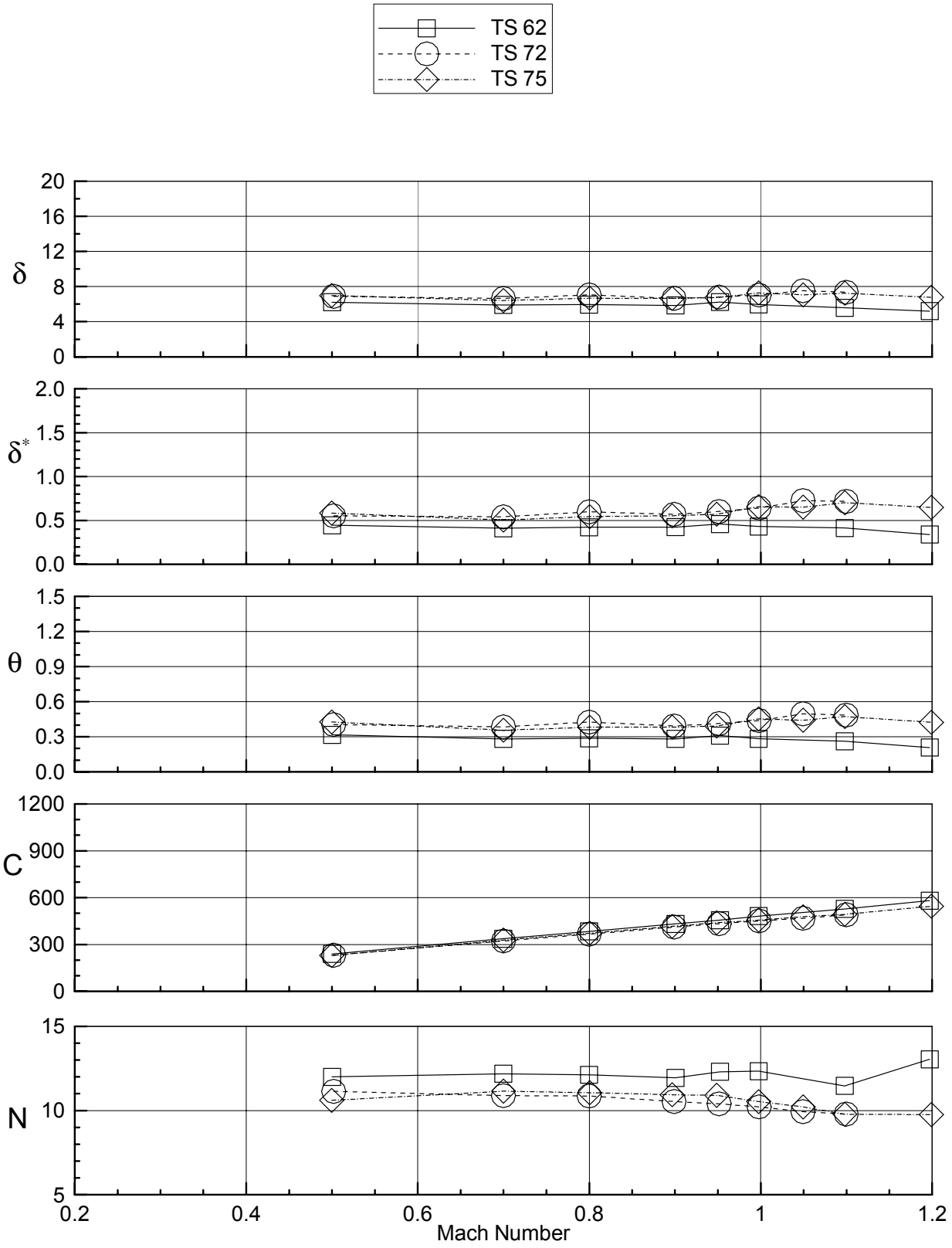

d) West wall rake

Figure 25. - continued.

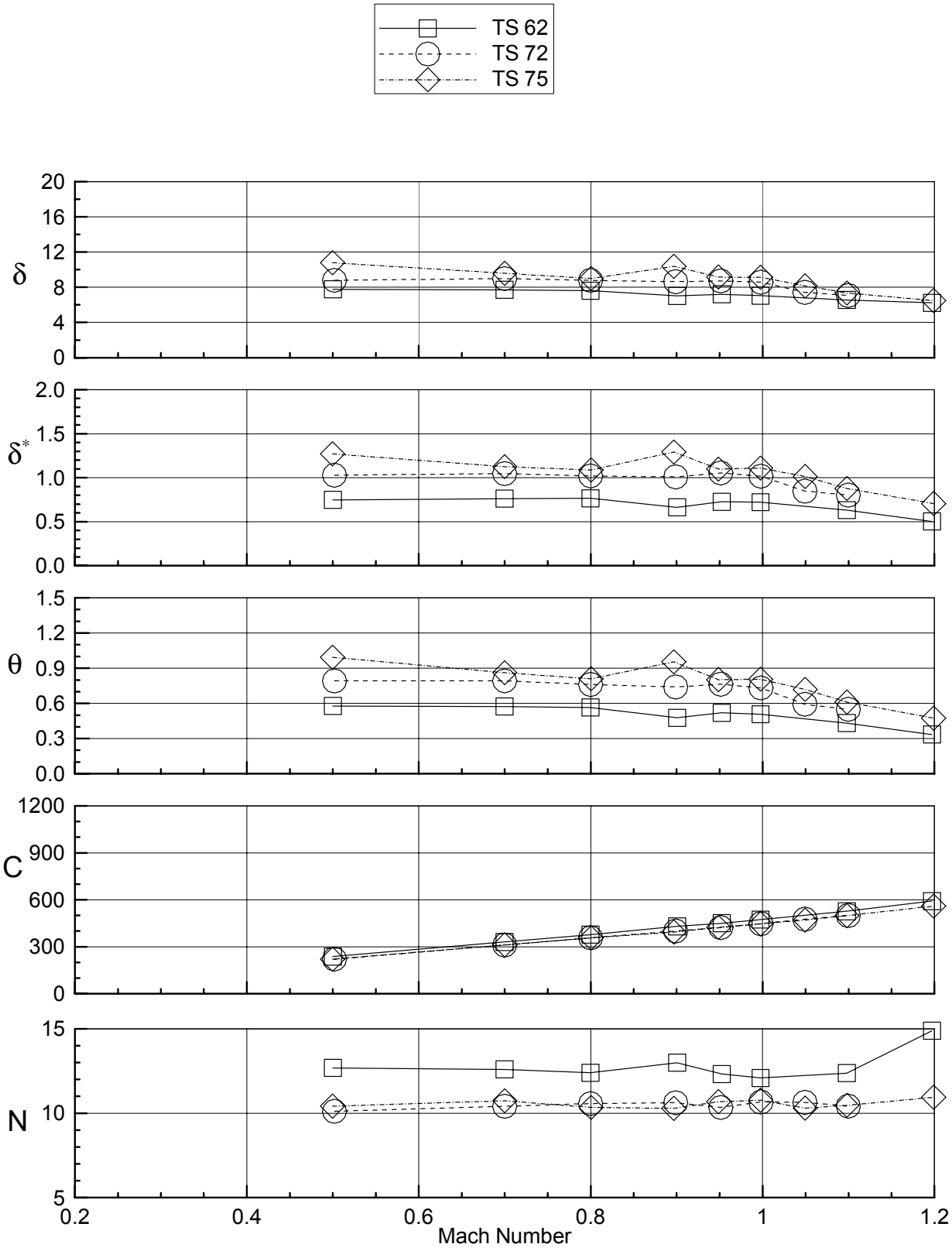

e) West floor rake

Figure 25. - continued.

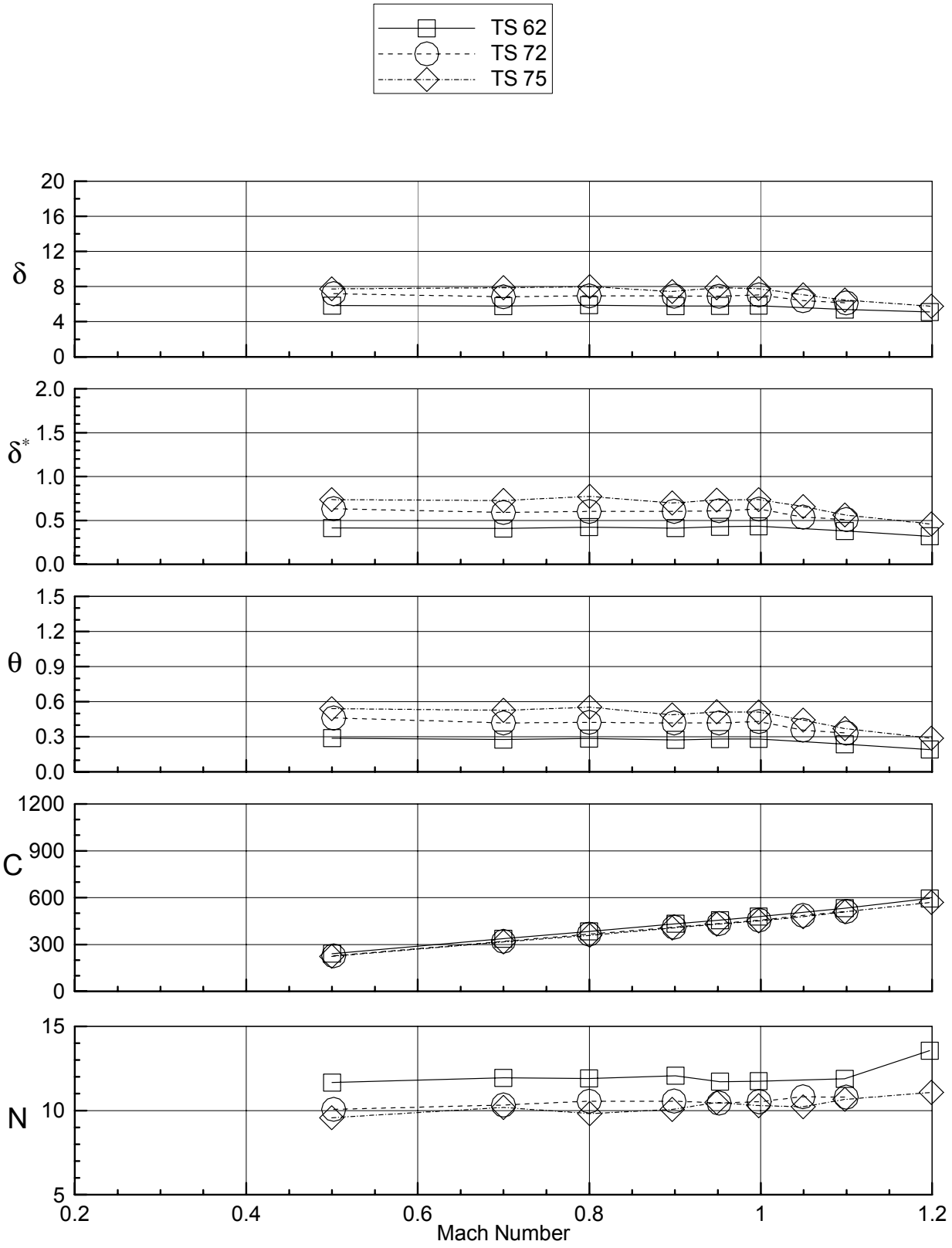

f) East floor rake

Figure 25. - continued.

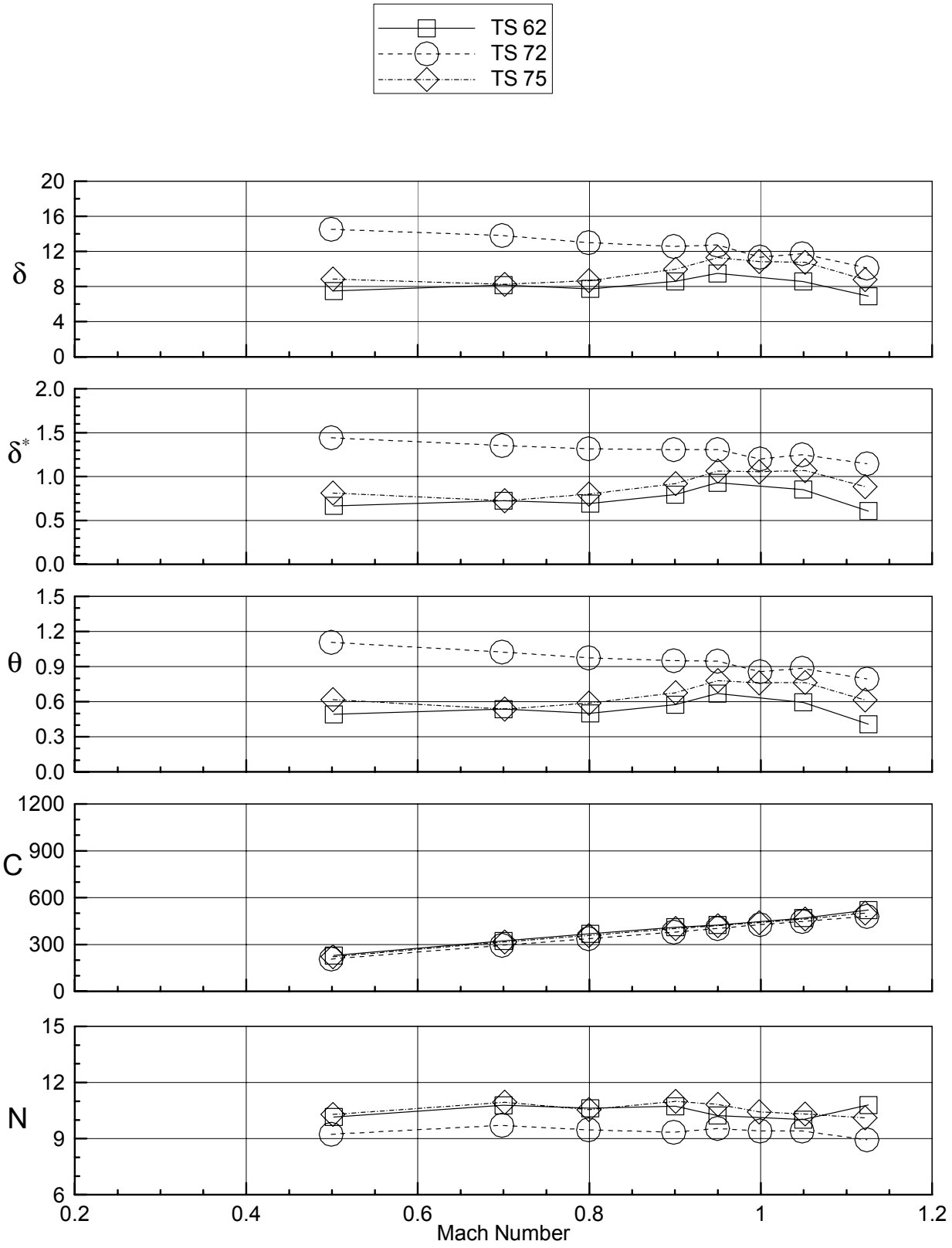

a) East wall rake

Figure 26. Boundary layer parameters for R-134a, East Wall slots closed, standard flap settings, P_t=1000 psf.

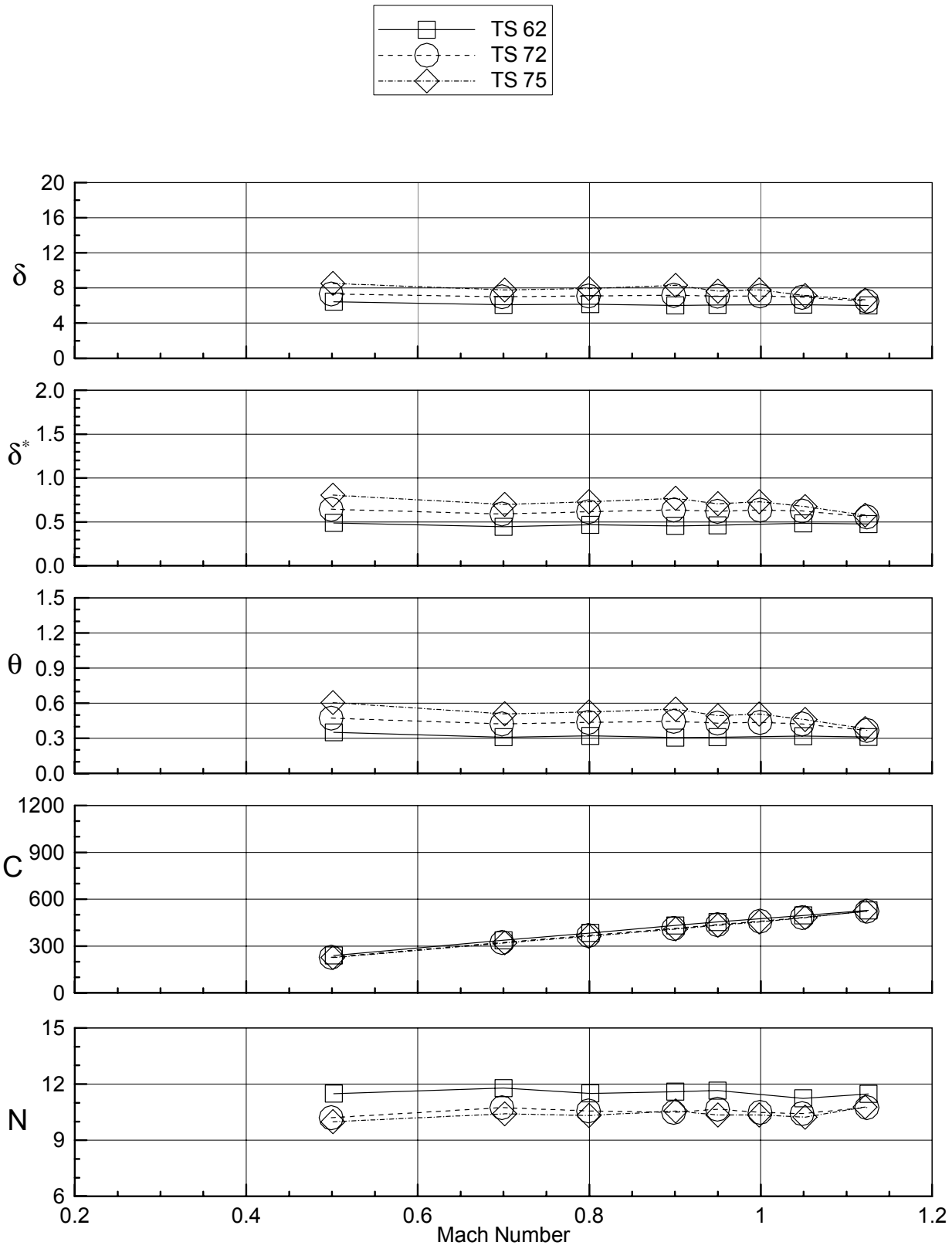

b) East ceiling rake

Figure 26. - continued.

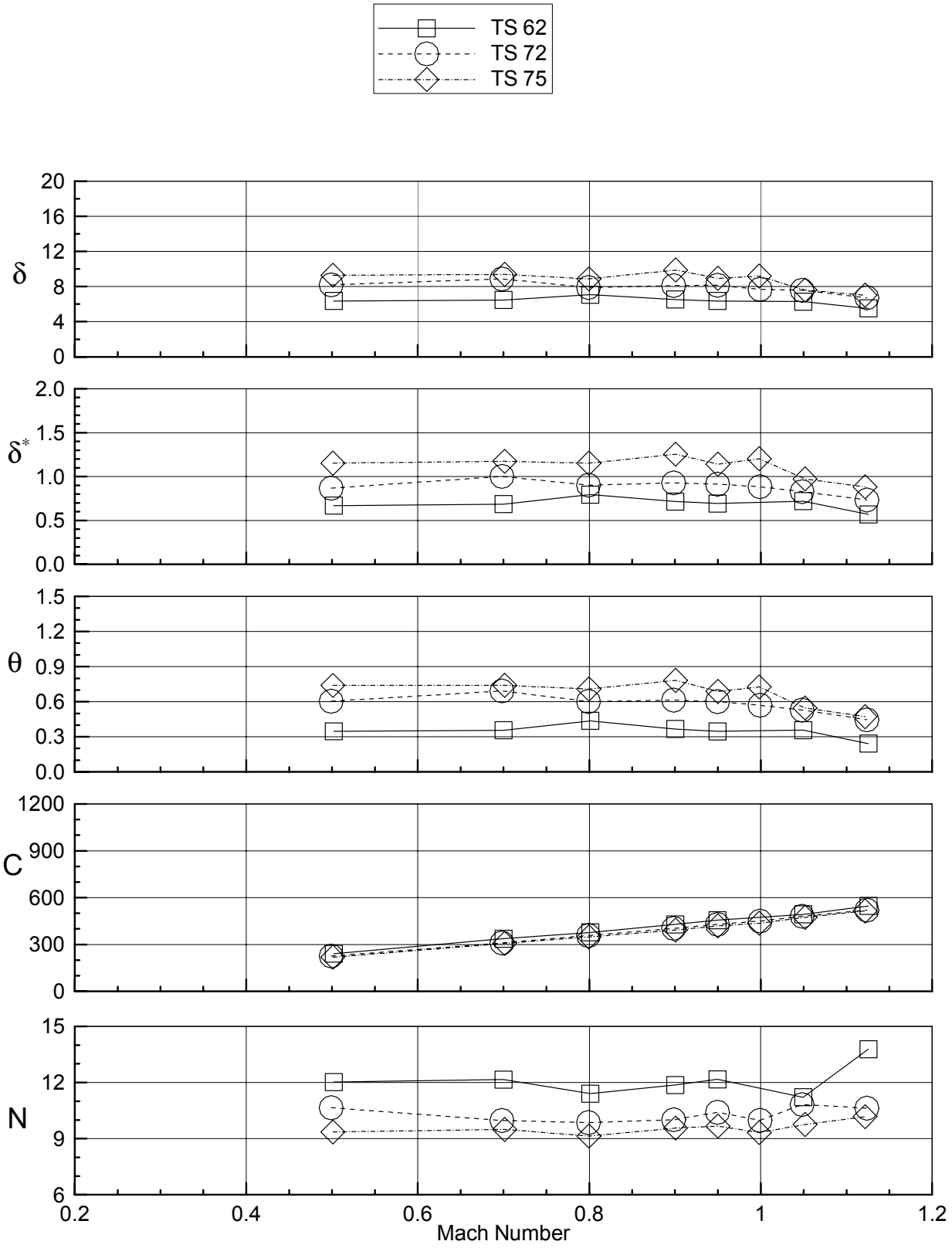

c) West ceiling rake

Figure 26. - continued.

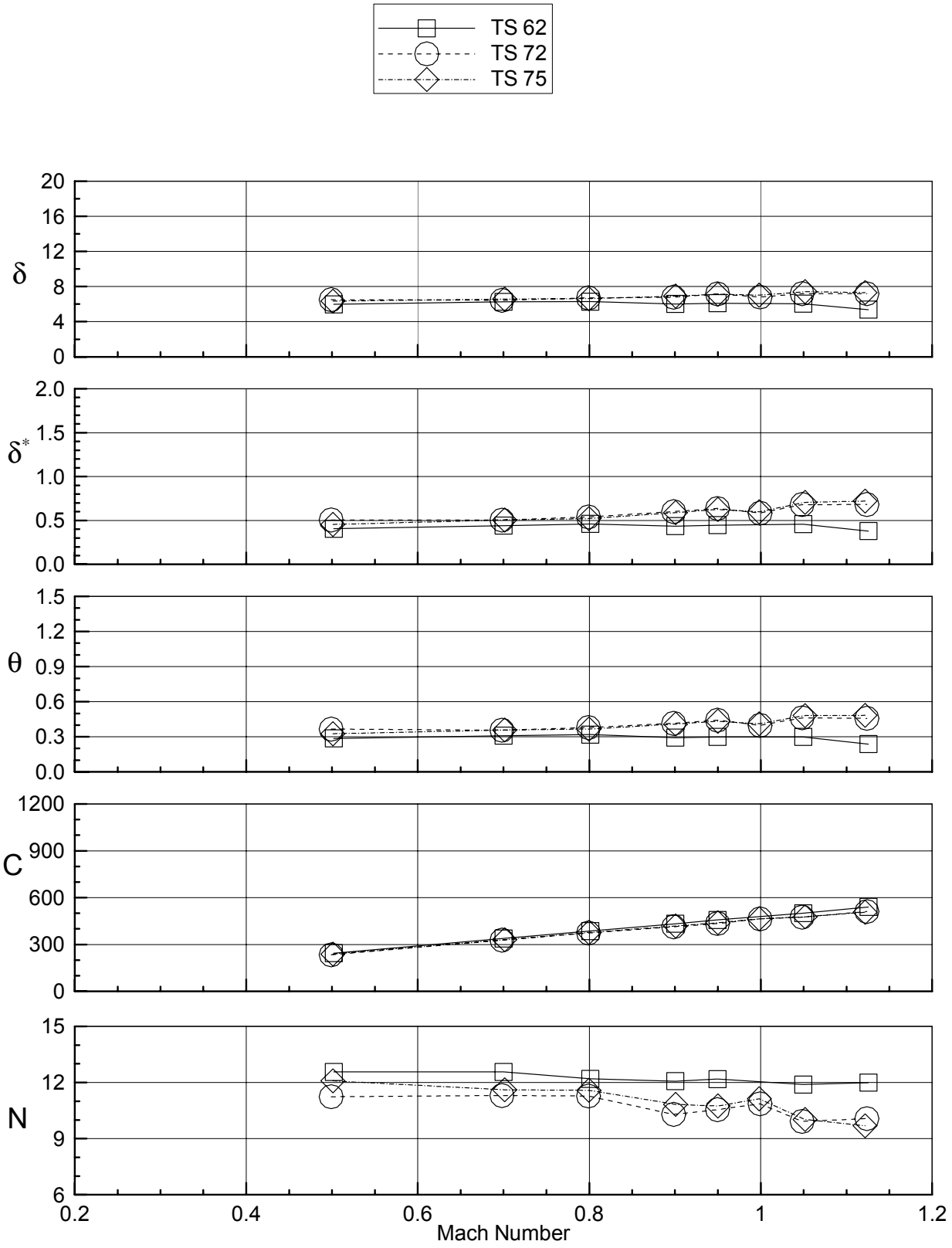

d) West wall rake

Figure 26. - continued.

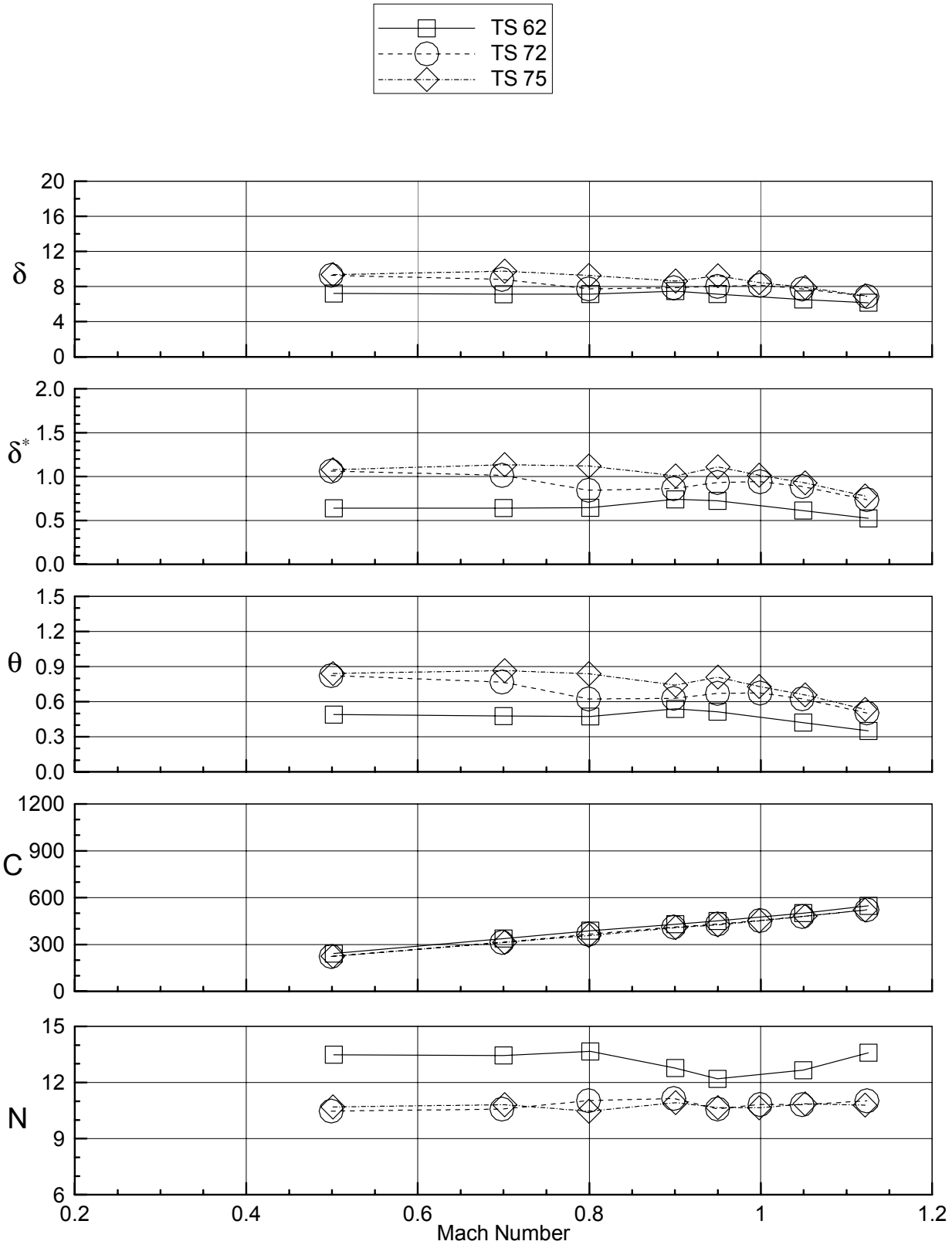

e) West floor rake

Figure 26. - continued.

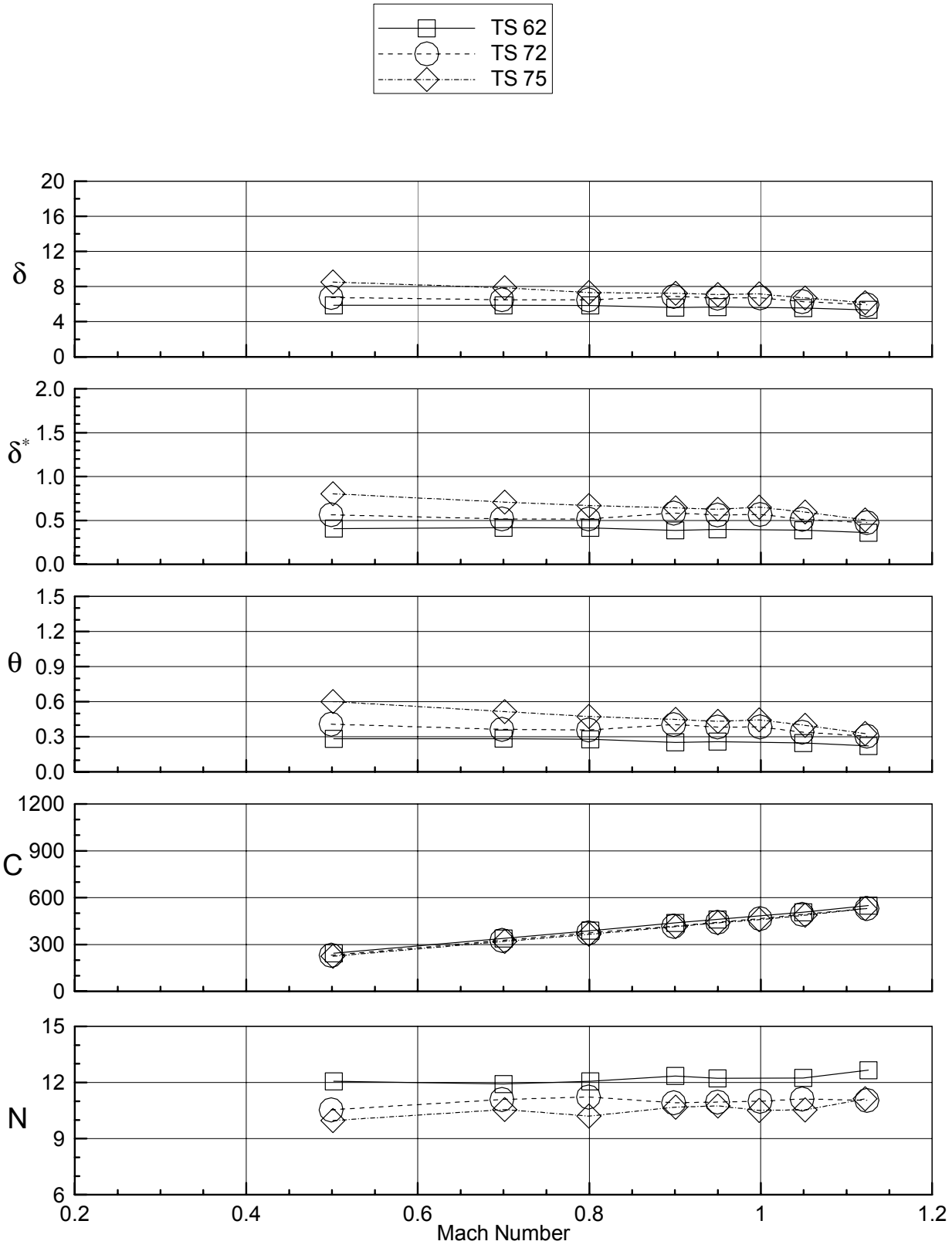

f) East floor rake

Figure 26. - continued.

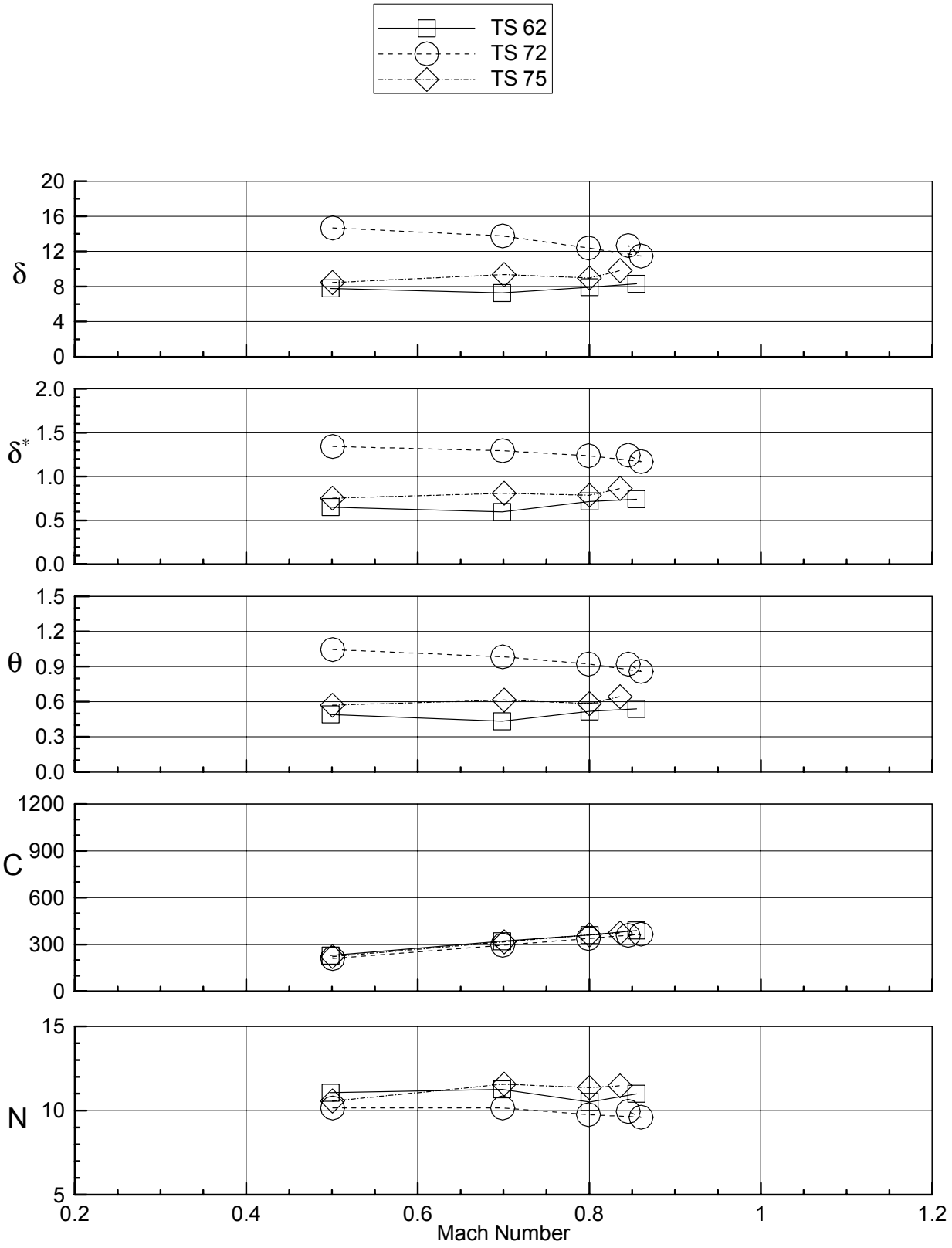

a) East wall rake

Figure 27. Boundary layer parameters for R-134a, East Wall slots closed, standard flap settings, P_t=1800 psf.

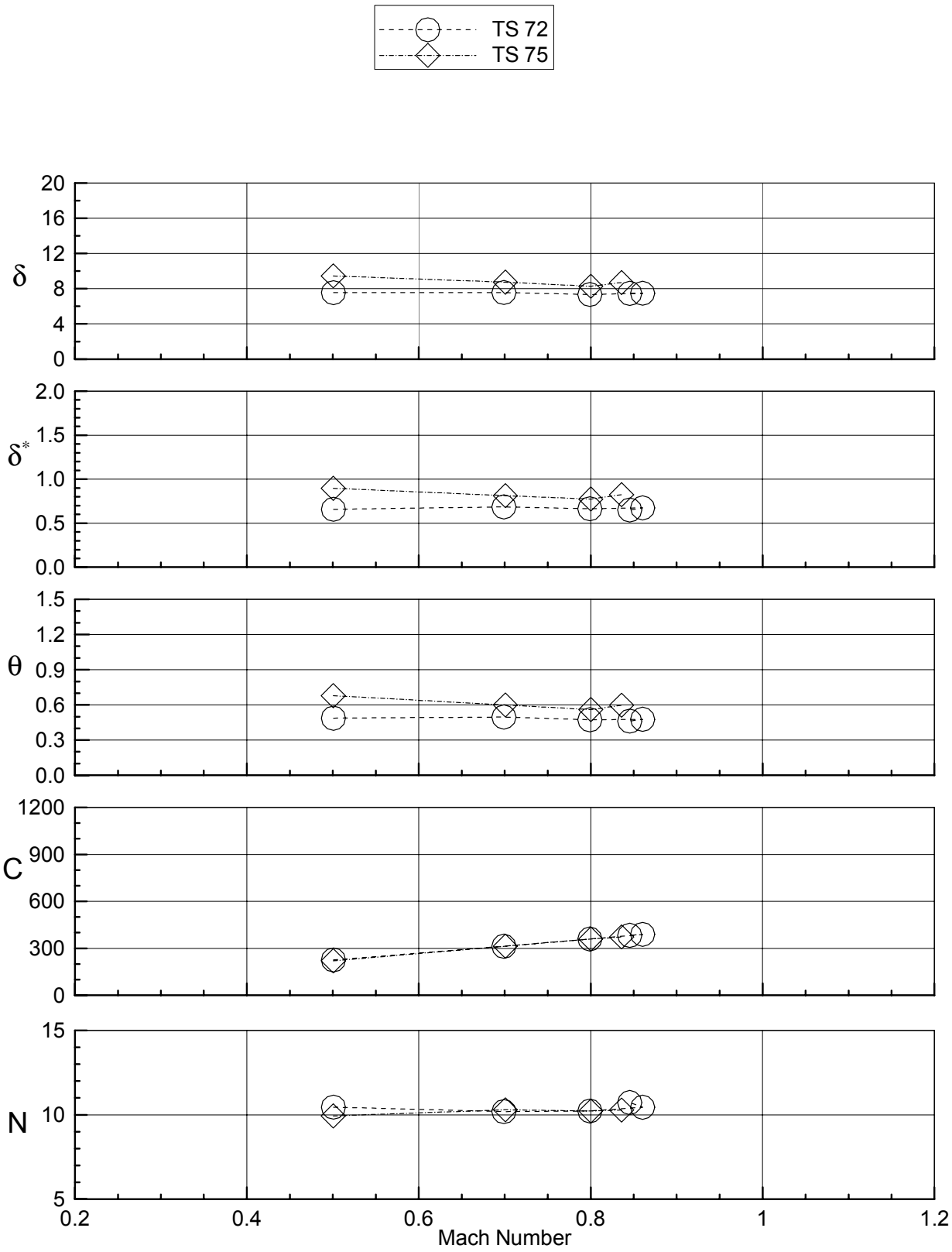

b) East ceiling rake

Figure 27. - continued.

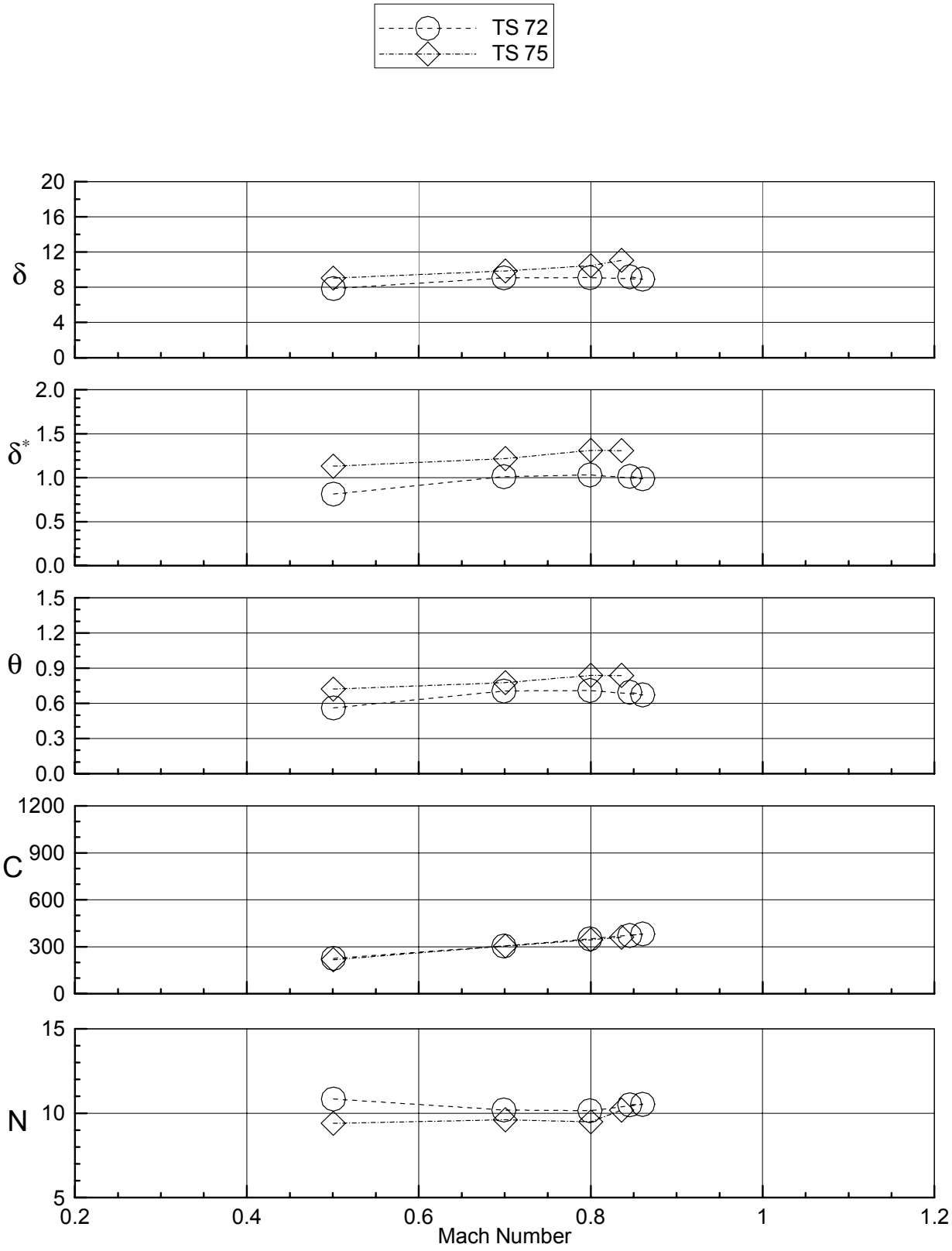

c) West ceiling rake

Figure 27. - continued.

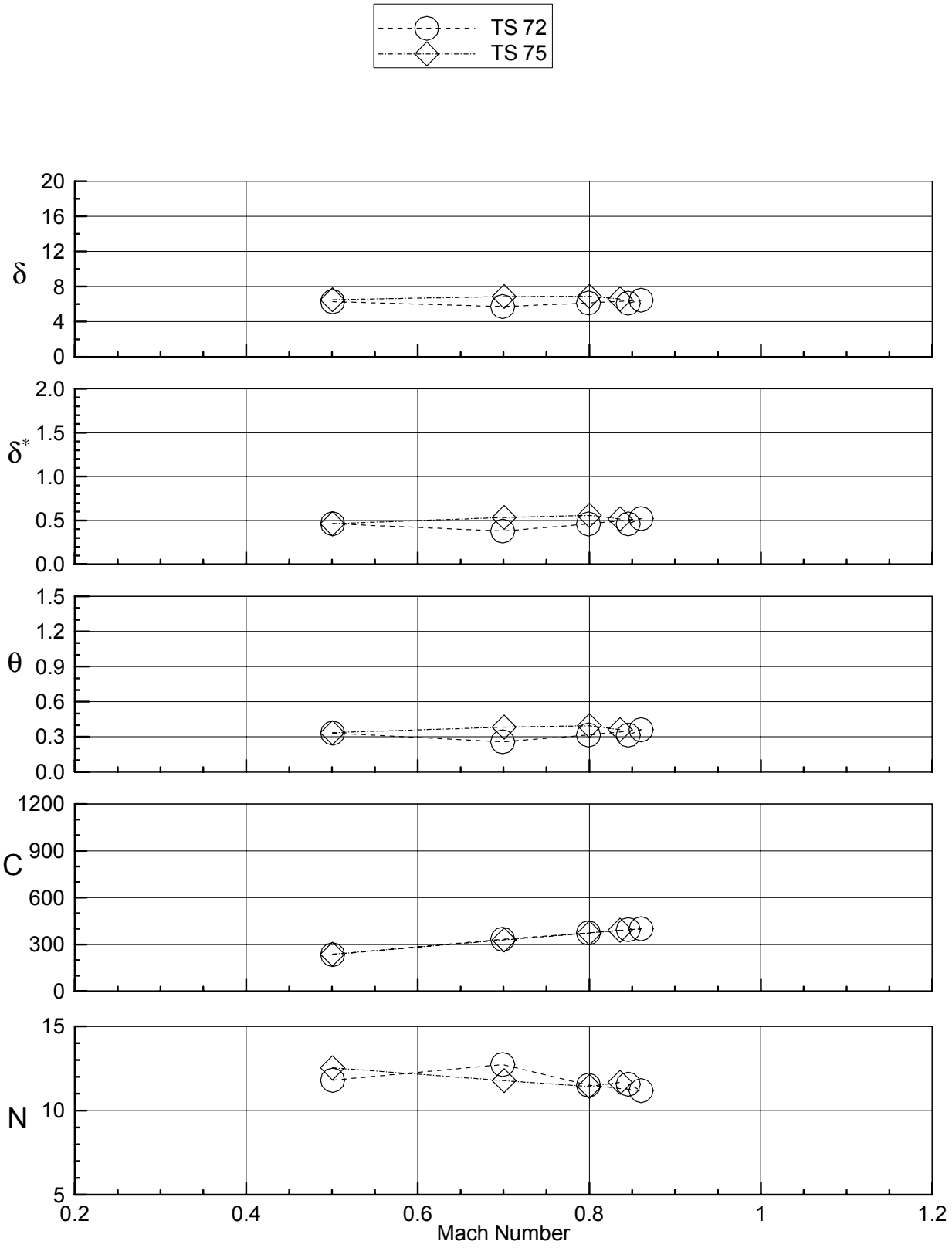

d) West wall rake

Figure 27. - continued.

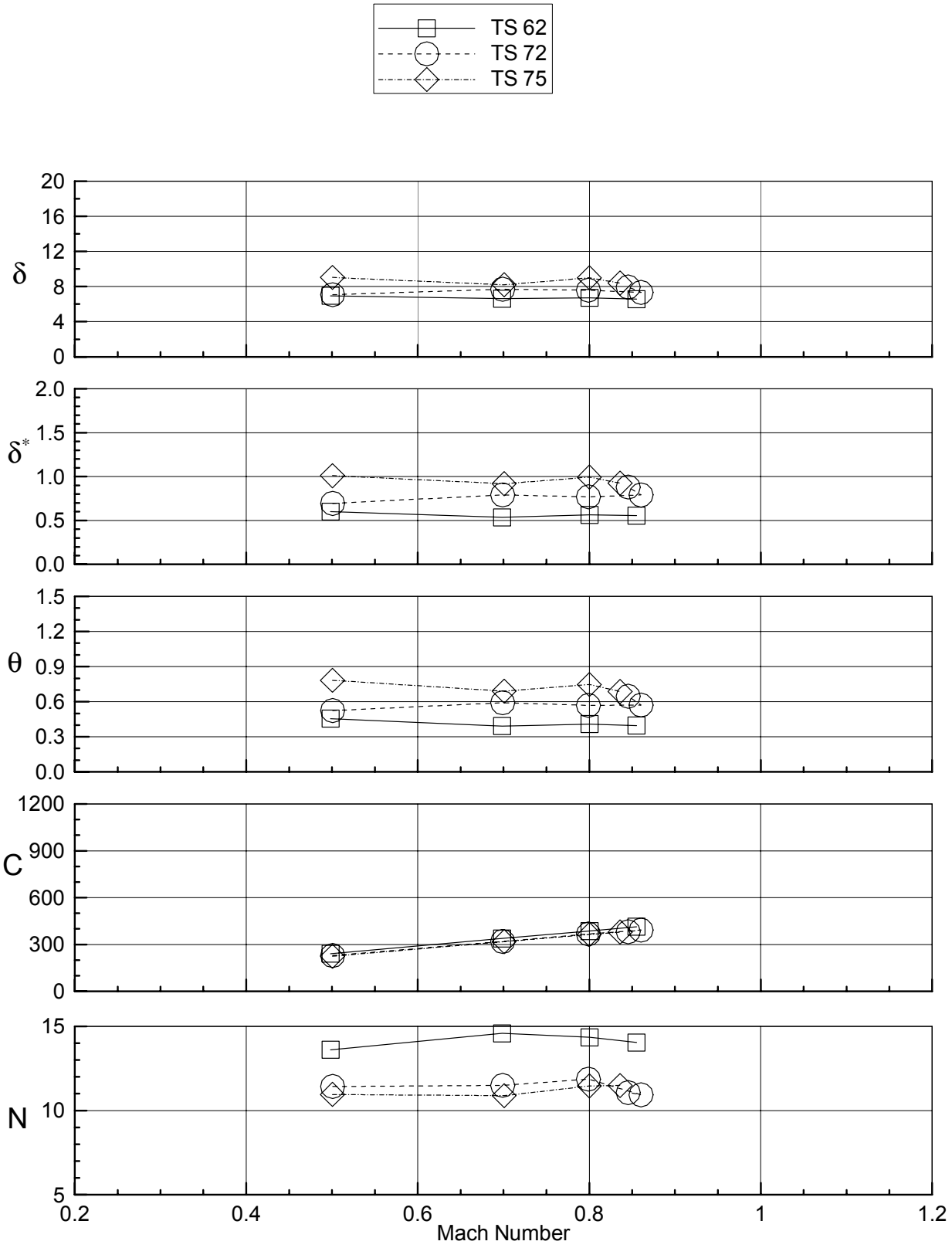

e) West floor rake

Figure 27. - continued.

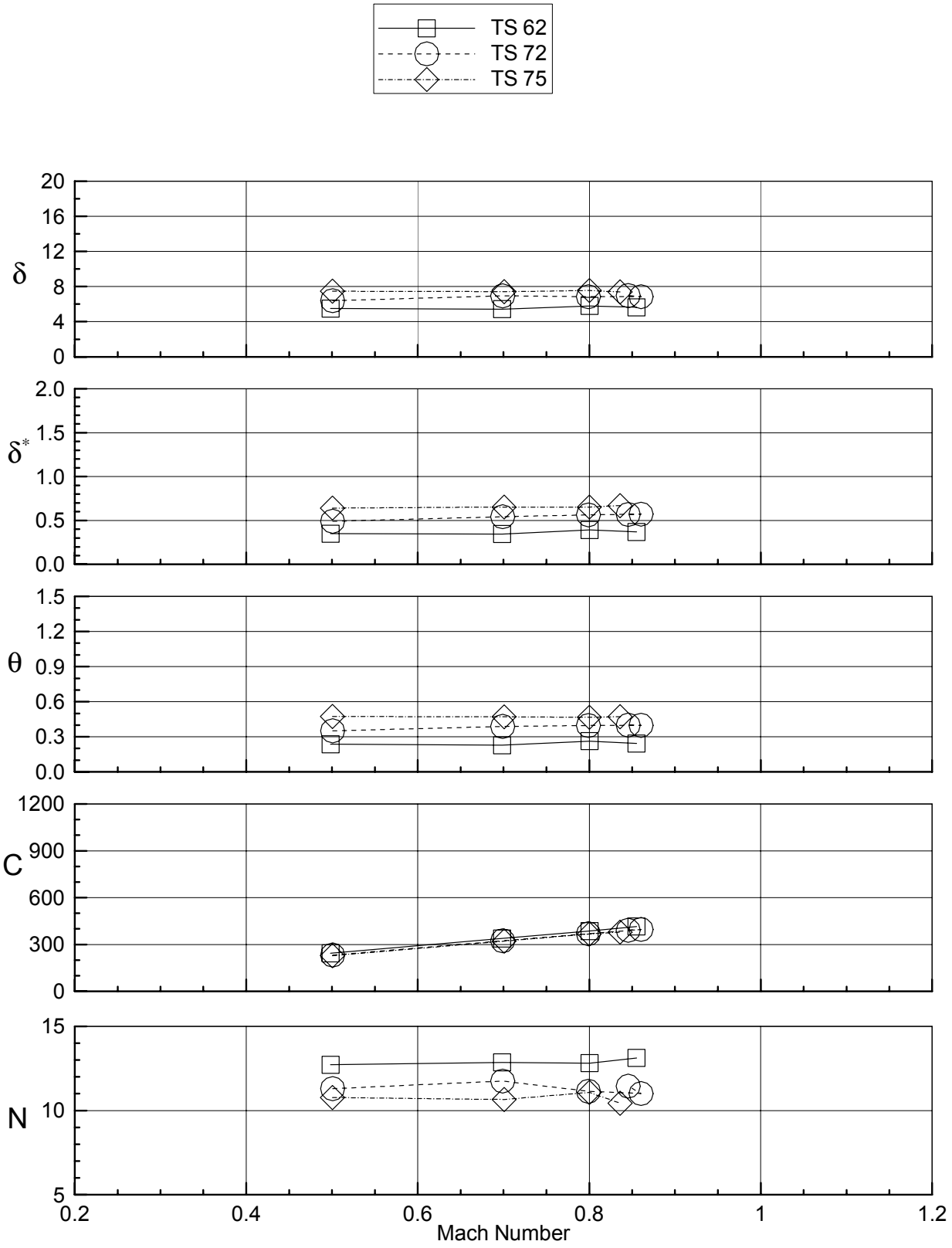

f) East floor rake

Figure 27. - continued.

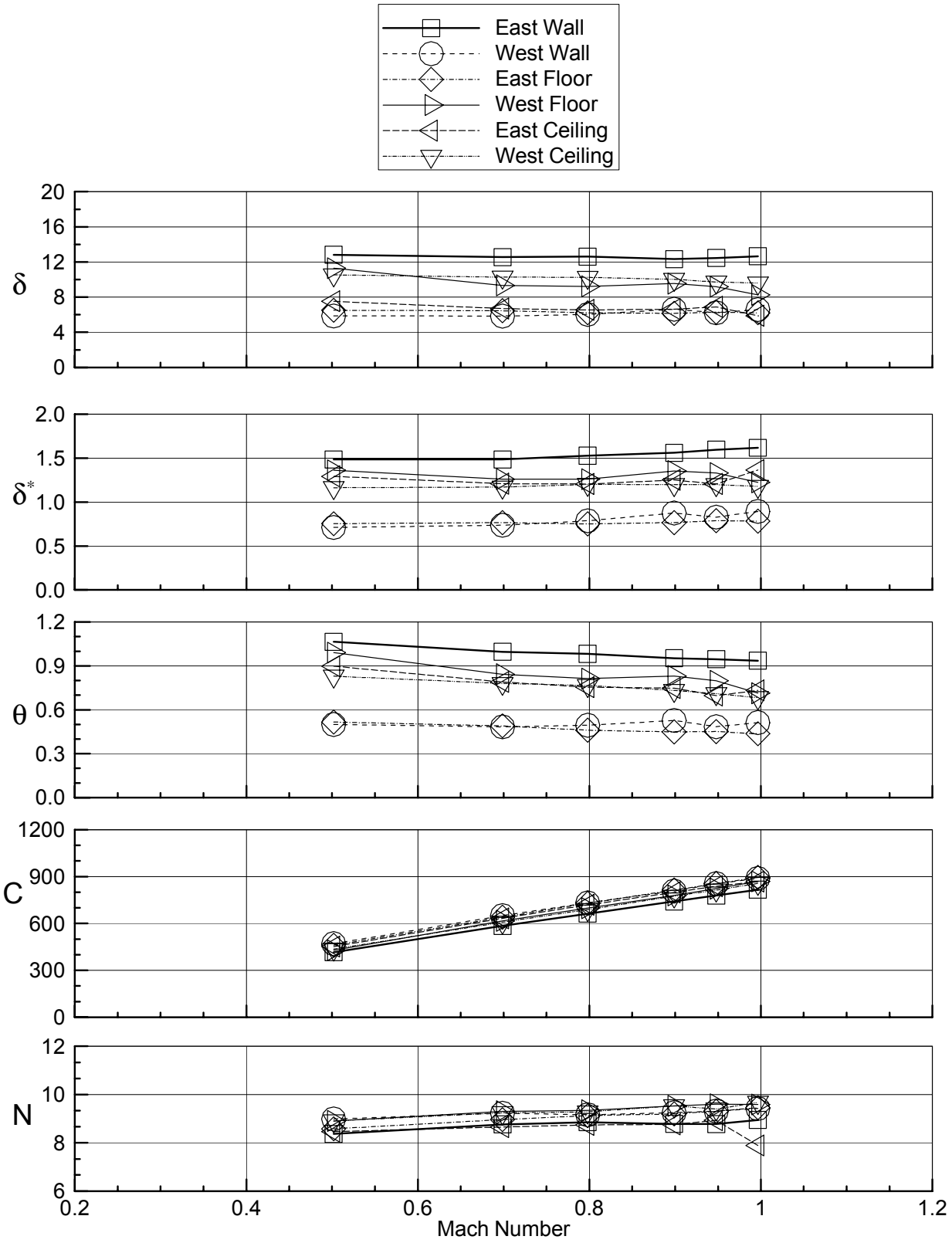

Figure 28. Boundary layer parameters for air, all slots open, standard flap settings, TS 72, P_t=400 psf.

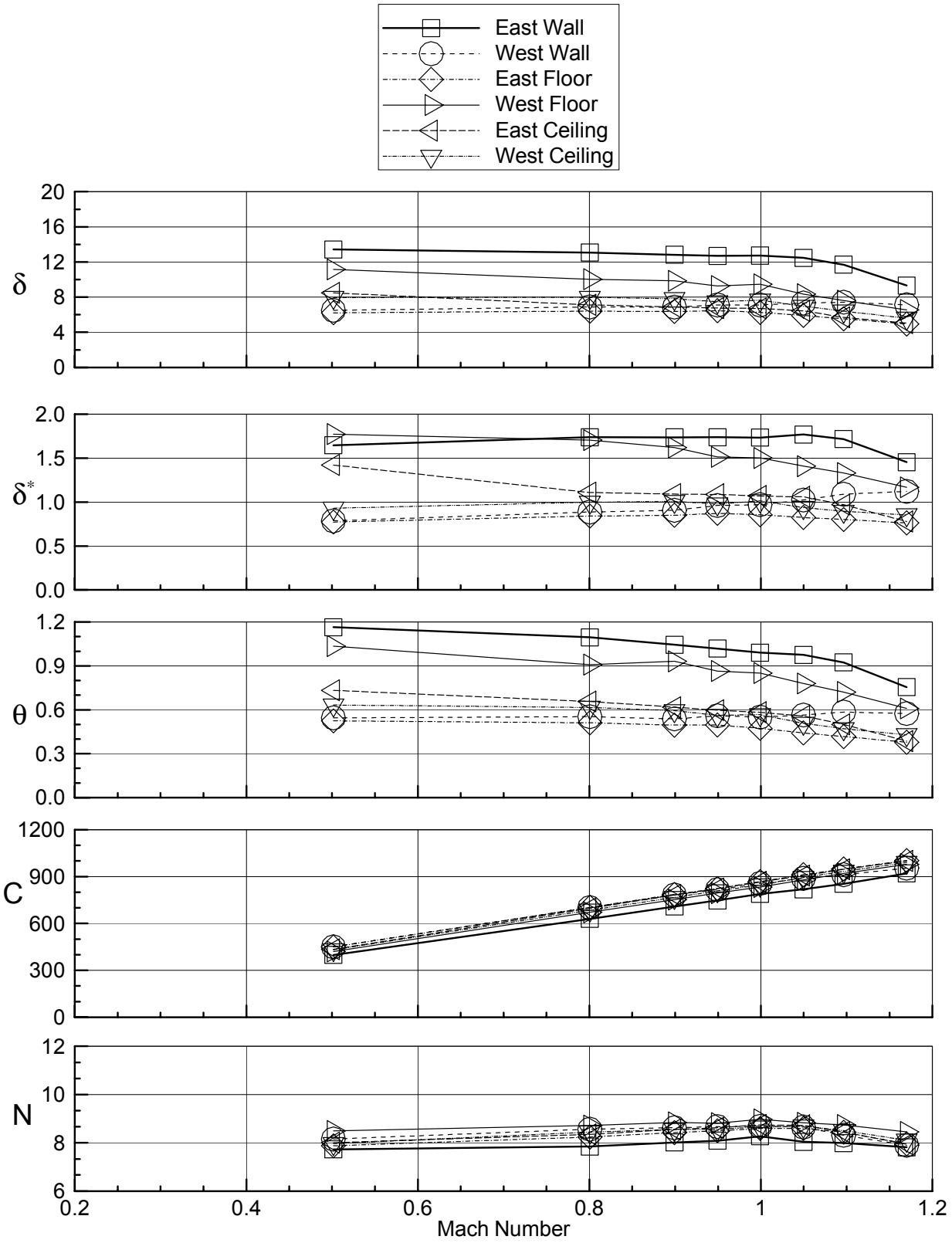

a) P_t=200 psf

Figure 29. Boundary layer parameters for air, East Wall slots closed, standard flap settings, TS 72.

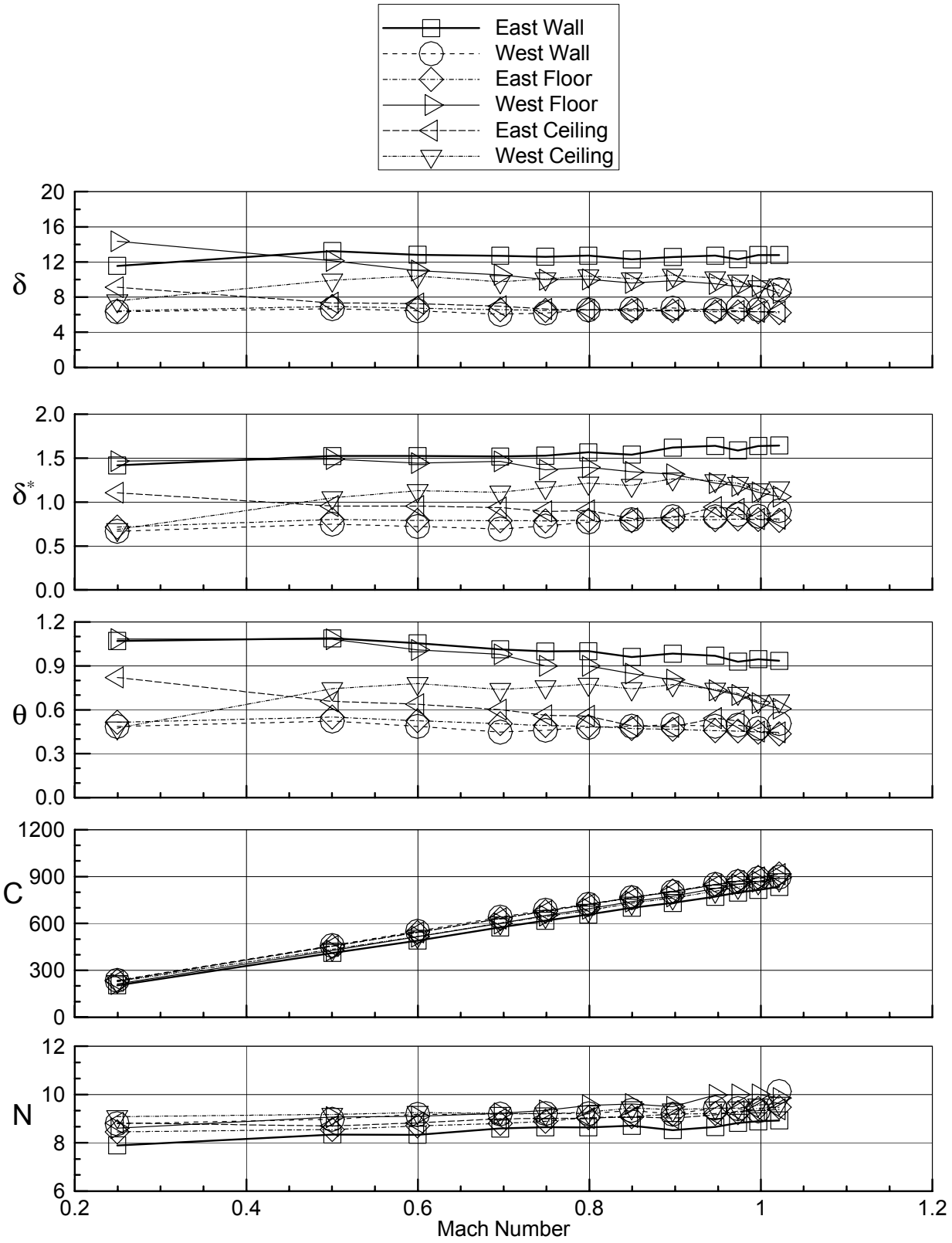

b) P_t=400 psf

Figure 29. - continued

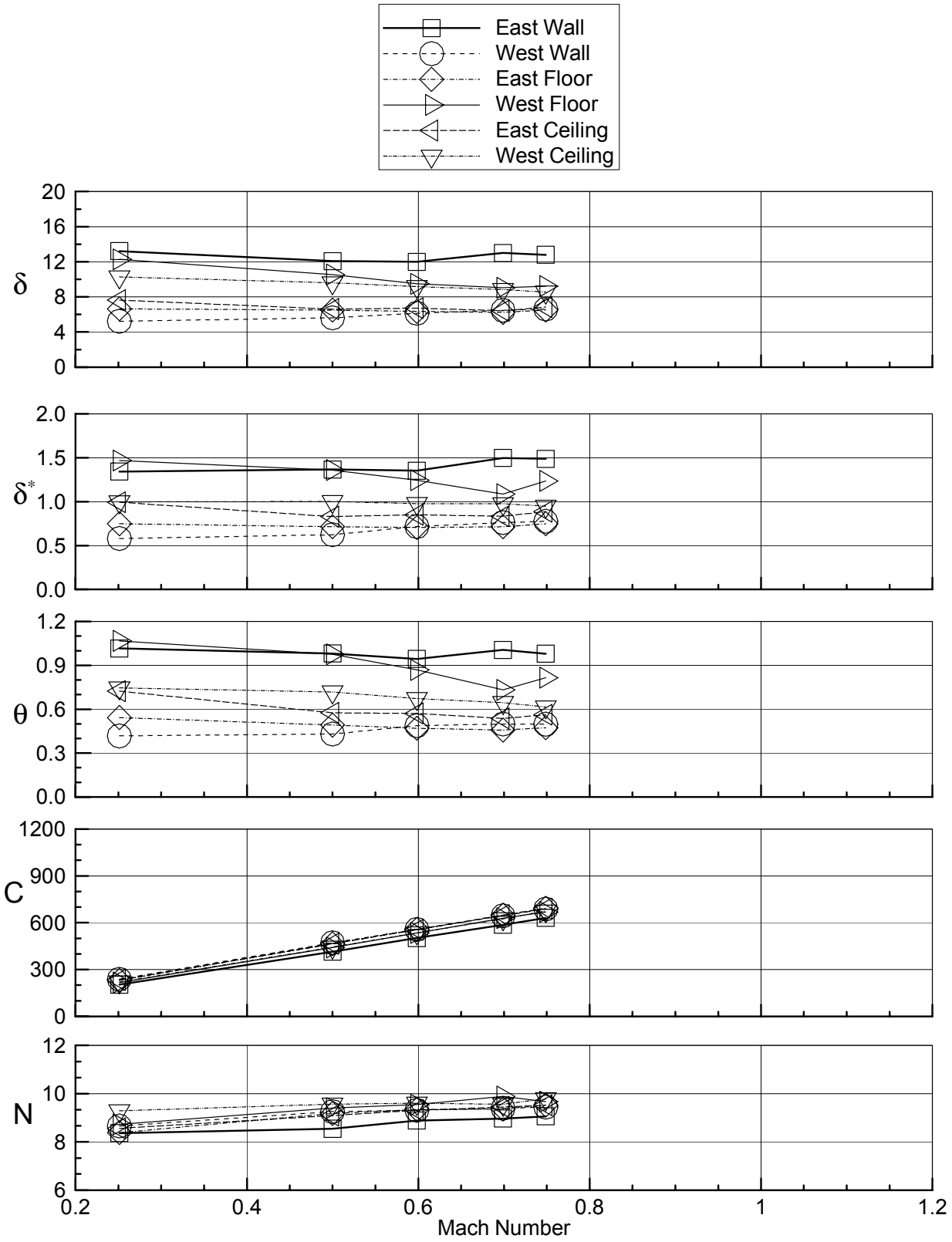

c) P_t=700 psf

Figure 29. - concluded

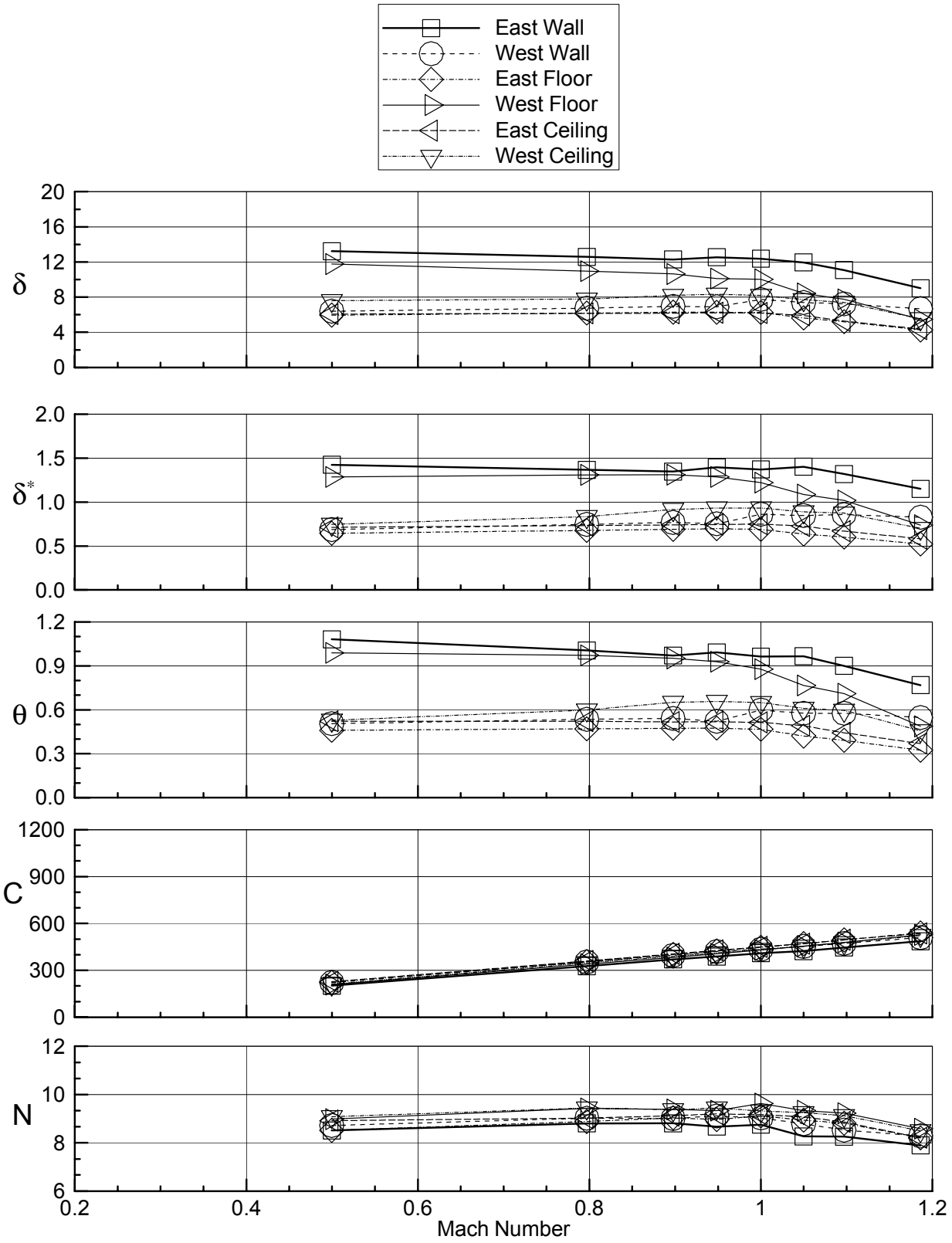

a) P_t=200 psf

Figure 30. Boundary layer parameters for R-134a, all slots open, standard flap settings, TS 72.

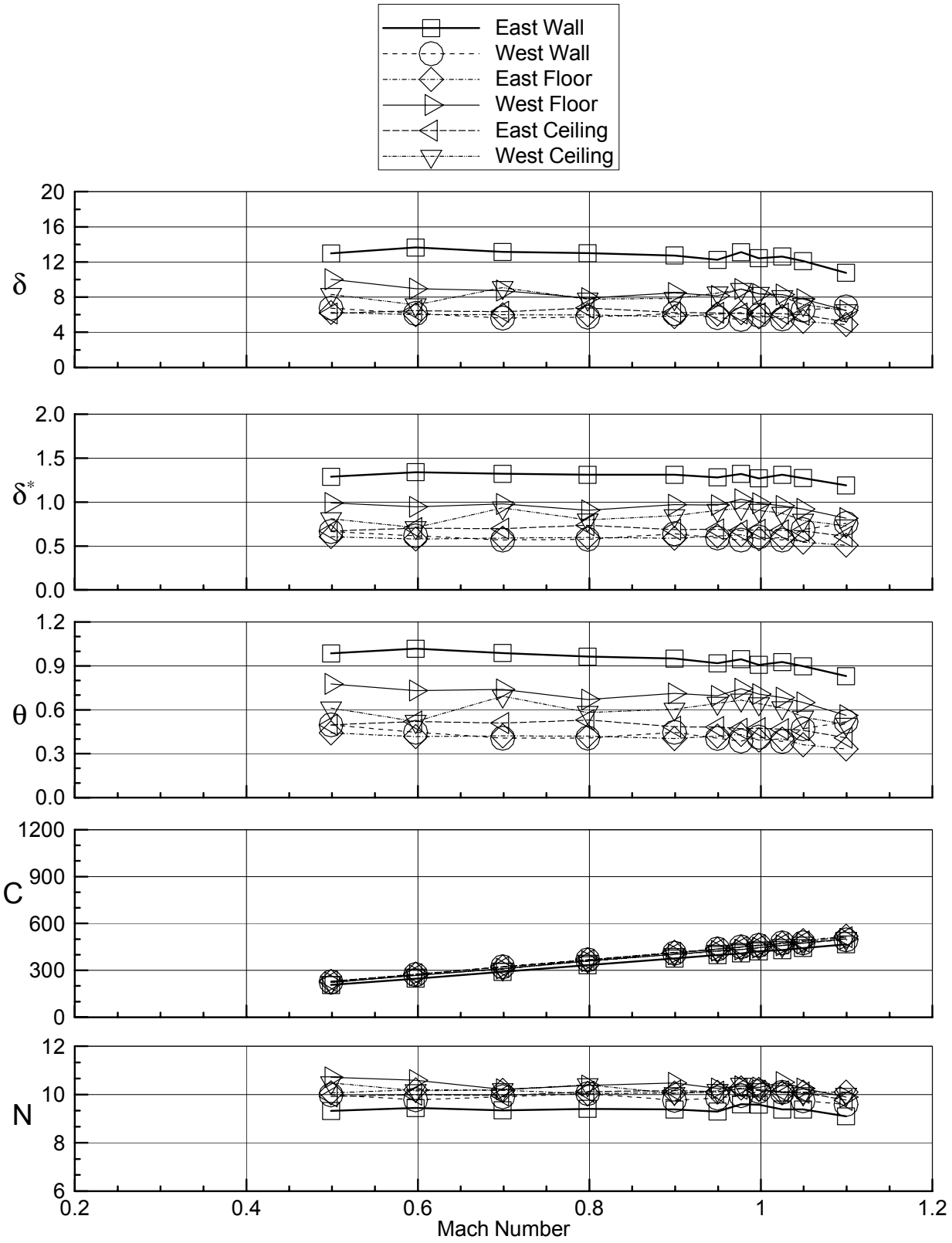

b) P_t=700 psf

Figure 30 - continued

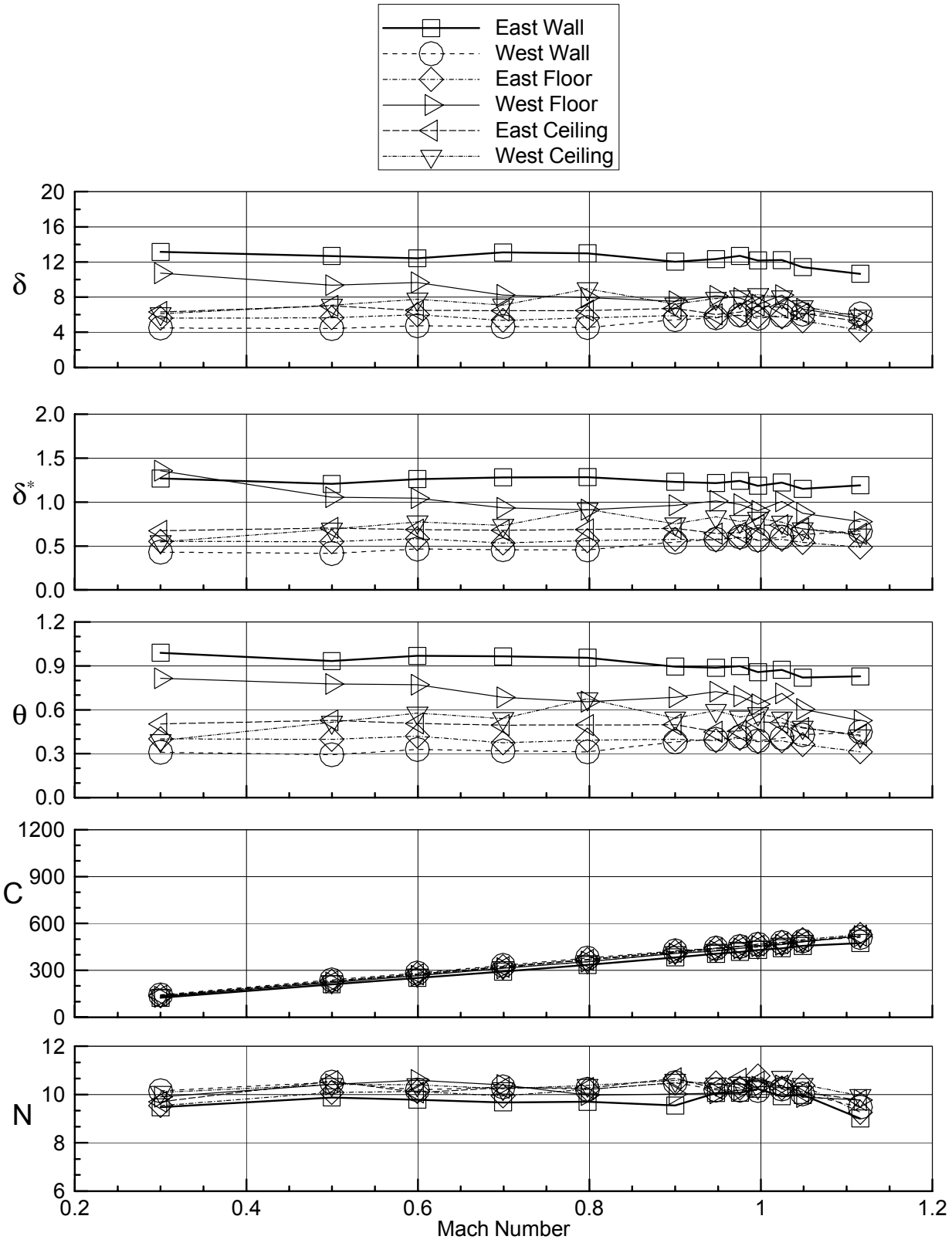

c) P_t=1000 psf

Figure 30 - continued

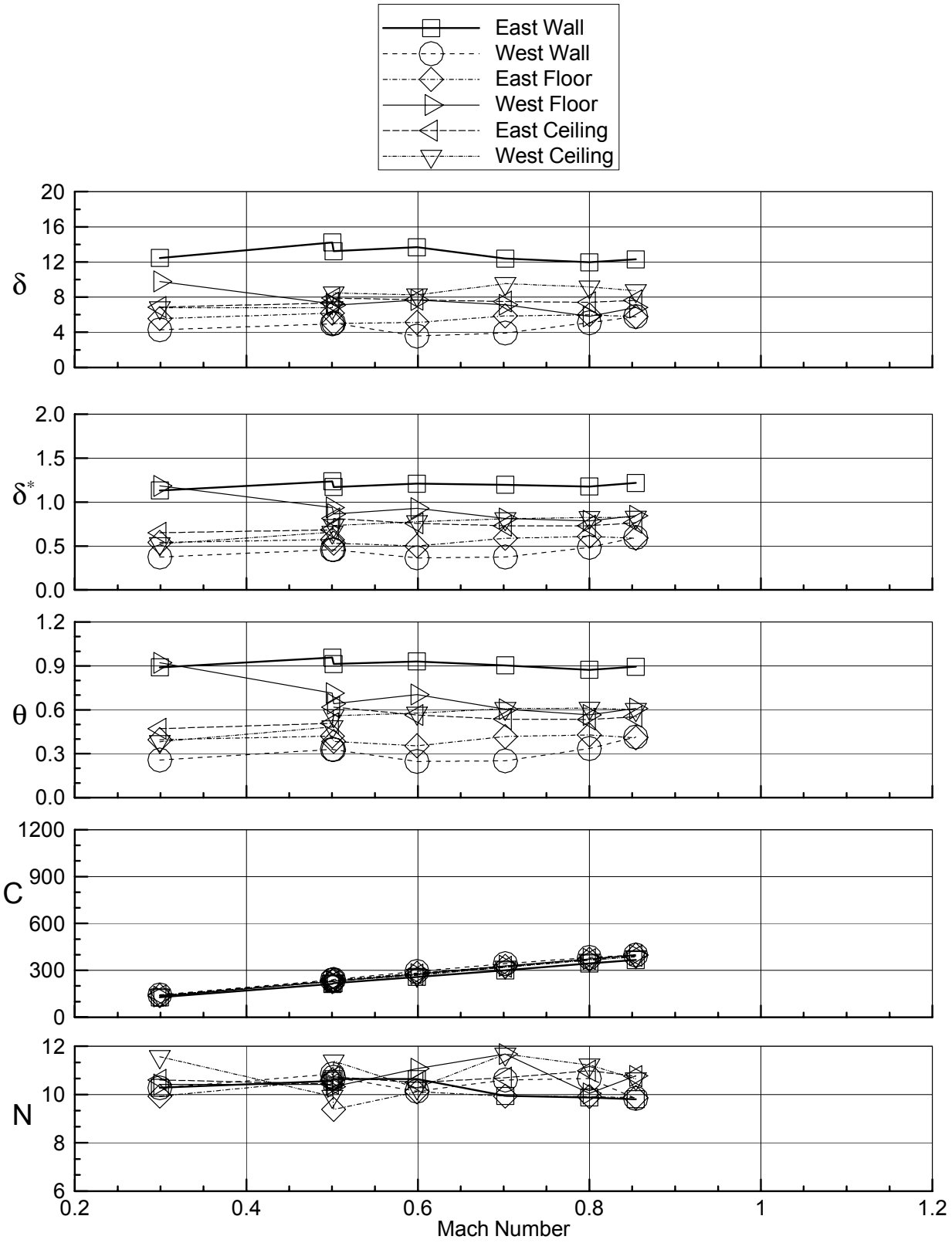

d) P_t=1800 psf

Figure 30 – concluded

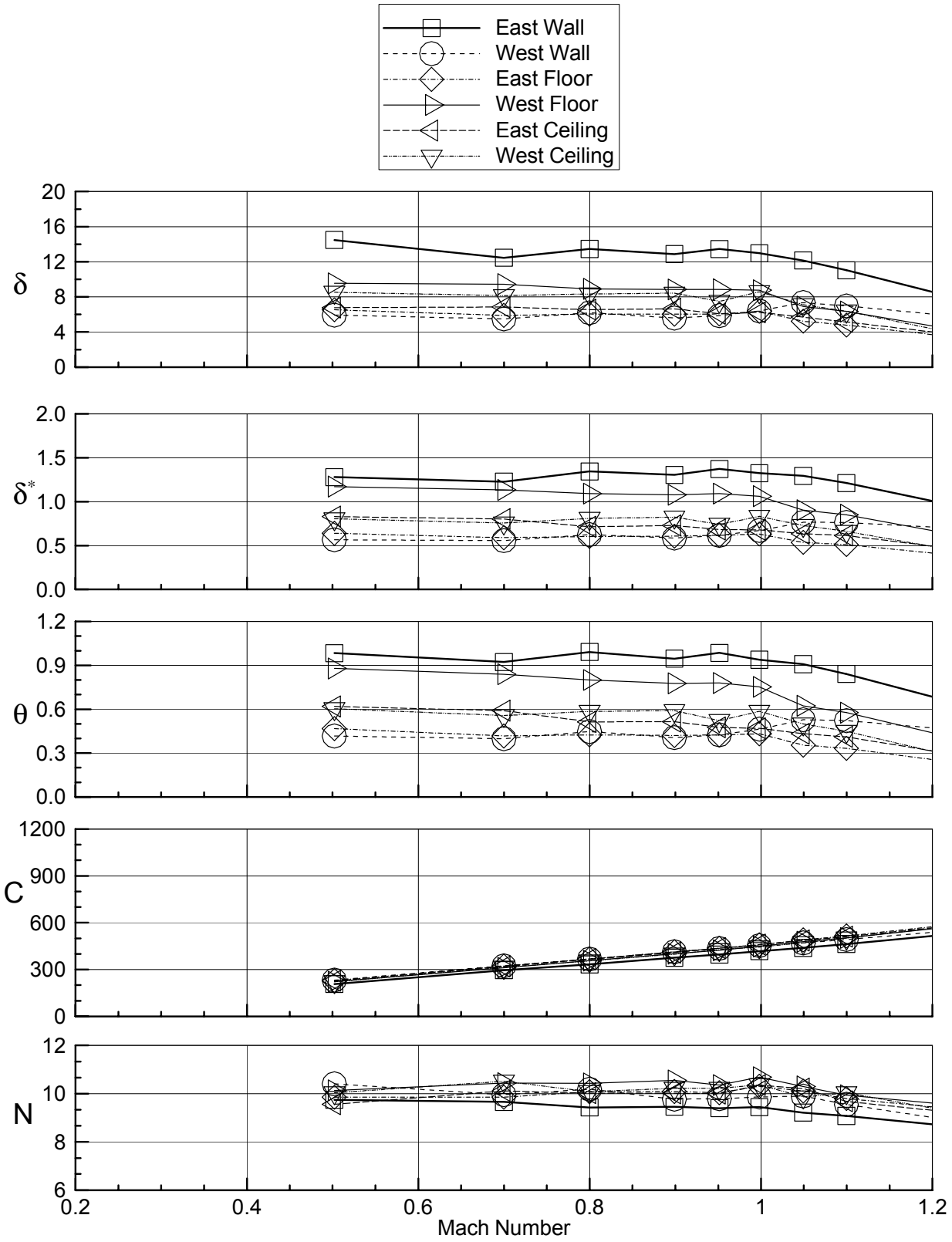

a) P_t=700 psf

Figure 31. Boundary layer parameters for R-134a, East wall slots closed, standard flap settings, TS 72.

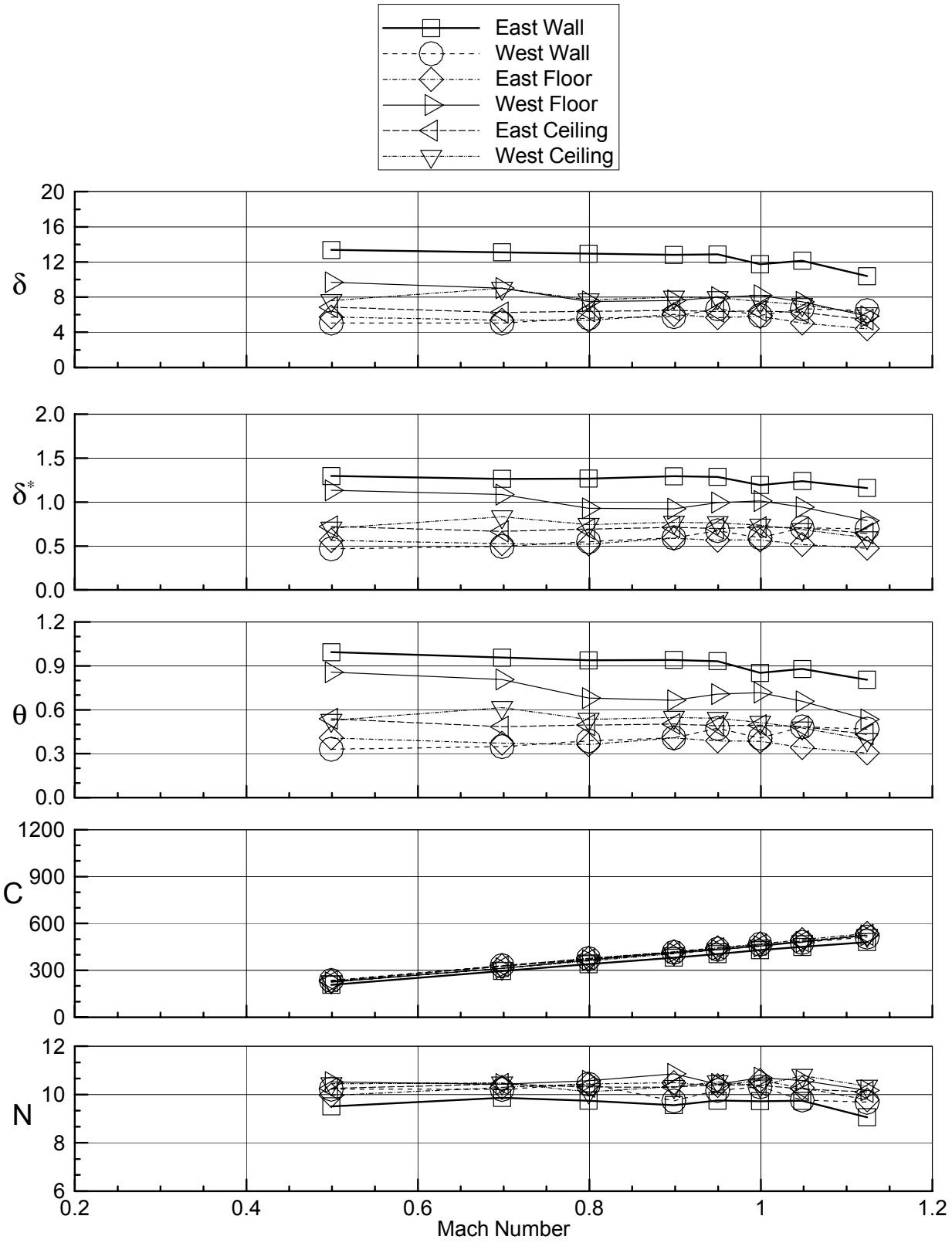

c) P_t=1000 psf

Figure 31 - continued

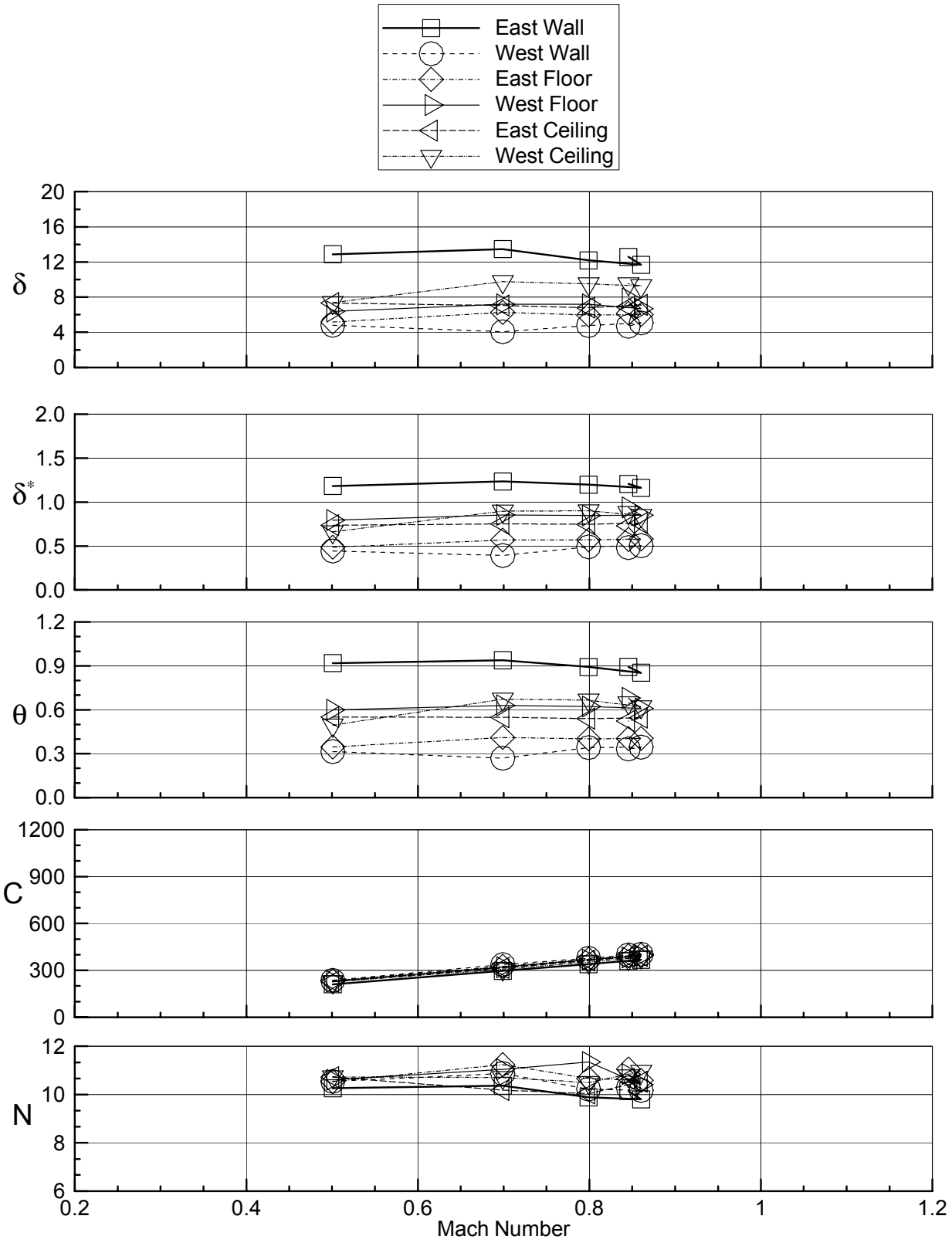

a) P_t=1800 psf

Figure 31 – concluded.

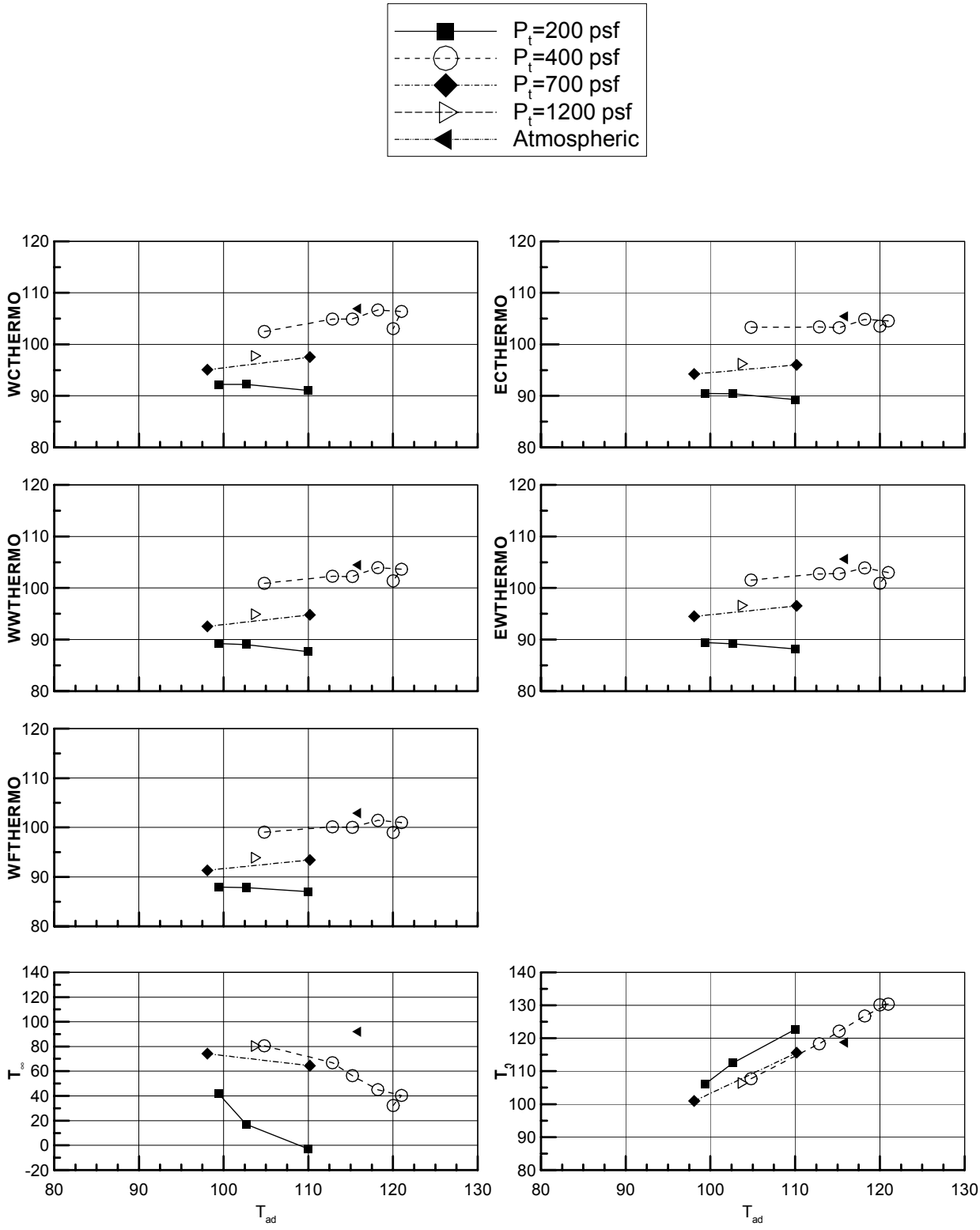

a) Air All slots open, Tunnel station 72

Figure 32. Temperatures as a function of adiabatic temperature, for Air, all slots open, all temperatures in degrees F.

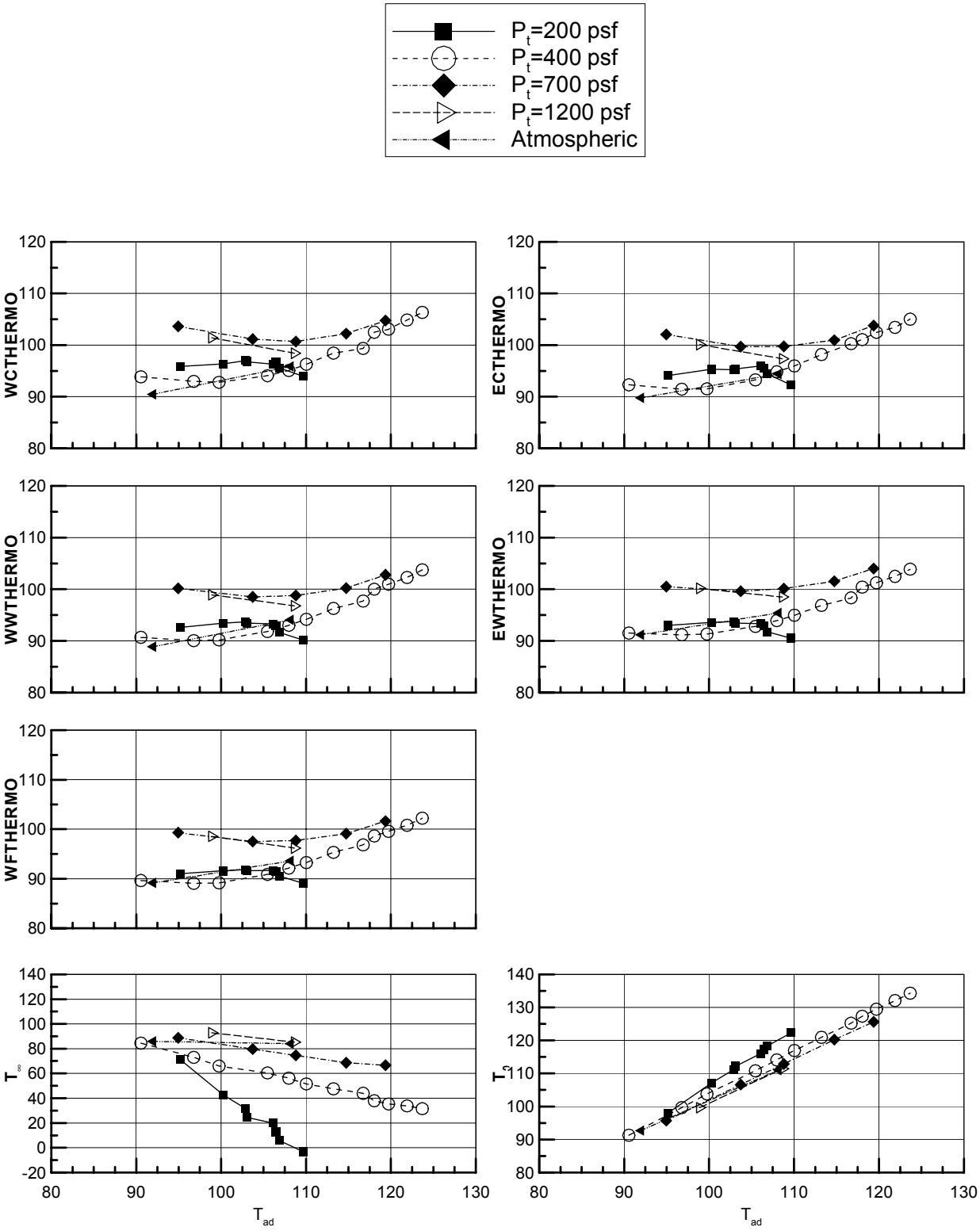

b) Air, East wall slots closed, Tunnel station 72

Figure 32. continued

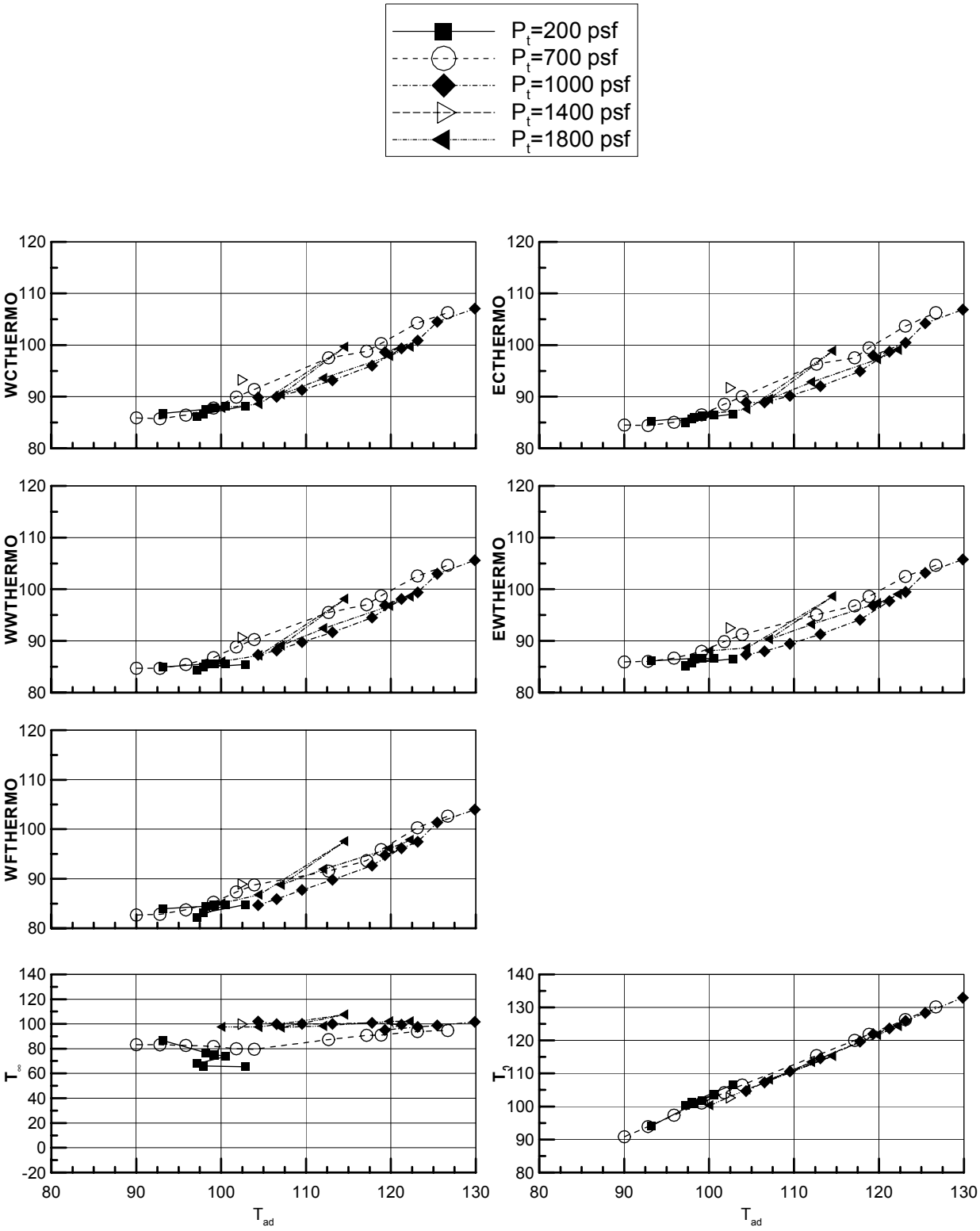

c) R-134a, All slots open, Tunnel station 72

Figure 32. continued

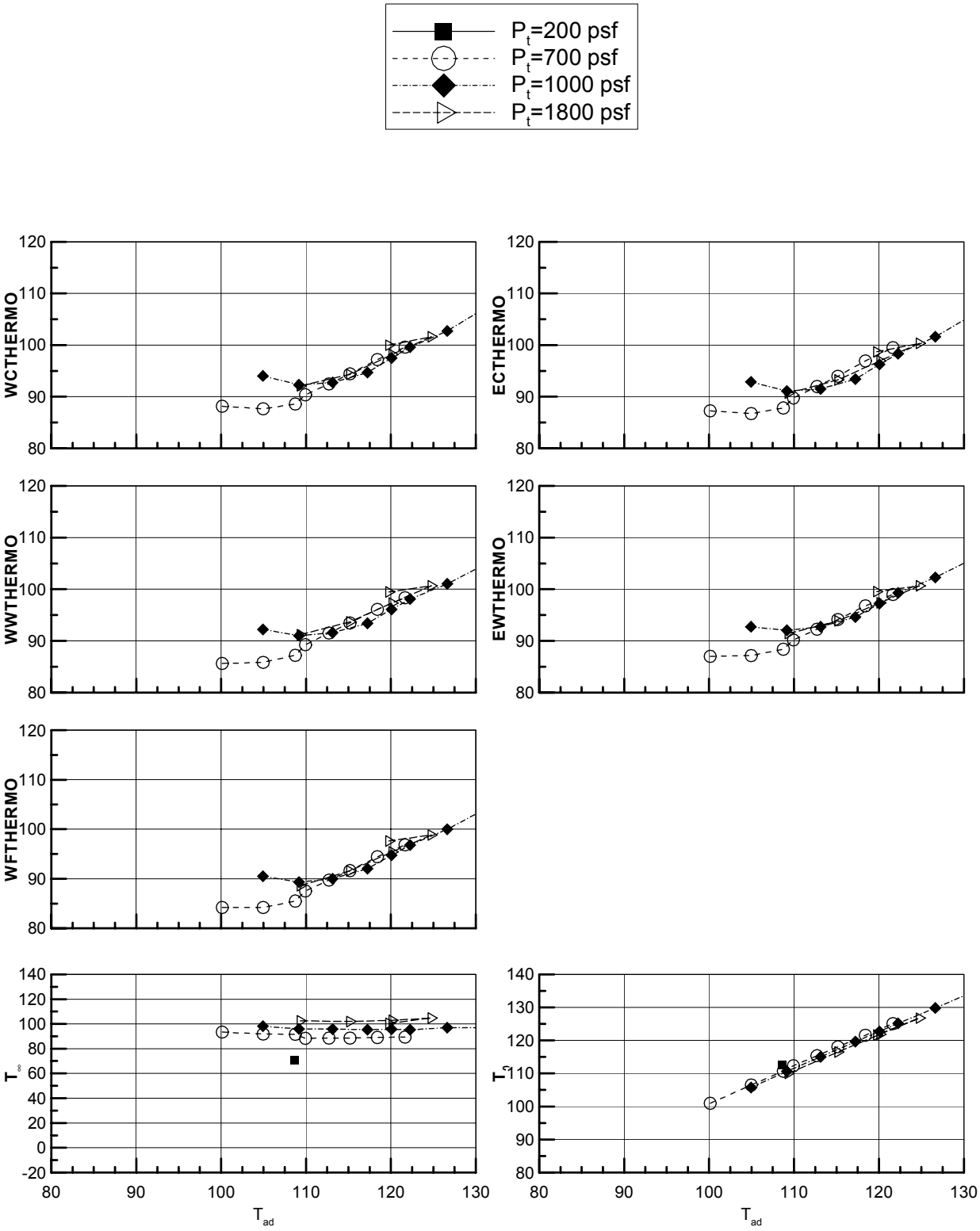

d) R-134a, East wall slots closed, Tunnel station 72

Figure 32. concluded.

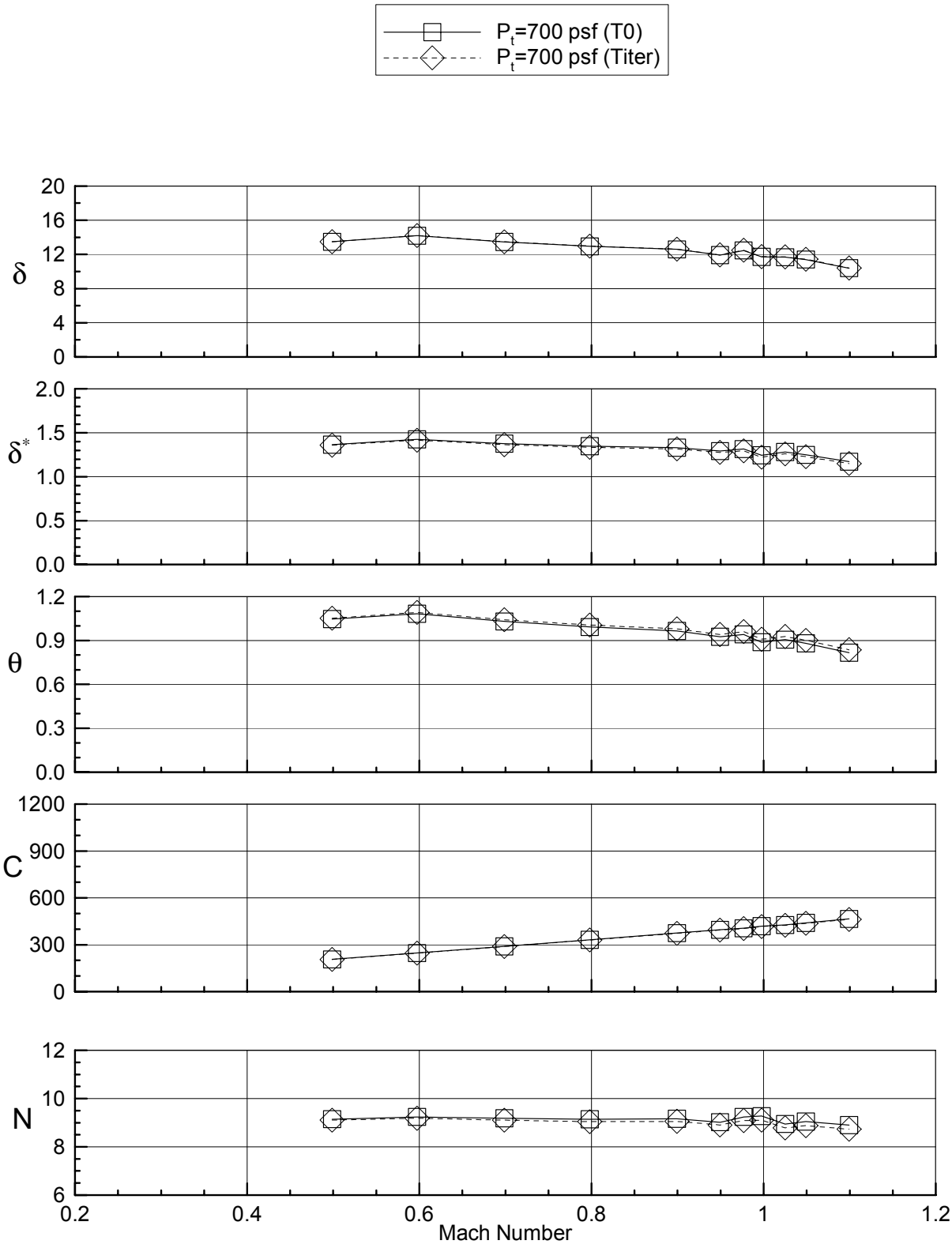

a) East Wall rake

Figure 33. Comparison of boundary layer results using tunnel stagnation temperature with iterating the temperature through the wall, R-134a, All Slots Open

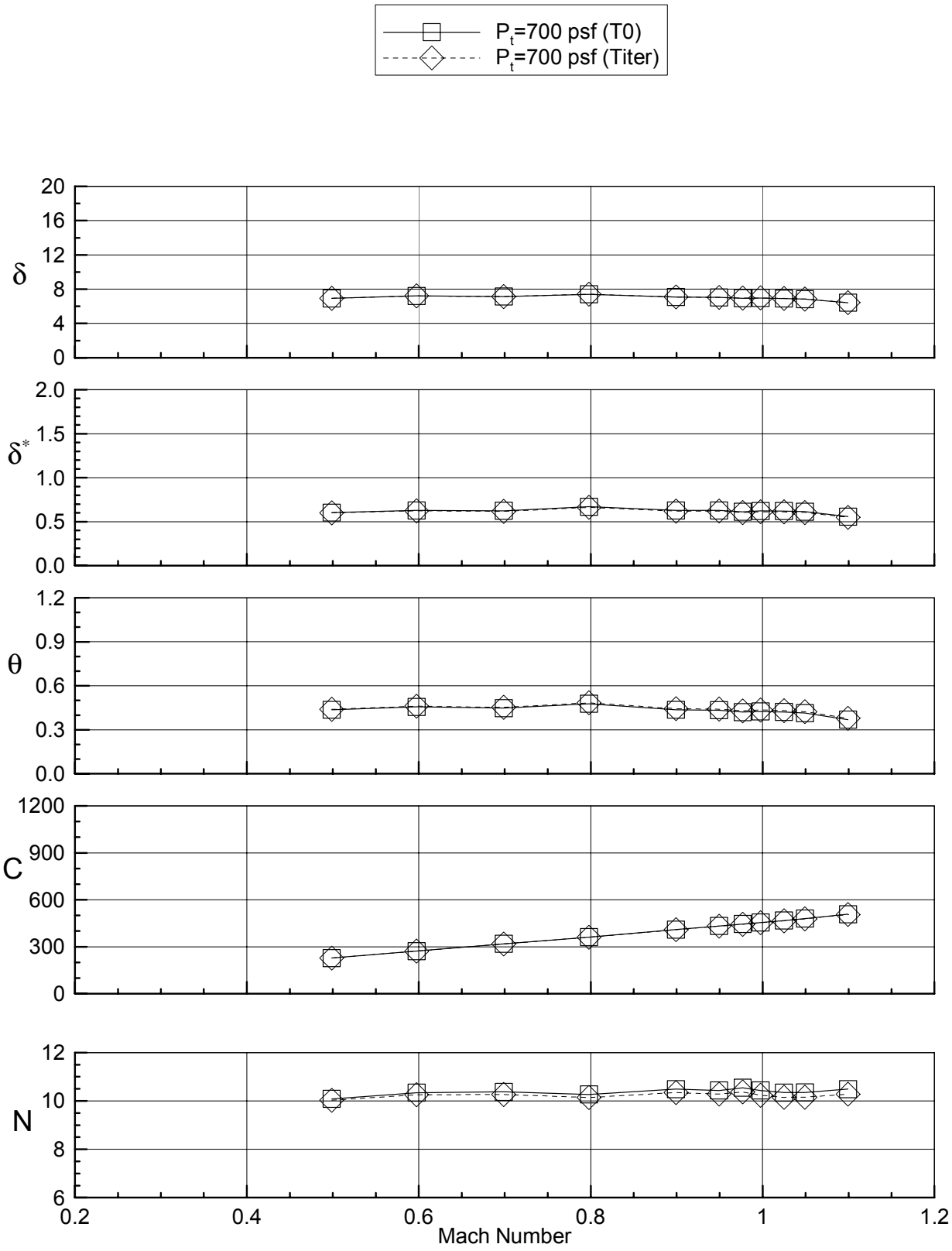

b) East Ceiling rake

Figure 33. continued.

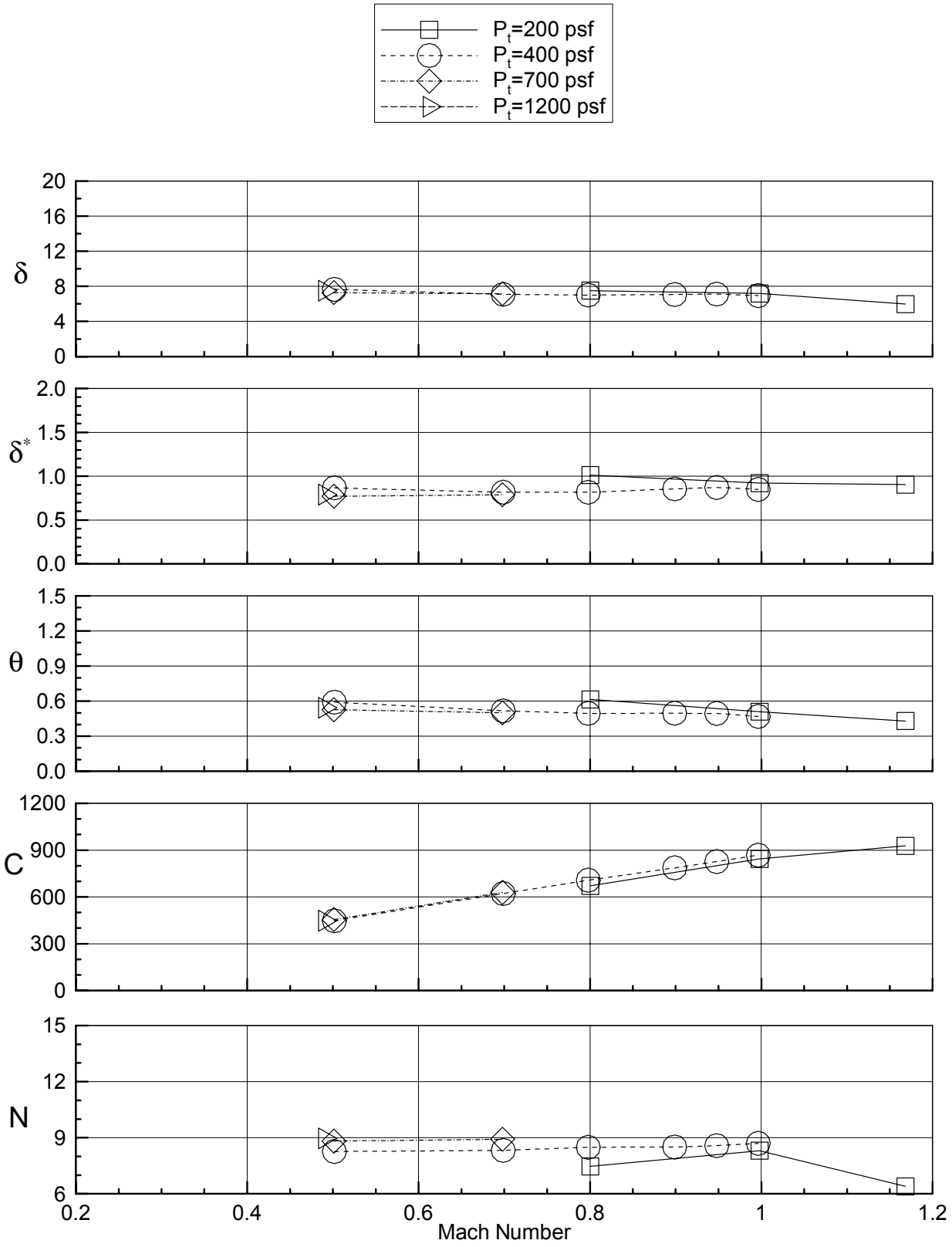
P_t=200 psf
P_t=400 psf
P_t=700 psf
P_t=1200 psf
δ
δ*
θ
C
N
Mach Number

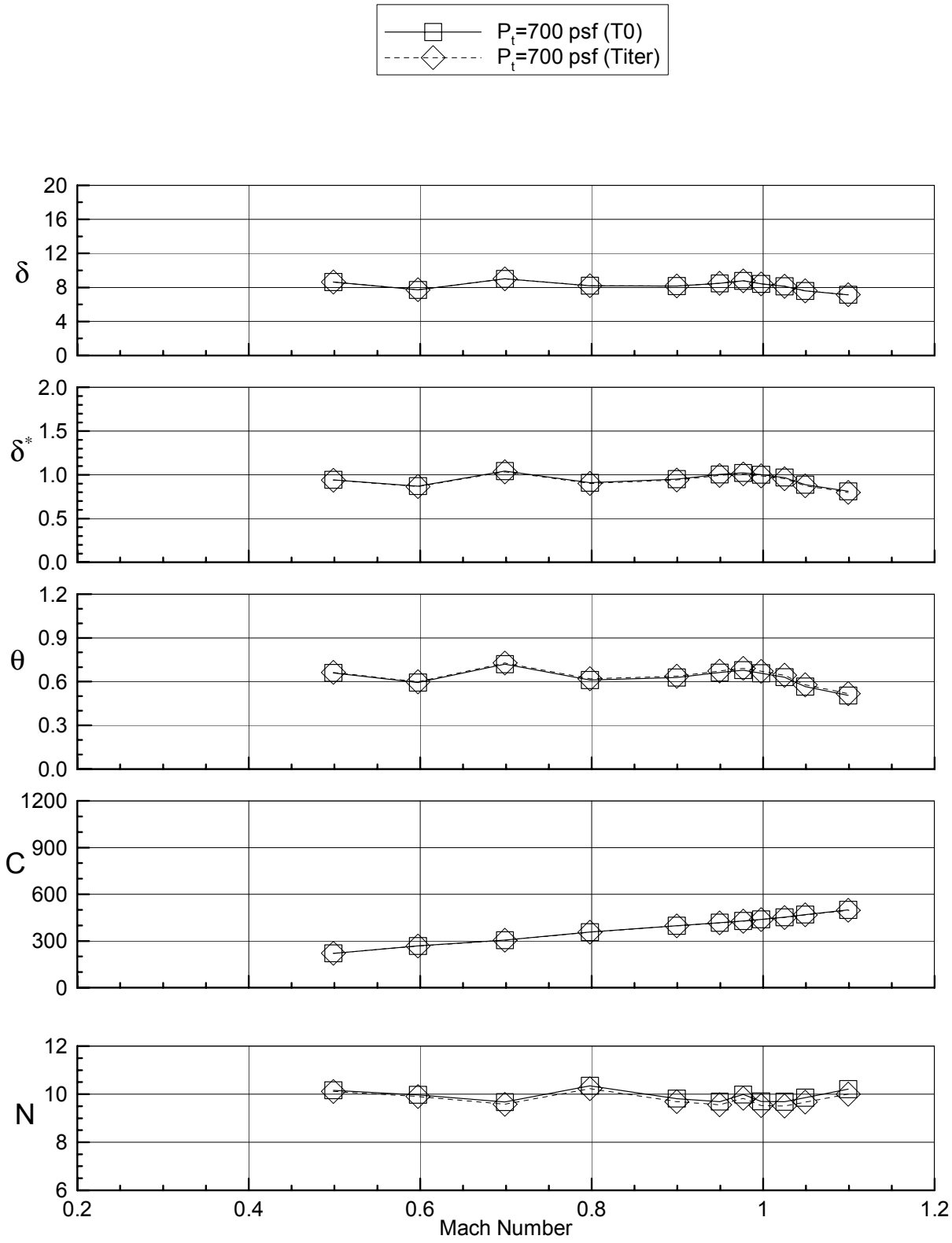

c) West Ceiling rake

Figure 33. continued.

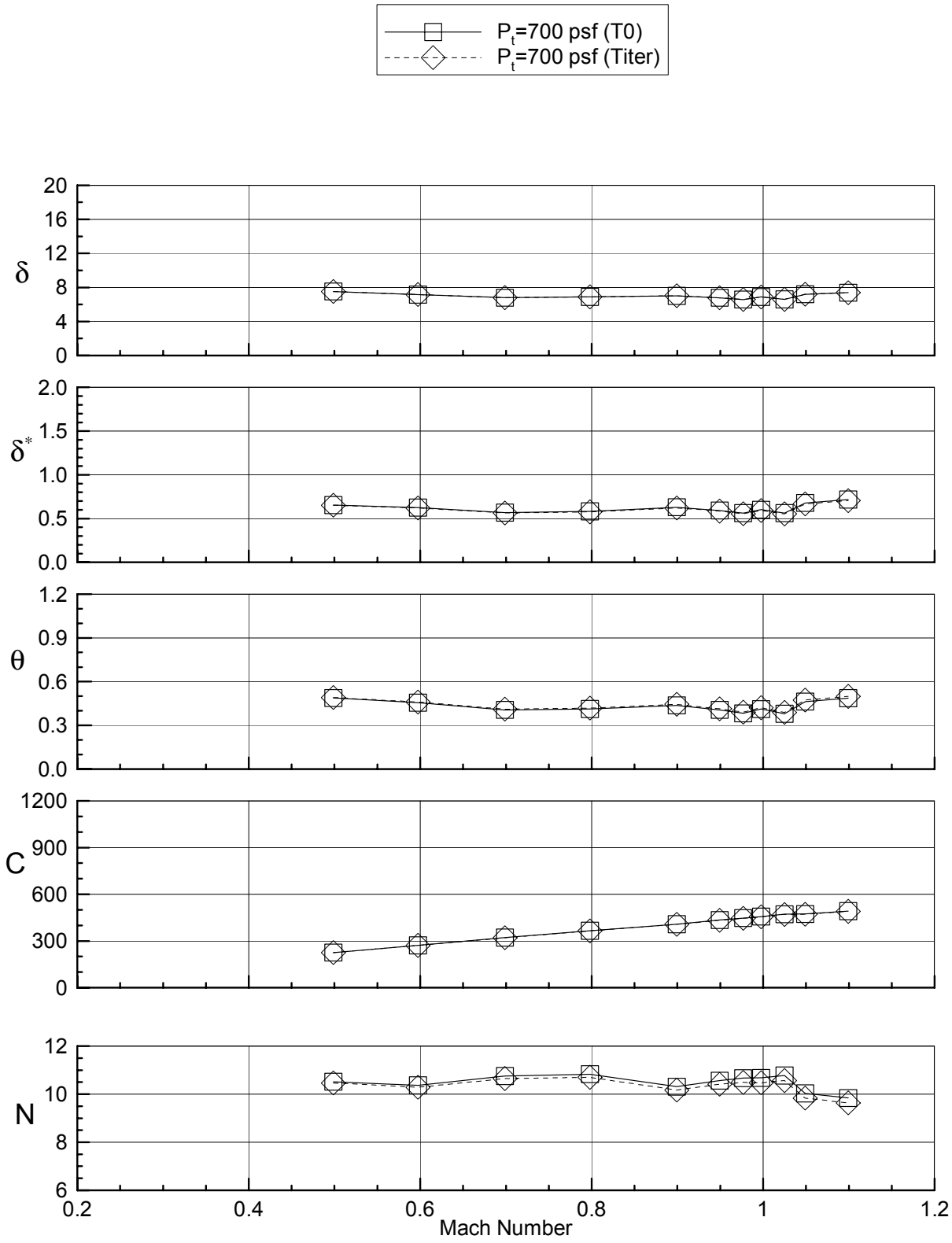

d) West Wall rake

Figure 33. continued.

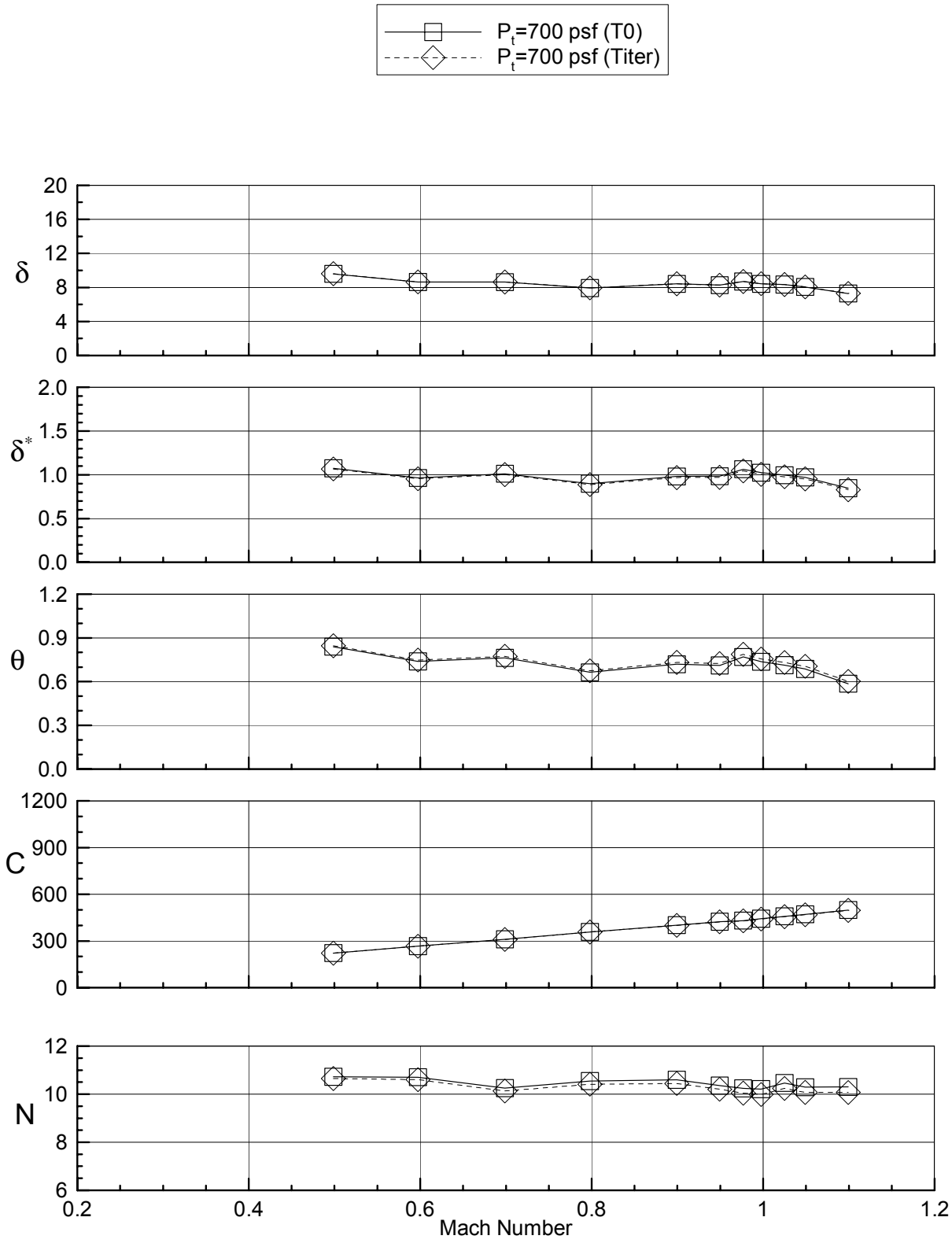

e) West Floor rake

Figure 33. continued.

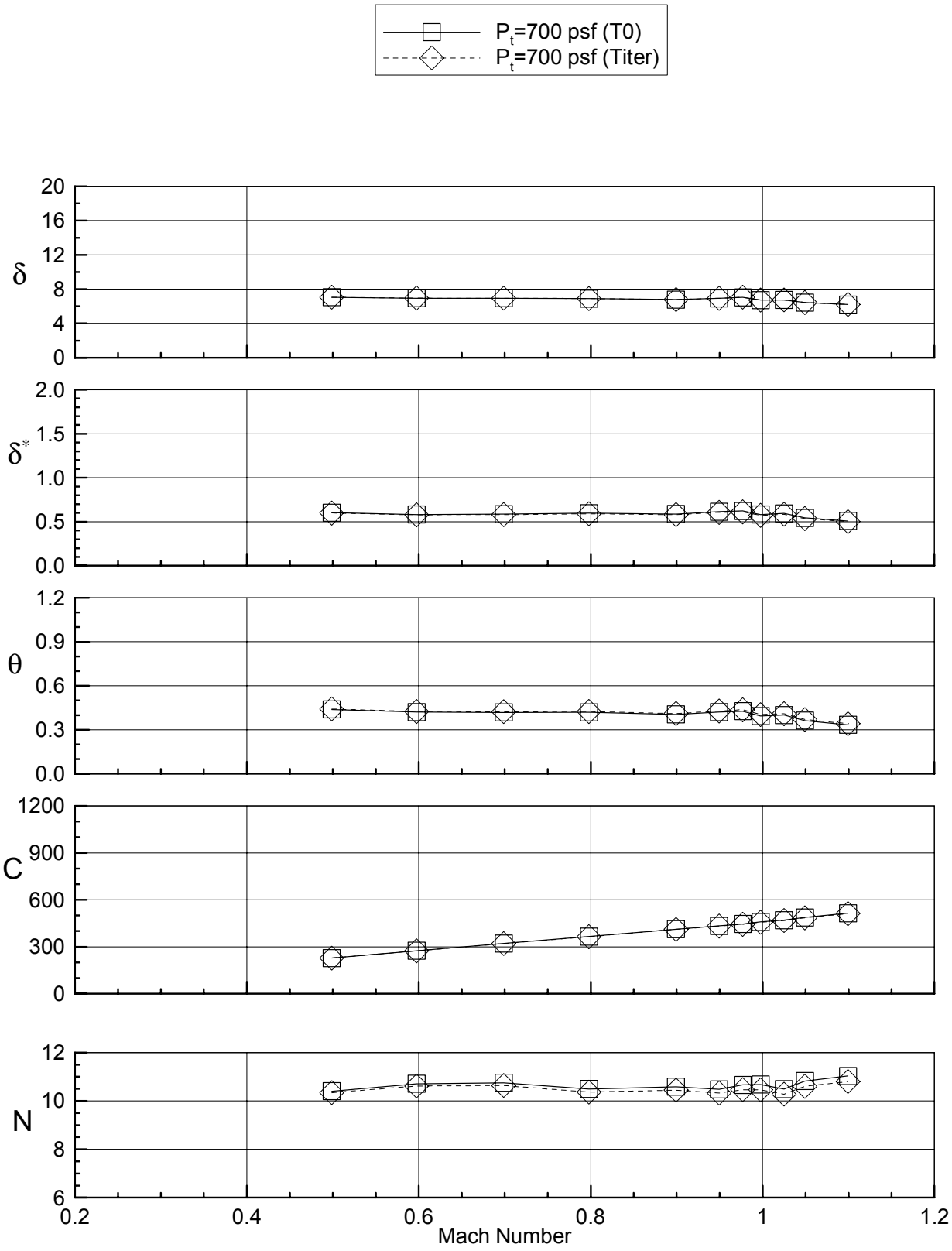

f) East Floor rake

Figure 33. concluded.

REPORT DOCUMENTATION PAGE

Form Approved
OMB No. 0704-0188

1. REPORT DATE *(DD-MM-YYYY)*	2. REPORT TYPE	3. DATES COVERED *(From - To)*
01- 04 - 2007	Technical Memorandum	

4. TITLE AND SUBTITLE

Wall Boundary Layer Measurements for the NASA Langley Transonic Dynamics Tunnel

5a. CONTRACT NUMBER

5b. GRANT NUMBER

5c. PROGRAM ELEMENT NUMBER

6. AUTHOR(S)

Wieseman, Carol D.; and Bennett, Robert M.

5d. PROJECT NUMBER

5e. TASK NUMBER

5f. WORK UNIT NUMBER

561581.02.08

7. PERFORMING ORGANIZATION NAME(S) AND ADDRESS(ES)

NASA Langley Research Center
Hampton, VA 23681-2199

8. PERFORMING ORGANIZATION REPORT NUMBER

L-19248

9. SPONSORING/MONITORING AGENCY NAME(S) AND ADDRESS(ES)

National Aeronautics and Space Administration
Washington, DC 20546-0001

10. SPONSOR/MONITOR'S ACRONYM(S)

NASA

11. SPONSOR/MONITOR'S REPORT NUMBER(S)

NASA/TM-2007-214867

12. DISTRIBUTION/AVAILABILITY STATEMENT

Unclassified - Unlimited
Subject Category 09
Availability: NASA CASI (301) 621-0390

13. SUPPLEMENTARY NOTES

An electronic version can be found at http://ntrs.nasa.gov

14. ABSTRACT

Measurements of the boundary layer parameters in the NASA Langley Transonic Dynamics tunnel were conducted during extensive calibration activities following the facility conversion from a Freon-12 heavy-gas test medium to R-134a. Boundary-layer rakes were mounted on the wind-tunnel walls, ceiling, and floor. Measurements were made over the range of tunnel operation envelope in both heavy gas and air and without a model in the test section at three tunnel stations. Configuration variables included open and closed east sidewall wall slots, for air and R134a test media, reentry flap settings, and stagnation pressures over the full range of tunnel operation. The boundary layer thickness varied considerably for the six rakes. The thickness for the east wall was considerably larger that the other rakes and was also larger than previously reported. There generally was some reduction in thickness at supersonic Mach numbers, but the effect of stagnation pressure, and test medium were not extensive.

15. SUBJECT TERMS

Boundary layer; Transonic; Tunnel calibration; Wind tunnel

16. SECURITY CLASSIFICATION OF:			17. LIMITATION OF ABSTRACT	18. NUMBER OF PAGES	19a. NAME OF RESPONSIBLE PERSON
a. REPORT	b. ABSTRACT	c. THIS PAGE			STI Help Desk (email: help@sti.nasa.gov)
					19b. TELEPHONE NUMBER *(Include area code)*
U	U	U	UU	136	(301) 621-0390